5

CENTRAL RESEARCH LIBRARY
DOCUMENT COLLECTION

OAK RIDGE NATIONAL LABORATORY LIBRARY
3 4456 0022211 3

ORNL-2787
Instruments

INSTRUMENTATION AND CONTROLS DIVISION

ANNUAL PROGRESS REPORT

FOR PERIOD ENDING JULY 1, 1959

CENTRAL RESEARCH LIBRARY
DOCUMENT COLLECTION
LIBRARY LOAN COPY
DO NOT TRANSFER TO ANOTHER PERSON
If you wish someone else to see this document, send in name with document and the library will arrange a loan.

OAK RIDGE NATIONAL LABORATORY
operated by
UNION CARBIDE CORPORATION
for the
U.S. ATOMIC ENERGY COMMISSION

CRL

Cy. 5

ORNL-2787
ERRATA

INSTRUMENTATION AND CONTROLS DIVISION ANNUAL PROGRESS REPORT
FOR PERIOD ENDING JULY 1, 1959

For Figs. 2 and 3, p 3, use ORNL-LR-DWG. Nos. 38815 and 38816.

For Fig. 43, p 67, use the corrected version given below:

Printed in USA. Price $3.00. Available from the
Office of Technical Services
Department of Commerce
Washington 25, D.C.

LEGAL NOTICE

This report was prepared as an account of Government sponsored work. Neither the United States, nor the Commission, nor any person acting on behalf of the Commission:

A. Makes any warranty or representation, expressed or implied, with respect to the accuracy, completeness, or usefulness of the information contained in this report, or that the use of any information, apparatus, method, or process disclosed in this report may not infringe privately owned rights; or

B. Assumes any liabilities with respect to the use of, or for damages resulting from the use of any information, apparatus, method, or process disclosed in this report.

As used in the above, "person acting on behalf of the Commission" includ[illegible] ny employe[illegible] contractor of the Commission, or employee of such contractor, to the ex[illegible] such em[illegible] or contractor of the Commission, or employee of such contractor [illegible]ctor.

ORNL-2787
ERRATA

Cy 5

INSTRUMENTATION AND CONTROLS DIVISION ANNUAL PROGRESS REPORT
FOR PERIOD ENDING JULY 1, 1959

Page	Line	Errata
15	Fig. 10	Line joining bottom of "carrier set" potentiometer to top of T_4 bus line should be deleted
32	Fig. 23	There is a common collector amplifier between the second feedback pair and the common collector cable driver that is not shown in the drawing
33	14	<u>for</u> common-base amplifier <u>read</u> common-collector amplifier
36	footnote	<u>for</u> $(1 - e^{\lambda T})\lambda$ <u>read</u> $(1 - e^{-T})T$

CRL

Cy. 5

ORNL-2787
ERRATA

INSTRUMENTATION AND CONTROLS DIVISION ANNUAL PROGRESS REPORT
FOR PERIOD ENDING JULY 1, 1959

For Figs. 2 and 3, p 3, use ORNL-LR-DWG. Nos. 38815 and 38816.

For Fig. 43, p 67, use the corrected version given below:

ORNL-2787
ERRATA

Cy 5

INSTRUMENTATION AND CONTROLS DIVISION ANNUAL PROGRESS REPORT
FOR PERIOD ENDING JULY 1, 1959

Page	Line	Errata
15	Fig. 10	Line joining bottom of "carrier set" potentiometer to top of T_4 bus line should be deleted
32	Fig. 23	There is a common collector amplifier between the second feedback pair and the common collector cable driver that is not shown in the drawing
33	14	<u>for</u> common-base amplifier <u>read</u> common-collector amplifier
36	footnote	<u>for</u> $(1 - e^{\lambda T})\lambda$ <u>read</u> $(1 - e^{-T})T$

ORNL-2787
Instruments
TID-4500 (15th ed.)

Contract No. W-7405-eng-26

INSTRUMENTATION AND CONTROLS DIVISION

ANNUAL PROGRESS REPORT

For Period Ending July 1, 1959

C. J. Borkowski, Director
C. S. Harrill, Associate Director

DATE ISSUED

OCT 21 1959

OAK RIDGE NATIONAL LABORATORY
Oak Ridge, Tennessee
operated by
UNION CARBIDE CORPORATION
for the
U. S. ATOMIC ENERGY COMMISSION

OAK RIDGE NATIONAL LABORATORY
3 4456 0022211 3

CONTENTS

A Pulser for the Duo Plasmatron Ion Source 1

2048-Channel Neutron Time-of-Flight Analyzer 4

Fission Fragment Time-of-Flight Spectrometer 10

Superheterodyne Electron Paramagnetic Resonance Spectrometer 12

A Versatile Instrument Camera with a Microsecond Electronic Shutter 16

Scaler Rate Meter Q-1743-13 22

Fast Neutron Dose Integrator 25

A Transistorized Data Tape Punch for Electronic Scaling Equipment 29

Transistorized Pulse Preamplifier Q-2032-1 RO 31

Thermal Neutron Survey Meter Q-2004 33

Portable Alpha Counter Q-1975 36

Grid Current in Electrometer Tubes 38

Personal Radiation Monitor 55

Small Concentric Cylinder Fission Chamber 62

Sodium Iodide Phosphor Mounting Techniques 64

Scintillation Spectrometer Shield 68

Systems Analysis 70

Temperature Control for Bulk Shielding Facility Single-Crystal Spectrometer 74

Radiation Effects on Thermocouples 77

Unsaturated Standard Cells 80

Additions and Modifications to the Instrumentation of the Fission Products Pilot Plant 82

Instrumentation for In-Pile Experiments 94

EGCR Fuel Element Capsule Tests in the LITR and the ORR 99

Instruments and Controls for the Maritime Ship Reactor Pressurized Water Experiment in the ORR 103

Transient Heat Transfer Temperature Measurements 116

Molten-Salt Experiments in the MTR 117

Homogeneous Reactor Project Instrumentation and Controls 119

Problems Relating to ORR Operation 142

Bulk Shielding Reactor II—SPERT I Tests 144

Servo Fission Chamber 145

A PULSER FOR THE DUO PLASMATRON ION SOURCE

C. D. Moak[1] R. F. King
H. E. Banta J. W. Johnson

A pulser has been developed for use with the duo plasmatron[2] ion source. The precepts used in the pulser for the r-f ion source are in general extended to this service. Oscillographic deflection of the ion beam across an aperture produces proton pulses with an estimated width at half height of 5×10^{-9} sec. Peak current at present is about 2 ma. Comparable figures for the r-f ion source are 400 μa and 7×10^{-9} sec. The 33-kev ion energy, about ten times the output energy of the r-f ion source, requires longer deflector plates and r-f deflector voltage on the lower plates of about 10 kv peak-to-peak at about 800 kc. The low duty cycle of the output heats the pulser assembly with more than 99% of the beam power. Forced cooling must be added to the assembly for continuous and/or higher current operation.

Figure 1 shows the pulser assembly. The ion beam diverges below the extractor electrode and is focused on the exit aperture by the central Einzel lens. This lens[3] was suggested by the work of Liebman.[4] The tungsten grids reduce lens aberrations. They are each 93% transparent, so that approximately 87% of the ion current goes through the lens. In operation these grids run at red heat and cool themselves by radiation. At the exit aperture the ion beam is approximately 0.10 in. in diameter. The beam is swept across, perpendicular to the long axis, a 0.10-in.-wide slit. The short bursts of ions which get through the slit twice per cycle of r-f deflector voltage are stopped in a Faraday cup of 50 ohms characteristic impedance. The transmission line continues to an oscilloscope, where it is terminated.

Figure 2 shows the pulse as displayed on an Edgerton, Germeshausen & Grier oscilloscope. This is a distributed deflection oscilloscope with no amplifier, and hence low deflection sensitivity. Its rise time is about 0.5×10^{-9} sec. Here the bias on the Faraday cup is reversed so as to collect the secondary electrons. This signal increases the pulse height but adds the electron collection time onto the rise and fall of the pulse. The ion source makes protons, mass 2, and mass 3; hence the three pulses shown here. The sweep is from right to left, and the time between the first two pulses is about 13×10^{-9} sec.

Figure 3 shows the Edgerton, Germeshausen & Grier oscilloscope presentation with no assistance from secondary electrons. The pulse width was estimated from such an oscilloscope presentation.

---

[1]Physics Division.

[2]C. D. Moak et al., "A Duo Plasmatron Ion Source for Use in Accelerators," to be published in Rev. Sci. Instr.

[3]Designed by C. D. Moak.

[4]G. Liebman, Proc. Phys. Soc. (London) B62, 213-28 (1959).

UNCLASSIFIED
ORNL-LR-DWG 38701

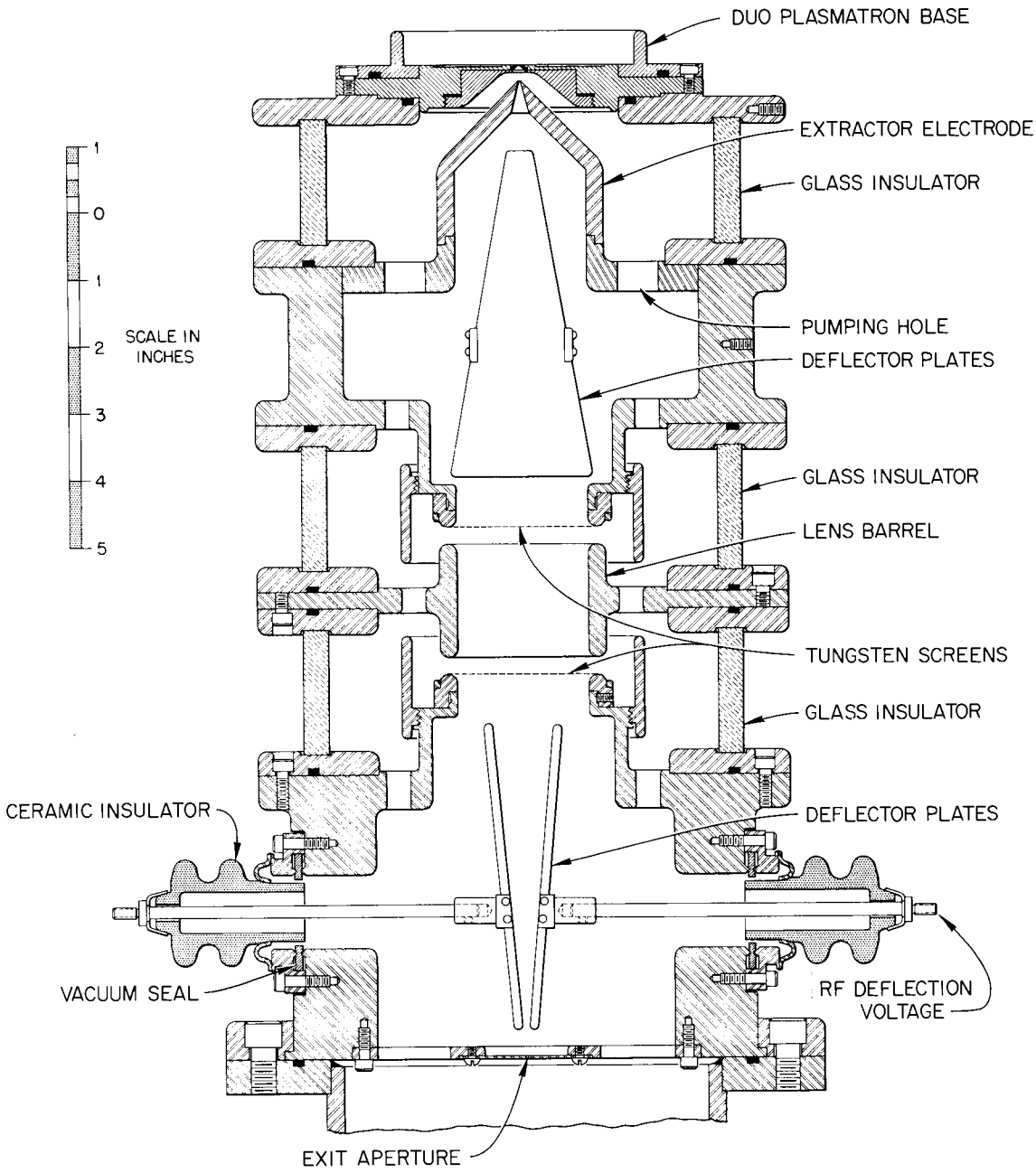

Fig. 1. Duo Plasmatron Lens, Pulser Model I.

ORNL-LR-Dwg UNCLASSIFIED ~~PHOTO~~ 38815

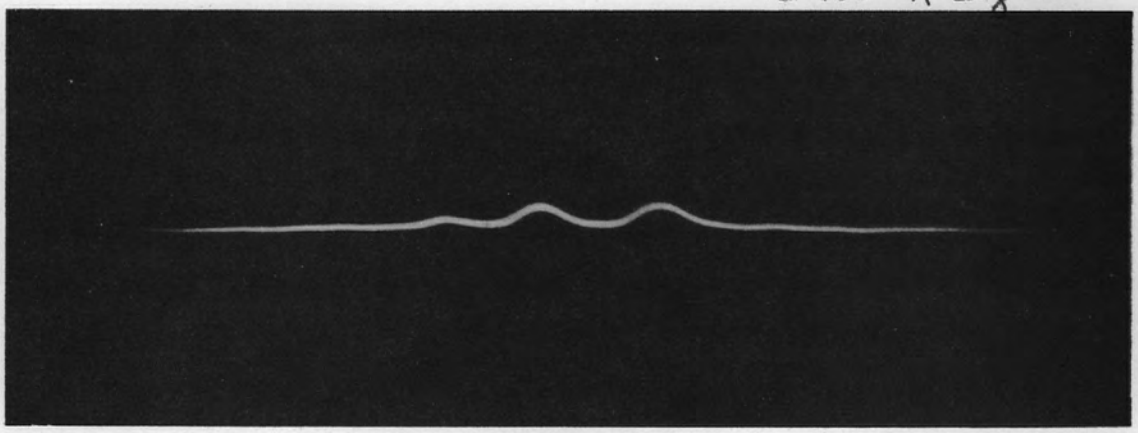

Fig. 2. Duo Plasmatron Pulse: Edgerton, Germeshausen & Grier Oscilloscope, No Amplifiers, with Electron Collection.

ORNL-LR-Dwg UNCLASSIFIED ~~PHOTO~~ 38816

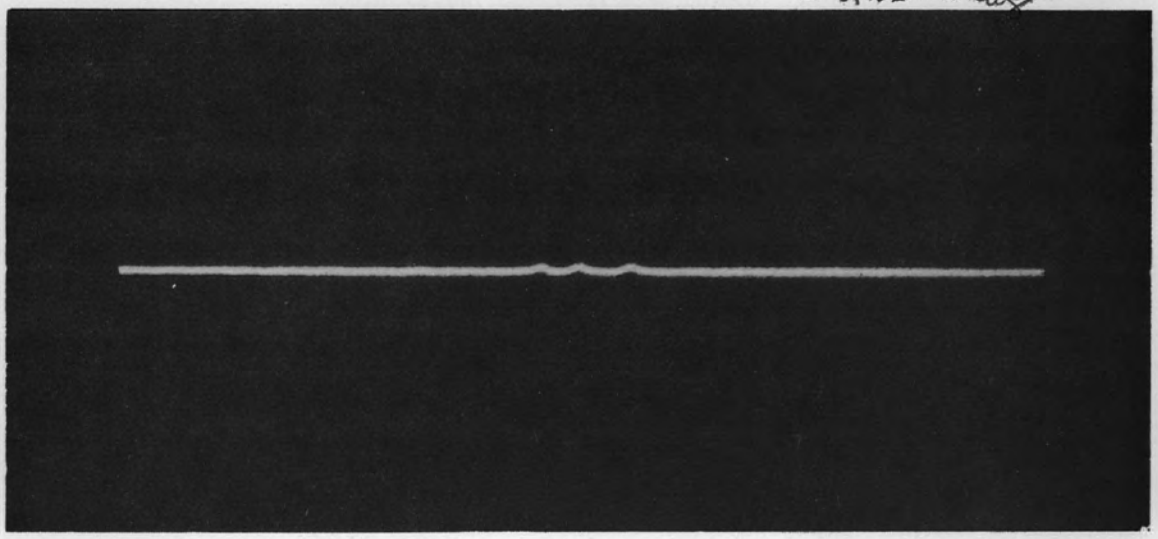

Fig. 3. Duo Plasmatron Pulse: Edgerton, Germeshausen & Grier Oscilloscope, No Amplifiers, No Electron Collection.

See errata

2048-CHANNEL NEUTRON TIME-OF-FLIGHT ANALYZER

N. W. Hill J. B. Davidson

A neutron time-of-flight analyzer having the following specifications has been designed and built for use with the fast chopper and 180-m neutron flight path at the Oak Ridge Research Reactor:

1. Type of storage: magnetic core (General Ceramic 0.080-in.-dia S-4 material).
2. Number of channels: 2048.
3. Capacity per channel: 65,535 counts.
4. Channel widths: 0.25, 0.5, 1, 2, 4, and 8 μsec selected by panel switch. Greater channel widths may be obtained by changing oscillator crystal.
5. Storage time: 16 μsec.
6. Multiple storage per neutron burst.
7. A maximum delay of 8192 channel widths in blocks of 256.
8. Memory separation into two or four parts corresponding to 1024 or 512 channels each.
9. Up to four detector inputs with counts from each stored in separate parts of the memory.
10. Automatic operation with sample changer and up to two detector inputs in which the "in" and "out" runs are stored in separate parts of the memory.
11. Data display on a 5-in. cathode ray tube.
12. Punched tape output of data for processing by a digital computer (Oracle).

The analyzer is based upon the designs of Schumann[1] and of Emmer et al.[2] It consists, basically, of a clock and a storage register or memory. The clock is started when a light beam is allowed to pass through the neutron chopper onto a photomultiplier tube at the instant the neutron beam starts through. The clock is stopped by a pulse from a neutron detector signaling the arrival of a neutron at the end of the flight path. A count is then stored in the memory channel assigned to the time of flight indicated by the clock.

---

[1]R. W. Schumann, Rev. Sci. Instr. 27, 686 (1956).

[2]T. L. Emmer, N. W. Hill, and J. B. Davidson, Instrumentation and Controls Ann. Prog. Rep. July 1, 1957, ORNL-2480, p 17.

In the present instrument the clock is a crystal-controlled oscillator operating at 4 Mc. Pulses from this oscillator can be gated on by the arrival of the photomultiplier pulse and gated off by the arrival of a neutron detector pulse. While the oscillator is on, pulses are being fed to an 11-stage binary "address" scaler. When the oscillator pulses are shut off by the detector pulse, the number of these pulses counted by the address scaler is a measure of the time of flight of the neutron. The number also designates the channel in the coincident-current ferrite core memory[3] in which a count is to be stored. The voltages representing the states of the address-scaler stages are combined in coincidence circuits and cause the memory driving circuits to be connected to the lines in the memory appropriate to this channel number. Upon a "read" command the number in binary form already in the channel is brought out of the memory and stored in the 16-stage "add-1" scaler. One count is added to this scaler, and on "write" the new number is returned to the memory. Sixteen microseconds is required to store a count after the arrival of a detector pulse. At the end of this memory storage cycle the clock pulses are again allowed to advance the address scaler until another detector pulse is received or until a "carry" pulse is obtained from the last stage. This carry pulse causes the oscillator to be shut off until the chopper opens again, giving another neutron burst and another light pulse.

The block diagram in Fig. 4 shows the main divisions of the instrument. The memory controls include the switches for selecting the mode of operation, for starting and stopping, clearing the memory, etc. There are five modes of operation: "Accumulate," "Static," "Test," "Complement," and "Punch."

"Accumulate" is the data-collecting mode. In this mode the time-of-flight control unit is used to accomplish two main functions: (1) The oscillator and its associated frequency dividers are turned on by the light pulse from the neutron chopper. This sends address advance pulses to the address scaler at a frequency determined by the channel width selected. (2) These address advance pulses are turned off by the neutron detector pulse arriving at one of the four detector inputs. The position of the "memory sections" switch indicates whether one, two, or four detectors are being used and determines the corresponding division of the memory.

It is frequently desirable to delay the start of the portion of the chopper cycle during which the analyzer is open to receive detector pulses. This delay is obtained by counting a predetermined number of the address advance pulses, using the address and delay scaler. The delay scaler consists of five stages which count the carry pulses from the 2^7 address stage.

---

[3]R. W. Schumann and J. P. McMahon, Rev. Sci. Instr. 27, 675–87 (1956).

The analyzer is able to store multiple counts per neutron burst as long as they do not occur within the 16-μsec memory storage cycle. After each storage the number in the address scaler must be corrected for the address pulses lost during the storage time. This is done by accurately setting the storage time at 16 μsec and by adding to the count in the address scaler after each storage a number equal to 16 divided by the channel width in microseconds.

"Static" is the display mode in which the data contained in the memory are brought out channel by channel at 10 kc and displayed on the oscilloscope. The display is accomplished by deriving voltages from the address and add-1 scalers which are proportional to the numbers contained in each. The address-scaler-derived voltage is used for the horizontal deflection, and the voltage from the add-1 scaler is used for the vertical deflection. The contents of the memory are thus continuously displayed in a series of horizontally and vertically displaced dots. By means of the vertical display switch and a base-2-to-base-8 converter the eight blocks of 256 channels may be observed one block at a time. Alternatively, the full 2048 channels may be viewed with eight channels allotted to each horizontal position. The vertical position of the individual channel is unchanged. For convenience in visual counting, alternate groups of eight channels are shown with the dots intensified.

The "Test" mode is similar to "Static Display." The contents of the memory are displayed at 10 kc. In "Test," however, unlike "Static" where the contents of the memory remain unchanged, one count is added to each channel in the process of displaying it. Hence, the content of the memory increases as in the "Accumulate" mode. The "Test" mode is, therefore, useful in checking the operation of the memory in the absence of photocell or detector inputs.

The "Complement" mode allows background subtraction and is also useful for testing the operation of the memory. By "Complement" is meant the changing of the binary number, N, such that $N = (2^{16} - 1) - C$. This is accomplished by bringing out, at a 10-kc rate, the number stored in a channel and putting it in the add-1 scaler. The states of each scaler stage are changed from "ones" to "zeros" and vice versa with the carrys between stages being prevented by raising the "carry bias." The number, N, is then written back into the memory.

On the "Punch" mode the information in the memory is called out channel by channel at an eight-channel-per-second rate, and the channel number and storage are punched on paper tape by a Teletype punch at the rate of 60 characters per second. A code word which indicates the switch positions on the time-of-flight control chassis, that is, the delay, the channel width, and the number of detectors, is automatically punched at the beginning of the tape.

The analyzer requires approximately 2000 w of power. All supplies are regulated within 0.1%, and, with the exception of the 300-v supply, employ transistors in the regulating circuitry. Avalanche diodes are used as reference elements and (in 10-w types) as protective devices for

the series regulator transistors. Large etched circuit boards and 21-conductor tape cable are used to advantage in organizing the memory circuitry and in distributing the address and add-1 scaler digits. The instrument is cooled by three fans mounted on top which pull air from the floor level through filters and over the circuitry.

The analyzer has been used successfully for five months with only minor adjustments after the initial checkout. Figure 5 shows the completed instrument. Figure 6 is a photograph of the oscilloscope presentation of a typical run.

The punch control unit was designed by C. H. Schalbe of the Computer Engineering Group.

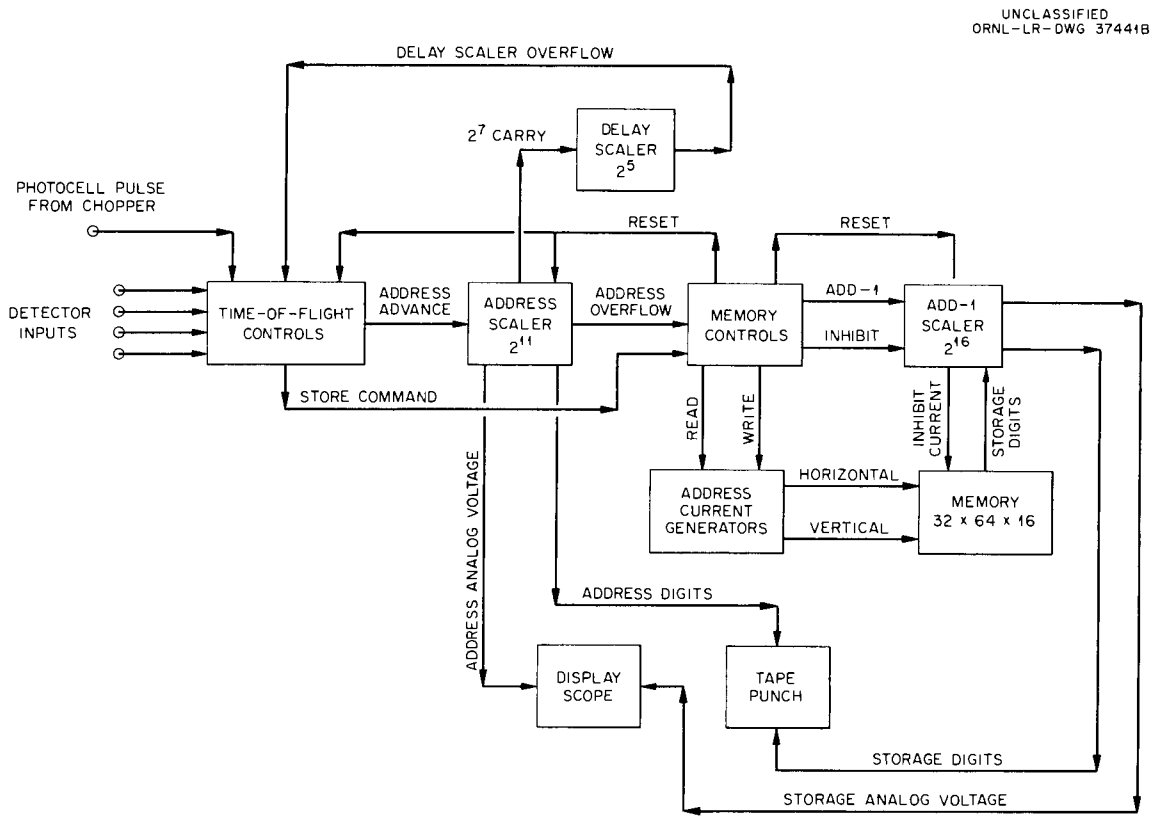

Fig. 4. Block Diagram of 2048-Channel Neutron Time-of-Flight Analyzer.

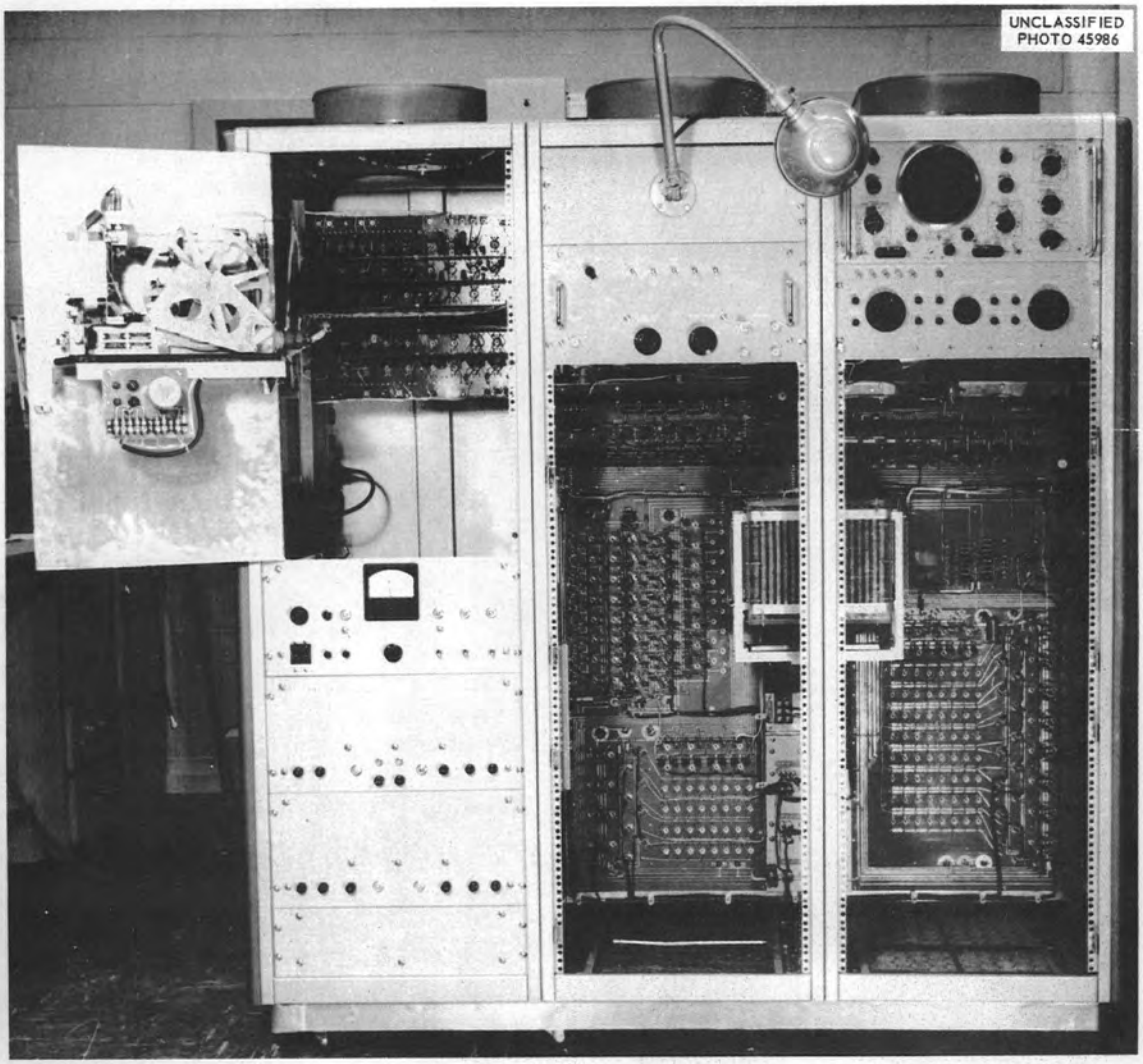

Fig. 5. 2048-Channel Neutron Time-of-Flight Analyzer.

UNCLASSIFIED
PHOTO 47754

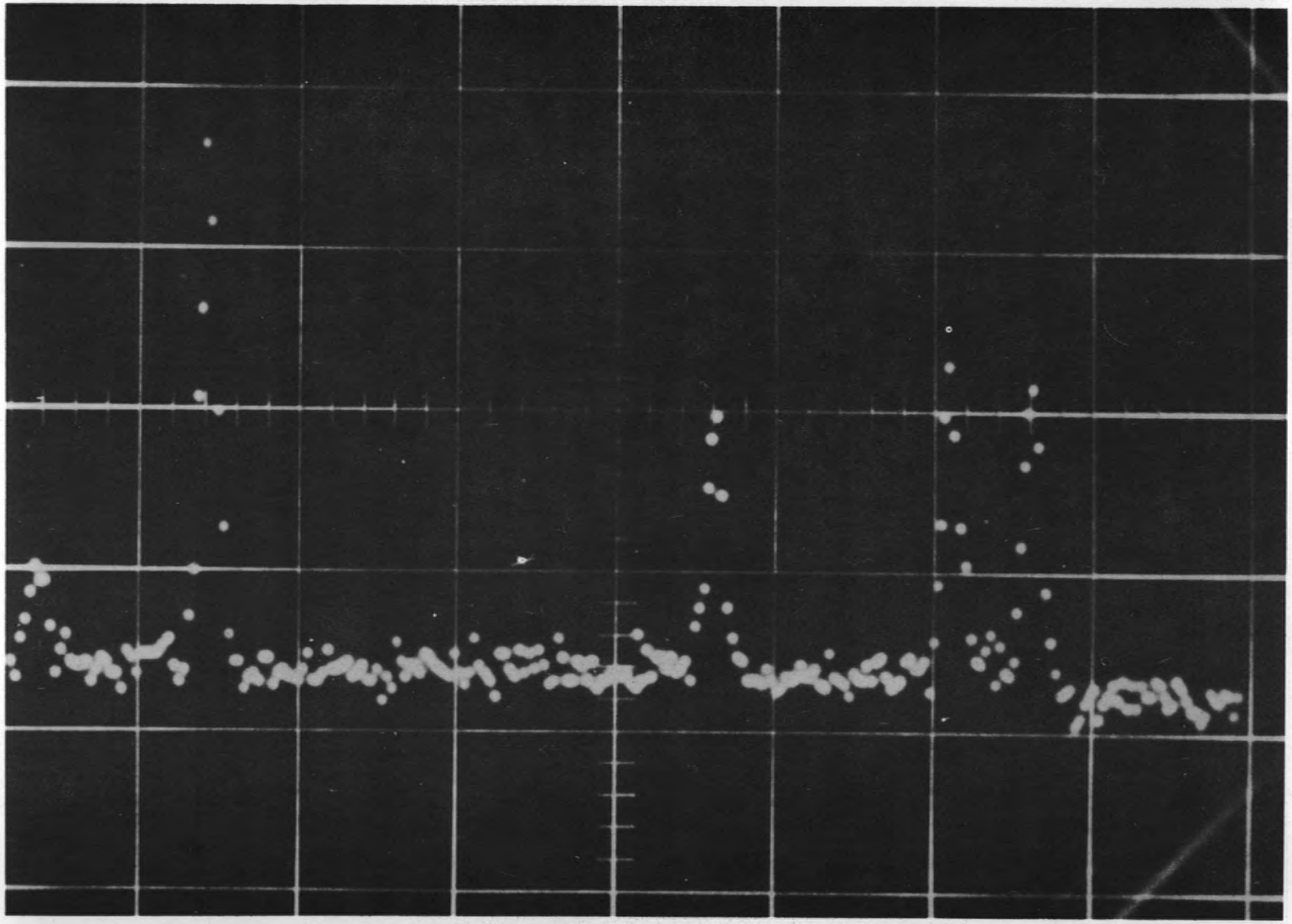

Fig. 6. Oscilloscope Display of Channels 256 to 512 Showing the Number of Neutrons Scattered from a 4-mil Silver Target. The energy range, from left to right, is approximately 180 to 40 ev.

FISSION FRAGMENT TIME-OF-FLIGHT SPECTROMETER

W. H. White, Jr.

A system for measurement of time of flight of fission fragments has been under development at ORNL. The daughter products of a fission event are collimated by two flight paths at 180° to each other. One flight path contains an energy-selecting magnet. The 4-m flight path provides a maximum expected time of flight of 500 mμsec for either daughter product. Both daughter products are to be timed, and the data will be presented on two 100-channel displays. The channel width is therefore 5 mμsec, which necessitates a system resolution of 3 mμsec or better.

In the system shown in Fig. 7 there are three detectors. An RCA 6810A photomultiplier is used to provide a zero time reference by detecting secondary electrons produced by interaction of one of the daughter products with a thin nickel plate. At the end of each flight path are RCA 7046 photomultipliers with thin plastic scintillators to detect the fission fragments.

A fast-slow system for analysis of fission events is used; that is, analysis is not started until a triple coincidence signal is provided through the slow-rise-time tenth dynode outputs from all three detectors. Noise rejection in the slow circuits is accomplished by using the pulse height selector outputs of the linear amplifiers.

The fast outputs from the anodes of the detectors are applied to time-to-pulse-height converter circuits. The time-to-pulse-height converters are similar to Neiler's circuit[1] and they operate in the following manner. The detector at the end of the flight path provides a fast rise pulse which is amplified, limited, and clipped and then applied to a diode stretcher. The stretched voltage is applied to the grid of a constant current tube, gating it on. The constant current tube begins charging the capacitance at the input of a linear amplifier. The arrival of the zero time pulse, which has been delayed by 600 mμsec, discharges the stretcher line and returns the constant current tube to cutoff. The integrated charge on the amplifier input capacitor determines the pulse height of the output pulse. The two time-proportional pulse heights are available for analysis by the time the slow coincidence signal has started the analyzers. The analyzers digitize the time signals in the following manner. The time-proportional pulse is stretched, and this voltage is then compared with a linear ramp voltage. The start of the analyzer and the ramp is provided by the coincidence signal, and the analyzer is stopped when the ramp reaches the time-proportional voltage of the stretched pulse.

The analyzer operates in a conventional manner: a 2-Mc oscillator is gated, divided, and counted using two decades of scalers for each channel. The scaler outputs are then printed out using conventional coded 1-2-2-4 outputs.

---

[1]J. H. Neiler *et al.*, Phys. Semiann. Prog. Rep. Sept. 10, 1955, ORNL-1975, p 66.

The fast outputs of all three detectors are coupled to the time-to-pulse-height circuits using Andrews type HO transmission cables. This cable was selected for its low attenuation at high frequencies, 1.6 db per 100 ft at 1000 Mc. Some sacrifice of signal is caused by the low (50-ohm) impedance of this cable, but the fast rise time which can be obtained is needed to provide good resolution. The two fragment detectors are coupled with 25-ft lengths to the time-to-pulse-height converters, and the 600-mμsec delay to the converters is accomplished by using 540 ft of this cable.

Because of the rather small solid angle subtended by the fragment detectors and the presence of the energy selection magnet, the counting rate of the system is low enough that the printer is satisfactory as a readout device. Data reduction is a problem, however, and the possibility of a Teletype paper punch which will provide data for computer reduction is being considered. A cathode-ray-tube—camera system for data presentation is also being considered. This will use X and Y deflection from the stretched time-proportional voltages. Intensity modulation from the triple coincidence circuits would allow photographic recording of each event.

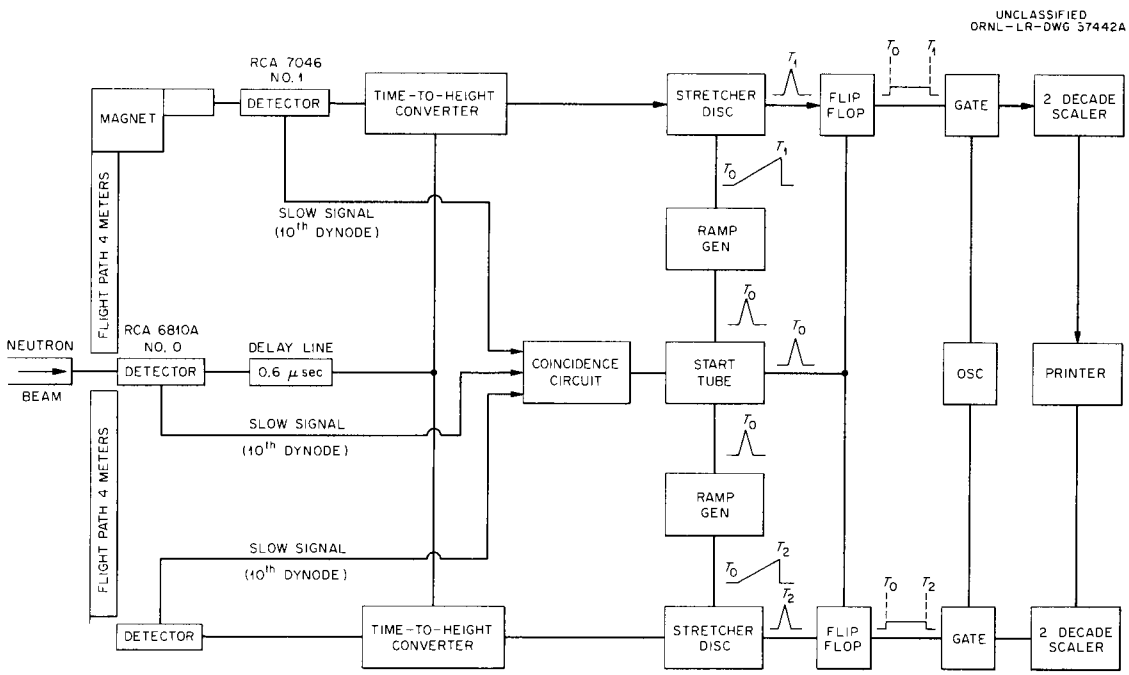

Fig. 7. Block Diagram of Fission Fragment Time-of-Flight Spectrometer.

SUPERHETERODYNE ELECTRON PARAMAGNETIC RESONANCE SPECTROMETER

J. L. Lovvorn

Introduction

The r-f generation part of a superheterodyne electron paramagnetic resonance spectrometer was designed for the Biology Division[1] utilizing commercially available 10-cm-band microwave components, 60-Mc i-f amplifiers, and d-c power supplies. The control panels, phase detector, and four-terminal d-c amplifiers were developed and fabricated. Frequency stabilization of the local oscillator is obtained by a conventional FM-type discriminator whose output is amplified and fed back to the local oscillator klystron reflector. The signal oscillator frequency is locked to the resonant frequency of the specimen cavity; thus automatic compensation is provided for the effects of paramagnetic dispersion.[2]

The output of the spectrometer is presented as a pattern on an oscilloscope of paramagnetic resonance absorption vs magnetic field. Provision is also made for presentation on a strip chart recorder as a graph of absorption vs magnetic field or the derivative of the absorption vs magnetic field.

Description

Microwave Components. — The microwave components are shown on Fig. 8. Care was taken that the attenuators should be of a type that gives minimum leakage of r-f energy from the wave guide. One high-quality calibrated attenuator with extremely small phase shift was obtained so that the power could be varied without upsetting the phase balance of the system. Ferrite load isolators were employed to prevent loading variations from affecting the klystron operation.

The signal oscillator feeds into the magic tee, where its power is split between arms 2 and 3. Arm 2 contains the reflection cavity with the sample, the reflected wave being bucked out with the aid of arm 3. For this purpose arm 3 has a phase shifter and attenuator. The desired signal appears in arm 4 and is fed into the balanced mixer, which receives the local oscillator power from the frequency-stabilized oscillator. The reflection cavity has modulation coils built in the walls. The output of the balanced mixer is fed through the i-f amplifier-detector to the oscilloscope.

---

[1] J. L. Lovvorn, Instrumentation and Controls Ann. Prog. Rep. July 1, 1957, ORNL-2480, p 28-30.

[2] J. M. Hirshon and G. K. Fraenkel, Rev. Sci. Instr. 26, 34 (1955).

Electronic Panels. — By using Varian low-voltage klystrons, a commercial laboratory power supply with a bias supply built in was employed as the klystron power supply. The filament supplies for the klystrons and the i-f amplifier were regulated by using semiconductors. Figure 9 shows a typical regulator circuit.

The control panel provides means for controlling the gain of the i-f amplifiers, monitoring the mixer crystal currents, and balancing the output of the lock-in mixer to ground for feeding the four-terminal d-c amplifier. The four-terminal d-c amplifier is a semiconductor modulated-carrier type[3] shown in Fig. 10. It employs a matched diode quad chopper excited by a transistor oscillator. The presence of an error signal from the receiver discriminator unbalances the net to pass the error signal to the transistor amplifier. The sign of the error signal determines whether the unbalance signal will be positive or negative phase. The error signal is amplified in a two-stage transistor amplifier. This amplified error signal is fed to the transistor phase discriminator. The transistors are used on a half-wave basis. The two transistors are powered, collector to emitter, on alternate half cycles at the carrier frequency from the transistor carrier oscillator. The amplified error signal gates the two transistors, base to emitter, on alternate half cycles. One or the other of the transistors will conduct, depending upon the error signal phase. The conduction current flows through the common load resistor, with the direction of the current in the load reversing for a reversal of signal phase. The entire circuit is isolated from ground potential. This permits inserting the output of the automatic frequency control (AFC) amplifier in series with the reflector supply to add or subtract the necessary correction voltage.

The equipment is in the final stages of checkout. Although no frequency checks have been made, the frequency control loop has been designed to keep the local oscillator in tune to an accuracy better than ±0.3 Mc at the receiver i-f regardless of transmitter and receiver drift.[3]

Two of the 60-Mc center frequency i-f amplifiers are commercial units selected for this application. One has 120-db gain with an amplitude detector in the output. The second has an FM-type discriminator in the output. These units were modified to provide a 60-Mc takeout point in each to feed additional amplifier stages for a lock-in-mixer-type phase detector.

Provision is made for disabling the AFC in testing, for modulating the signal oscillator and for metering the error signal. Care in layout and shielding were required to prevent carrier signal and 60-Mc signal leakage.

Although equipment shakedown tests have not been completed so as to allow complete evaluation, it is expected that the superheterodyne electron paramagnetic resonance spectrometer will have a sensitivity approaching 10^{13} spins with 1-diphenyl-2-picrylhydrazyl.

---

[3]M. C. Harp, Electronics 32, 68–70 (1959).

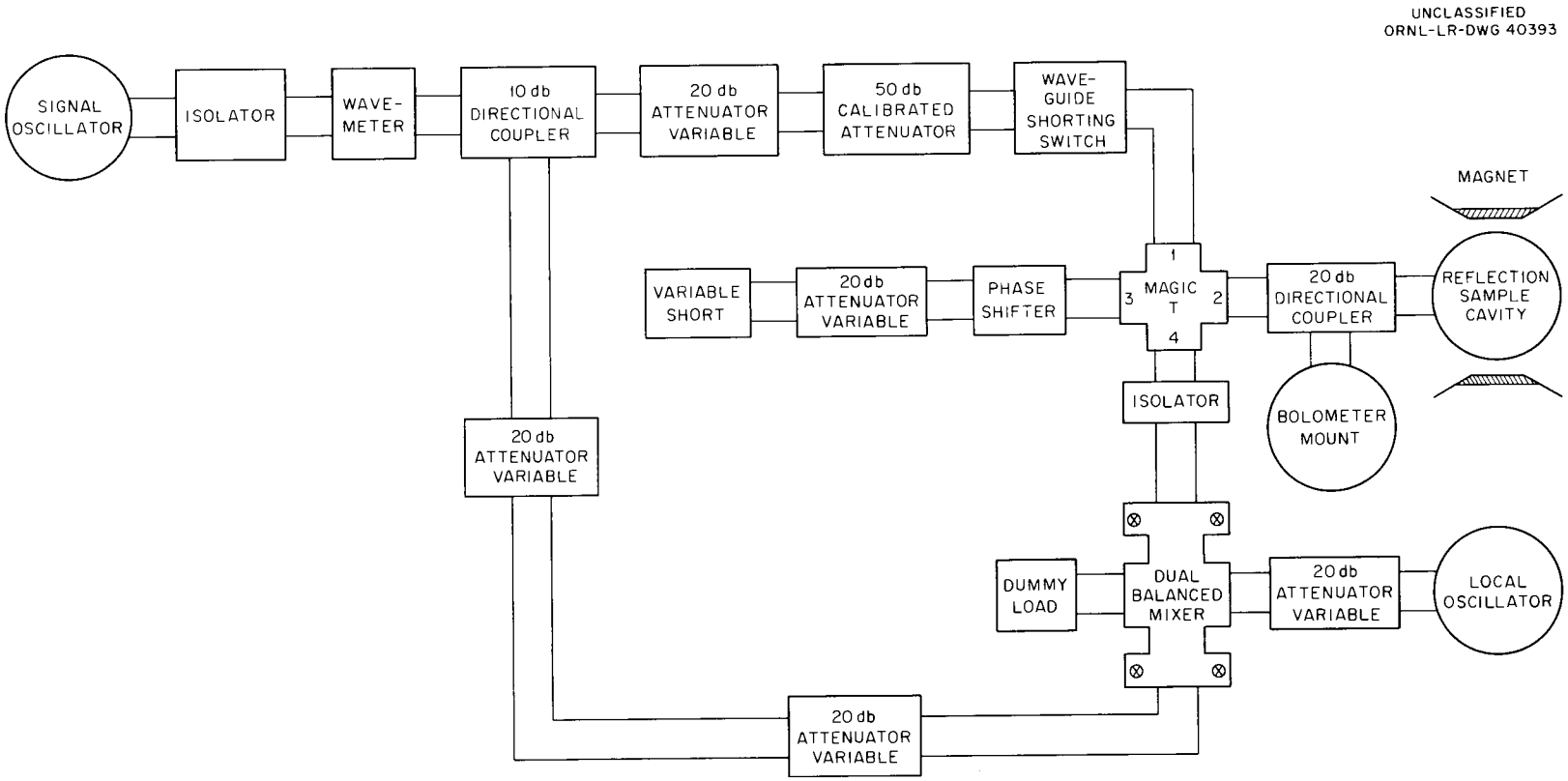

Fig. 8. Block Diagram.

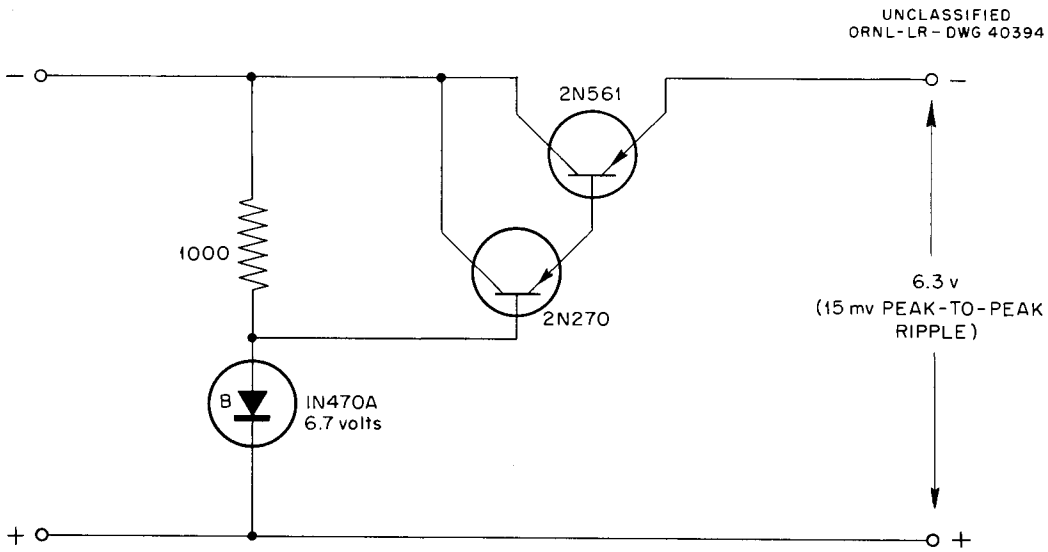

Fig. 9. Typical D-C Filament Regulator Circuit.

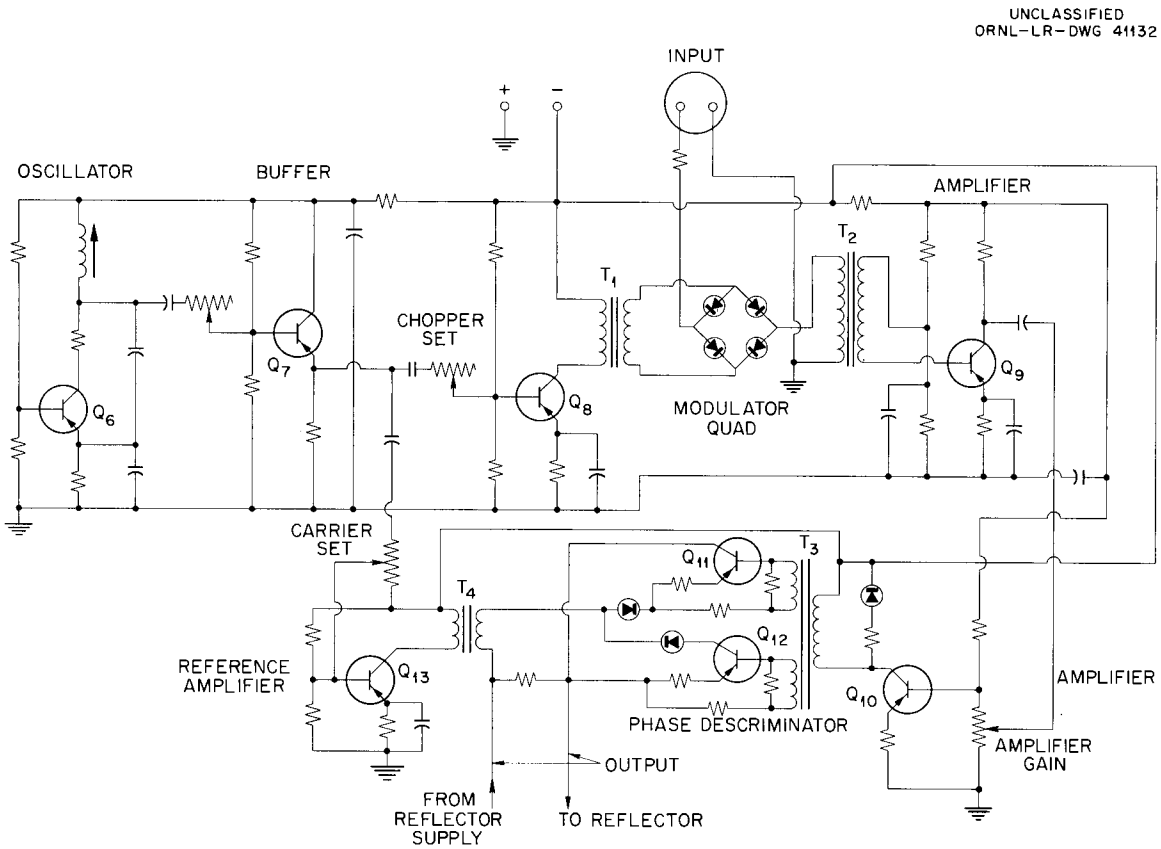

Fig. 10. Four-Terminal Carrier D-C Amplifier.

15 **Fig. 10** Line joining bottom of "carrier set" potentiometer to top of T_4 bus line should be deleted

A VERSATILE INSTRUMENT CAMERA WITH A MICROSECOND ELECTRONIC SHUTTER

C. H. Schalbe

Introduction

The camera to be described was developed for the study of high-current, low-pressure arcs such as are encountered in controlled nuclear fusion experiments. This type of arc is characterized by a relatively low level of energy output in the visible region and by the presence of strong magnetic fields. Because of these factors, and because exposures in the microsecond range were desired, mechanical shutters and cameras using Kerr cells were not feasible.

Within the limitations outlined above, an attempt was made to produce as versatile an instrument as possible. In general, the problem was to design a medium-speed camera adapted for nonlaboratory environments. The operating parameters had to be easily adjusted over a fairly wide range, and mobility was important.

Description of Camera

The camera constructed to satisfy these requirements uses an image converter tube which provides high-speed shutter action and also light amplification under the proper operating conditions. Figure 11 is a view and representative diagram of this tube, which is manufactured on a developmental basis by Radio Corporation of America. It features a semitransparent photocathode (S11), a control grid for gating the electron beam, an electrostatic lens system, and a pair of deflection plates for positioning a series of time-sequential images side by side on the phosphor screen (P11). Exposures as short as 10^{-8} sec are possible, and, with an incident light of about 4400 Å and an accelerating potential of 15,000 v, a conversion gain of 12 minimum is obtained.

A simplified block diagram of the electronic control is shown in Fig. 12. Timing pulses for exposures and for the interval between exposures are generated by two phantastrons. Controls on the operating panel permit selection of exposure times from 0.6 to 100 μsec and intervals between successive exposures from 1 to 1000 μsec. A three-stage counter is used to properly sequence the selected number (either 1, 2, 4, or 8) of images and also to position these images in steps vertically down the phosphor screen. Vacuum tubes rather than thyratrons were used throughout because of their advantages in making a flexible system.

Exposures are obtained by application of a 300-v pulse to the cathode of the image converter tube, which is normally cut off by a bias of 100 v. Since the image will be in focus at only one particular voltage configuration, the shutter pulse must be flat-topped and rise and fall rapidly. Figure 13 is a schematic diagram of the screen-coupled positive-feedback circuit devised to obtain the desired pulse. This circuit generates a pulse which has a total rise and fall time of 0.45 μsec, and it is flat-topped to within 0.5%.

Photographs of the phosphor screen are taken with a 35-mm oscilloscope camera using Linagraph ortho film, which has a maximum sensitivity in the blue region. A 50-mm f/1.5 lens and a 50-mm f/1.0 lens are available for use with this camera. The film transport and shutter are electrically operated, and both single-frame and continuous film movement types of operation can be performed.

Camera Performance

Figures 14 and 15 are views of the electronic camera. The large rack houses all the d-c power supplies and regulators and also the power control panel. The camera head is mounted on a standard black-and-white television camera tripod and dolly. The front lens on the camera head is a 180-mm f/1.5 lens. Three other lenses are available: an f/0.8 50-mm lens, an f/1.5 90-mm lens, and an f/2.5 310-mm lens.

Figure 16 is a reproduction of a photograph taken with the image converter camera. It is a view of a d-c arc taken in a series of 2.5-μsec exposures with an interval between exposures of 3 μsec. The voltage of the arc was 7 kv and it occurred in air at a pressure of about 90 mm Hg. The frontal lens used to take this picture was the 180-mm f/1.5 lens stopped down to f/8.0.

The performance characteristics of the camera are as follows:

Exposure time	0.6 to 100 μsec
Exposure spacing	1.0 to 1000 μsec
Number of exposures	1, 2, 4, or 8
Frontal lenses	50 mm f/0.8, 90 mm f/1.5, 180 mm f/1.5, 310 mm f/2.5
Rear lenses	50 mm f/1.0, 50 mm f/1.5
Synchronization	External trigger or local control
Conversion gain (measured)	Approximately 10 at 13 kv anode voltage using photospot PSP2 as the light source

UNCLASSIFIED
PHOTO 46425

UNCLASSIFIED
ORNL-LR-DWG. 37513

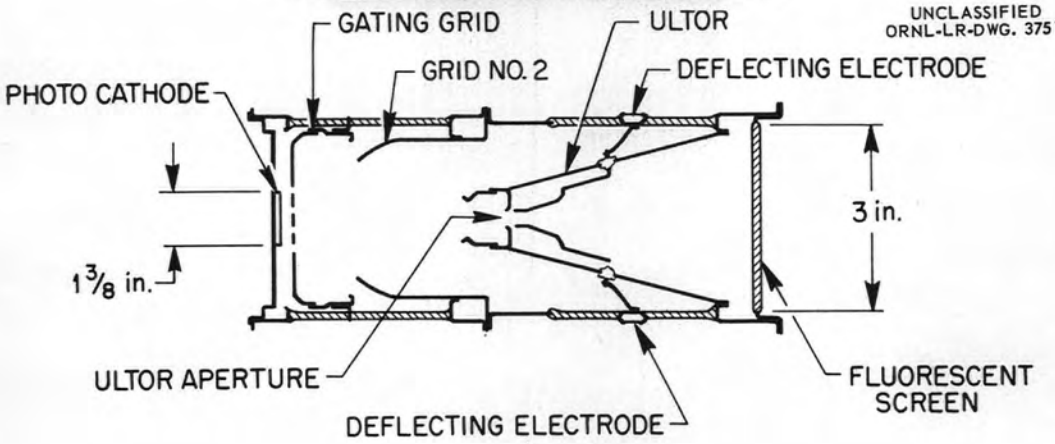

Fig. 11. Image Converter Tube, RCA C73435B.

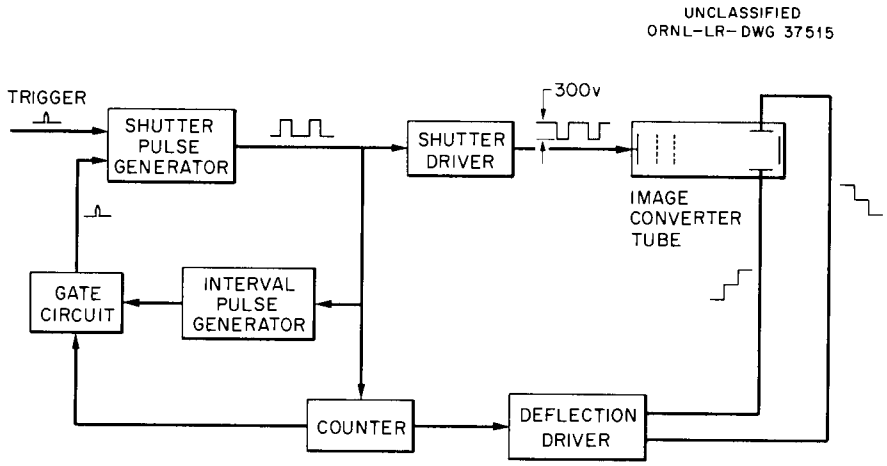

Fig. 12. Block Diagram of Camera.

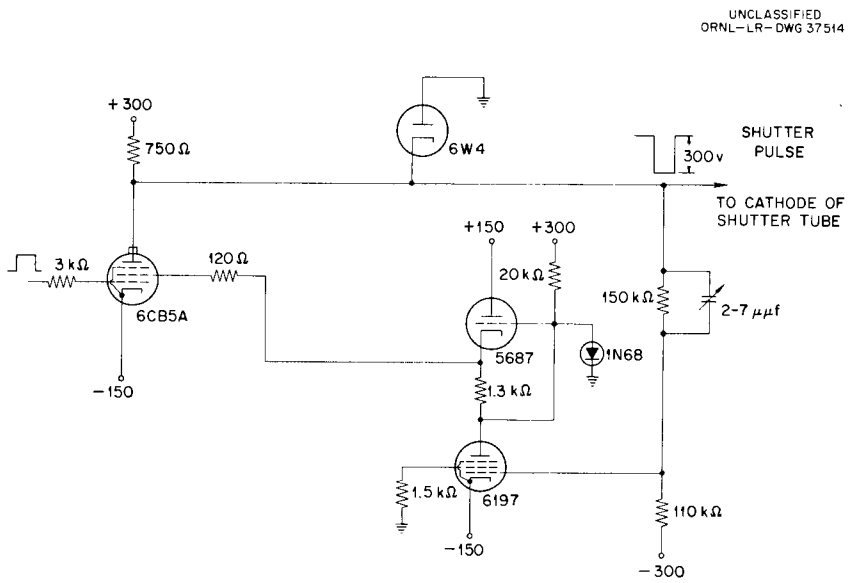

Fig. 13. Circuit of Shutter Driver.

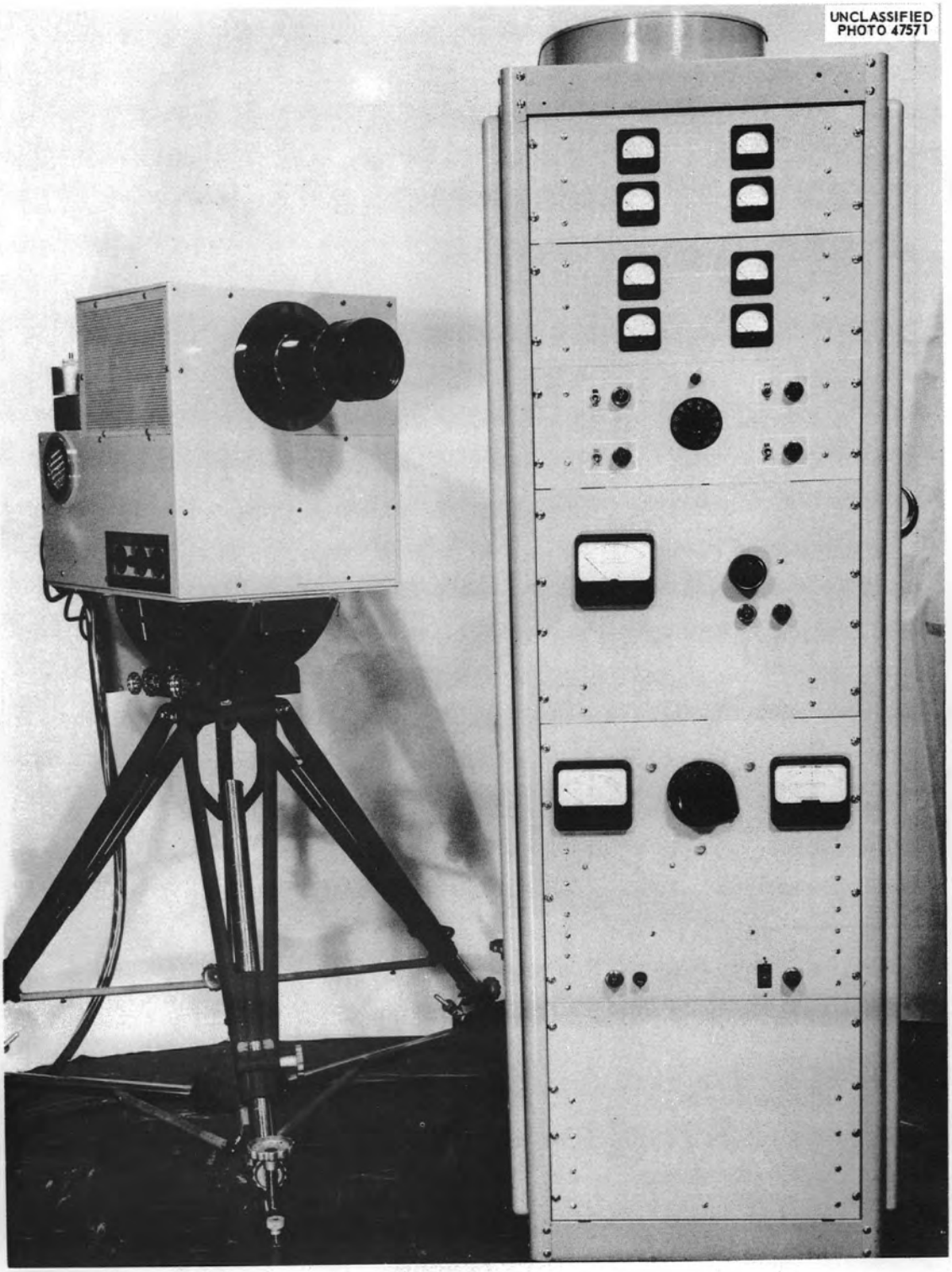

Fig. 14. Electronic Camera with Associated Components.

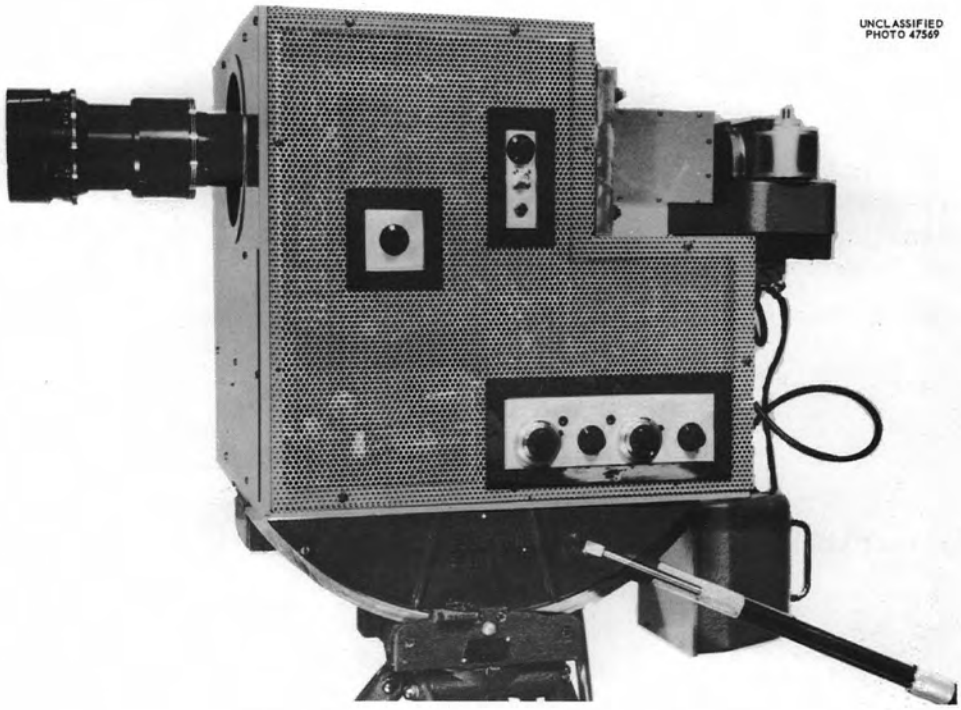

Fig. 15. Closeup View of Camera Head.

UNCLASSIFIED
PHOTO 47422

Fig. 16. Arc Discharge at 6.5 mm Hg Pressure. Exposure time, 2.5 μsec; exposure interval, 3.0 μsec.

SCALER RATE METER Q-1743-13

H. N. Wilson F. M. Glass
B. C. Behr G. A. Holt

A combination decade scaler and linear count-rate meter with a positive high-voltage supply has been developed for use at health physics monitoring stations. The instrument is for use with G-M tubes or alpha scintillation detectors.

Specifications for the meter are as follows:

Input sensitivity	40-mv negative pulse
Scaler	Scale of 100 composed of two glow-tube decades and a four-digit Sodeco mechanical register with electrical reset
Scaler resolving time	12 μsec
Rate meter	Linear duty cycle type with ranges of 500, 5000, and 50,000 counts/min
Aural monitor	Variable volume "poppy" for use with low-count-rate alpha monitoring
High-voltage supply	Positive shunt-regulated supply continuously variable from 700 to 1700 v
Recorder outputs	Both 10-mv and 1-ma outputs from the rate meter for recorders
Panel size	7 × 19 in. – suitable for rack mounting

This combination instrument is an outgrowth of the original Q-1743A-1 decade scaler which was designed on a semimodular construction basis. This type of construction permits the easy alternations of modules to include the features desired. The original Schmitt trigger input and coupling stage has been replaced with a two-stage cathode-coupled dual-triode amplifier and a trigger pair which acts as a discriminator and pulse shaper. The fast input decade of the original circuit, composed of a beam switching tube and its associated drive circuit, has been removed as it is of no value for Geiger counting or low-level alpha counting. In its place physically has been substituted the shunt regulator circuit of the high-voltage supply. The original Veeder-Root register and drive circuit have been replaced with a Sodeco four-digit register with electrical reset and a simplified drive circuit. This change was made to conserve space and for ease of operation. The rate-meter module has been added, and the circuit used is basically the same as in instruments Q-1951 and Q-1957, which are count-rate meters for area monitoring.[1] Recorder outputs

---

[1]F. M. Glass, Instrumentation and Controls Ann. Prog. Rep. July 1, 1958, ORNL-2647, p 2.

have been made available so that the instrument may perform the function of a background monitor when not being used for other purposes. Also, the aural output has been included to act as an aid in monitoring for alpha contamination.

Most of the circuitry consists of conventional vacuum tube elements; however, there are a few pertinent design features that will be mentioned. The input amplifier section, being of the dual-triode, cathode-coupled design, handles negative signals only and can gracefully handle large signals, such as those from halogen G-M tubes, without double pulsing. A differentiation and clipper network is placed between the two amplifier stages so that the output pulse is back to the base line in about 3 μsec for small signals, and for a 10-v input signal the pulse width spreads to only about 6 μsec. Thus in the case of G-M tubes, the recovery time of the detector itself becomes the limiting factor. The rate-meter section is composed of a trigger pair having a stable output pulse width and a biased-off pentode stage. The pentode stage operates between B- and ground, so that the meter and 10-mv recorder output signal are essentially at ground potential. With this circuit there is no need for a zero adjustment since a tube with good cutoff characteristics was selected. A recorder driver circuit was necessary to give the 1-ma recorder output, but the input voltage sensitivity of the circuit is approximately 2 v, so that the zero stability is good. The high-voltage supply has a 6842 shunt regulator. The cathode is tied to the +155-v regulated supply as a reference, and the screen is supplied by the +270-v regulated supply. This simple regulator circuit is quite adequate for Geiger counting and alpha scintillation counting.

A block diagram of the instrument is shown in Fig. 17, and a photograph in Fig. 18.

UNCLASSIFIED
ORNL-LR-DWG 40395

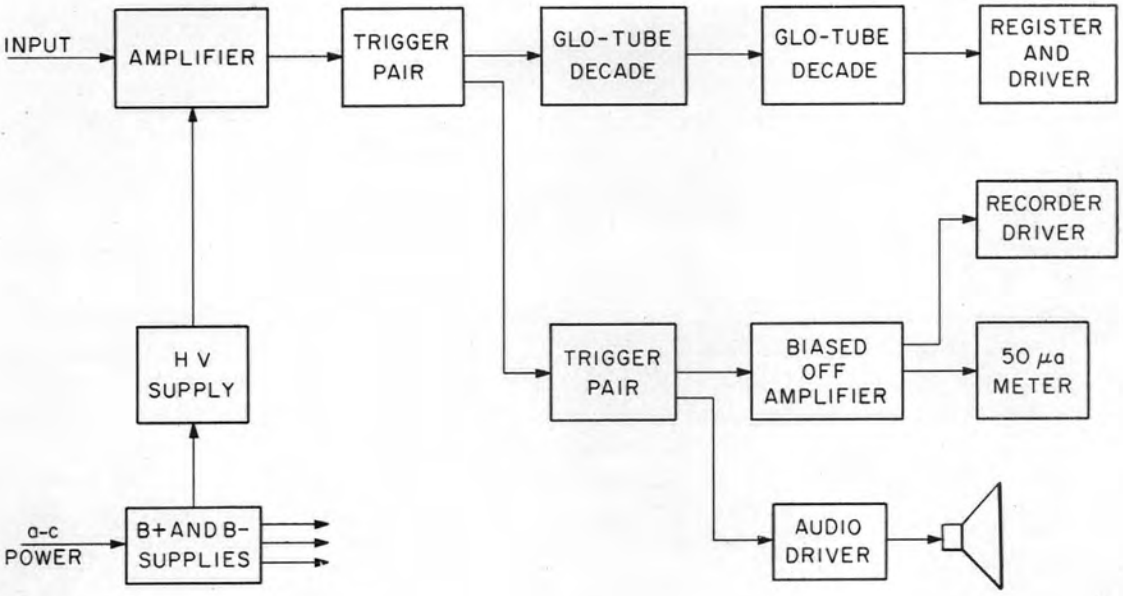

Fig. 17. Block Diagram of Scaler Rate Meter.

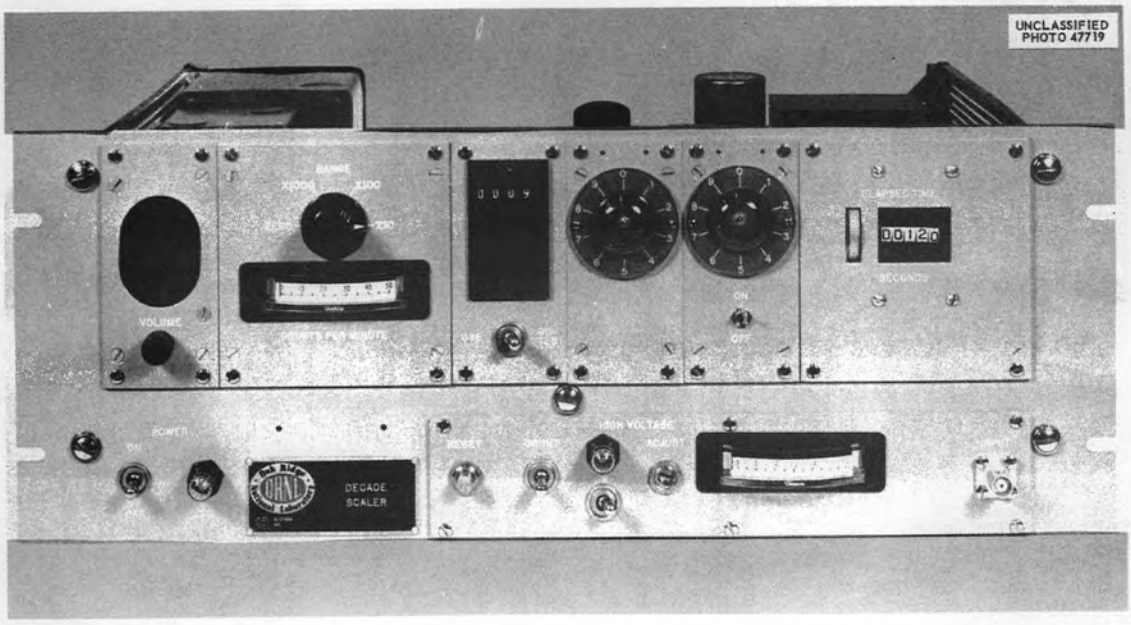

Fig. 18. Front View of Scaler Rate Meter.

FAST NEUTRON DOSE INTEGRATOR

J. T. DeLorenzo

Introduction

An a-c—powered fast neutron dosimeter, using vacuum tubes, has been designed to measure and indicate directly the dose rate (in millirads per hour) received from fast neutrons in the presence of gamma radiation. The accuracy of the instrument is within ±5% of the tissue-absorbed dose over the energy range 0.5 to 14 Mev.

The design of the dosimeter is based on the early concepts of the ORNL Health Physics Division[1–3] in cooperation with Instrumentation and Controls Division personnel. These concepts led to the construction of an accurate direct-reading instrument which would measure the tissue dose (energy per gram of tissue) of fast neutrons in the presence of gamma radiation. This instrument was reported in 1958.[4]

The instrument (Q-1995) reported here represents a transition from an experimental instrument to one which can be constructed and maintained with a minimum of effort. The basic changes incorporated over the original instrument are as follows:

1. The gating of the counting circuits with mechanical timers has been replaced with an electronic timer controlled from a stable R-C multivibrator with five decade glow tubes for countdown.
2. The r-f high-voltage supply has been replaced with one of more conventional design employing shunt regulation.
3. The manually reset register has been replaced with one that is electrically reset, thereby permitting a complete reset operation with one push button.
4. The vacuum tube rectifiers have been replaced with silicon rectifiers.
5. The binary pulse integration has been simplified, permitting the use of fewer tubes. Also, solid-state diodes are used to drive the various binary stages.
6. The signal-to-noise ratio of the amplifier section has been improved by making a direct connection to the detector signal electrode and by using a cascode input stage in the preamplifier.

---

[1] G. S. Hurst, R. H. Ritchie, and H. N. Wilson, Rev. Sci. Instr. 22, 981–86 (1951).

[2] F. M. Glass and G. S. Hurst, Rev. Sci. Instr. 23, 67–72 (1952).

[3] G. S. Hurst and R. H. Ritchie, Radiology 60, 864–68 (1953).

[4] E. B. Wagner and G. S. Hurst, Rev. Sci. Instr. 29, 153–58 (1958).

Description

General. – The main instrument (Fig. 19) is contained on two 17 × 13 × 2 1/2 in. chassis with 7 × 19 and 5 1/4 × 19 in. panels. Both chassis are mounted in a cabinet with over-all dimensions of 21 3/4 in. width, 18 in. depth, and 14 5/8 in. height. The cabinet is supplied with side-mounted, collapsible handles. The over-all weight of the instrument in the cabinet is approximately 75 lb.

The upper chassis contains all the power supplies and the decade scaler. The lower chassis contains the main amplifier, binary integrator, and glow-tube timer and gate circuits.

The preamplifier chassis is shock-mounted and is contained within a 3 3/8-in.-dia × 7 1/2-in.-long anodized aluminum case. The detector is attached to the case by four of its flange screws (elongated). The preamplifier can be connected to the main unit with any cable length up to 75 ft.

Power requirements for the entire unit are 115 ± 10 v, 60 ± 5 cps, 195 w, and 1.7 amp. The operating temperature limits are 0 to 122°F.

Circuit. – Reference is made to Fig. 20, which is a block diagram of the over-all instrument. The detector is a proportional counter of special design which conforms to the Bragg-Gray principle. Construction details and performance characteristics can be found in the literature cited earlier. The detector has a self-contained Pu^{239} source which is used to calibrate the instrument.

The detector pulses are amplified by a preamplifier mounted on the counter and a main amplifier. The preamplifier is characterized by a cascode input stage for low noise and has an over-all gain of about 6. The main amplifier consists of three feedback sections, one section occurring before the differentiator. This section, with a gain of about 6, gives a total gain of about 36 before differentiation. The amplifier is designed for a 1.5-μsec clipping time constant. Single R-C clipping is employed. The amplifier is essentially linear to about 90 v.

The measurement of neutron dose requires an integration of the amplitude of the pulses produced by the recoil atoms. Upon amplification, these pulses are fed into a four-stage binary integrator which gives an output pulse rate proportional to dose rate. Details of operation of this unique circuitry are given in the earlier references. The count rate is determined by gating the integrator to count for a specified time. The count is indicated on a decade scaler. The timing interval is measured with an electronic timer employing a stable R-C multivibrator and five decade glow tubes for countdown.

When the unit is properly calibrated, the dose rate (in millirads per hour) is indicated directly on the decade scaler upon counting for specific time intervals. Three timing intervals are provided – short, medium, and long. The medium interval is a factor of 10 longer than the short, and the long interval is a factor of 10 longer than the medium interval. A decimal light is changed with the timing interval. A manual

count position and an elapsed-time indicator are available for manual operation. The elapsed-time indicator is also useful for a check of the electronic timer.

The various power supplies include a well-regulated +260-v supply, a VR-tube-regulated -150-v supply, a well-regulated high-voltage supply (adjustable from 1800 to 2400 v), a 6-v solenoid supply (for shutter control on Pu^{239} source), and a +460-v supply for the decade glow tubes.

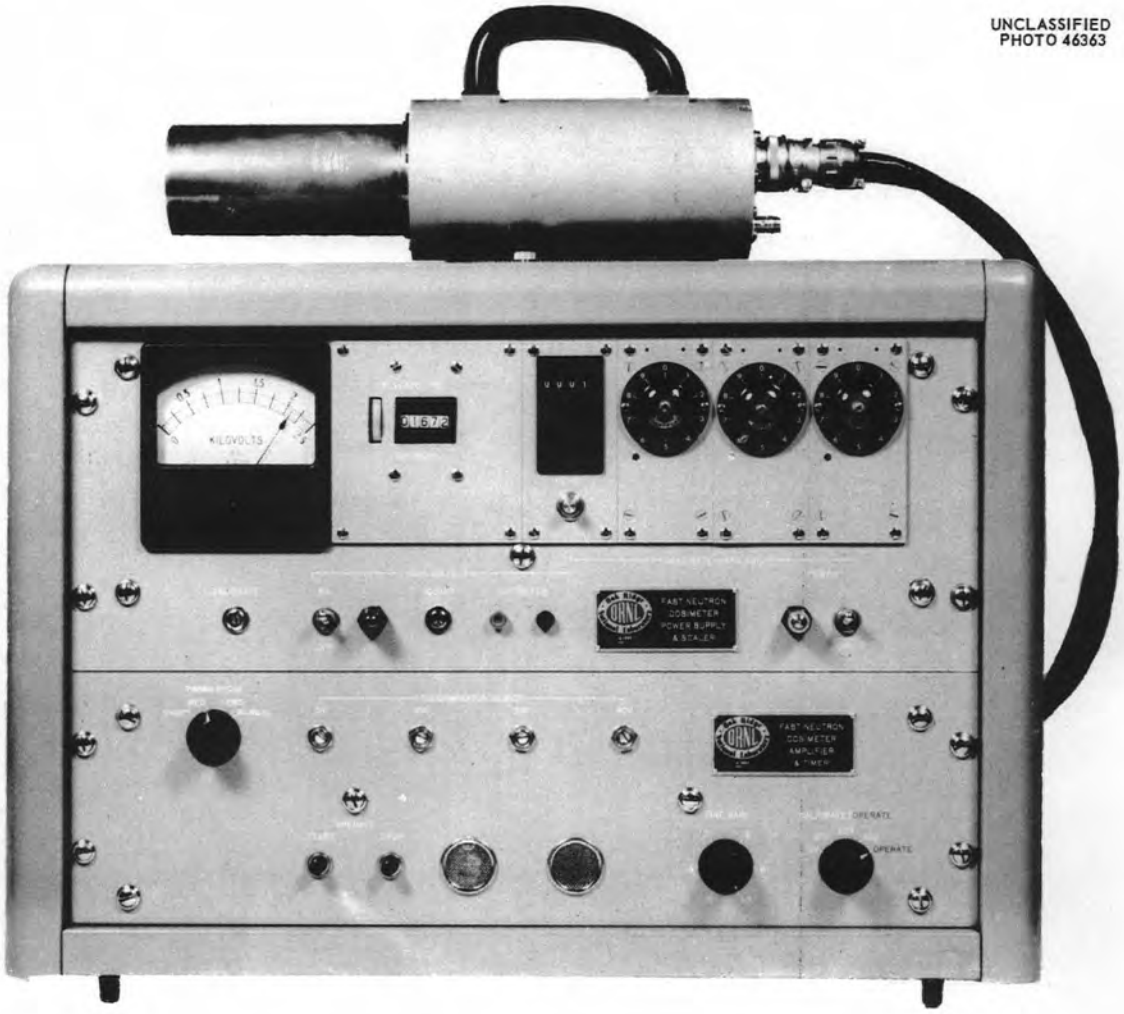

Fig. 19. Front View of Fast Neutron Dosimeter, with Detector and Preamplifier on Top.

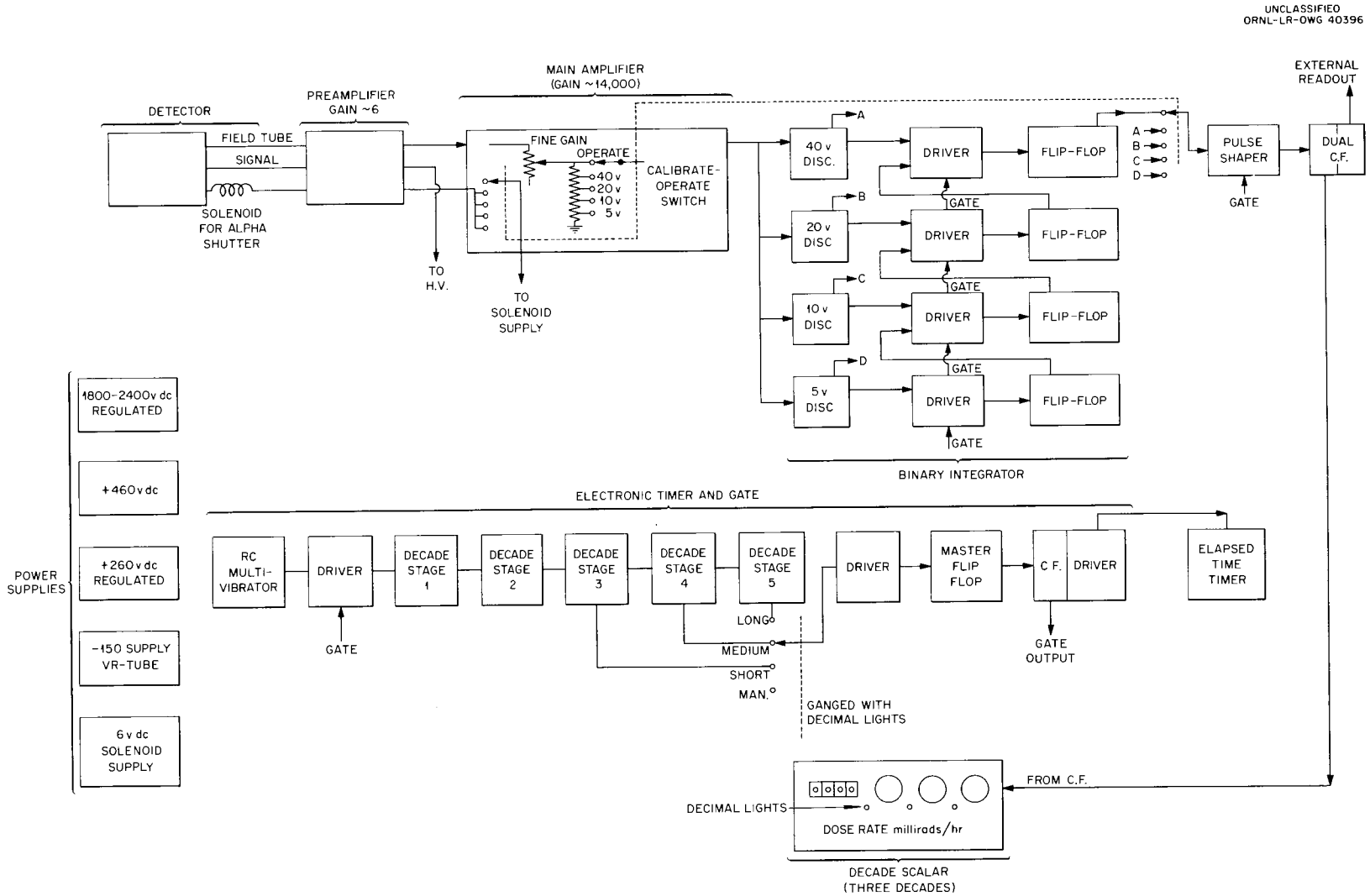

Fig. 20. Block Diagram of Fast Neutron Dosimeter Q-1995.

A TRANSISTORIZED DATA TAPE PUNCH FOR ELECTRONIC SCALING EQUIPMENT

J. W. Woody, Jr.

As was mentioned previously,[1] data handling and processing is becoming a problem of rather large proportions at ORNL. In view of the fact that the Oracle is available for work of this type, interest has been growing in instruments which reduce data directly into a form compatible with the Oracle input. The instrument discussed here falls into this category.

The EPUT meter punch (Q-2016C) is a completely transistorized device which takes the digital outputs from a Berkeley "events-per-unit-time" (EPUT) meter (model 7360) and automatically produces a punched paper tape while the experiment is in progress. This tape is in Oracle format and can be fed into the computer directly.

Although this unit (see Figs. 21 and 22) was designed to be used with the above-mentioned EPUT meter, it can be used with a wide variety of electronic scaling equipment, provided slight modifications are made.

The EPUT meter punch consists of the following:

1. A printed circuit input gating matrix (composed of transistors and diodes) for sequentially selecting the digital outputs from the six decimal counting units in the EPUT meter.
2. A transistorized control section to perform the operations required to select and punch in proper synchronism the above-mentioned outputs.
3. A motor-driven paper tape punch, which is a modified Teletype BRPE type (seven channels plus sprocket) with a magnetic pickup for synchronizing the punch cycle with the EPUT meter. Printed circuit, transistor drivers are provided to drive the punch solenoids.
4. A transistor-regulated power supply providing three voltages (+12 v, -12 v, and -30 v) each capable of delivering more than 500 ma.

These are all housed in a standard 17 × 13 × 3 in. rack mount chassis with a 14-in. front panel.

The control section performs the logical functions as indicated above, and is composed mainly of commercially available plug-in transistor packages manufactured by Engineered Electronics Company. These packages are approximately the size of a nine-pin miniature tube and plug into a standard noval socket.

The maximum punching speed of this particular unit is 30 decimal characters per second. However, with modification, a speed of 60 characters per second can be obtained.

---

[1]J. W. Woody, Jr., Instrumentation and Controls Ann. Prog. Rep. July 1, 1958, ORNL-2647, p 7.

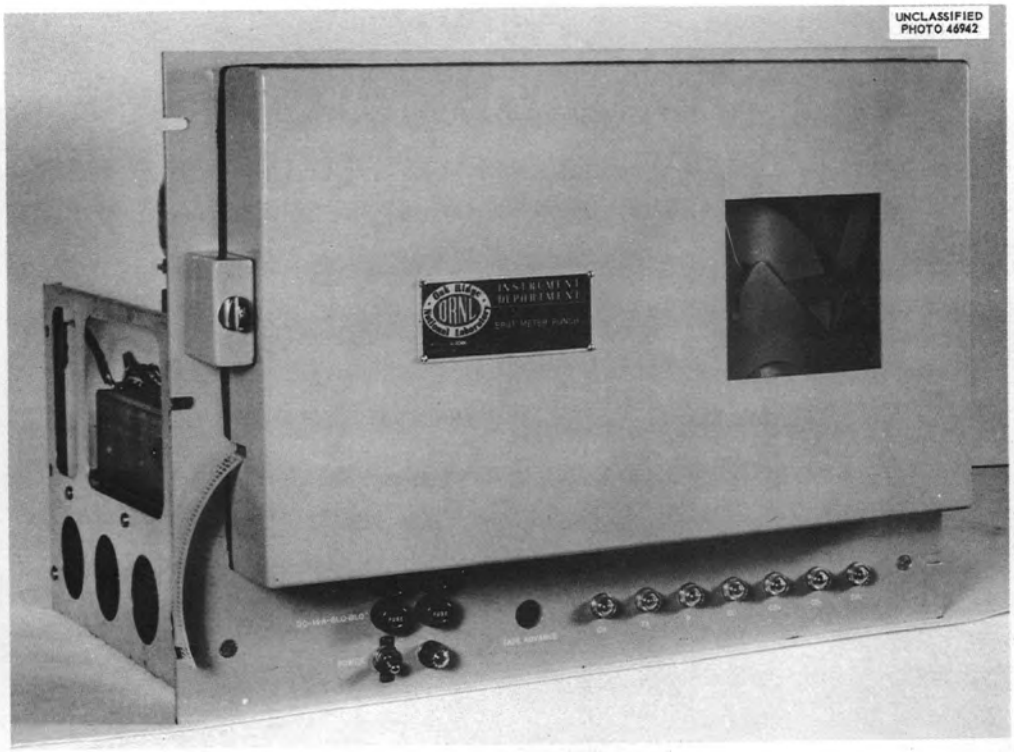

Fig. 21. EPUT Meter Punch.

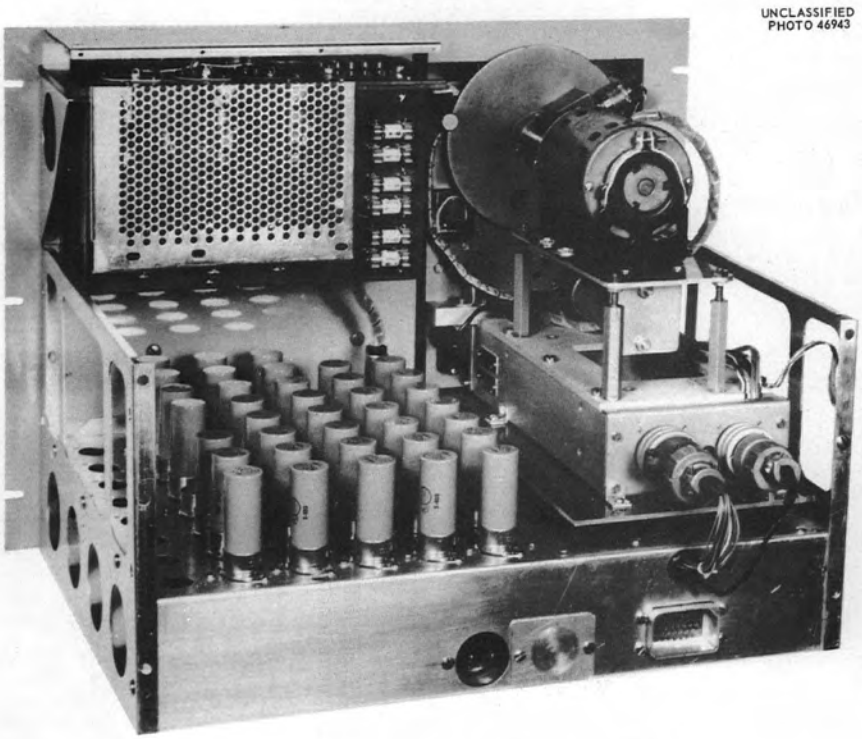

Fig. 22. Rear View of EPUT Meter Punch.

TRANSISTORIZED PULSE PREAMPLIFIER Q-2032-1 RO

F. M. Glass

A preamplifier was designed to be used with A-1 pulse amplifiers where extremely long cable runs present a problem. One of the attractive features of this preamplifier is its low power requirement, which is less than 100 mw. Therefore, the d-c power can easily be transmitted over the same terminated cable that serves as the pulse transmission line.

The input stage consists of a 3N35 emitter follower directly coupled to a 2N384 emitter follower (see Fig. 23). The 3N35 is a silicon UHF tetrode having an alpha cutoff of 150 Mc and a high beta at very low collector currents. The 2N384 is a germanium p-n-p having an alpha cutoff of 100 Mc. By using this combination with the lowest possible collector current that will maintain the minimum permissible bandwidth, the noise figure of this preamplifier has been made comparable to that of a good pentode such as the 6AK5 or 5654. Direct-current feedback from the second collector to the first emitter also improves the noise figure by regulating the collector voltage at or near the optimum value. The input impedance to this stage averages 750 kilohms and the output impedance averages 65 ohms.

The input stage is followed by a feed-back pair consisting of a 2N247 and another 3N35 having a loop voltage gain of 36. Approximately 40 db of feedback results in good gain stability, an input impedance of 10 kilohms, and an output impedance of approximately 65 ohms. The trimmer in the feedback network makes it possible to adjust for the fastest rise time obtainable without ringing as a result of phase lag. This adjustment, however, does not make it possible to use transistors having alpha cutoffs below 10 Mc. No amount of compensation will prevent oscillation when this much feedback is employed if the alpha cutoff is too low. A second feed-back loop to the input base passes dc only and serves as a means of stabilizing the collector current in both transistors.

A single 2N247 emitter follower drives the 75-ohm terminate cable. The input impedance with the 75-ohm line attached is approximately 4000 ohms with the average 2N247, and the output impedance is about 8 ohms.

The 3N35 is used as a triode in order to obtain a better noise figure. By eliminating the extra base current it is possible to obtain equivalent noise resistances as low as 100 ohms. However, one must also resort to starved current operation, thereby sacrificing bandwidth in order to reduce the noise to this low level. The input stage of this amplifier is a compromise design, as the specifications will indicate:

Power requirements	12 v at 7 ma
Rise time	150 mμsec
Gain	2.5×10^{-11} coulomb/volt (with 10 μμf shunt capacity and 100 mμsec collection time)
Noise	3.5 μv rms referred to the input with the input shorted; 8.8 μv rms with input open

With 27 μμf shunting the inputs, this preamplifier and one having a 6AK5 have the same noise figure. With less than 27 μμf the 6AK5 is slightly better than the 3N35, and with more than 27 μμf shunting the input, the 3N35 is slightly better than the 6AK5.

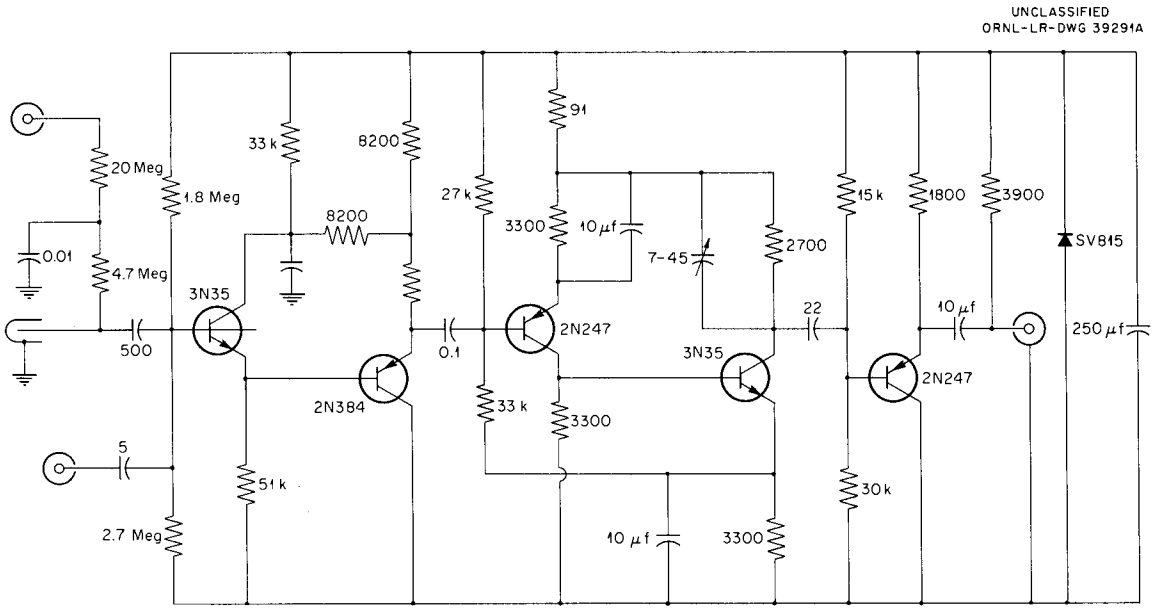

Fig. 23. Circuit Diagram of Transistorized Preamplifier Q-2032.

32 **Fig. 23** **There is a common collector amplifier between the second feedback pair and the common collector cable driver that is not shown in the drawing**

THERMAL NEUTRON SURVEY METER Q-2004

F. M. Glass

This instrument is a transistorized counting-rate device which has the desirable features of compactness, light weight, and permanent-type rechargeable batteries. As the name implies, it is a survey-type health physics instrument. The detector ($B^{10}F_3$ counter) is fastened directly to the front of the case. The entire instrument is not much larger than the probe on the vacuum tube model it replaces (see Fig. 24). There are three ranges, having calibrations of 200, 2000, and 20,000 neutrons$\cdot$cm^{-2}. sec^{-1}.

The circuitry (see Fig. 25) consists of a pulse amplifier, a discriminator, a duty cycle meter, a transistorized 1200-v regulated supply, and a built-in battery charger. There are two 2N384 transistors and two 2N169A transistors in the amplifier. The first feed-back pair consists of a 2N384 in the input directly coupled from its collector to the base of a 2N169A. The 2N169A serves as a common-~~base~~ collector amplifier* with its emitter coupled through an R-C integrating network back to the input base. This type of current feedback is employed in order to achieve gain stability without impedance-matching the detector to the amplifier. Since the output impedance of this pair is very low, voltage feedback can be used in the second amplifier pair to stabilize the gain. Current (d-c) feedback is also employed to stabilize the collector current of the second pair. The gain of the first feed-back pair should be considered in terms of output voltage in relation to input charge. It is 0.016 v per 10^{-12} coulomb. The voltage gain of the second loop is 40, and the sensitivity of the discriminator is 130 mv. The resultant over-all sensitivity of the instrument is 2×10^{-13} coulomb.

*see errata

The discriminator normalizes the pulses at a fixed amplitude and at three different pulse widths, depending on the range. The width is such that regardless of the range in use, the normally cut-off transistor in the meter circuit is keyed on for a 2% duty cycle when the meter reads full scale. This means that the fractional counting loss is the same for all ranges and has a linear relation to the meter scale. Therefore, it is possible to compensate for this loss in the initial calibration, so that the meter indicates the true counting rate.

The meter circuit consists of a normally cut-off 2N335 silicon transistor with an R-C-damped 50-μa meter in the collector circuit. There is enough resistance in series with the meter and transistor to make the peak current fairly independent of beta and collector saturation characteristics.

The high-voltage supply is a Universal Transistor Products Corp. model C 1200 R/12/10. This supply delivers a regulated 1200 v at 10 μa.

The specifications are:

Thermal neutron detector	BF_3 proportional counter
Cabinet size	8 × 5 1/2 × 5 in.
Weight	4 lb
Battery drain	18 ma
Battery	500 ma-hr, rechargeable
Resolution	No apparent counting loss
Accuracy	±6% over operating range of battery and temperatures from 40 to 100°F

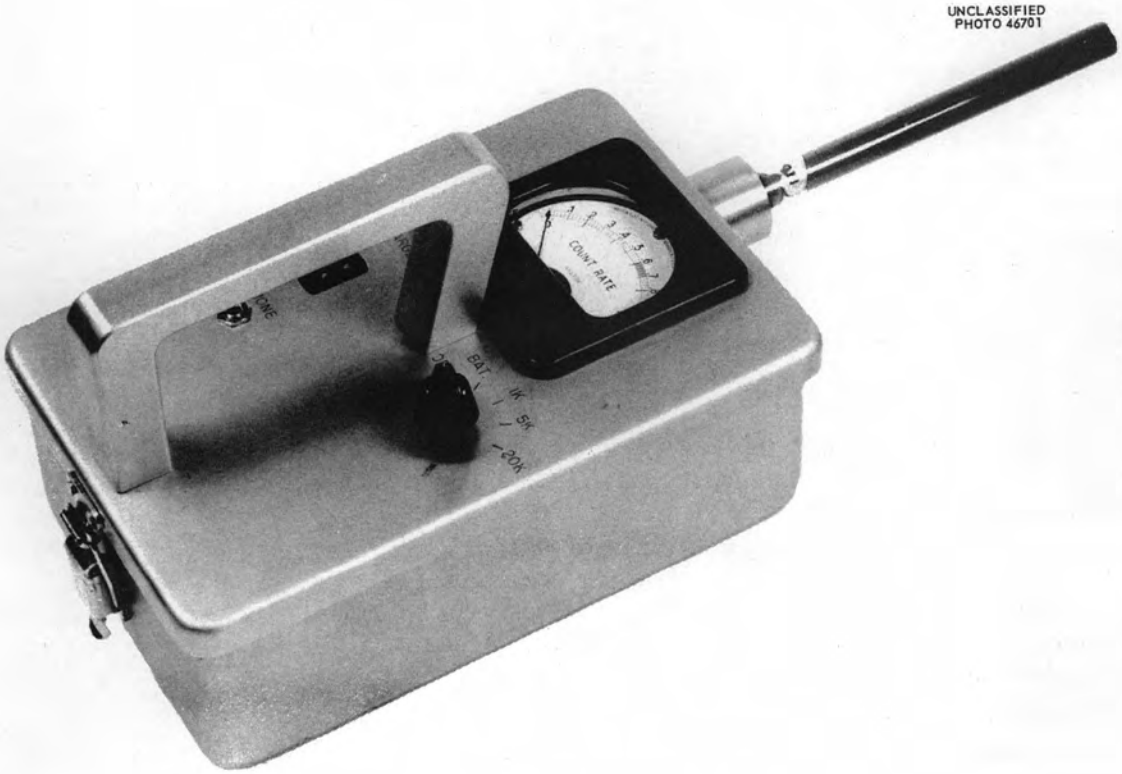

Fig. 24. Thermal Neutron Survey Meter.

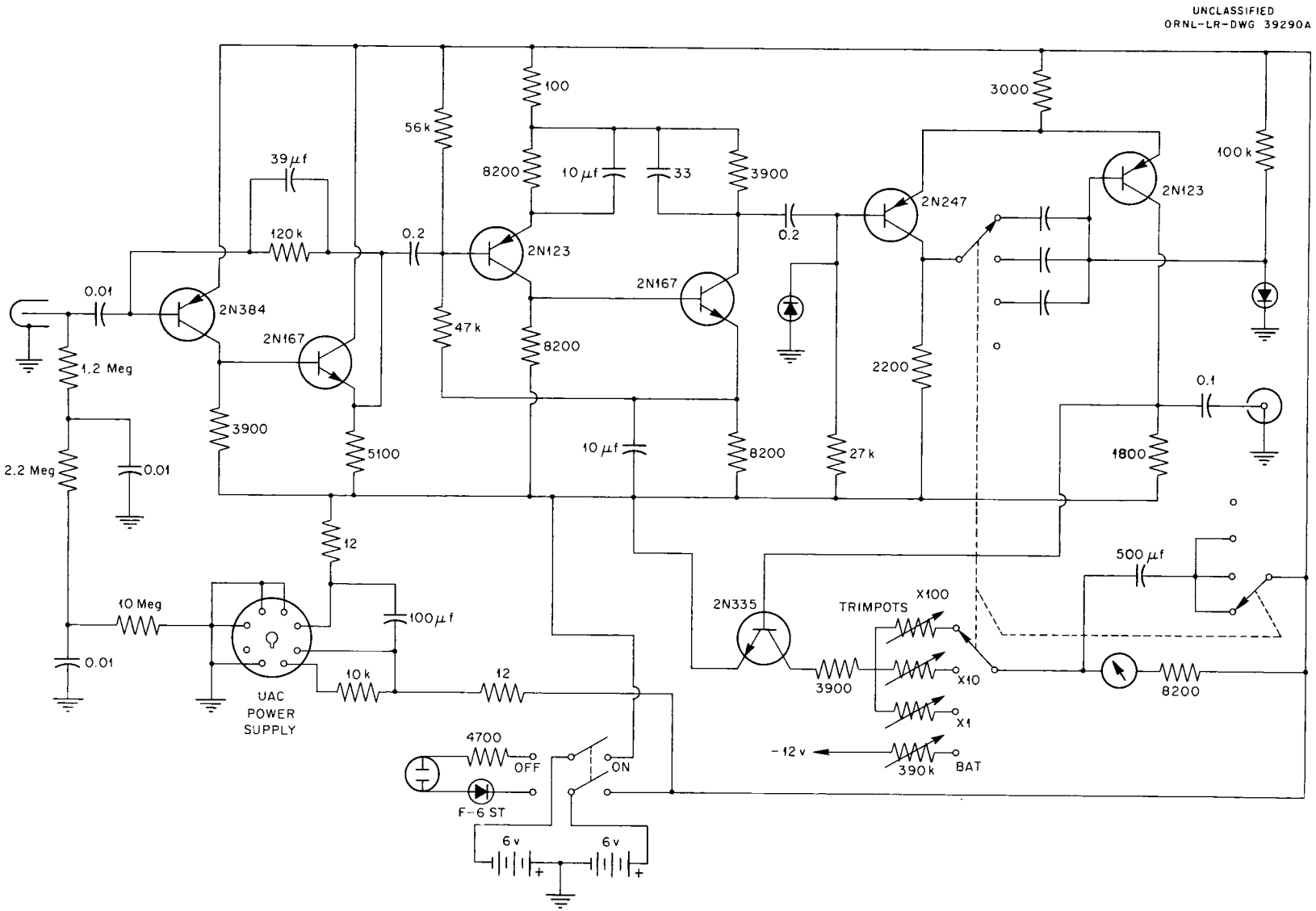

Fig. 25. Circuit Diagram of Thermal Neutron Survey Meter Q-2004.

PORTABLE ALPHA COUNTER Q-1975

F. M. Glass

A transistorized portable alpha scintillation counter has been designed, and five are currently being tested in the field. Although this is the first attempt by the instrument development group to transistorize pulse-type counting equipment, the results of the test have been quite gratifying. As of this date there have been no failures, and the stability as a function of temperature and battery voltage is adequate.

The circuitry (see Fig. 26) consists of a feed-back amplifier pair, a trigger pair which functions as a discriminator, a scale of 2, a pulse shaper and register driver, a 900-v regulated supply for the photomultiplier tube, and a built-in battery charger. The amplifier has approximately 40 db of a-c voltage feedback to stabilize the gain and sufficient d-c current feedback to stabilize the collector current. Since the photomultiplier is a current source and the feedback employed is voltage feedback, transformer coupling is used to couple the detector to the amplifier. No attempt has been made to temperature-compensate the discriminator, as the stability is adequate for this type of instrument.

The 2N123 and 2N167 transistors used in this instrument were selected on the basis that they were the best of the industrial types that were carried in stock at the time this work was done. They are not necessarily our first choice for some of the applications in which they are used.

The built-in charger is so designed that it is impossible to exceed the gassing potential of the cells (1.49 v). Batteries have been left on charge for 60 days with no apparent damage.

The specifications are:

Size	6 × 5 × 4 1/2 in.
Weight	3 lb 10 oz
Battery drain	20 ma
Battery	12 v, 500 ma-hr (rechargeable with life expectancy in excess of 15 years)
Sensitivity	5×10^{-12} coulomb
Resolution*	Counting loss = 2 1/2% at 100 counts/min
Stability	Count rate increases 0.14% per °C for Pu^{239} within the temperature limits of 0 to 60°C

---

*Since the resolving time of the scale of 2 (20 μsec) is very short in comparison to the resolving time of the mechanical counter (0.06 sec), it can be shown that the number of counts missed per minute is $(1 - e^{-T})T$, where λ is half the actual count rate and T is the resolving time of the register.

* see errata

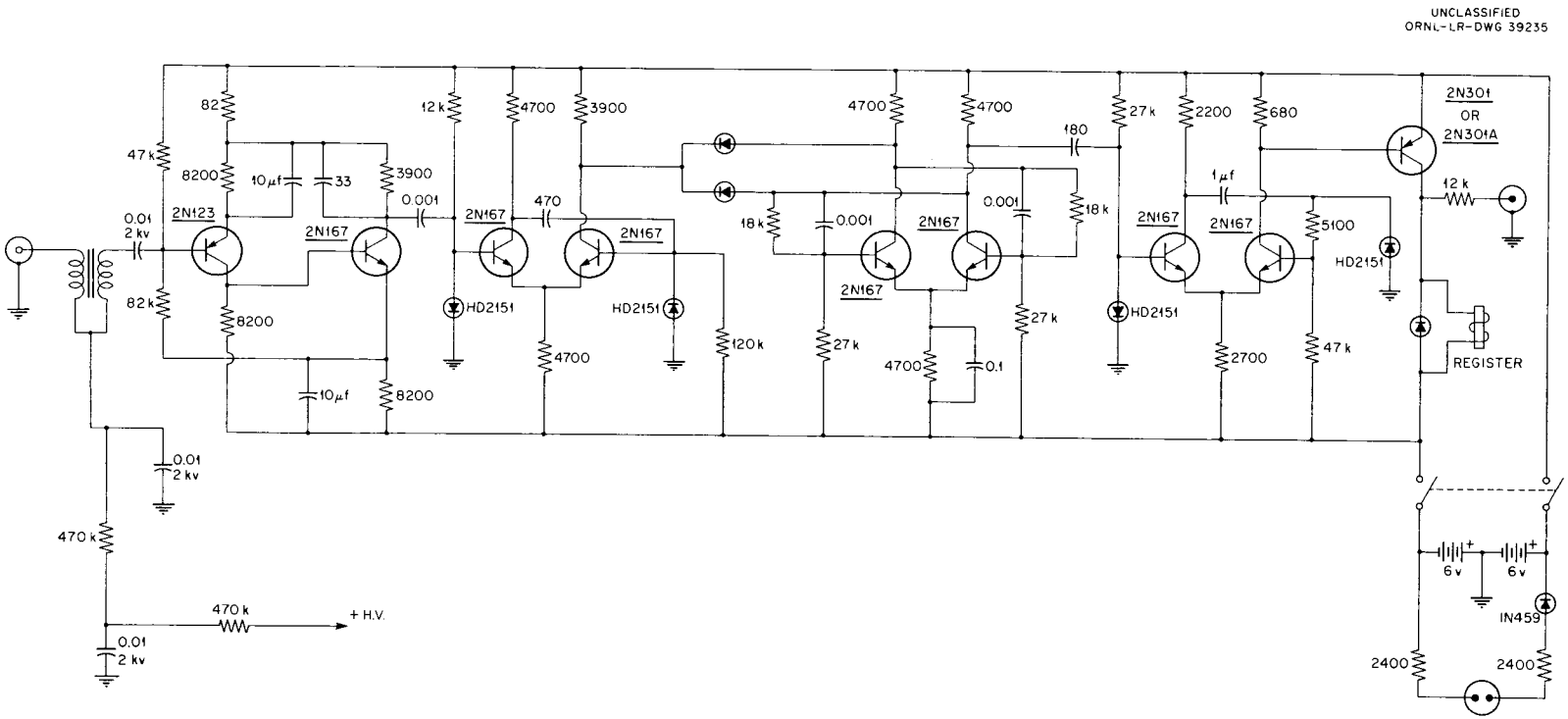

Fig. 26. Portable Alpha Counter Q-1975.

GRID CURRENT IN ELECTROMETER TUBES

E. Fairstein

More than 200 vacuum tube electrometers are in use at the Laboratory, and there is a continuing need for tubes having low grid current. The factors affecting grid current are well known, but the lack of specific information regarding modern electrometer tubes prompted a study, the results of which are given here.

Tubes from three manufacturers were tested — Philips, Raytheon, and Victoreen. Emphasis was placed on the testing of pentodes.

Since the measurement of currents in the range below 10^{-14} amp is very time consuming, a test instrument was built to permit the measurements to be made in the least possible time. The testing device consisted of two parts — a chamber for housing the tube and a feed-back amplifier. Currents as low as 10^{-16} amp could be measured with confidence. A short description of the instrument follows.

The rate-of-drift technique was used exclusively in the grid current measurements. Data were taken in the range from 10^{-16} to 10^{-11} amp, although currents as low as 10^{-17} amp were detectable. The basic circuit is shown in Fig. 27. It can be seen that the electrometer tube is part of a feed-back loop. In operation, S_2 is first placed in the "check" position and the amplifier "A" is adjusted for $E_o = 0$. The switch is then moved to the "use" position. The action of the feedback is to hold the cathode of the electrometer tube within millivolts of ground, regardless of the operating conditions of the tube. With S_1 closed, E_o is the grid bias of the electrometer tube necessary to establish the preset plate and screen voltages E_p and E_{C_2}, and the preset cathode current 150/R. When S_1 is opened, the grid current charges C at a constant rate. Since the feed-back action holds the cathode very nearly at ground, the changing voltage drop across C appears as a changing E_o; dE_o/dt was determined from the relationship

$$I = C\ dV/dt = C\ dE_o/dt \quad .$$

Because of the feedback, dE_o/dt was independent of E_o for any given tube up to a maximum E_o of 65 v.

A view of the chamber cover with the tube in place is shown in Fig. 28. (During measurements the chamber was evacuated to eliminate the effects of moisture-produced surface leakage and the collection of ions produced by background radiation.) The grid of the tube is shown connected to a single threaded Teflon feed-through insulator, the stud serving both as a switch contact and as one of the capacitor plates (S_1 and C_1, respectively, in Fig. 27). The switch arm was insulated from the chamber cover by a vacuum-tight O-ring seal which permitted the arm to slide in and out. The lower contact moved through a small hole in the lower capacitor plate. The shielding action of the plate plus gold-plated contacts minimized switching transients. The capacitor C was trimmed to 1.00 ± 0.03 pf by several turns

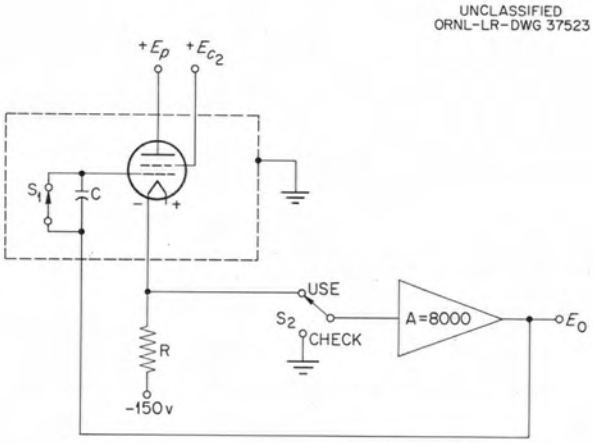

Fig. 27. Grid Current Tester: Basic Circuit.

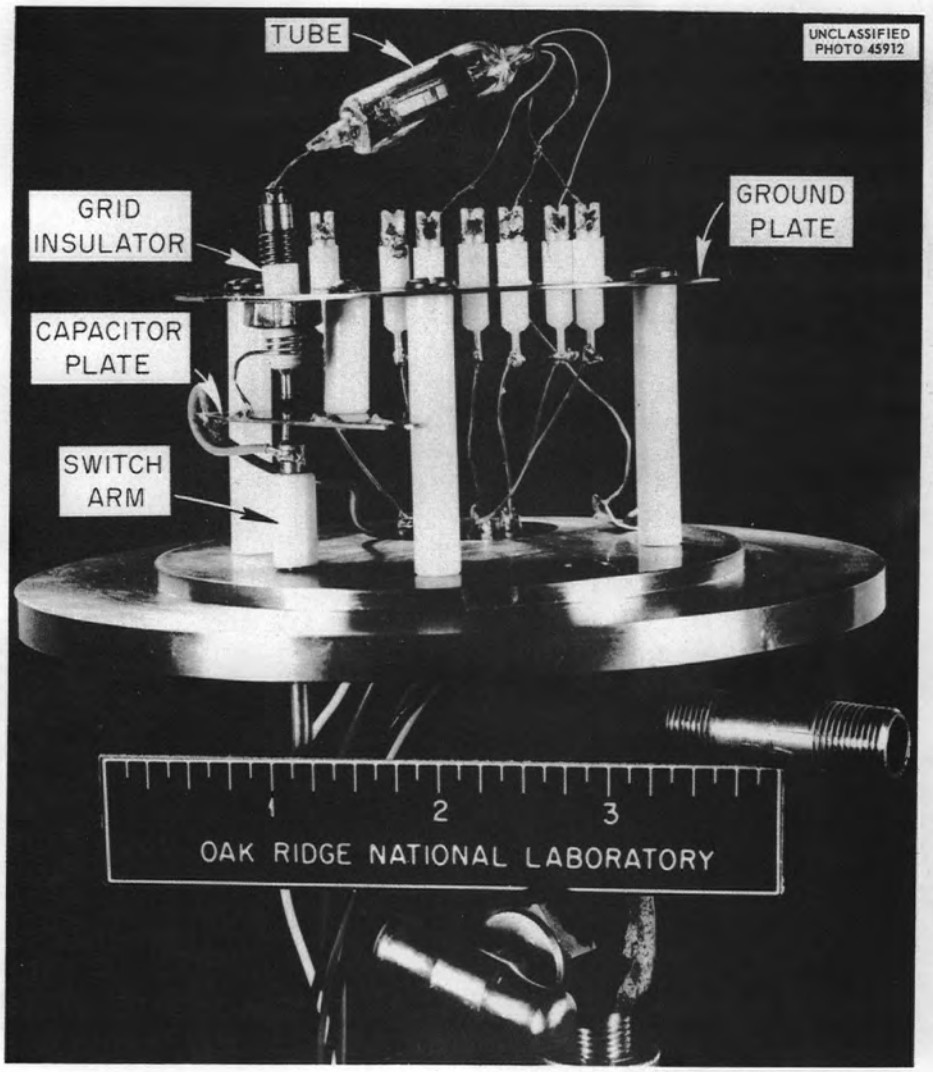

Fig. 28. Test Chamber Cover Plate.

of wire wrapped around the grid insulator (1 picofarad = 10^{-12} farad). This wire was connected to the lower plate. The apparently flimsy arrangement proved to be quite stable in use; repeated operation of the switch and attempts to change the capacity by flexing the switch arm resulted in no more than ±1.5% variation in capacitance. Changing tubes had no effect, partly because the ground plate completely shielded the tube from the moving switch contacts and partly because the feedback resulted in an effective grid-to-ground capacity of less than 0.002 pf. (A feed-back factor in excess of 5000 was used.) All leads leaving the chamber were at a low impedance level. A multiple Kovar seal was used for these leads, and the glass insulators were packed with Apiezon Q to make them opaque.

A complete circuit of the tester (less power supply) is shown in Fig. 29. The section to the left of the dotted line was contained in the chamber; the section to the right was contained in a closed box to prevent air movement in the room from producing changing thermal gradients. The layout and choice of tubes and components resulted in a drift rate of less than 1 mv/hr. The power supply, though conventional in circuitry, was built with similar care and did not degrade the performance of the tester. Electrometer tube parameters could be preset by calibrated controls. The output circuit made it possible to buck the output signal against an adjustable voltage for those dE_o/dt measurements where the change in voltage was small compared with the absolute voltage.

For most of the measurements, a KinTel model 203 vacuum tube voltmeter was used at the E_o position. In a typical measurement, the observed root-mean-square random voltage fluctuation (noise) was 40 μv or less and was probably due to flicker noise in the carbon resistors used to set the cathode current of the tube under test. (It was impractical to use wire-wound resistors at this location.) The smallest value of ΔE_o used in a measurement was 2 mv, resulting in an rms error of approximately 2%. With a current of 10^{-17} amp, a capacitance of 1 pf, and a ΔE_o of 2 mv, a ΔT of 100 sec was required. In all the measurements, the precision of reading did not limit the over-all accuracy. Errors were 3% or less for currents between 10^{-12} and 10^{-15} amp, increasing to 10% for the decades above and below. The errors were far less than the variation between tubes.

A capacitance of 1 pf is small compared with the commonly encountered standard capacitance, and a direct measurement with the equipment on hand would not have resulted in the desired accuracy. The measuring technique used is described in Appendix I of this section. The absolute error in measurement did not exceed 3%. For the purposes of these tests, a 10% error would have been acceptable.

The leakage resistance of the grid insulator could also affect the accuracy of the results. By applying a large, known voltage to the ground plate in which the insulator was mounted, it was possible to determine that the leakage resistance was approximately 5×10^{17} ohms. Under measuring conditions where this leakage resistance would have the greatest effect (at a grid current of 10^{-16} amp), the leakage produced a background current of approximately 4×10^{-18} amp. No attempt was made to correct for it.

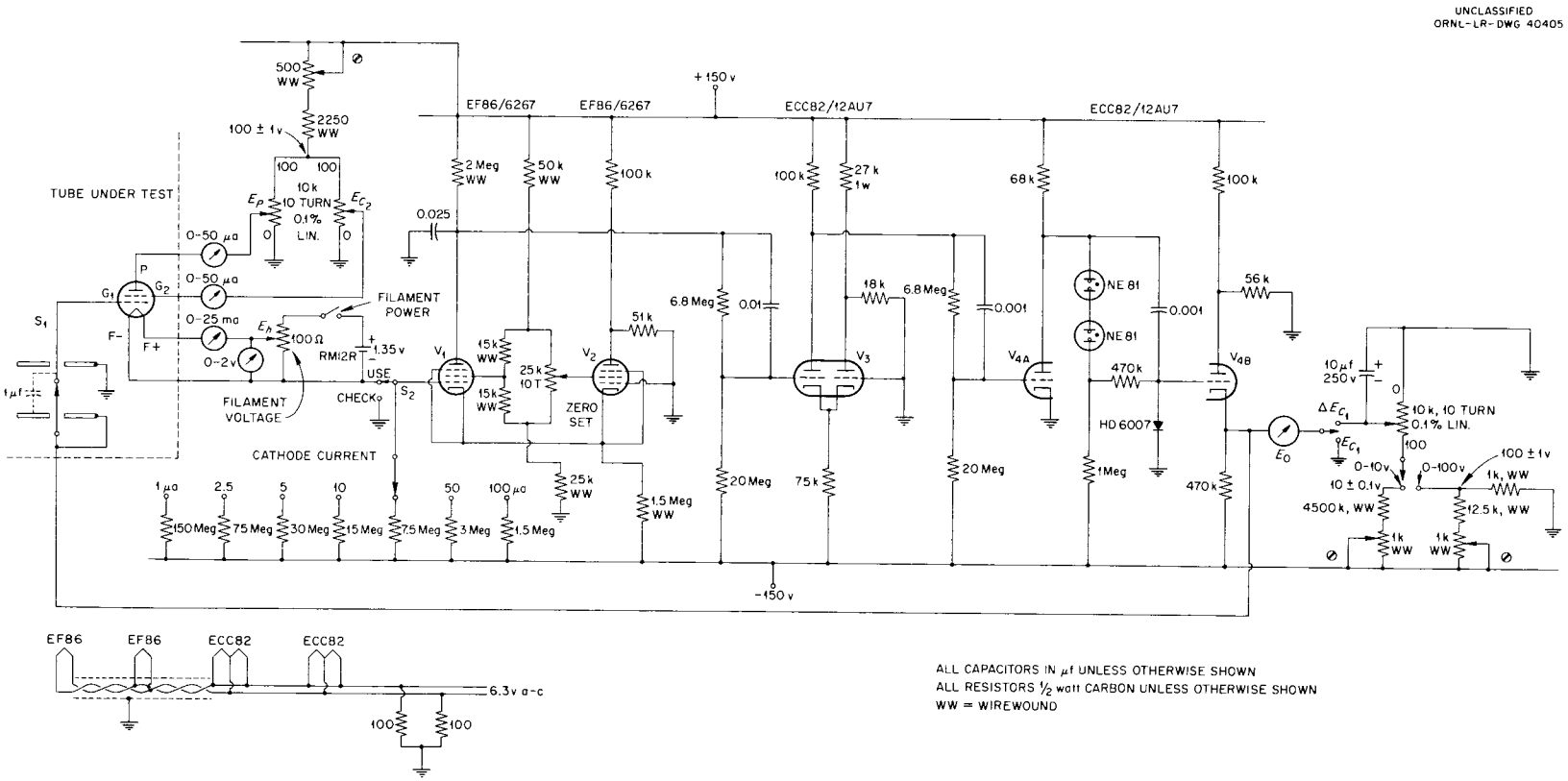

Fig. 29. Grid Current Tester: Complete Circuit (Less Power Supply).

In summary, the features which justified the construction of this tester are the following:

1. Plate voltage, screen voltage, and cathode current could be individually set without interaction between parameters.
2. The use of feedback made it possible to degenerate the input capacitance of the tube under test to a value of less than 2×10^{-15} f.
3. This low input capacitance permitted the use of a 10^{-12}-f standard capacitor, in turn making it possible to measure a current of 10^{-16} amp in a time as short as 10 sec. The degeneration also made it possible to change tubes without the necessity for recalibration.
4. The circuit configuration eliminated the need for anything but a single insulator to be connected to the grid of the tube under test.

Table 1 is a summary of test results for all the tubes tested. The 5886 and 5889 tubes were manufactured by Raytheon, the VX55 and 5803 by Victoreen, and the 4068 by Philips.

The voltages $E_p + |E_{C_1}|$ are the sums of the absolute values of the plate-to-filament and grid-to-filament voltages. This particular parameter was chosen because it is a measure of the total energy imparted to the electrons leaving the filament (the grid current in a particular tube is known to be a function of the electron energy). Since in every case the triode-connected amplification factor μ is approximately 2, one-third of the voltage represents bias while the remaining two-thirds represents the plate voltage.

The last two columns give a measure of the grid current with the tube biased beyond cutoff (-45 v), first with a cold filament and then with a hot filament (see Appendix II of this section for the test circuit). With a cold filament, the grid current is an approximately linear function of applied voltage, indicating ohmic resistance. With the filament hot, the grid current contains two components, one of which is due to the aforementioned resistance and the other due to positive ion emission from the filament. The ion emission is independent of applied voltage above a threshold of a few volts.

In every case, plate and screen voltages were equal. All tubes were aged at 5 μa plate current for at least 24 hr preceding the test. The tube envelopes near the grid lead were not cleaned; neither were they touched. It was felt that evacuation would remove most of the surface moisture – the leading cause of surface leakage. Plate power was always removed by switching S_2 in Fig. 29 to "check" before switching the filament supply on or off. Equilibrium conditions were always established before taking readings.

5886. – Samples 1, 2, 3, 4, 5, and 8 were supplied by Raytheon as samples. It is not known whether these were selected for low grid current or were typical of normal production. Since the worst tube was one of the samples, the tubes were probably unselected.

Table 1. Electrometer Tube Grid Current Tests

$E_h = 1.0$ v
$I_k = 5\ \mu a$

Tube Type	Sample No.*	Filament Current (ma)	Grid Current (10^{-15} amp)					
			$E_p + \lvert E_{C_1} \rvert$				$E_{C_1} = -45$ v	
			9 v	12 v	20 v	35 v	Filament Off	Filament On
5886	1	9.5	1.2	1.9	10	2,200		
	2	8.9	1.9	2.1	7.3	1,040	0.6	6.3
	3	8.6	2.5	4.6	13.3	625	0.3	11.8
	4	8.5	5.9	7.2	17.7	2,500	0.6	10
	5	9.25	8.5	9.5	18.5	1,400	0.7	14.3
	6	8.9	10.5	13.3	25	861		
	7	9	11	13.3	27.8	848	1.4	20
	8	8.7	14.2	16.4	29	790	0.6	28
5889	1	6.4		0.33	4.9	2,180		
	2	6.6		0.37	5.7	2,180	0.59	0.47
	3	6.25		0.47	8.5	5,700		
	4	7.0		0.57	5.1	3,340	1.6	0.94
	5	8.9	0.22	0.83	17	10,000	0.46	0.47
	6	6	Faulty	Faulty	Faulty	Faulty		
VX55	1	8.2	2		42	340	1.3	8.3
	2	8.8	2.3	6.1	36	410	2.7	5.3
5803	1			1.7	14	410	1.2	1.8
	2						2.0	2.8
	3	8.0	0.67	1.0			0.9	1.2
	4	8.0	0.76	2.5			0.5	
4068	1	6.5		0.47	8.8	834		
	2	6.7	0.48	0.84	10	1,400	0.77	1.2
	3	6.8	6.4	10	25	750	46	55
	4	6.5	10	15.4	31	110	82	84
	5	6.7	12.5	32.2	85.8	263	185	208
	6	6.3	+2.5	+0.25	8.5	130	0.6	0.8

*For each tube type, the samples are listed in the order of increasing grid current at the 12-v level.

The performance ranged from fair to poor, using the best of all the tubes tested as a criterion of performance. There is no correlation between biased-off leakage current and grid current in the normal operating range. The positive ion emission from the filament was high, with an apparent correlation between the ion emission and the grid current.

5889. – These tubes were supplied by Raytheon as samples. As with the 5886's, it is not known how representative of current production they were. (The faulty tube appeared to have a cracked seal, which probably occurred in transit.) Accordingly, five more tubes were purchased (not as samples) and spot checked. The evidence indicates that the original tubes are typical of current production.

The 5889's were the best of all those tested. In fact, the grid current at $E_p + |E_{C_1}| = 9$ v was so low ($\sim 2 \times 10^{-16}$ amp) that in four of the five usable samples the current was not recorded, on the assumption that the tubes were operating too close to the floating grid potential for the numbers to be meaningful. Later measurements proved this assumption to be false.

Only three tubes were tested for grid current under cutoff conditions. In two of these, the current with the filament hot was lower than with the filament cold. This is the reverse of the expected results, and the writer is unable to explain the anomaly.

These tubes are the only ones to have the grid lead emerge from the end of the envelope opposite to that of the remaining leads. The external leakage path between the grid and the other electrodes is approximately ten times greater for the 5889 than it is for other tube types; the long leakage path probably accounts for the low grid current.

VX55. – This tube is a triode, and little testing time was spent on it. The two tubes tested were fair, and both had relatively high positive ion emission from the filament.

5803. – This tube is also a triode; it is not in current production. Unfortunately, approximately 200 Laboratory instruments use the tube, and replacements are required.

The first two samples tested were unused tubes which had been on a shelf for approximately five years. The last two were recently made laboratory models (by Victoreen). All the tests indicated satisfactory performance.

4068. – Of the six tubes tested, three were excellent and three were relatively poor. There is a definite correlation between the cutoff grid current and the performance in the normal operating range, indicating leaky insulators in the three poor tubes. In sample No. 6, the grid current over part of the range was opposite in polarity to that expected. The effect was too large to be satisfactorily explained by leakage resistance. It may have been caused by a charged dielectric film on the grid wires.

Additional information was obtained in graphical form for one tube (a good one, but not the best) of each type tested. Except for changes in scale, all the curves had much the same shape. Complete data are presented for the 5889 only.

Figure 30 shows curves of grid current, grid bias, and μ as a function of plate-to-filament voltage for a constant cathode current of 5 μa. The μ curve was derived from the bias vs plate voltage curve using the equation

$$\mu = \left.\frac{\Delta e_p}{\Delta e_c}\right|_{I_k \text{ const}} .$$

Filament voltage was held constant at 1.00 v.

The left-hand spur of the grid current curve corresponds to the positive grid current region between the floating grid potential and zero bias. In this region over the range shown, the grid current varies as the 21st power of the plate voltage!

The right-hand spur represents the commonly used negative grid current region. In the range between $E_p = 5$ and $E_p = 10$, the grid current varies approximately as the 4th power of the plate voltage, increasing to the 15th power in the region between 14 and 20 v, and dropping off to the 3/2 power above 50 v.

In the region between 5 and 10 v, individual points gave evidence of several breaks in the curve. While the curve shown did not have enough points in it to definitely establish the existence of the breaks, carefully taken data on other tubes showed that in many cases these breaks are indeed real. They correspond to the ionization potentials of the materials of construction and/or residual gas in the tube. The marked change in slope of the curve between 10 and 15 v is certainly real. The second ionization potential of the iron-cobalt-nickel group is between 16.5 and 18.2 ev, and these values lie within the $E_p + |E_{C_1}|$ values corresponding to the points between 10 and 15 v.

All the tubes for which grid current curves were drawn yielded curves of nearly the same shape, differing only in the magnitude of the grid current for a given operating voltage and in the details of the irregularities occurring in the region below 10 v.

All the tubes tested had triode-connected μ's in the range between 1.5 and 2.0.

In another test, the results of which are not graphed, the effect on the grid current of varying the plate voltage while holding the screen grid voltage constant was tried. Since the grid current in a tube having low insulator leakage is due primarily to the soft x rays produced at the plate and screen, it is to be expected that the relative contributions by the two elements should be proportional both to the currents to plate and screen and to the applied voltages. With the plate voltage lower than the screen voltage, the x rays should be predominantly due to the screen. This was confirmed by measurement — as the plate voltage was reduced, the grid current decreased, eventually reaching a saturation value approximately 35% lower than in the triode-connected case. Saturation set in when the plate voltage was reduced below 40% of the screen voltage.

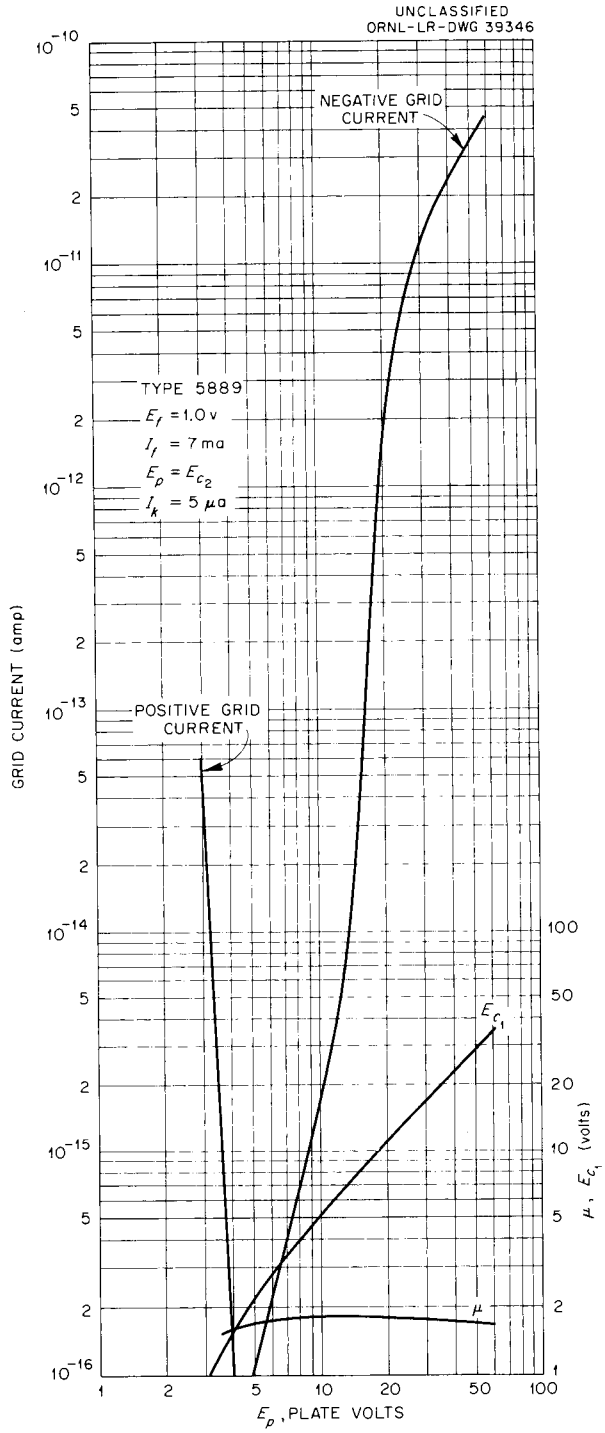

Fig. 30. Grid Current, Grid Bias, and Amplification Factor μ vs Plate Voltage for a Type 5889 Electrometer Tube, Triode-Connected.

With the plate voltage higher than that of the screen, the x rays should be predominantly due to the plate. However, since the control grid is shadowed by the screen grid, the grid current should always be lower than for the triode-connected case. This was also confirmed by the measurements. The grid current curve was parallel to that of Fig. 30 in the region above $E_p = E_{C_2}$, but was displaced from it on the low side by a factor of 2 to 3 in grid current.

Figure 31 shows curves of grid current vs cathode current for the 5889 and the 4068. Plate and screen voltages were held at 8.0 v. The dip in the 5889 curve is atypical and is probably a manifestation of the same phenomenon discussed earlier in connection with sample No. 6 of the 4068.

Grid current should be directly proportional to cathode current. The fact that it is not in the case of the 4068 is due to two effects: (1) as the grid current decreases, the effects of leakage resistance and positive ion emission from the filament become increasingly more important, eventually setting a lower limit to the measured current; (2) because of the low μ of the tubes, the bias change of approximately 3 v which accompanies the cathode current variation from 1 to 100 μa is an appreciable fraction of the applied plate voltage of 8 v. The grid current is a steep function of the energy of the cathode-emitted electrons. The energy of these electrons is directly proportional to $E_p + |E_{C_1}|$. Combining these facts, it can be seen that an increasing cathode current is accompanied by a decreasing grid bias (plate voltage held constant), causing the grid current to increase at a diminishing rate. The observed results confirm this conclusion.

Figure 32 is a set of curves of the ratio of plate to screen grid current as a function of the ratio of plate to screen grid voltage, taken at a screen grid voltage of 8 v and a cathode current of 50 μa. The ratios are nearly independent of the absolute values of voltage and current over the normal operating ranges of the tubes.

The curves are useful for circuit design purposes. For example, the plate resistance may be obtained from the equation $v_p = \Delta e_p/\Delta i_p$.

Figure 33 gives curves of triode-connected transconductance vs cathode current, and curves of grid voltage vs cathode current. The transconductance to plate or screen may be separated from the triode-connected transconductance by noting that the separate transconductances are directly proportional to the electrode currents (see Fig. 32).

Figures 34a and 34b are curves of grid bias necessary to establish a constant cathode current vs filament voltage, with cathode current as a parameter. The slope of the curves in the relatively flat region reflects the fact that the d-c drop along the filament wire makes up part of the grid bias. Near the knees, the slope changes sharply because the tube becomes emission-limited.

The slopes of the 10- and 100-μa curves of the 4068 indicate that its emission capability is relatively poor compared with that of the 5886, 5889, or VX55.

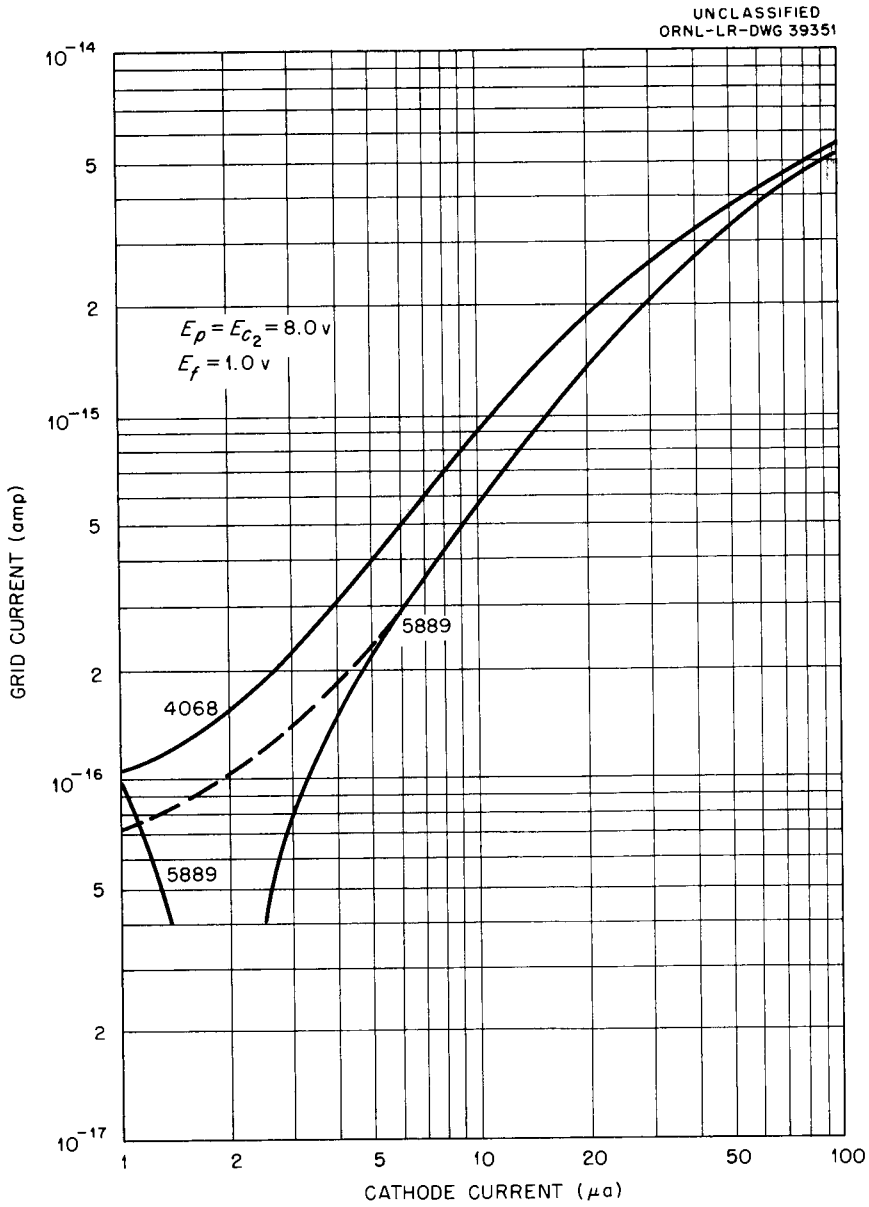

Fig. 31. Grid Current vs Cathode Current, Types 4068 and 5889.

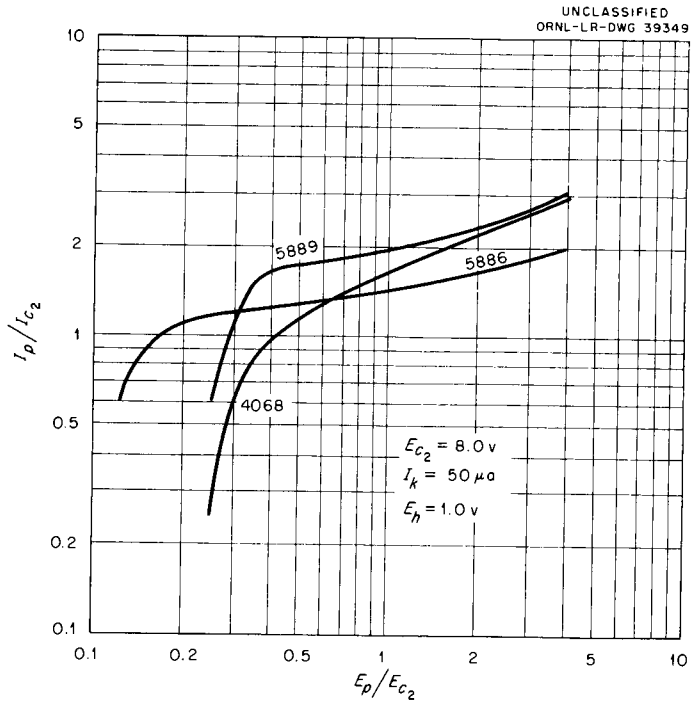

Fig. 32. Ratio of Plate to Screen Grid Current vs Ratio of Plate to Screen Grid Voltage, Types 4068, 5886, and 5889.

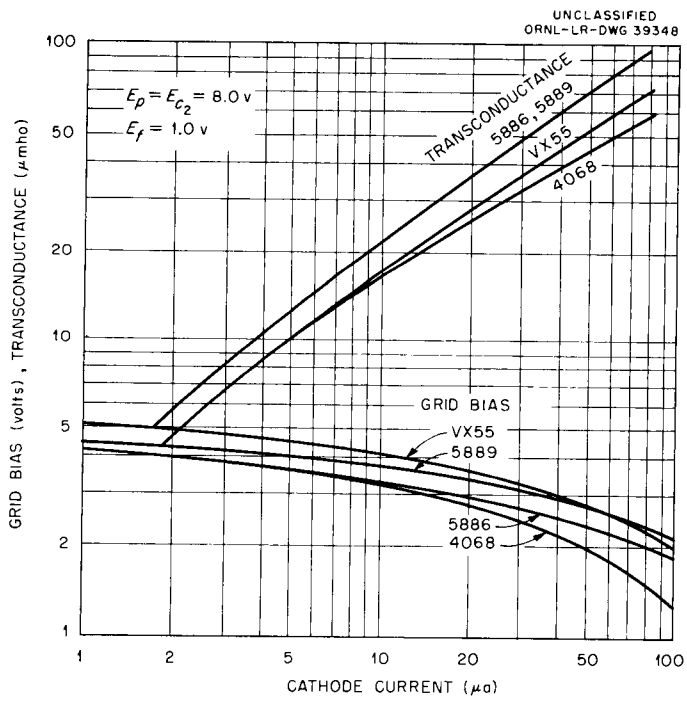

Fig. 33. Transconductance and Grid Bias vs Cathode Current, Types 4068, 5886, 5889, and VX55. The pentodes were triode-conncected, with $E_p = E_{c_2} = 8.0$ v.

All the tubes exhibited a transient response to a change in operating conditions. The time constant of the transient was more than 8 hr in some instances, and because of the time scale no quantitative measurements were made. However, the qualitative data bear some discussion.

If the tube is operated with approximately 20 v on the plate and/or screen and the voltage is then reduced to 6 v, the grid current remains at a high value for a time which may be only 30 min or as long as a day. The time depends on the tube type, on the difference between the initial and final voltages, and on the difference between the initial and final grid currents. It was noted that the recovery time was much longer for the 5886 and the 5889 than it was for the other tubes. The 5886 and 5889 use mica insulators, while the other tubes use ceramic. The transient is probably due to dielectric hysteresis in the glass, the tube element spacers, and the Teflon insulator in the test ring. It may be that the dielectric hysteresis in mica is larger than in ceramic, accounting in part for the longer recovery time in the 5886 and 5889. It should be noted that there was no evidence indicating that the mica spacers are inferior to ceramic spacers regarding leakage resistance or outgassing.

A large change in cathode current also produced a transient effect. This may have been due to a change in the surface charge, either on the element spacers or the oxide film on the grid, if such a film existed. It also may have been due to slight changes in the emitting surface of the filament which may have resulted in the release of positive ions.

On the basis of information obtained in the preceding tests, some conclusions may be drawn regarding the design of practical electrometer circuits and the means by which the tube manufacturers may improve their products.

Drift in Operating Point. — If drift is to be limited to the first stage in a multistage amplifier, the first stage must have a gain of at least 5. In the case of an electrometer, this means that the input tube must be pentode-connected. This restriction does not apply to those circuits in which the input tube is followed by a meter.

From Figs. 34a and 34b it can be seen that a 10% change in filament voltage (at rated voltage) has the same effect on the plate current as a 100- to 200-mv change in input signal. Compensating techniques can reduce the effects of filament voltage changes by a factor of 10 or more. Filament voltage regulation can give a further improvement.

With a μ of only 2, a change of Δv at the screen grid will have the same effect as a change of $\Delta v/2$ at the control grid. Evidently, the screen grid voltage regulation must be no worse than twice the desired offset at the grid.

Under carefully controlled conditions, stability can be very good. In one test performed on a 5889 having a 10^{10}-ohm resistor (shunted by a 100-pf capacitor) in series with the grid, the peak-to-peak fluctuation of the base line (referred to the grid) was 200 μv for an 8-hr period, and the mean drift in the base line for this same period was not more than 50 μv. This compares favorably to a vibrating reed instrument. At least part of the fluctuation was due to thermal noise in the resistor.

Grid Current. – In radiation measurements it is rarely necessary to measure currents of less than 10^{-13} amp. Examination of Table 1 shows that at least 50% of each of the electrometer tube types can be operated under conditions which will ensure grid currents of 10^{-14} amp or less. In the case of the 5889, the yield is 80% of tubes exhibiting grid currents of 10^{-15} amp or less.

It was stated earlier that electrometer tubes should be operated on the negative bias side of the floating grid potential. Experience has shown that the difference between the operating bias and the floating grid potential should be approximately 0.75 v. This figure represents a compromise between the lowest possible grid current and that value of bias which will prevent the normally encountered contact potential variations from ever causing the operating point to fall on the wrong side of the floating grid potential. The contact potential varies by as much as 0.5 v from tube to tube; superimposed on this is the variation due to the choice of cathode current and plate (and screen) voltage, which will account for an additional 1 v. The latter variation is usually under the control of the circuit designer – the former is not.

In the best of the tubes (the 5889), the lowest practical operating grid current appears to be about 5×10^{-16} amp. Grid currents appreciably lower than this will be subject to large variations caused by surface charges on the various insulators within the tube structure. In selected tubes, grid currents as low as 10^{-17} amp may be possible, but the occasions demanding that an electrometer tube be used for such measurements are rare.

Possible Improvements. – The tests performed on these tubes are artificial in that it is unusual for a tube to be encapsulated in an evacuated chamber. The usual environment is a closed but nonhermetically sealed box. Surface leakage then becomes very important. The construction of the 5889 is ideal in this respect since it has not only an external leakage path equal to the length of the tube, but a guard ring as well.

It may be desirable to replace the mica spacers within the tube with ceramic spacers, not because of their insulating properties, but because of their possibly lower dielectric hysteresis.

It would be desirable to surface the tube elements, particularly the control grid, with a noble metal. This would reduce the possibility of insulating oxide patches and improve the stability of the grid current at low grid currents.

The grid current could be further reduced if the μ of the tube were lowered, thereby permitting a reduction in plate and screen voltage. In view of the already coarse control grid pitch, such a change may prove to be impractical.

Less than half of the filament emits all of the cathode current (see Appendix III for an explanation). By halving the length of the internal structure, filament power would be halved and the structural rigidity would increase eight times.

Appendix I
Measurement of the 1-pf Standard Capacitor

An accurately measured (±1%) capacitor having a capacitance of approximately 1000 pf was connected between the electrometer tube input grid and ground. A sine-wave signal was applied to the low-impedance side of the shorting switch (S_1 in Fig. 27). A low-pass filter was added to the feed-back line to remove the oscillator signal. Then, by measuring the a-c signal at the amplifier output terminal with and without the 1-pf capacitor shorted, it was possible to compute its exact size in terms of the known capacitance from grid to ground, and the signal attenuation.

Appendix II
Measurement of Tube Leakage Resistance and Ion Emission from the Filament

The test circuit is shown in Fig. 35. The tube on the left is the tube under test; the one on the right is a tube selected for low grid current. Leakage current to (or from) the grid of the tube under test was measured as the difference in current resulting from the application and removal of the 45-v test battery.

Appendix III
Effect of Filament Length on the Transconductance

Assume that a 5886 or a 5889 is operating at a cathode current of 3 μa. The transconductance at this current is 8 μmho (see Fig. 33). At the mid-point of the filament, the actual bias voltage is 0.5 v more negative than the externally applied bias because of the d-c drop along the filament wire. The product of this voltage drop and the transconductance is 4 μa, which is larger than the mean cathode current. Evidently, more than half of the tube structure is biased beyond cutoff. As a check on this theory, an experiment suggested by R. J. Klein was performed.

The circuit of Fig. 36 was connected. The filament was powered by a square-wave generator whose output was +1 v peak to ground. The grid was biased to produce a plate current of 2 μa (and therefore a cathode current of about 3 μa) when the filament was on. A sine wave whose frequency was high compared with the square wave was superimposed on the bias voltage to permit incremental gain measurements. The observed wave form is shown in Fig. 37.

Filament power was applied at t = 0. The filament was fully heated within 0.25 sec after the application of power, and a plate current of 2 μa resulted. At t = 6 sec, the filament power was removed, thereby reducing the voltage drop along the filament wire to zero. The plate current shot up to 20 μa, but decayed to zero in 0.15 sec as the filament cooled. By means of the sine wave signal (not shown in Fig. 37) it was determined that the g_m increased by 3.5 times when the drop along the filament wire was suddenly removed. This increase indicates that little more than one-third of an electrometer tube is contributing to the transconductance. The remaining two-thirds adds to the grid current, the

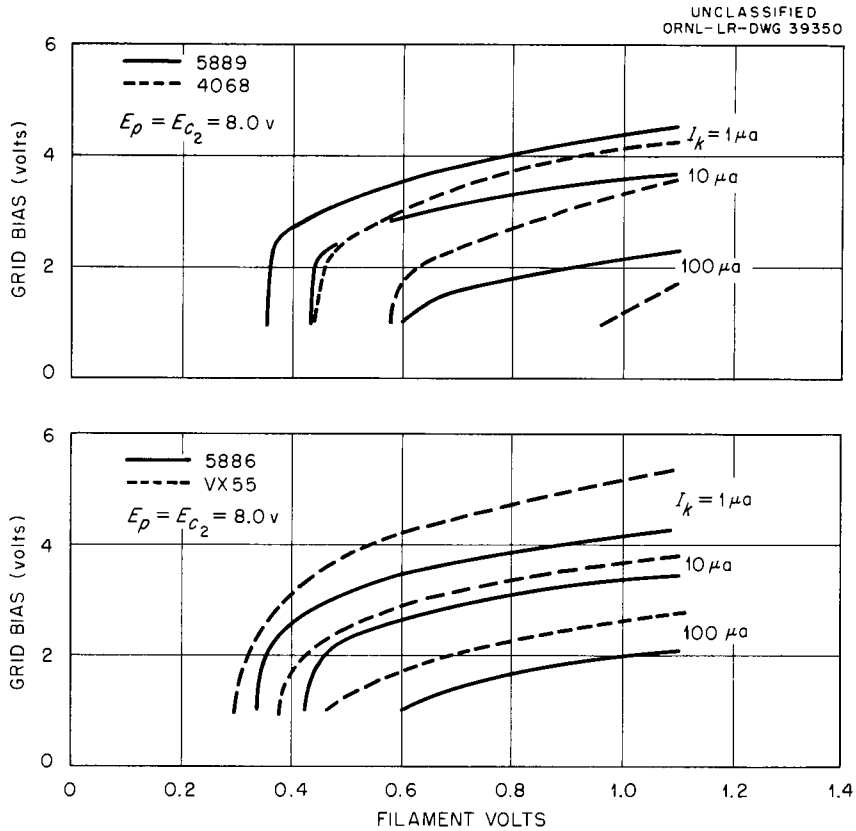

Fig. 34. Grid Bias Necessary To Establish the Stated Cathode Current vs Filament Voltage: (a) Types 5889 and 4068; (b) Types 5886 and VX55.

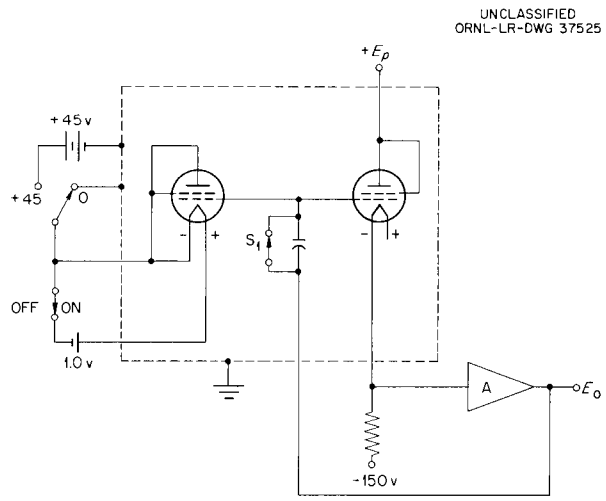

Fig. 35. Leakage Test Circuit. The tube on the left represents the tube under test.

microphonics, and the filament dissipation, but nothing to the gain. This same condition is probably true of all 1.5-v battery-operated tubes.

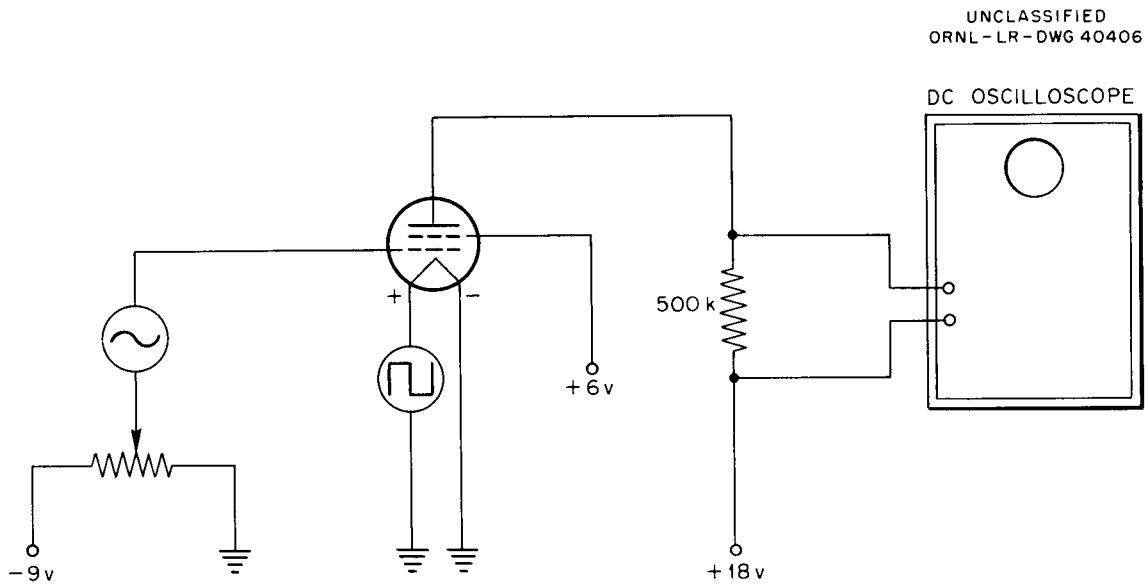

Fig. 36. Circuit for Testing the Effect of Filament Length on Transconductance. The 500-kilohm load resistance includes the input resistance of the oscilloscope.

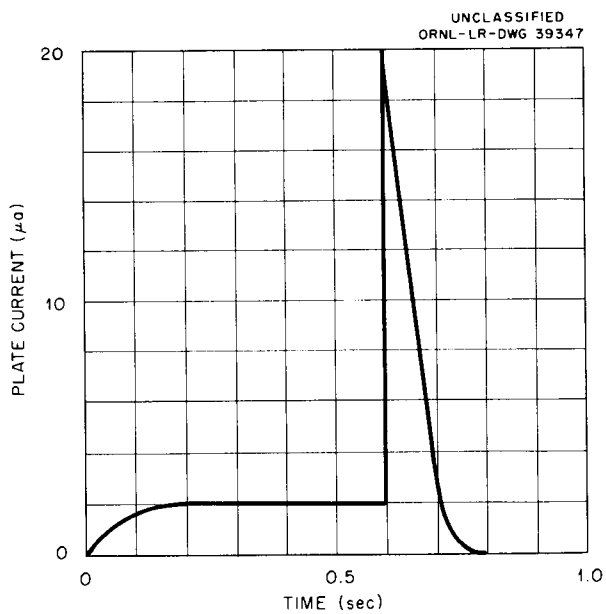

Fig. 37. Plate Current Wave Form Resulting from Filament Voltage Switching.

PERSONAL RADIATION MONITOR

R. H. Dilworth C. J. Borkowski

The instrumental protection of personnel from accidental radiation exposure is usually accomplished by area monitoring instrumentation. However, when it is realized that protection is actually desired not for areas but for people, the possibility of providing radiation monitoring instruments that can be worn directly on the person becomes very attractive. Still another advantage of personal monitors lies in the fact that few people work alone in those areas most susceptible to radiation accident, and if several different monitors in the pockets of several different workers alarm simultaneously, there will be little doubt in their minds that an accident has really occurred. This is in contrast to the all-too-frequent reaction of workers hearing a single area alarm sound and then leisurely wondering whether the instrument has failed or whether someone has carried a source too close to the detector assembly.

Radiation detectors worn on the person are already in very common use in the form of film badges, pocket ion chamber dosimeters, and self-reading quartz fiber pocket dosimeters. None of these types of monitors give any warning to the user; they merely give after-the-fact information on dosage already received. There has been some use of personal-warning-type instruments of the accumulating dosimeter type, notably the R-Vox, developed by F. M. Glass of this Laboratory in 1953, and the PTW Monitor, a recent German development. These instruments are worn on the belt of the user, and they emit a loud tone alarm when they have accumulated some chosen dose — typically 100 mr — since the last time they were reset. Instruments of this category are particularly useful in preventing overdose to workers who must enter areas where radiation is known to exist. They have inherent disadvantages when used as warning instruments by persons who do not normally expect to encounter dangerous radiation because of the uncertainties of when in the accumulating period the dangerous field was encountered and where the encounter took place.

These and other considerations point to the need of an on-the-person radiation monitoring instrument that is sensitive not to accumulated dose but rather to the dose rate or intensity of radiation. Such an instrument could sound an alarm immediately should the radiation intensity exceed a predetermined threshold. Furthermore, a rate-sensitive instrument can be made to provide a proportional indication of intensity above the threshold so as to aid the user in locating the source. The Personal Radiation Monitor about to be described is an attempt to satisfy these needs just expressed.

In considering the design of a dose-rate-sensitive monitor to be worn on the person, the question of size is of paramount importance. There has been some objection to instruments whose size required that they be worn on the belt of the user or carried in some special harness. Such seemingly minor objections to instruments of this type actually have a drastic effect on the user's acceptance of the instrument and his probability of actually using it when he needs it. On the other hand, there is little if any

opposition to the use of ion chamber or quartz fiber pocket instruments that have the shape of a fountain pen and a clip for wearing in a shirt or coat pocket. It was therefore decided to confine the new instrument to fountain pen size and shape if at all possible.

Another design philosophy was that of not merely trying to miniaturize with special tiny components some existing monitoring circuits, but instead to attempt to devise new circuits and methods which inherently required few components of small size and which insofar as possible made multiple use of those components and circuits that are used. Further aims in the design were to obtain exceptionally long battery life and to keep the cost of the instrument at a minimum, so as to make widespread use practical.

Figure 38 illustrates the exterior of a current version of the instrument along with a fountain pen for size comparison. It is 5 1/2 in. long – about the same length as most fountain pens. However, the diameter is a bit larger at 3/4 in. A spring clip is provided for attachment to the pocket. There is no "ON-OFF" switch, since if there were the human element would figure in the usefulness of the device to an intolerable extent. A mercury battery is installed under a screw cap at the lower end of the case. Early models of the instrument on which we now have some field experience obtained one month of operation from a 9-v battery that costs $1.75. An experimental newer version obtains a conservative three months of operation from a 5-v battery that costs 76¢.

The neon lamp at the top of the instrument flashes at a rate that is proportional to radiation intensity. At normal background this rate is about once every minute or so. At a few hundred milliroentgens per hour the flashing rate will exceed the point where the eye can discern changes in rate. At an intensity of somewhat above 10 r/hr the lamp ceases to flash and glows continuously.

The instrument also has a sound output heard through the series of holes surrounding the neon lamp. Each time the lamp flashes, a slight tick can be heard. This tick is quiet enough and infrequent enough so as not to be disturbing even in a quiet office; yet it furnishes reassurance to the user that the instrument is functioning. It can also apprise him of a several-fold increase in background if he notices the accompanying increase in tick rate. As the intensity exceeds a certain threshold – typically 100 mr/hr – the tick begins to lengthen into a continuous tone of greater amplitude. The pitch of this tone rises as the intensity rises above the threshold. The tone pitch is proportional to intensity up to a dose rate of several roentgens per hour. Above this rate the tone remains at the maximum pitch.

The instrument will continue to give both visual and aural alarm even in very high radiation fields. Extrapolation of tests made up to 100 r/hr would indicate no failure up to perhaps 100,000 r/hr. Extension of the nonblocking range much beyond this level is unwarranted since at such levels the time required to accumulate a lethal dose becomes only a few seconds.

UNCLASSIFIED
PHOTO 46416

Fig. 38. Exterior of Instrument and Fountain Pen.

Since the output indications of the instrument depend entirely upon subjective interpretation of sight and sound by the user, the accuracy with which dose rate can be estimated is perhaps only to order of magnitude by a user with some experience with the instrument in known fields. However, it is quite practical to calibrate an individual instrument and obtain accuracies of better than 10% of measured dose or dose rate in the suitable dynamic range by use of a stop watch or even by "counting" seconds. Such calibrations can be either a certain number of milliroentgens per neon flash for dose measurement or a calibration that relates time between flashes to dose rate.

To illustrate the types of circuitry being used in the instrument, the circuit of the newer 5-v instrument is shown in Fig. 39. The radiation detector is a miniature Philips halogen-filled G-M tube. It is operated in an externally quenched mode rather than the usual self-quenched mode for purposes of securing a higher charge transfer per ionization event. High voltage is obtained from a transistor blocking oscillator and voltage quadrupler. The voltage developed by G-M tube current across the resistor and thermistor in series is duplicated by the emitter follower transistor at a lower impedance and fed back to the blocking oscillator so as to increase its repetition rate as G-M current increases. This results in a supply having a moderately constant efficiency and thus uses the minimum battery drain possible for a given situation.

The neon lamp indication is obtained by having the G-M tube current charge the 0.1-μf capacitor up to the point where the neon lamp will discharge it in the usual relaxation oscillator method. The sound alarm is obtained by passing the blocking oscillator wave form — which increases in frequency with radiation — to an amplifier transistor and hearing-aid earphone. The threshold is obtained by inserting a silicon junction diode in the emitter of the amplifying transistor and thus muting it until the base bias — taken from the emitter follower — exceeds the 1/2-v forward conduction knee of diodes of this type. The tick output is obtained by passing the neon lamp discharge current into the emitter and thus through the amplifying transistor.

Examples of special methods and dual use previously mentioned are the external quenching of the G-M tube to gain 100-fold higher output current — thus eliminating circuit complexity; the use of CR1 both as a rectifier and as a regulator by having it limit the quadrupler input voltage to its inverse Zener breakdown; the use of the blocking oscillator both as a high-voltage generator and as a source of proportional tone alarm signal; and the use of the amplifier transistor both in grounded emitter service for the warning tone and in grounded base service for the tick.

A useful range change toward lower sensitivity can be had simply by inserting a 2-megohm resistor in series with the G-M tube, thereby changing it to self-quenched operation. The sensitivity of the instrument will then be decreased by a factor of about 100, making the upper limit of proportional sound output about 100 r/hr. The addition of a highly reliable switch and indicator to make this range change available on the prototype

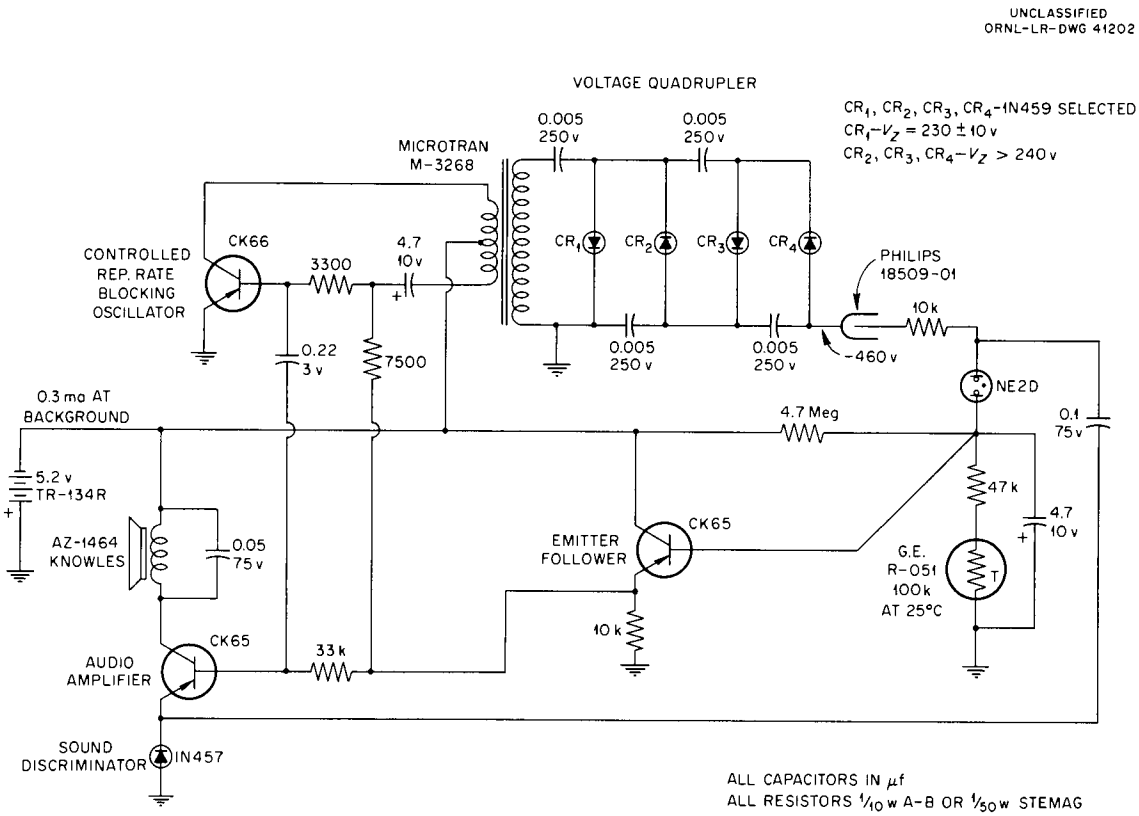

Fig. 39. Schematic Diagram of Personal Radiation Monitor Circuit.

instruments is being considered because of the great value of such a range in identifying the source of radiation in a high-level exposure accident.

Figure 40 illustrates some of the components from which the circuit is assembled. Those familiar with the usual size of components having these values will recognize considerable size reduction. The location, procurement, and testing of these components has been a major part of the effort in developing this instrument.

The physical construction of prototypes already made has been with an anodized aluminum case and a machined Bakelite top cover. Humidity protection and mechanical support for the electronic circuit are obtained by encapsulation with epoxy resin. A battery holder has been devised which eliminates all mechanical current-carrying contacts except the gold-plated surfaces which contact the battery itself under heavy spring compression.

A controlled field test of 25 instruments of the older 9-v design is in progress in order to gain experience with the reliability and suitability of the instrument under conditions of actual use. At this writing about 40,000 instrument hours of operation are complete. There is no instance of component failure. Infrequent failures have been recorded due to mechanical causes such as shorts and breakage. These mechanical failures are relatively meaningless, since those instruments now in the field were intended only as electrical prototypes and not mechanical prototypes. Some tendency of the G-M tubes toward afterpulsing or hangover following exposure has been related to the high peak current occurring in the unconventional circuit. Tests are under way to determine the degree of current limiting that can be provided and the extent to which this will solve the problem.

The 25 instruments are in use in diverse locations at the Laboratory where activity levels warrant their use. Comments received from the users are favorable and indicate that the instrument is of genuine value to them in ensuring against inadvertent exposure. The most frequent suggestions are for increased battery life and increased audible output. Circuit development toward these ends is now in progress. Preliminary work indicates that superior performance will be obtained from a design using 4- or 5-v batteries and a two-transistor push-pull blocking oscillator power supply. Increased output and dynamic range of the audible alarm may require using a separate voltage-controlled tone oscillator instead of using the power oscillator repetition rate. Resolving of these and other problems and the construction of final prototypes of the instrument will be complete by November 1959.

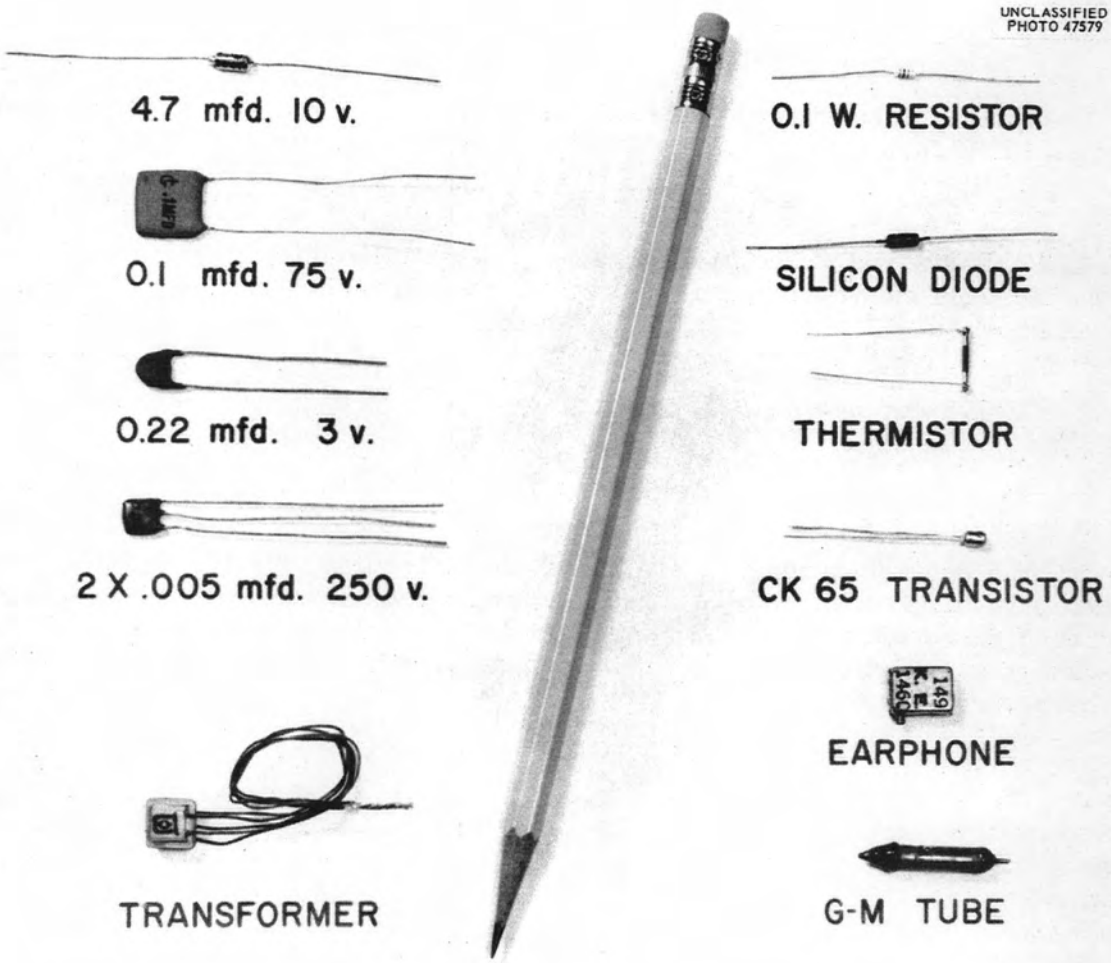

Fig. 40. Photograph of Typical Components.

SMALL CONCENTRIC CYLINDER FISSION CHAMBER

R. E. Zedler

A small-diameter concentric cylinder fission chamber has been designed and fabricated for the Tower Shielding Reactor II.

The chamber (Q-2014) is composed of four concentric stainless steel cylinders, the largest being 11/16 in. in diameter and the smallest being a 1/8-in.-dia rod. The spacing between the cylindrical surfaces is 1/16 in. The effective length is 6 in. and the over-all length (exclusive of filling tube) of the hermetically sealed chamber is 6 7/8 in.

The total surface area available for uranium coating is 271 cm^2, of which 241.5 cm^2 was actually plated with 93.18% U^{235} at a density of 1 mg/cm^2.

The fission chamber is filled to 15 psig with an argon–3% carbon dioxide gas mixture.

The endwise detection efficiency as determined by the Tower Shielding group is 0.038 count per neutron per square centimeter at an alpha background count of less than 1 count/sec. The efficiency is roughly 0.075 count per neutron per square centimeter for a neutron flux entering the chamber radially.

Figure 41 shows the pulse height distribution characteristic curve for the chamber.

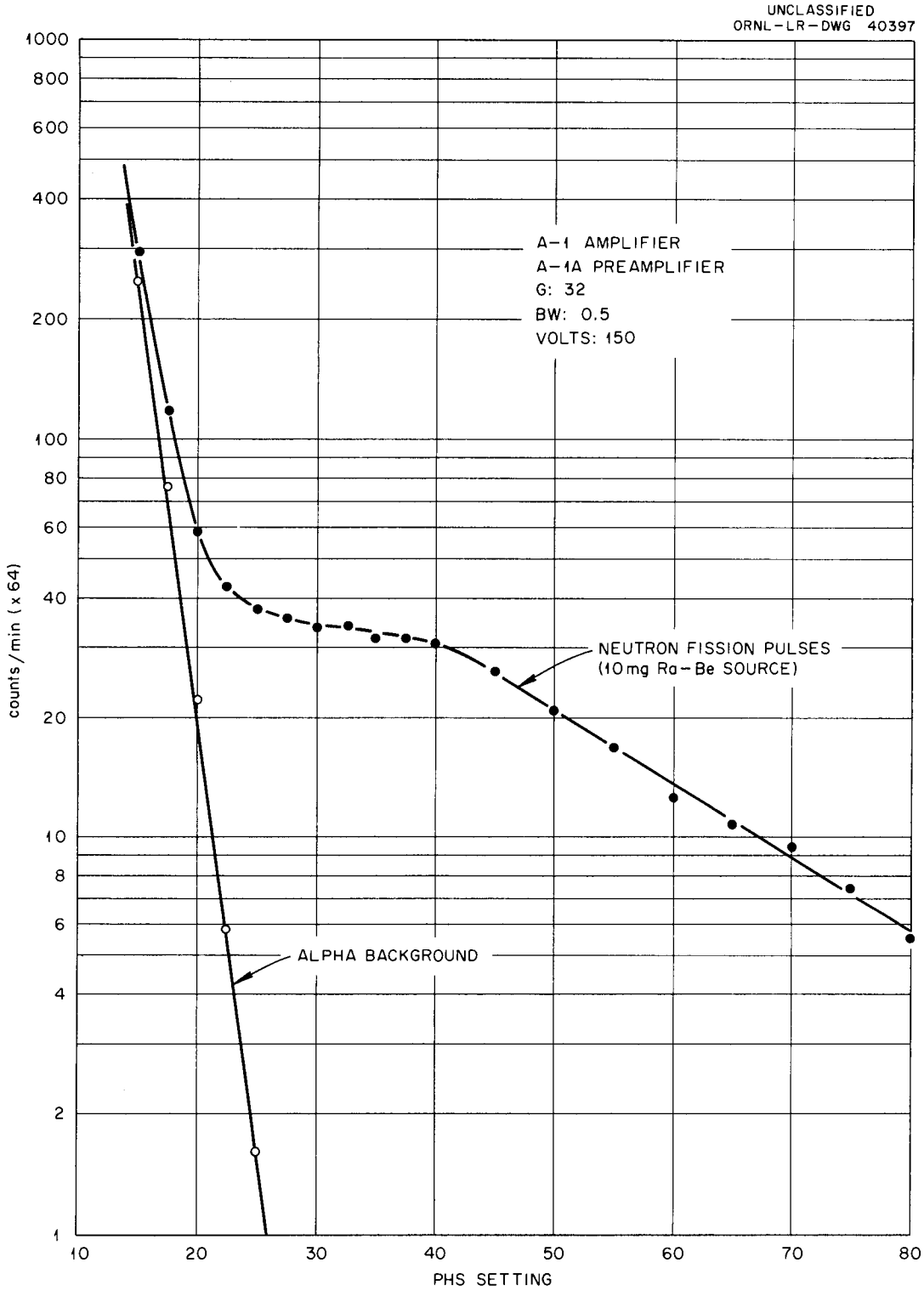

Fig. 41. Integral Pulse Height Characteristic for TSR-II Fission Chamber.

SODIUM IODIDE PHOSPHOR MOUNTING TECHNIQUES

V. A. McKay

The sodium iodide mounting techniques will be presented in two parts: first, the preparation of the crystal, and second, the encapsulation of the crystal.

The string-sawed crystal blank is first machine-cut to dimension (±0.005 in.) either by the vendor or by the Instrument Department. Most crystals that are presently purchased are machined before shipment. They are shipped in sealed cans containing a desiccant and protective paper.

After the crystal has been machined it is placed *in vacuo* for 24 hr or more to remove the surface moisture. Subsequent to this operation the crystal is transferred to a dry box. The hydrate is removed with 00 steel wool and 400-grit abrasive paper.

The better face is selected for polishing. This will face the photocathode of the photomultiplier tube. This face is first sanded with 400-grit abrasive paper that is backed by a large piece of plate glass. This step assures a flat surface. Then 600-grit paper is used in the same manner. Subsequently, finer grits may be used. These operations are followed by very light buffing with a pad of 0000 steel wool. The surface is then ready to be polished.

A firm cotton buffing wheel, with generous amounts of jewelers' rouge, is used at 100 rpm to buff the surface. This is continued until a high gloss is obtained. To protect against thermal damage, the crystal is buffed for short intervals of time and allowed to cool for 10 to 15 min between buffing operations. The residual rouge is constantly removed with absorbent cotton. Kleenex is sufficiently rough to scratch the polished surface.

Subsequent to the rouge buffing, a soft cotton buffer is used to clean away the rouge that may remain. A third buffer is used to obtain the finished gloss.

The remaining surface is abraded with 180-grit 3/4-in.-dia disk paper mounted on a rotating fixture. The speed is held to approximately 100 rpm, and the paper is only lightly applied to the crystal. The abrader must not dwell in one spot because heating may break the crystal. When this operation is finished, the crystal should be covered with 3/4-in. swirls. This gives a reasonably diffuse surface.

This completes the preparation of the crystal for encapsulation.

Presently there are two general capsule classifications. Low-mass capsules are formed with 5-mil aluminum foil and are fabricated over appropriate mandrels. Medium-mass capsules are usually made of machined aluminum parts.

Crystals are usually mounted similarly in either capsule. The crystal is usually coupled directly to the phototube with 2.5-million-centistoke DC-200 fluid and provided with a packed MgO reflector. The capsule

is sealed to the phototube with epoxy resins and evacuated. Each detector is leak-tested on a helium leak detector before it is sealed.

In general, crystals and phototubes are matched in diameter; however, there are some detectors with crystals that are smaller than the phototube. On rare occasions, some detectors have crystals that have larger diameters than the phototube. In this latter case the crystals may be coupled either to the tube or to a light piper.

Figure 42 shows a 3 × 3 in. crystal mounted on a 6363 phototube. Other lengths are mounted in this manner by simply using a can of appropriate length. Smaller diameters may be accommodated by shaping the capsule to accept both the crystal and tube.

Figure 43 shows a 2 × 2 in. well crystal mounted on a 2-in. phototube. Obviously a 2 × 2 in. solid crystal requires a small modification of the cap. For dimensions other than 2 × 2 in. the capsule needs only to be shaped to the desired crystal dimensions.

The same general scheme is applied to 1 1/2-in. tubes. With slight modifications beryllium windows have been used with crystals as small as 3/4 in. in diameter and 0.008 in. in thickness. These mounting schemes lend themselves readily to specialization and in general provide reliable and enduring detectors.

UNCLASSIFIED
ORNL-LR-DWG 40398

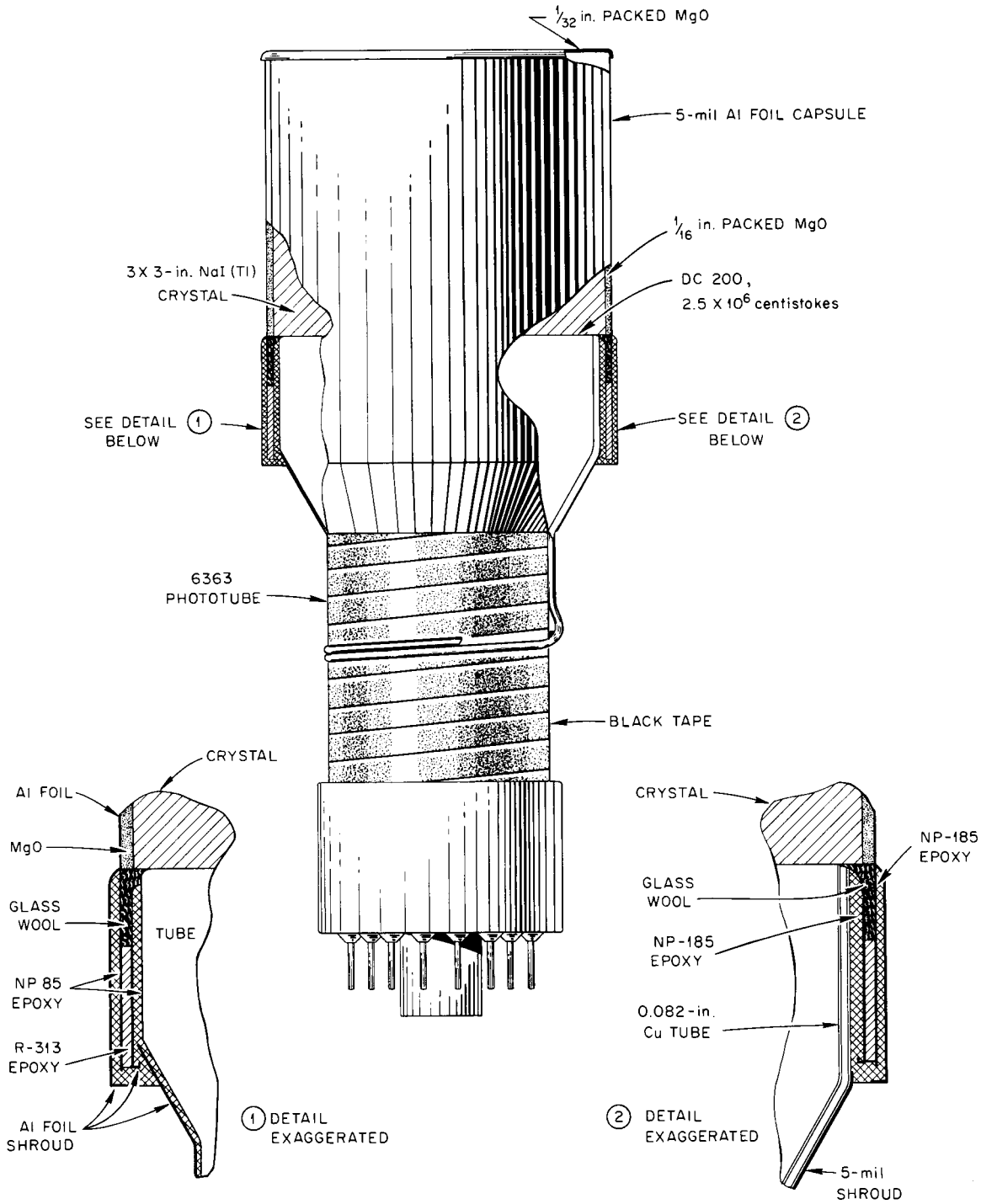

Fig. 42. 3 × 3 in. Crystal Mounted on a 6363 Phototube.

UNCLASSIFIED
ORNL-LR-DWG 40399

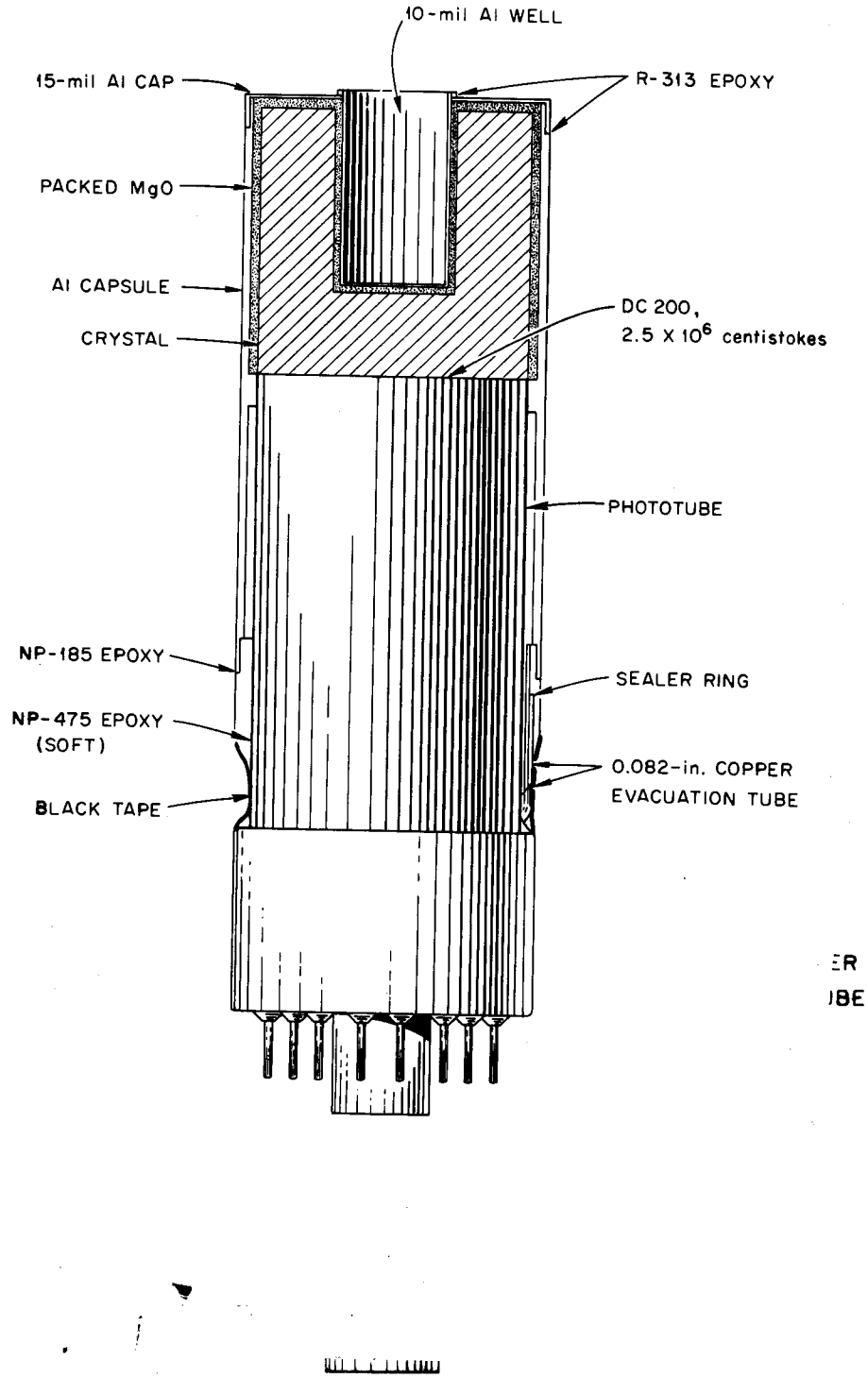

Fig. 43. 2 × 2 in. Well Crystal Mounted on a 2-in. Phototube.

See errata

SCINTILLATION SPECTROMETER SHIELD

V. A. McKay

A lead shield having an inside diameter of 12 in. and an inside height of 18 in. has been designed and placed in ORNL stores. This shield has a 3-in. thickness with stepped base, lid, and cable access.

The lid is a casting, the base is composed of 1-in. disks, and the walls are laminated with 1-in.-thick sectors. The shield is assembled on a steel base and lid actuation mechanism.

The lid is raised 2 1/2 in. by a 1 1/2-ton hydraulic jack; it is then rotated through 90° of arc to complete the opening.

The wall sectors are V tongued and grooved to prevent localized reduction in shield thickness. The sector sizes and weights are nominal and permit disassembly and movement of the shield, easy washing or decontamination, or sector replacement. Two men can readily handle any single part of the shield for these purposes. Disassembly can be accomplished within 1 hr.

The shield is completely lined with a cadmium-copper laminate that acts as a shield against lead x-ray fluorescence.

The present shield cost is approximately $1200. For an additional $100 the shield can be mounted on a dolly that will facilitate movement from one location to another.

A method for electromechanical lid actuation is being developed for those users who require frequent changes.

Figure 44 shows the interior of the shield. The phototube socket and leads are visible. The lid has been rotated clockwise exposing the shield interior. Figure 45 shows the lid actuating mechanism on the right side of the shield and the dolly to the left of the shield.

A smaller shield is available for 2 × 2 in. well-type scintillation spectrometers. It has 3-in. walls, base, and lid. The interior is 4 in. in diameter and 10 in. high. The small shield costs approximately $350.

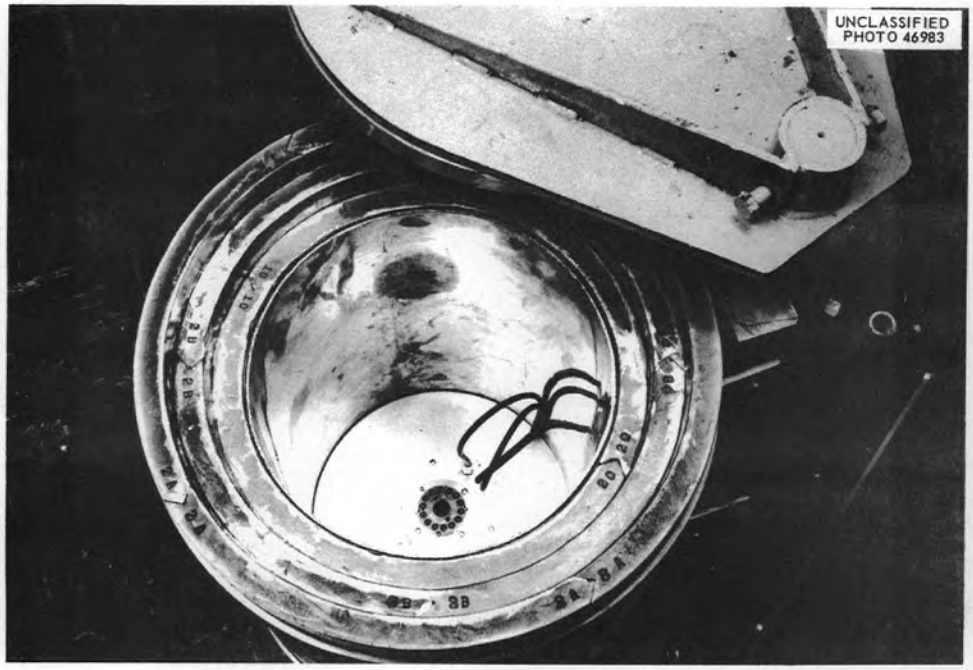

Fig. 44. Interior of Shield.

Fig. 45. Completed Scintillation Spectrometer Shield and Dolly. The lid-actuating mechanism is on the right side of the shield.

SYSTEMS ANALYSIS

R. K. Adams

In the past year the Instrumentation and Controls Division has undertaken a series of projects aimed toward providing a comprehensive systems analysis service for the research divisions. In addition to conducting basic studies in process control theory and performing dynamic instrument evaluation tests, the Process Control and Instrumentation Section has completed two significant process analyses. The description of these projects will illustrate some of the techniques which are being brought to bear on control problems at the Laboratory.

Tower Shielding Reactor II Analysis

Early in the design of the cooling water system for Tower Shielding Reactor II (TSR-II) the existence of a difficult temperature control problem was realized. As shown in Fig. 46, the cooling water supplied to the reactor must pass through long lengths of pipe and hose between the heat exchanger and the reactor. Temperature changes caused by heat gain or loss through these long lines, and the unavoidable delay before a temperature change effected at the heat exchanger could be felt at the reactor, severely limited the application of conventional temperature control equipment. There was also the necessity of determining the extent of "cold slugging" of the reactor, which could be caused by a rapid increase in heat removal rate at the heat exchanger.

By means of the Analog Computer Facility, the complete Tower Shielding Reactor cooling water system was simulated. The reactor was also simulated in order to study the interrelation of reactor power changes on the temperature control system. Because of the afore-mentioned difficult control problem, the computer simulation was used to design the temperature control system. This was done by simulation of a typical control system directly connected to the simulation of the cooling water system. In this manner the precision of temperature control resulting from a specific control system design was investigated. The temperature control system which gave the best compromise in performance when confronted with reactor power level changes, ambient temperature changes, wind and rain loading, etc., was used as the design for the control hardware now installed on the Tower Shielding Reactor cooling water system. It is interesting to note that a cascade-type control system was the approach suggested by normal control experience, but simulation proved it to be an unworkable system. This cascaded system and the system resulting from the study on the analog computer are shown in Fig. 46. Although the flow plan of the cooling water system for TSR-II is straightforward, the simulation necessitated the use of the full capacity of the Analog Computer Facility.

Volatility Pilot Plant HF Vaporizer Analysis

The design of the hydrofluorinator addition to the Volatility Pilot Plant also suggested possible control problems. The control system for

the HF vaporizer presented a problem which would be very difficult to study analytically. For this reason the HF vaporizer and its control system were simulated on the analog computer. A schematic diagram of the control system and HF vaporizer is shown in Fig. 47. It may be seen that the instrumentation for this system involves three basic control loops. It is also apparent that each of these control loops interacts in some fashion with the other loops. For instance, a change in HF liquid level might produce both a change in HF vapor flow rate and a change in vapor pressure. In an effort to closely simulate these interacting control systems, pneumatic process controllers identical to the type to be used in the plant were linked to the analog computer by means of appropriate transducers. The panel in which the pneumatic recorder-controllers and their associated transducers are mounted may be seen at the left side of Fig. 48.

In determining the system parameters required in such an analog simulation it is necessary to examine in considerable detail such things as heat transfer area as a function of liquid level in the vaporizer, the control characteristics of the vaporizer steam valve, the change in heat transfer coefficient with temperature, and the change in dissociation factor of HF with temperature. In the course of this detailed investigation a number of side benefits of system simulation are realized. It is often possible to recommend design changes or systems operating parameter modifications on the basis of this preliminary work without actually running the problem on the analog computer.

The study of the Volatility Pilot Plant HF vaporizer on the analog computer included the investigation of process controller adjustment for best control. Because of this investigation, startup of this portion of the plant need not be delayed by field controller adjustments. The nature of the physical facility of the analog computer allows a problem which has been programed previously to be rerun at some future time. Because of this the Volatility Pilot Plant control system simulation will allow some operator training at a time near the plant startup date. This is particularly advantageous because the control equipment used in the simulation is identical to that which will be installed in the plant and the simulation will act like the process without the embarrassing repercussions of overflowing tanks, boiled-dry evaporators, etc., due to operating oversight.

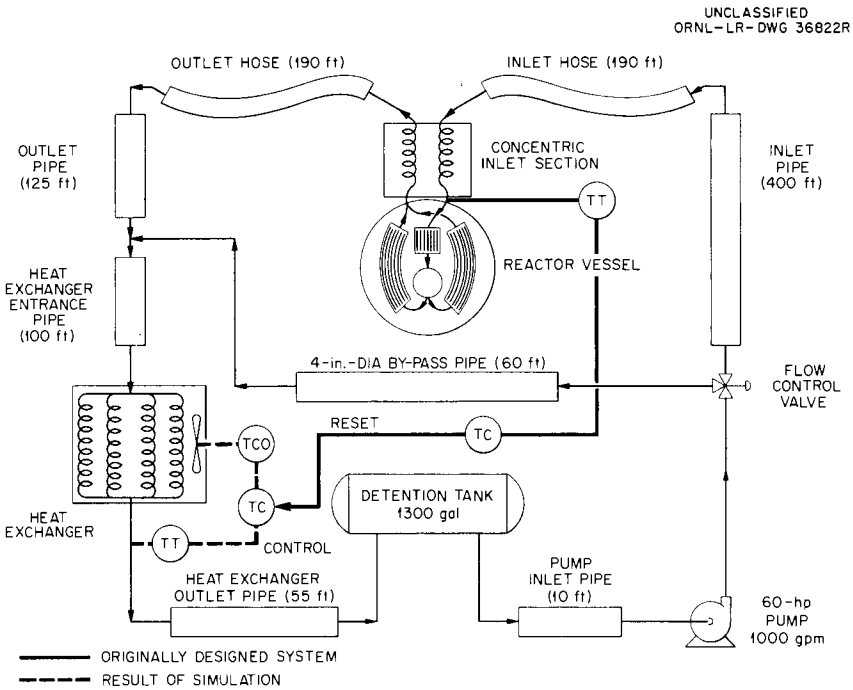

Fig. 46. TSR-II Cooling Water System and Temperature Control.

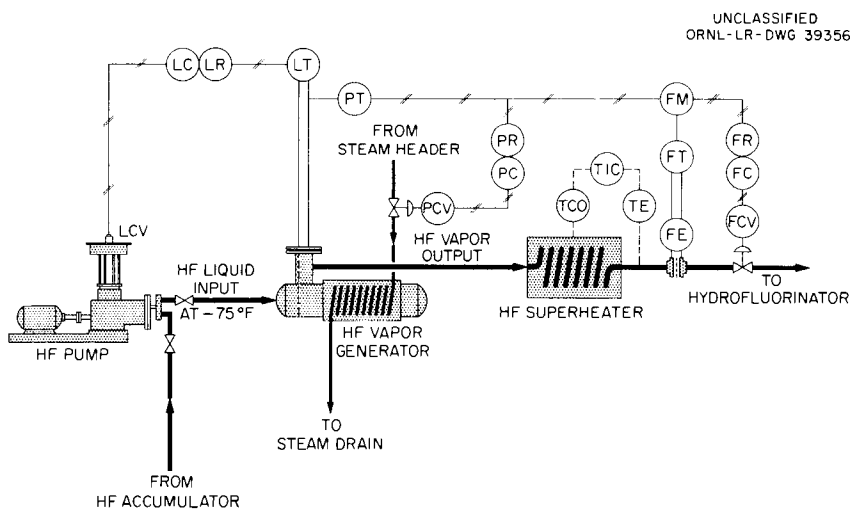

Fig. 47. HF Vapor Generator Control System.

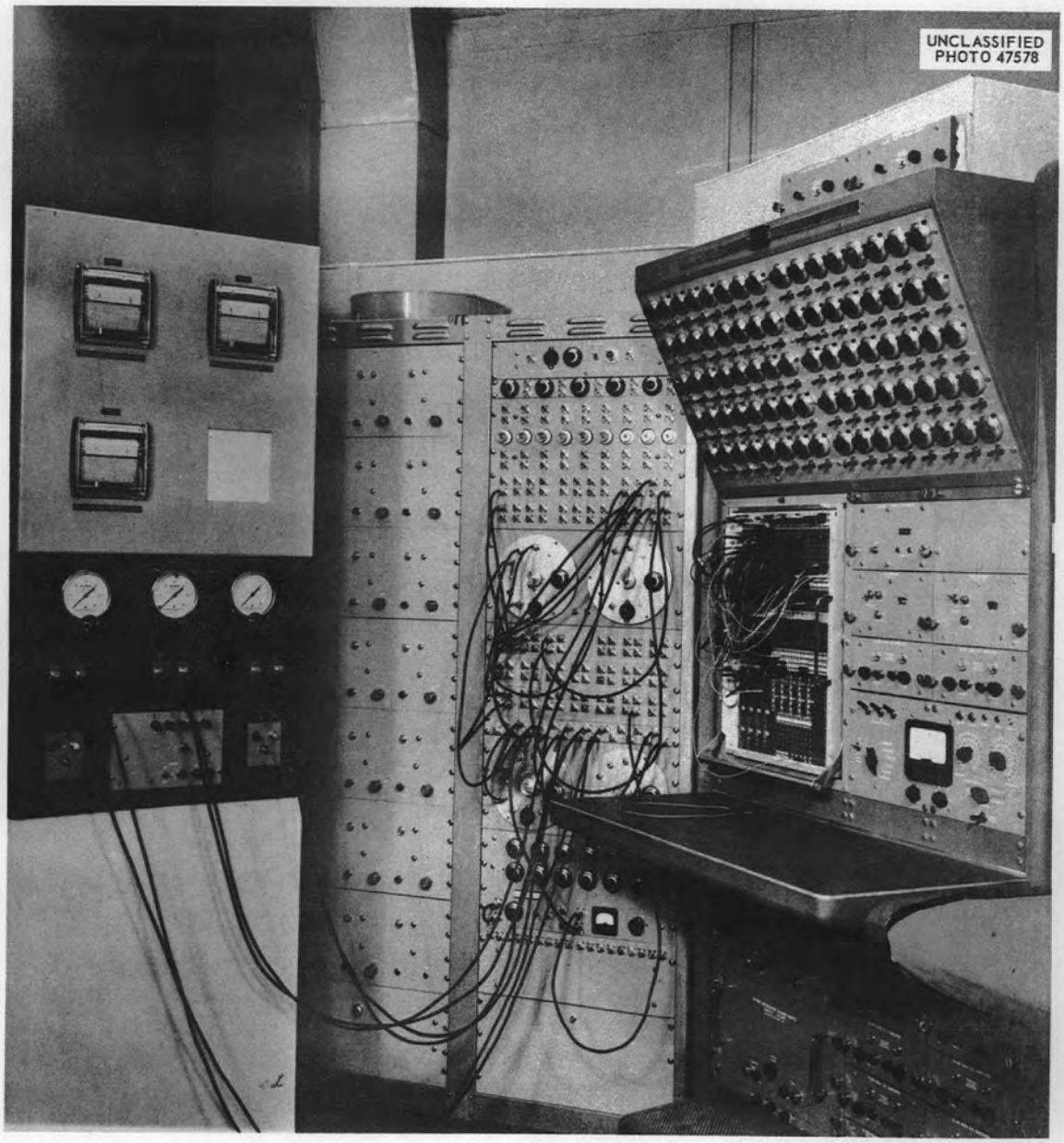

Fig. 48. Pneumatic Process Controllers Linked to Analog Computer.

TEMPERATURE CONTROL FOR BULK SHIELDING FACILITY SINGLE-CRYSTAL SPECTROMETER

R. K. Adams B. C. Duggins

The new single-crystal spectrometer for use at the Bulk Shielding Facility, as described by Knowles in an earlier report,[1] requires a control system to maintain its interior at a constant temperature to maintain constant gain of the spectrometer and to prevent thermal shock to the 9-in.-dia crystal. Room temperature (75°F) was selected as the control point since maintenance would be facilitated if the spectrometer could be removed from the pool and worked on immediately. Since the water temperature of the pool may vary from 60 to 80°F, the temperature control system must be capable of both heating and cooling. Additional requirements for the temperature control system were that it must be small in size, must operate under 25 ft of water, and must be supplied by flexible hoses.

Unique in this control system is the use of a vortex or Hilsch tube to provide the necessary small amount of cooling capacity. The Hilsch tube, Fig. 49, is an expansion refrigeration device which consists of a length of smooth tubing 12 or more diameters long into which compressed air is introduced tangentially at one end. At the end adjacent to the air inlet, there is an orifice plate with a hole approximately half the diameter of the large tube. The inlet air stream splits, with a portion spinning rapidly down the tube away from the orifice to exit at a temperature significantly higher than the inlet air and the remainder passing through the orifice and leaving at a temperature lower than the inlet. A throttling valve at the hot outlet controls the flow split. Increasing the cold air flow as a fraction of the total reduces the temperature differential between inlet and cold outlet.

A 3/8-in.-dia Hilsch tube with a 90-psig air supply provides a cooling capacity of 70 w at 13.6 scfm total air flow, with 36°F temperature differential and approximately equal flow split. The flow split for maximum cooling capacity is nearly the same as that for the largest temperature differential.

The Hilsch tube is used in combination with an electrical heater, as shown in Fig. 50, to provide the required heating or cooling. The 3- to 15-psig output of the pneumatic temperature controller is split; from 3 to 9 psig, heating is varied from maximum to zero, and from 9 to 15 psig, cooling is varied from zero to maximum. Control is accomplished on the heating cycle by the use of a pneumatically operated Variac and on the cooling cycle by a pneumatic valve on the outlet of the Hilsch tube. After the air is heated or cooled as required it is passed through the jacket of the spectrometer and exhausted to the atmosphere.

---

[1]D. J. Knowles, Instrumentation and Controls Ann. Prog. Rep. July 1, 1958, ORNL-2480, p 24.

Chief advantages of the Hilsch tube are its simplicity and small size. These features allow it to be installed directly on the spectrometer, thereby eliminating the necessity for insulated air lines to the top of the pool.

Tests on the inner vessel of the spectrometer indicate that a temperature control precision of 1°F may be attained using the system of Fig. 50.

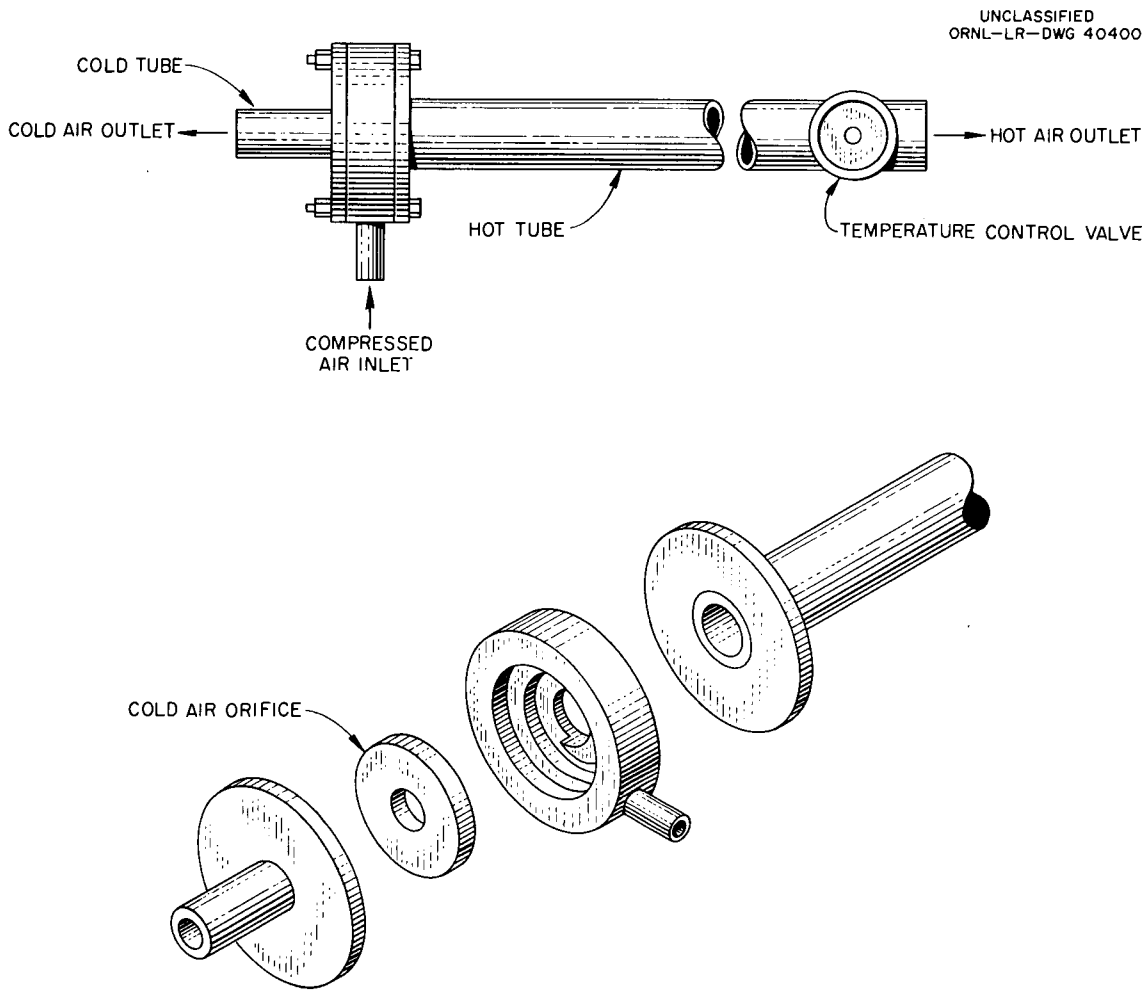

Fig. 49. A Simple Hilsch Tube.

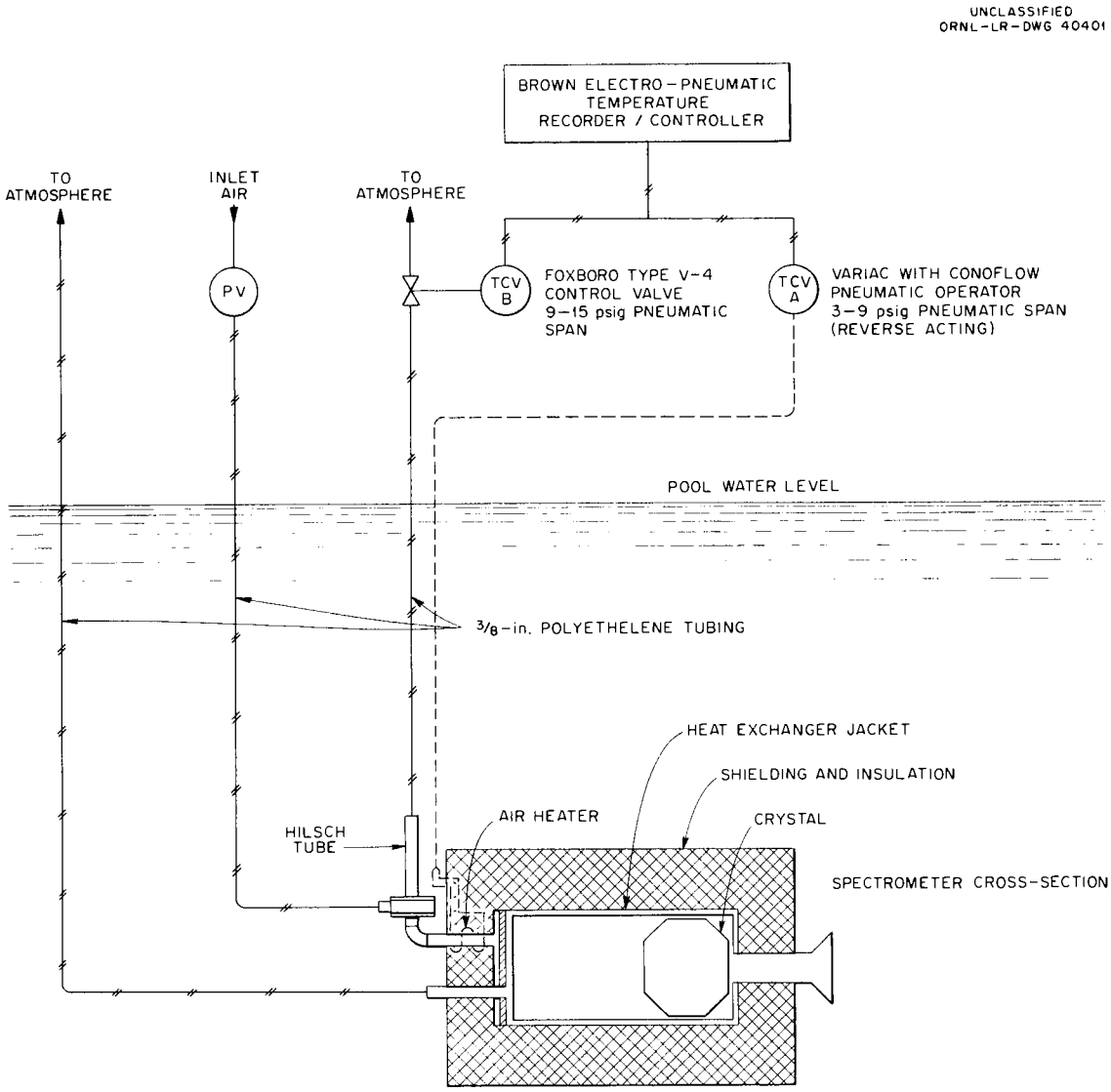

Fig. 50. Schematic Diagram of Temperature Control for BSF Spectrometer.

RADIATION EFFECTS ON THERMOCOUPLES

M. J. Kelly W. W. Johnston

In a previous report in this series[1] the effect of neutron flux on platinum—platinum-rhodium thermocouples was discussed. Additional data have been obtained, and the results are shown on Fig. 51.

The data are plotted as percentage error at 1900°F vs neutron exposure in nvt. Errors which would be obtained in a reactor are dependent on the relationship of the temperature gradient vs the neutron flux gradient. Errors shown are the maximum which should be expected, since in the test setup the temperature gradient was held within the area of maximum neutron exposure.

Figure 52 is a typical deviation curve of thermocouple error vs output. It can be seen that the effect of neutron exposure is not linear with output until fairly high temperatures are reached (900°F). This is probably due to the effect of palladium formation from the rhodium-neutron transmutation.

Chromel-Alumel thermocouples have also been irradiated up to an nvt of approximately 4×10^{20}. These thermocouples showed no effects attributable to the neutron exposure. Deviations from calibration of 20°F at 2000°F were noted but could not be correlated with neutron exposure. These results are reasonable since all irradiated couples were annealed prior to calibration. This should have eliminated the gross cold working or lattice defects caused by neutron exposure but undoubtedly left small amounts resulting from the remote handling in the hot cells. Simple calculations[2] reveal that an nvt exposure of the order of 4×10^{20} will cause net composition changes of the following magnitude in commercially available alloys: Chromel-Alumel, 0.02%; platinum vs 90% platinum—10% rhodium, 0.97% (mostly palladium from rhodium).

It can be seen that the small percentage change in Chromel-Alumel probably would not affect the calibration. The 90% platinum—10% rhodium leg of the platinum-rhodium thermocouple has, however, now approached a 90% platinum—9% rhodium—1% palladium composition, which probably causes the errors shown in calibration.

Compilation of data on this project is still in progress. A separate final report will be issued at the conclusion of this project.

---

[1]M. J. Kelly, Instrumentation and Controls Ann. Prog. Rep. July 1, 1958, ORNL-2647, p 36.

[2]D. L. McElroy, personal communication.

UNCLASSIFIED
ORNL-LR-DWG 40402

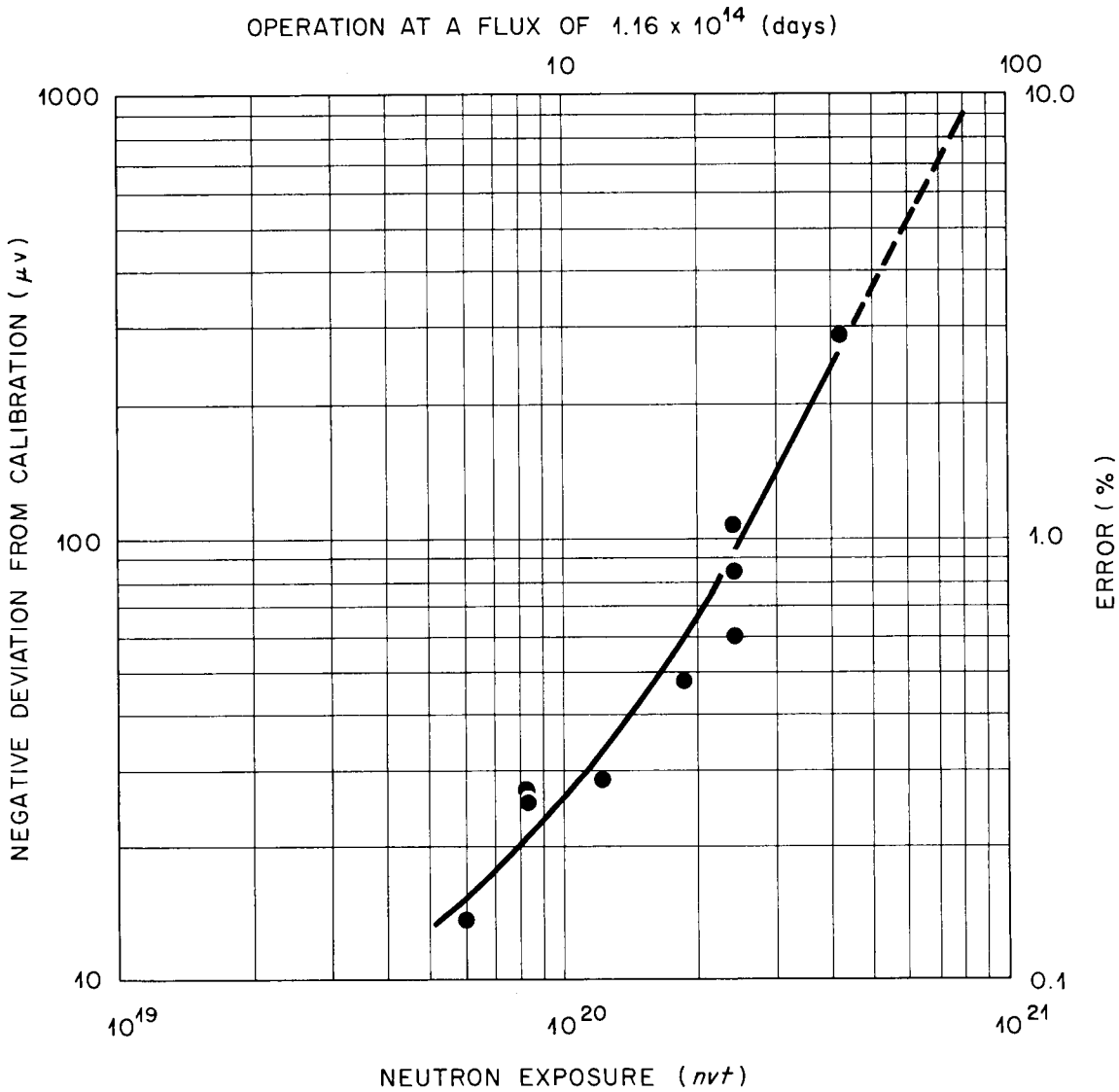

Fig. 51. Error Observed from Platinum vs Platinum–10% Rhodium Thermocouples at 10.000 mv Output (1900°F) as a Function of Neutron Exposure.

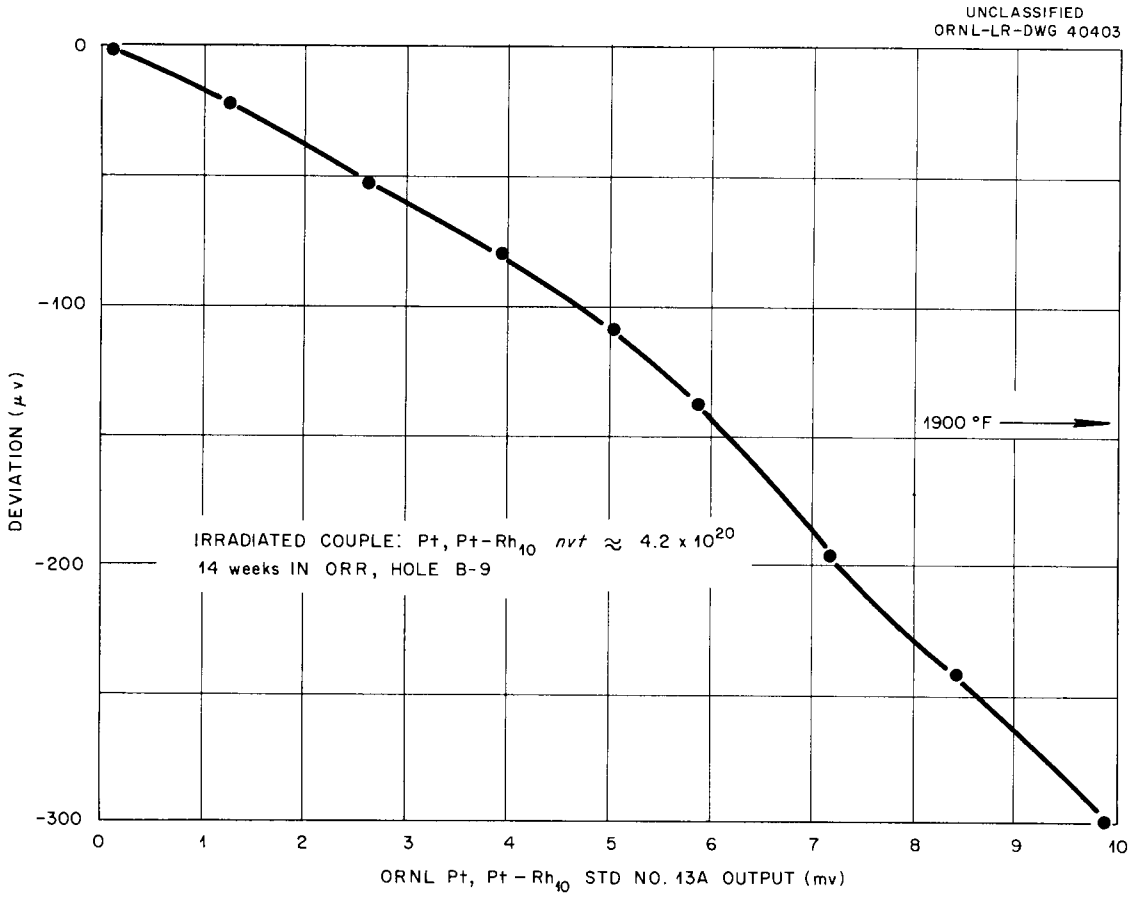

Fig. 52. Typical Deviation Curve of Irradiated Thermocouple.

UNSATURATED STANDARD CELLS

W. W. Johnston

Many research personnel at ORNL use the unsaturated type of Weston or cadmium cell as their source of primary calibration voltage. From time to time questions have arisen concerning their accuracy, and recently some specific complaints have been received. The reported errors were in general greater than those which might be expected. The reported errors were: (1) temperature coefficients greater than 4 μv (4 ppm) per °C, (2) voltage drifts in excess of 40 μv (40 ppm) per year, and (3) random fluctuations of emf of 200 μv and greater.

The Information and Controls Division Standards Laboratory, in attempting to check some of these effects, set up a bank of unsaturated cells in a chamber so that temperature could be closely controlled and measurements could be made outside the chamber. Observations were made over several weeks under varying conditions. Under stable conditions the average temperature coefficient of these cells was found to be between 3 and 4 μv/°C, over the range 25 to 35°C. During periods of changing temperature, variations of 100 to 200 μv were observed. Different periods of time, 12 to 72 hr, were required for the cells to restabilize after each temperature change. The periods were apparently related to the age of the cells.

Records maintained over the past seven years on cells supplied to this Laboratory, and observations on recertification of these cells, indicate a drift of 30 to 50 μv per year. From this information we feel that the manufacturer's stated drift rate is correct.

However, certain other spurious emf's have been noted which could not be attributed to either thermal upset or drift. In an attempt to determine their cause, one of the cells in the controlled bank was defined as the standard reference. The other four were bucked against this one, and differences were read with the aid of a microvolt amplifier whose output was fed into a recorder (50 μv full scale). One of the four cells showed abnormal disturbance patterns of the order of 50 to 200 μv under stable conditions, while the remaining cells showed no appreciable errors. Further investigation of the physical condition of the questionable cell revealed a drop of mercury in the cadmium sulfate solution above the septa. This damage to the cell was probably due to improper handling and possible inversion during shipment. Such damage could easily account for these spurious emf's, as the surface potential of mercury to cadmium sulfate is quite unpredictable and immeasurable.

One further test was made of the effect of mechanical shock on these cells by very gently sliding the temperature-controlled chamber along the bench. Shifts in the emf's of all five cells were noted. After being allowed to restabilize, all cells came back to their original emf's. Repeated tests of physical shock on this bank of cells as a bank and as individual cells resulted in temporary emf shifts of 10 to 150 μv. These shifts were completely random in magnitude and direction within this range, and restabilization times were comparable to those of thermal upset. Degree of shock had no apparent effect on these shifts, as very gentle

motion caused more error in some instances than more violent shocks in others in the same cell. In some cases movements would cause no observed error in a cell and at other times there would be an induced error. This clearly indicates that for precise work physical location stability is demanded.

The observations indicate that unsaturated standard cells may be relied upon to ±200 μv (0.02%) for normal use. When the cells are used in an air-conditioned laboratory free from drafts or hot- or cold-zone exposure and allowed to thermally and physically stabilize for 72 hr, a reliability of ±50 μv (0.005%) can be expected. To obtain better accuracy careful selection of the cells is required and they must be maintained in a constant (±0.1°C) temperature environment. Accuracies of about 5 ppm can be expected with extreme care.

ADDITIONS AND MODIFICATIONS TO THE INSTRUMENTATION OF THE FISSION PRODUCTS PILOT PLANT

L. H. Chase T. M. Gayle
H. E. Cochran P. D. Koster
B. Lieberman

During the year major modifications and additions have been made to the Fission Products Pilot Plant (F3P) facilities. The changes were necessitated by process improvements and the requirement for the separation of three additional isotopes, Pm^{147}, Cs^{137}, and Ce^{144}. These process changes have resulted in an addition or substitution of approximately 500 instrument components, representing a 50% increase in the plant instrumentation. Figure 53 gives an over-all conception of the process scheme. The following six major additions or modifications have been made:

1. Modifications of Original Process. – The piping in the tank farm was revised for greater flexibility of process solution transfer. Inside cell 6, the evaporator was modified so that instead of being a continuous operation, initial evaporation of the feed material became a batch-type operation. Two new tanks were added to the F3P tank farm, and spare thermocouples were installed in all the process vessels.

2. Cell 9 – Rare Earth Separation. – In cell 9 the Y^{91} and Ce^{144} are separated from the trivalent rare earths by extracting in batch mixer-settlers. The trivalent rare earths, including Pm^{147}, are precipitated as oxalates prior to removal to Building 3028, where the Pm^{147} is separated by ion exchange. The Ce^{144} is transferred to cell 11 for final processing.

Shown in Fig. 54 is 6 ft of panel board which was added for cell 9. Process measurements to be made are liquid level, density, temperature, and liquid interface position in the mixer-settler units. Since the success of the operation depends in part upon the successful separation of the aqueous phase (containing the promethium) from the organic phase in the mixer-settler unit, two interlocking systems are used. Measurement and control of the phase separation are pneumatic. A Taylor differential pressure transmitter is used in conjunction with a Foxboro ribbon-type indicator for measurement of the position of the interface, and the system is designed so that the aqueous solution transfer is terminated when the interface position is 2 in. from the bottom of the tank. A secondary control system consisting of a pair of conductivity electrodes is installed in order to sense the interface (by virtue of the difference in conductivity of the two phases) as it passes by the extreme bottom of the tank. This is intended to allow precise separation of the two process phases in the mixer-settler unit. The conductivity probes did not prove successful due to the fact that after one or two runs precipitate became coagulated between the probe and the shell of the vessel. This caused the probes to indicate the presence of the more conducting medium whether or not this was actually the case. Consequently, during radioactive operation the conductivity probes were not used, and satisfactory operation was obtained from the pneumatic interface position indication.

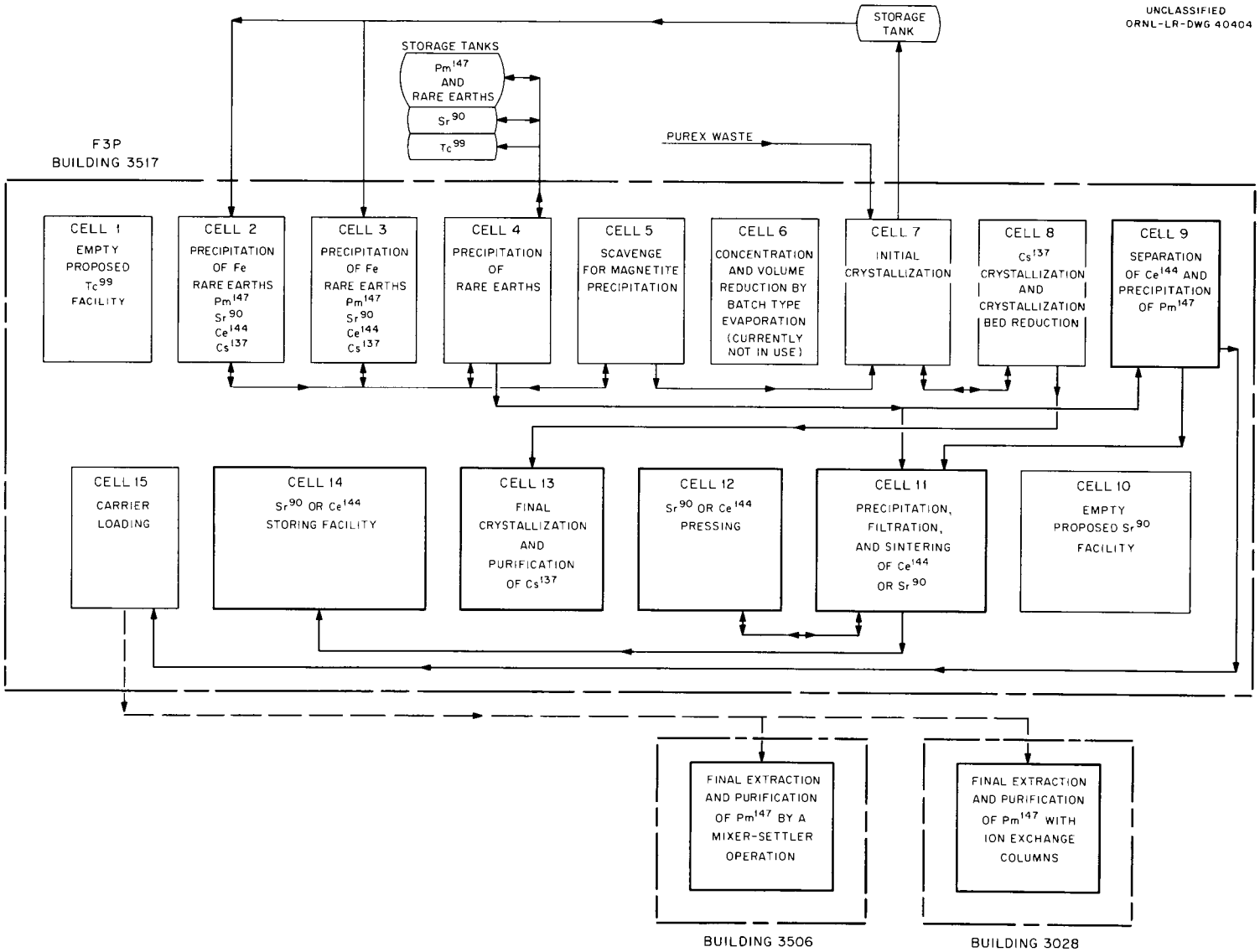

Fig. 53. Schematic Diagram of Fission Products Pilot Plant.

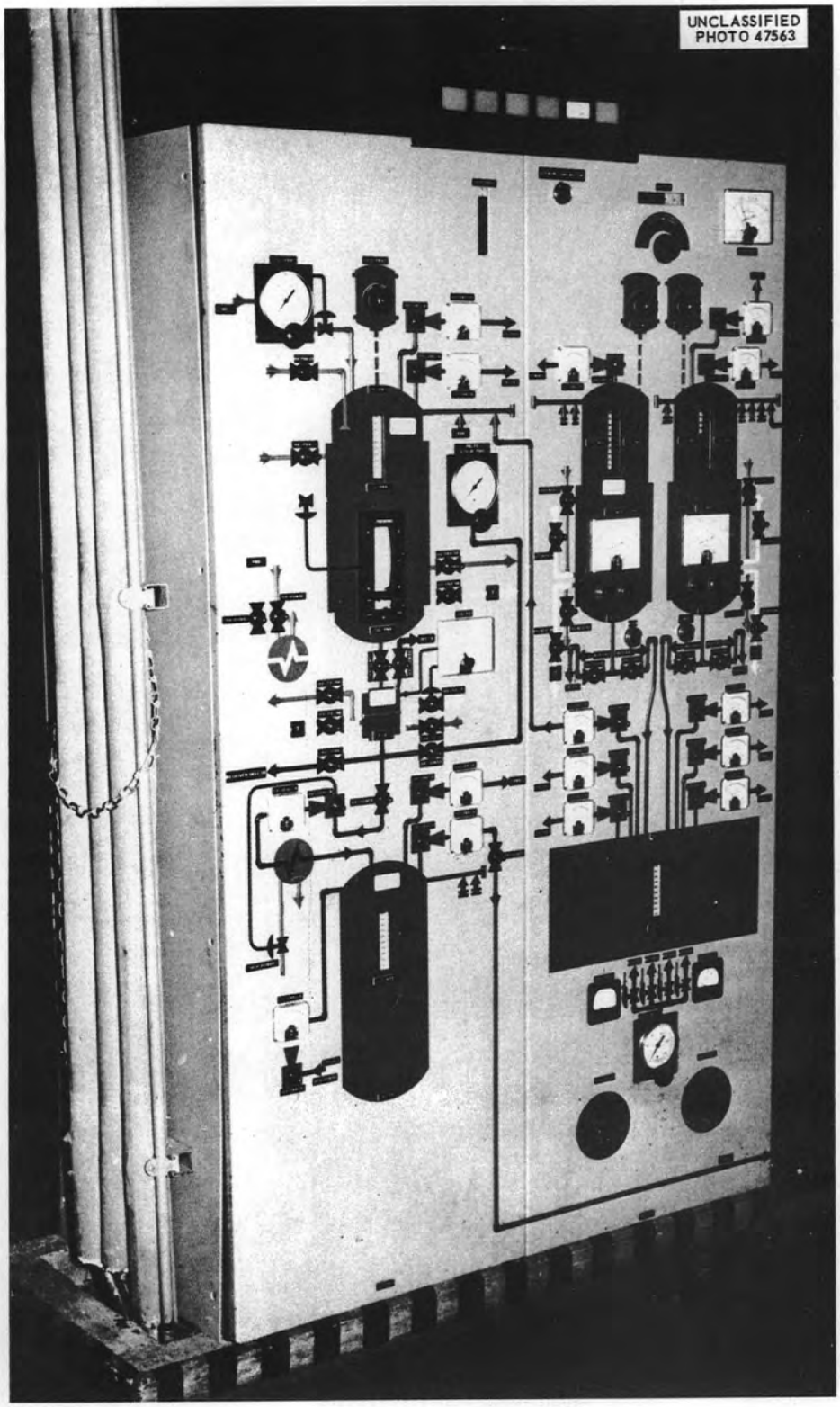

Fig. 54. Cell 9 Panel Board.

In addition to rendering the conductivity probes inoperative, the precipitate formed in the mixer-settler tank caused a last-minute change in design. Originally, solution was transferred out of the mixer-settler by gravity with metal-seated process valves provided for shutoff. After one cold run it was found that the precipitate caused the valves to leak. At this time it was decided to abandon the gravity transfer idea with attendant valve problems and use an air lift for process solution transfer. This has been found to be a satisfactory solution to the problem

3. Building 3028 – Pm^{147}. – The process facilities in Building 3028 were designed and built for the purpose of extracting Pm^{147} in its pure form from the feed material obtained from the Multicurie Fission Products Pilot Plant. The actual final extraction of Pm^{147} from neodymium, europium, traces of Ce^{144}, and remaining inactive rare earths is effected by passing the stream through ion exchange columns.

The instrumentation phase of the job cost $30,000 and involved 8 ft of panel board (see Fig. 55) with 8 ft of transmitter rack. The bulk of the instrumentation involved measurement of liquid level, temperature, and remote switching of process valves. All the process valves were of the electrical solenoid type equipped with 24-v coils so that the power cabling could be run in the open.

In this type of process the ion exchange columns are more efficient if they are operated at an elevated temperature. This was attempted by electric heating, but a uniform temperature could not be attained over the length of the column, and so the idea was abandoned.

Initially, plastic diaphragm closure solenoid valves were used. These valves were not successful due to their inability to operate under certain upstream and downstream pressure conditions. They were replaced with stainless steel body valves, which have proved successful.

4. Building 3506 – Pm^{147}. – The facilities in Building 3506 were designed and are currently being built to effect the separation and purification of Pm^{147} by a continuous countercurrent mixer-settler operation on the feed obtained from the rough extraction made in cell 9 of the Multicurie Fission Products Pilot Plant.

Eight feet of panel board (see Fig. 56) was provided, with 10 ft of associated transmitter rack. Conventional measurements to be made are temperature, liquid level, and liquid density. Two significant features are worthy of note. First, mixer-settler efficiency can be optimized by controlling the throughput. Because of the nature of the equipment, the flow must be measured by determining the position of the interface and controlled by raising and lowering a weir at the outlet. The measurement of the interface level is done in several stages of the mixer-settler units by means of probes which detect the change in conductivity as they are lowered through the interface of the two phases. Both the positioning of the probes and the weir height adjustment are done pneumatically. Second, the manner of checking the output of the feed pump is novel. The output of the pump is run to the highest point in the process cell into

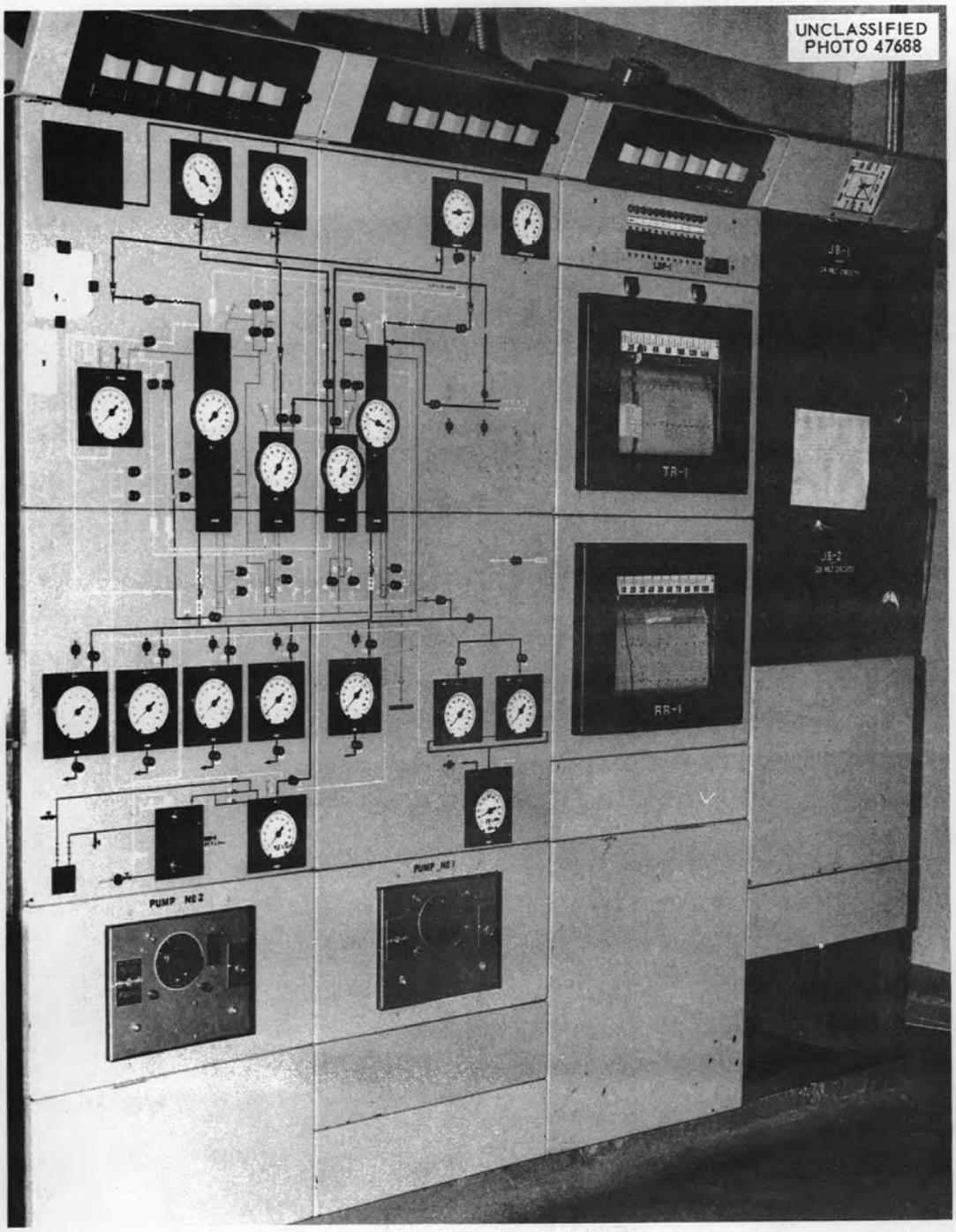

Fig. 55. Building 3028 Panel Board.

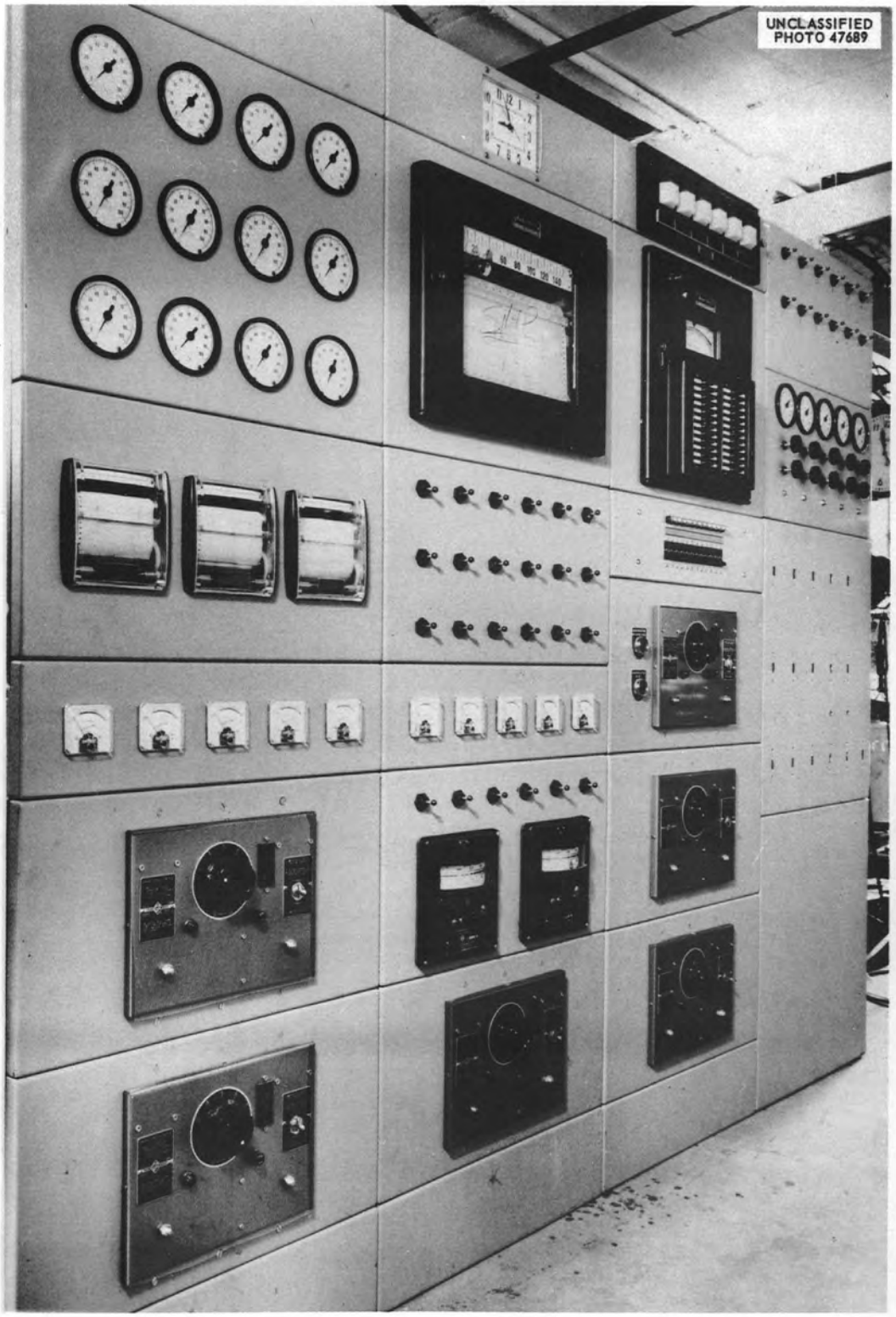

Fig. 56. Building 3506 Panel Board.

a box with a perforated wall which presents an obstruction to the flow path in the center of the box. After passing through the perforated wall the fluid is gravity-fed to its destination. This arrangement gives the effect of a weir except that the variation in level at the inlet side is greater than that normally encountered in a 90° V-notch weir. The liquid level in the upstream side is then measured and the system calibrated for liquid level vs fluid flow.

5. Cell 13 – Cs^{137}. – The facilities in manipulator cell 13 were designed for the final purification of Cs^{137}. The process equipment is largely glass and was not extensively instrumented. Two feet of panel board was supplied (see Fig. 57) which contained a strip chart temperature recorder, an indicating controller for an evaporator high-temperature cutoff, and a remote igniter system for a Bunsen burner.

The final purification of the Cs^{137} is a crystallization operation. In order to determine the point at which crystals are formed in the two crystallizers in the process, a single-point temperature recorder with a four-point switch was provided. By recording the decreasing temperature of the crystallizers the operator is enabled to note the point of actual crystal formation, which shows as a break in an otherwise smoothly decreasing temperature curve for the crystallizer being used, since this is an exothermic reaction.

The remote igniter system for the Bunsen burner which supplied heat to the evaporator consisted of a 115-v/10,000-v transformer and a pair of movable platinum electrodes located near the Bunsen burner inside the manipulator cell. When fired, the arc was 1/4 to 3/8 in. long and proved quite satisfactory. There was little, if any, evidence of electrode burn-up, as the arc was drawn only for a short period of time.

6. Cells 11, 12, and 14 – Ce^{144}. – Manipulator cells 11, 12, and 14 are used for the purification of Ce^{144}. The feed material comes from the main process cells of F3P into a hold tank in cell 11. From this hold tank it is transferred by jet into a precipitator in cell 11, where the Ce^{144} is precipitated. The slurry is run through a filter screen which catches the precipitate and allows the remaining solution to enter the receiver tank. The precipitate of Ce^{144} remaining on the filter bed is dried, ground up, and transferred to cell 12 to be pressed into a cylindrical shape. The cylinders go back to cell 11 for sintering. From there, they are moved by means of an intercell conveyor to cell 14 for weighing, measuring, and storing.

The instrumentation for these cells involves 8 ft of panel board (see Figs. 58, 59, and 60). The instrumentation requirements for cell 14 include only rotameters, hand valves, and pressure gages for the distribution of the sparge air and cooling water for the storage containers.

Cell 12 required no instrumentation, since all the operations are mechanical in nature and visually controlled.

Cell 11 required the bulk of the instrumentation, involving liquid level, temperature, and pressure measurement. In this job, the problems

produced when an accessible semiradioactive area for the pneumatic transmitters is not provided can readily be seen. As such an area was not available it was necessary to place the transmitters in a cubicle fabricated of 3 1/2-in. armor plate (see Fig. 61). Although cell 11 has not yet operated, problems involving the maintenance of the transmitters in this cubicle are inevitable.

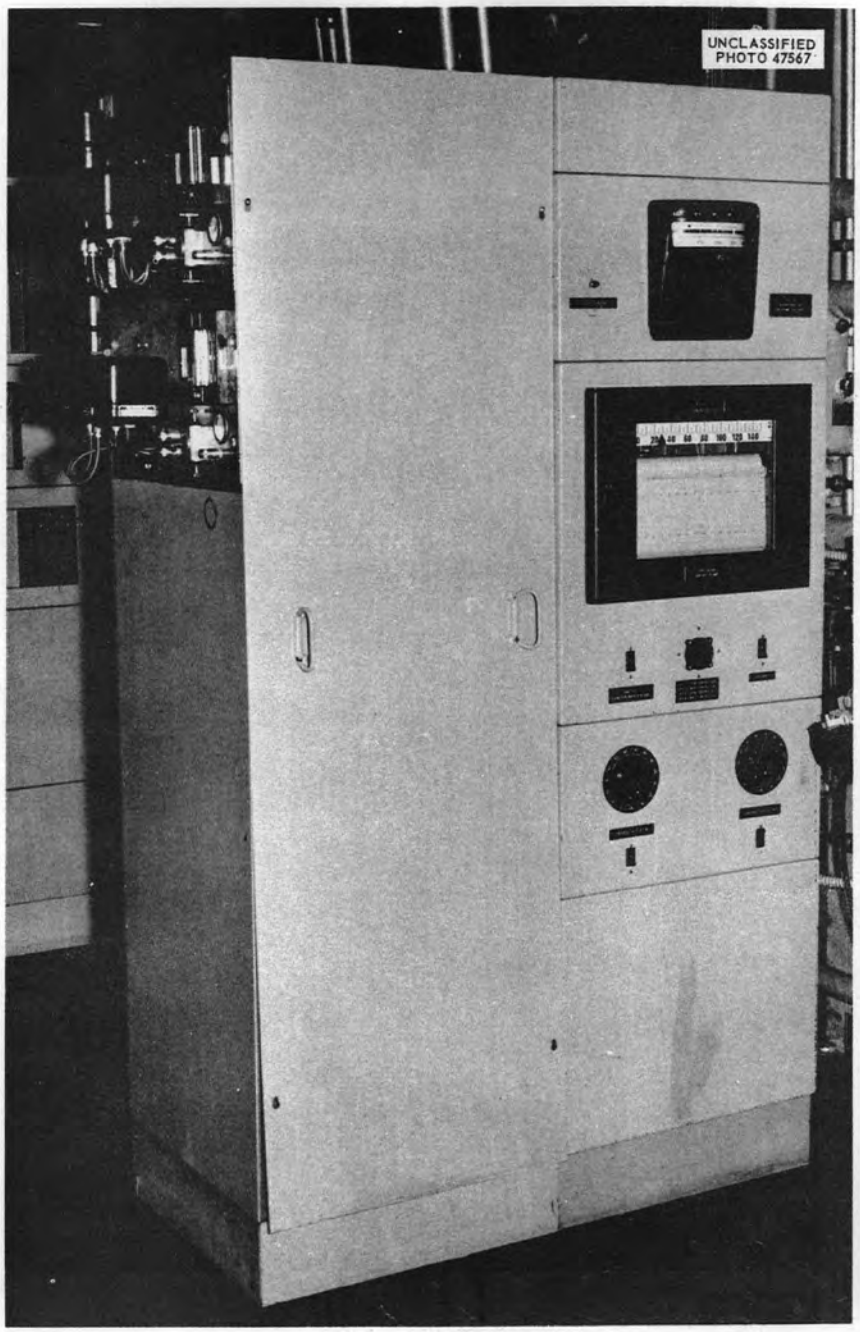

Fig. 57. Panel Board for Cell 13.

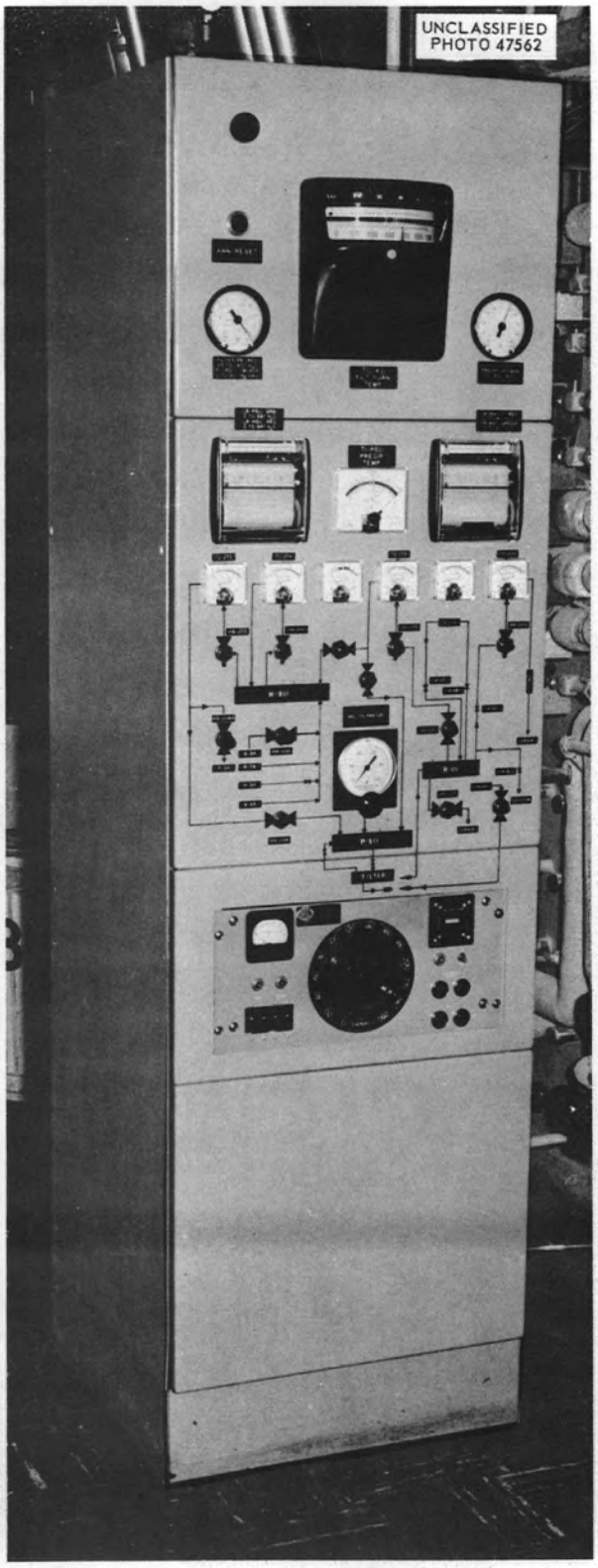

Fig. 58. Cell 11 Panel Board.

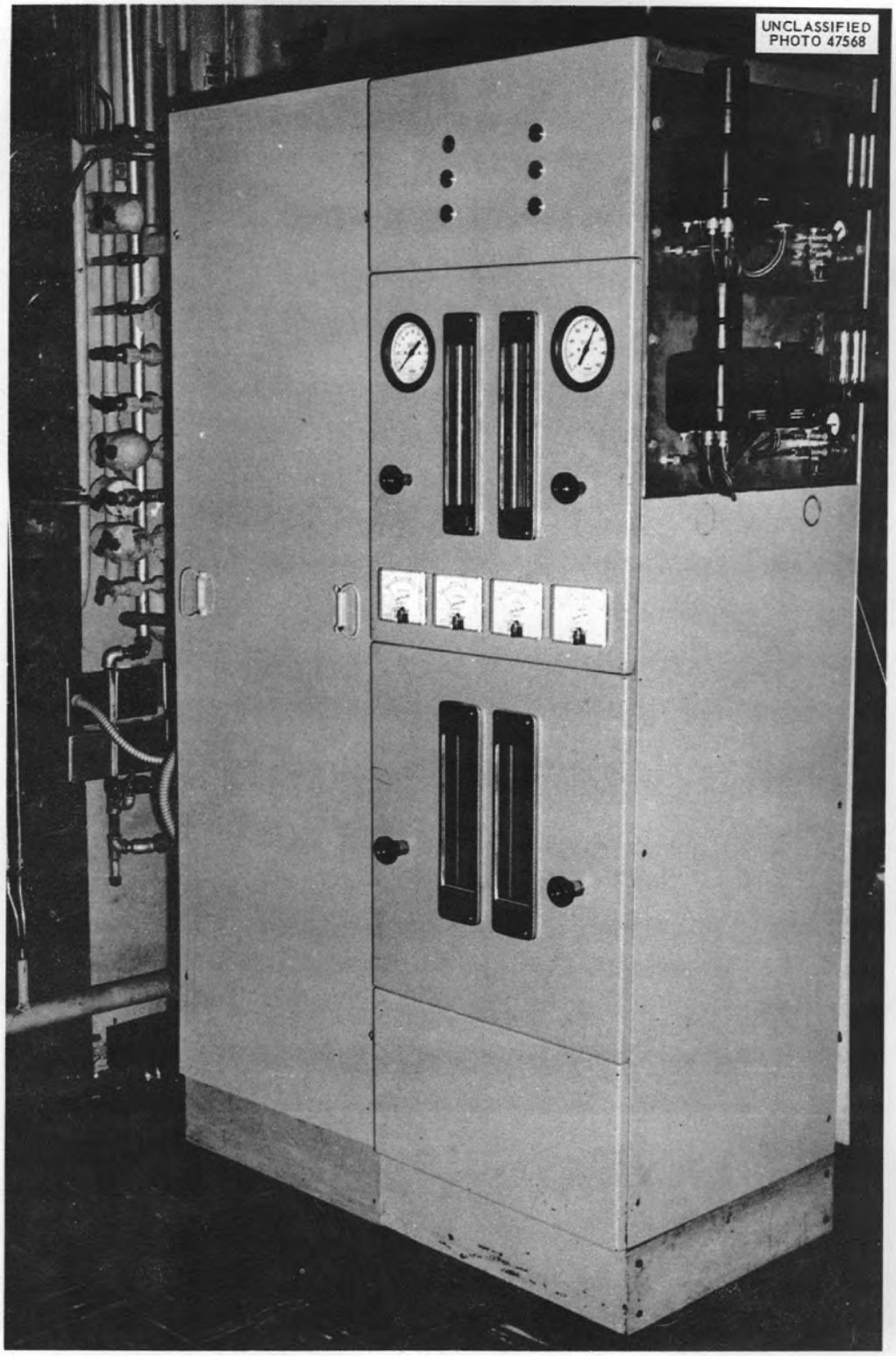

Fig. 59. Cell 14 Panel Board.

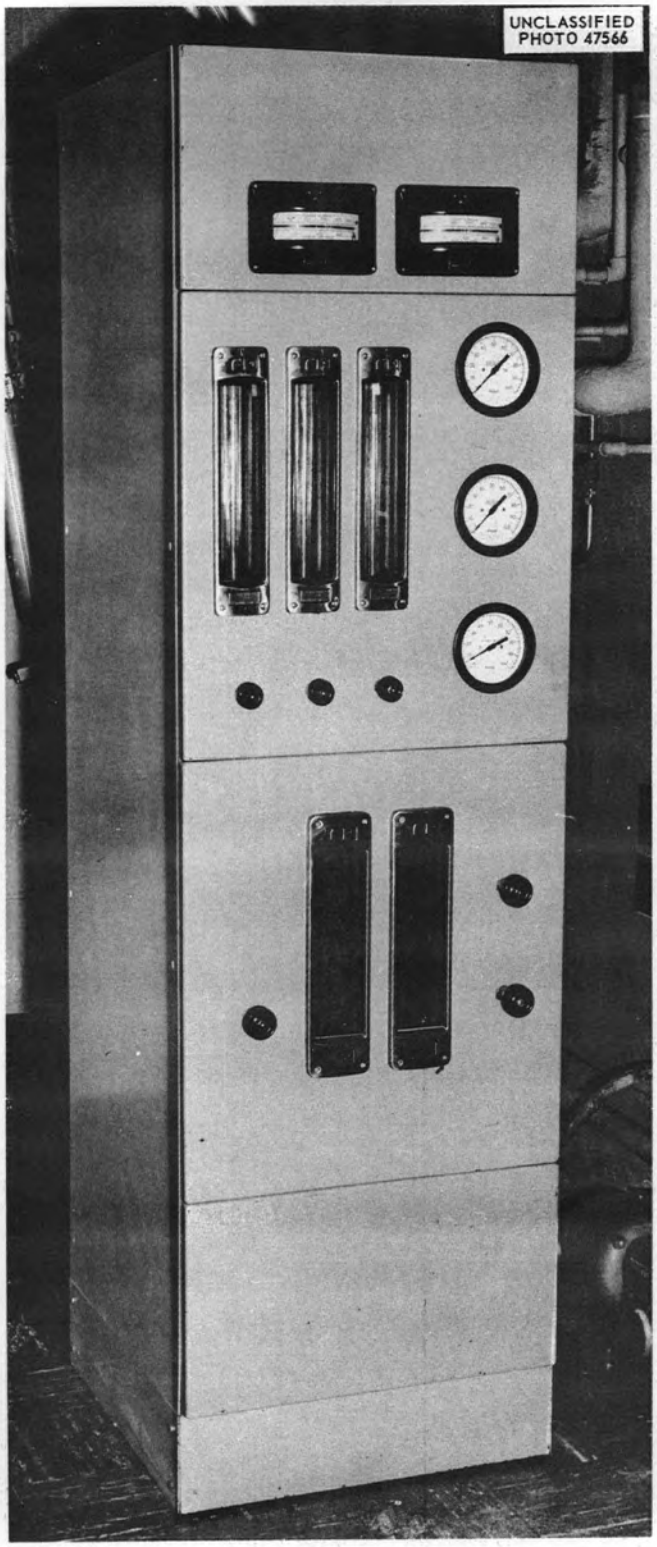

Fig. 60. Additional Panel Board for Cell 14.

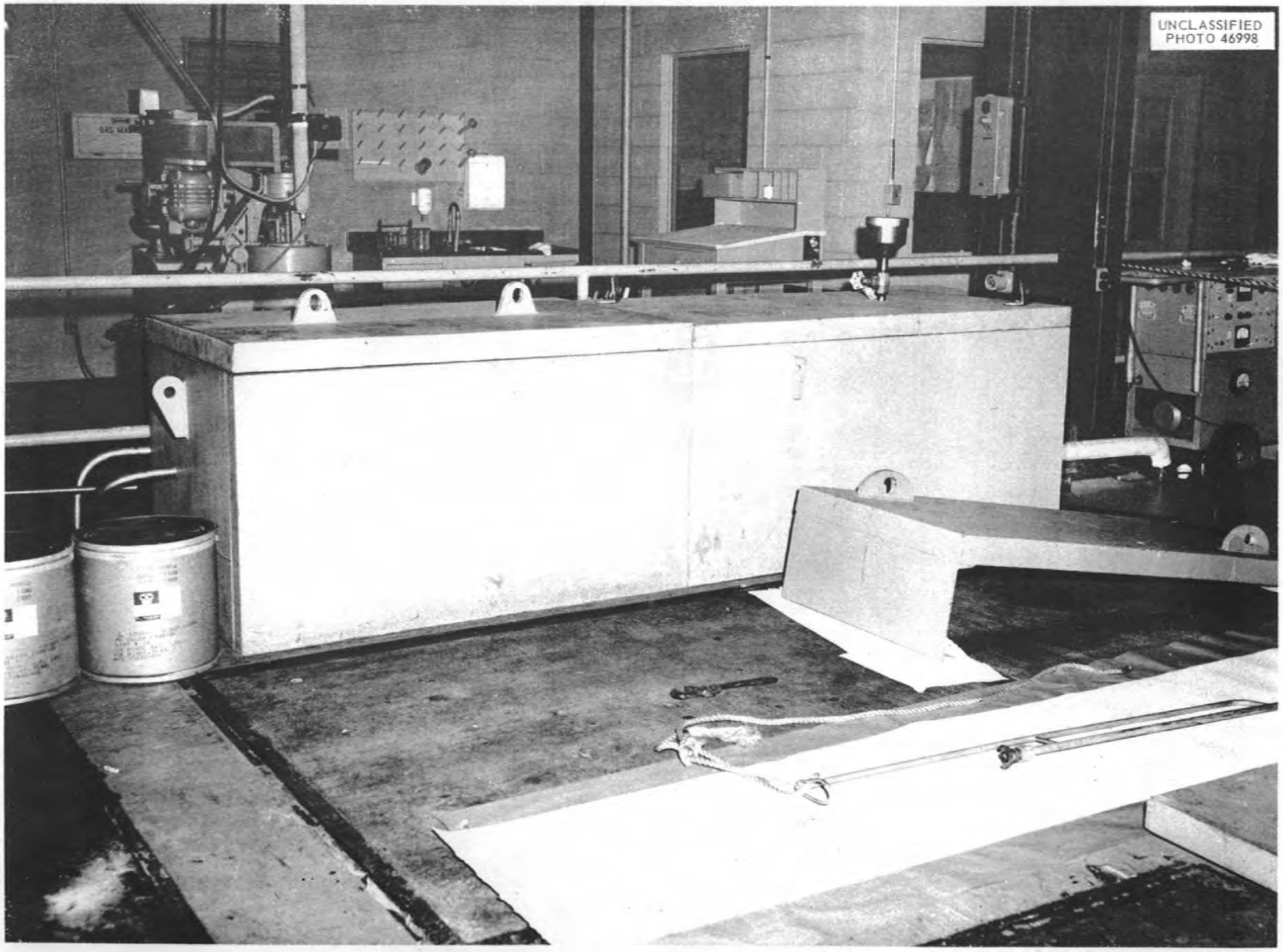

Fig. 61. Transmitter Cubicle for Cell 11.

INSTRUMENTATION FOR IN-PILE EXPERIMENTS

L. H. Chase J. L. Horton C. S. Lisser

The Oak Ridge Research Reactor (ORR) has presented problems not encountered with in-pile experiments in the other ORNL reactors due to its short allowable down time and the larger number and greater complexity of experiments. After operating the reactor at full power for some time, a shutdown for longer than a few minutes (depending on the period within the fuel cycle) will allow xenon poisoning to prevent the reactor restarting. A scram requires a minimum of 5 to 10 min for rod recovery, which further limits the allowable down time. Shutdowns exceeding the restarting time necessitate a fuel change requiring 4 to 6 hr. If the ORR is to operate a reasonable percentage of the time the unscheduled shutdowns must be kept to a minimum and the duration of these shutdowns must be kept less than the xenon buildup time. Operating experience at the Graphite Reactor and the LITR indicated that a serious re-evaluation of the instrumentation and instrument practices had to be made to meet the requirements of the ORR. As a result of this evaluation the following changes have been made to provide more reliable instrumentation:

1. An In-Pile Instrumentation and Controls Committee was appointed to formulate instrument philosophy, review instrumentation design, and serve in an advisory capacity to the Experiment Review Committee and the Operations Division.
2. An Instrument Coordinator for experimental instrumentation was appointed to serve between the Operations Division and the Instrument Department.
3. The safety system has been redesigned to provide standard safety circuits, equipment, drawings, and procedures for connecting experiments to reactor control.
4. The Instrumentation and Controls Division has prepared a list of preferred industrial instruments and associated hardware to provide greater reliability, availability of replacement parts, and ease of maintenance.
5. The design of control panel boards and other instrumentation is standardized wherever possible to minimize maintenance troubleshooting.

Instrumentation was installed in the ORR by the Instrumentation and Controls Division on the following experiments:

1. lattice position C-1: Solid State Division fuel element capsule for the spectrometric analysis of fission gases released by ceramic fuel elements (see Fig. 62);
2. lattice position B-9: Solid State Division gas-cooled test facility for determining performance of ceramic-clad fuel elements (see Fig. 63);
3. lattice position B-1: General Electric ANPD water-cooled capsule for material evaluation (see Fig. 64);

4. lattice position F-2: General Electric ANPD air-cooled facility for the evaluation of fuels and other materials pertinent to their reactor (see Fig. 65);
5. pool face position 6: Physics Division helium recoil experiment;
6. pool face positions 1, 2, 3, 7, 8, and 9: Reactor Projects Division Gas-Cooled Reactor capsules (instrumentation provided by the Instrumentation and Controls Division's RPD Instrumentation Group) (see the following section, "EGCR Fuel Element Capsule Tests in the LITR and the ORR");
7. north horizontal facility HN-1: HRP corrosion loop (instrumentation provided by the Instrumentation and Controls Division's HRP Instrument Group).

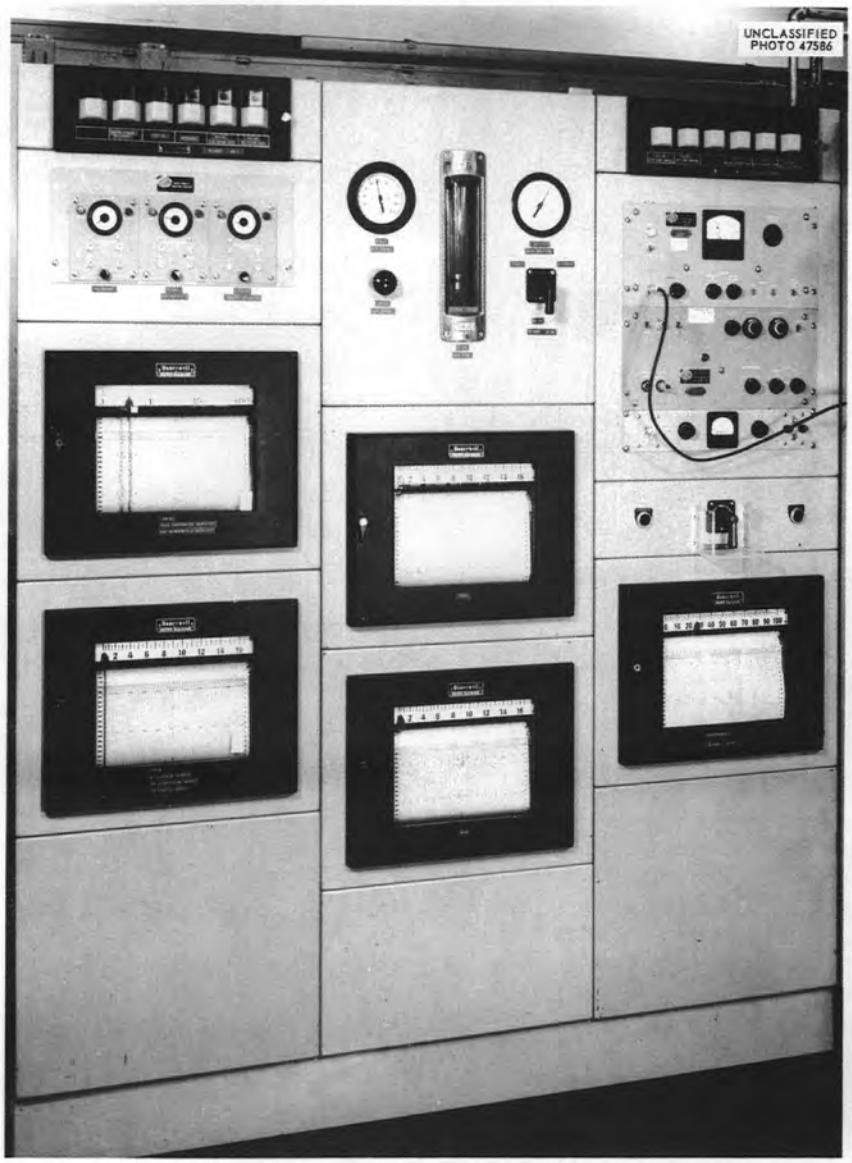

Fig. 62. Panel Board for Lattice Position C-1.

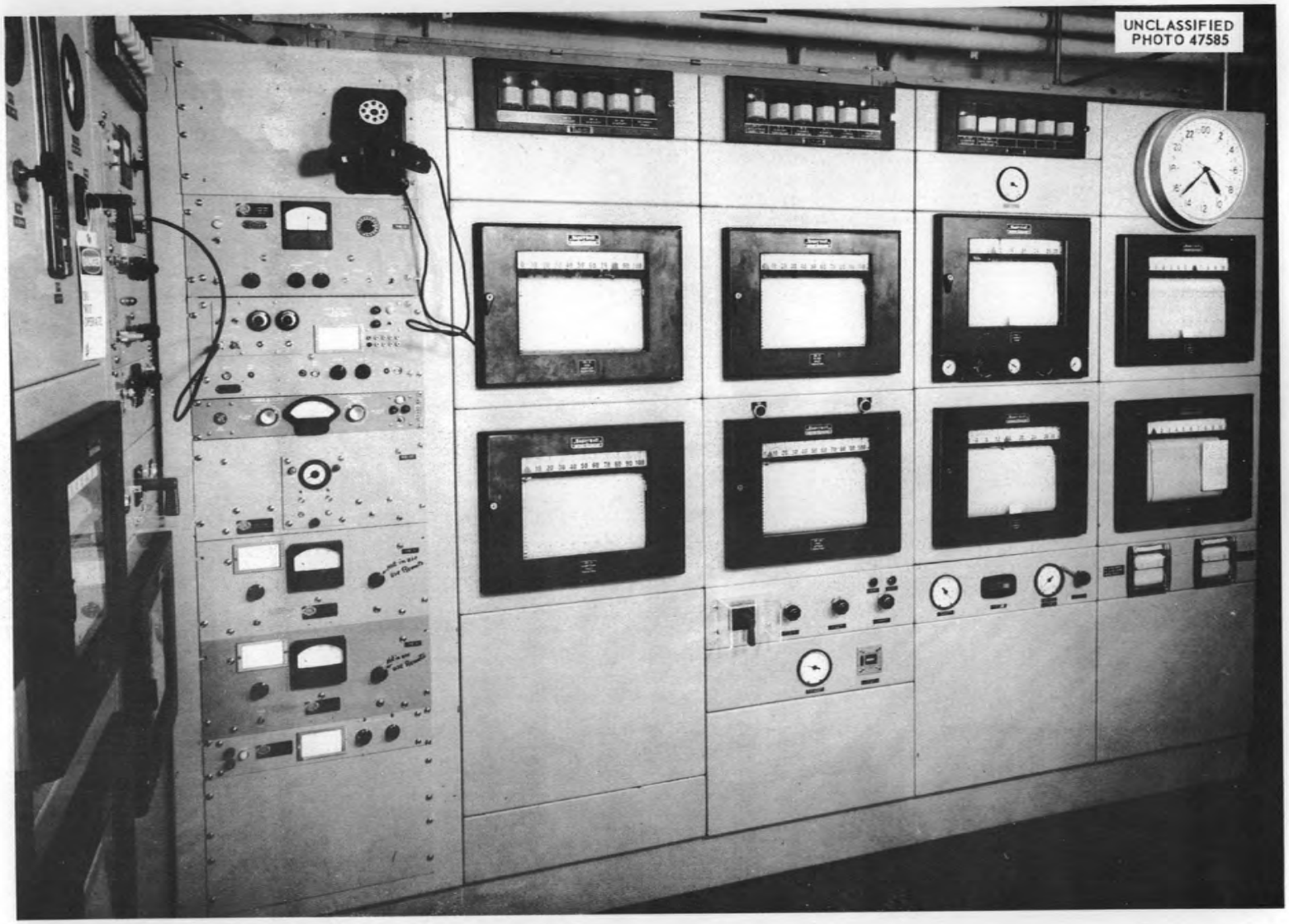

Fig. 63. Panel Board for Lattice Position B-9.

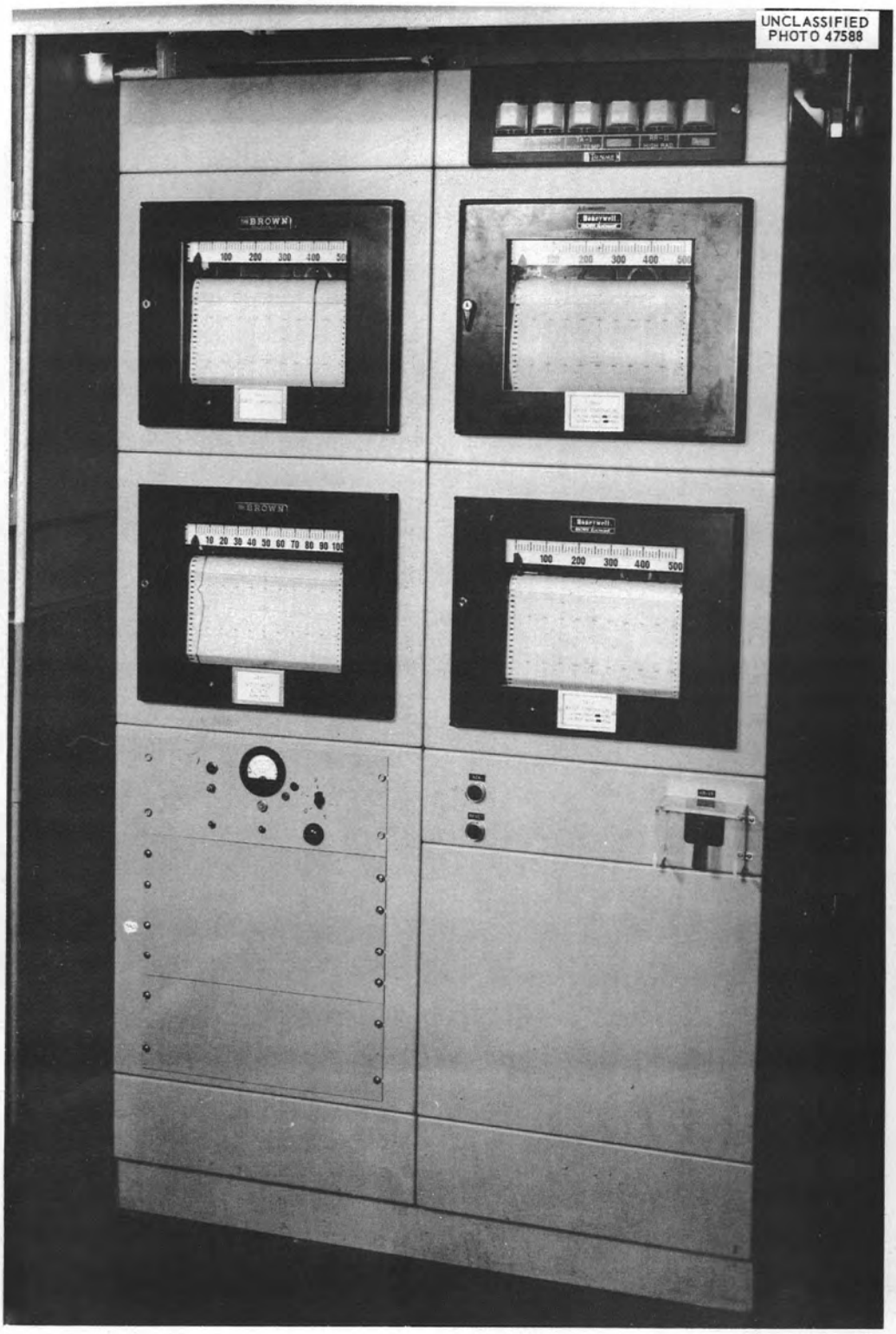

Fig. 64. Panel Board for Lattice Position B-1.

Fig. 65. Panel Board for Lattice Position F-2.

EGCR FUEL ELEMENT CAPSULE TESTS IN THE LITR AND THE ORR

C. M. Burton

Introduction

Inconel-clad UO_2 fuel element pellets are being irradiated and post-irradiation analyses made. The LITR and ORR tests are part of a large irradiation program for the Experimental Gas-Cooled Reactor. Identical experiments are being run in six core positions in the LITR (C-28, C-42, C-46, C-47, C-57, and C-58), and eight experiments in the ORR. Many experiments are needed so that various fuel enrichments, densities, burnup times, etc., can be evaluated. Information on the quantity of fission products released and the consequent pressure buildup, and on the kinds of fission products produced is also needed.

LITR Tests

The capsules are in the center of two concentric aluminum tubes. Cooling air goes down the inner tube and returns through the annulus. Each capsule contains two sets of pellets in separate compartments, one above the other.

Measurement and Control. — The six experiments required twelve 2-ft panels, which are in the LITR west room. These experiments were the first to use the ORNL E-panel and S-box arrangement to tie in-pile experiments to a reactor's safety system.

The first capsules had one inside and three outside thermocouples. The center hole in the pellets allowed a thermocouple to be put into the top pellets. Its leads came out through a hermetic seal. Three 1/16-in.-OD thermocouples, with Chromel-Alumel wires, MgO insulation, and Inconel sheaths, were put in grooves on the outside of the fuel can, and the tips were Heliarc-welded in place. The temperature of each Chromel-Alumel thermocouple was recorded on a separate recorder. Two 0–2000°F single-pen recorders (with upscale burnout) recorded capsule wall temperatures, alarmed on high temperature, and scrammed the reactor at a still higher temperature. Temperature recorders with pneumatic control held the wall temperatures constant by varying the cooling air flow with air-to-close valves. The hottest thermocouple was held to about 1300°F. The controllers had switches that could be tied into the reactor safety circuits. These were to be used if one of the single-pen recorders became inoperative, or if one of the other two outside thermocouples failed. Two wall thermocouples must work and be read out on separate instruments for the experiment to be permitted to continue to run in-pile.

These thermocouples were flattened to 0.045 in. and put in grooves in the capsule wall to clear the air tube and to give better wall temperature measurement. Temperature differences between adjacent thermocouples were as much as 400°F early in the program. Some of this difference could have been caused by the fuel pellets shifting position, or by cracking up of the

fuel pellets. It was noticed that the Heliarc-welding of some thermocouple tips left voids which could allow cooling air to pass between the thermocouples and fuel cans. The voids could not be filled by welding without melting through the thermocouple's thin sheath. The later capsules had these voids filled with brazing material for 1/8 to 3/16 in. from the tip. Then the indicated temperature differences were only 10–60°F between adjacent thermocouples. Only one outside thermocouple has open-circuited. The oldest thermocouples have been in the reactor 30 calendar weeks. The reactor was at power approximately 80–85% of this time.

Proper postirradiation analysis of the fuel requires that the center temperature be known, at least initially. When the program was started, center temperatures were low, within range of platinum-rhodium–platinum. Later, thermocouples that would operate up to 3500°F were needed to allow proper evaluation of the UO_2 fuel.

As center temperatures reached 2200–2500°F, the platinum-rhodium–platinum thermocouples deteriorated rapidly. It was then learned that platinum reacted with UO_2 at and above these temperatures. This forced the use of sheathed platinum-rhodium–platinum thermocouples, or of other high-temperature thermocouples, earlier than was anticipated. The most promising thermocouple combination seemed to be rhenium-tungsten with BeO insulation in a 1/16-in.-OD tantalum sheath, or rhenium-tungsten with a BeO two-hole insulator. Rhenium-tungsten was tried in three capsules, and two of these apparently open-circuited on initial heatup. The third, in capsule L-8, indicated about 2660°F at first and fell to about 2300°F in five weeks.

Recently, the capsule was redesigned to have a center thermocouple in the bottom half, as well as the top half. A platinum-rhodium–platinum thermocouple is used in the top half, which runs cooler than the bottom half, and a rhenium-tungsten thermocouple is used in the bottom half. Such a capsule was installed on June 16, 1959. The capsule was expected to have a center temperature of the order of 2500°F. However, the indicated temperatures were 1800°F in the top and 2050°F in the bottom. These temperatures correlated well with wall temperatures.

Radiation detectors caused an alarm if a capsule leaked fission products into the cooling air.

ORR Tests

The eight experiments are on the west face of the ORR core. In each experiment a fuel element is immersed in NaK. Between the NaK container and the outside tube, a gas annulus restricts heat flow to the pool water. Thus, the fuel elements can be held at temperatures up to 1600°F by changing the gas composition in the annulus. Thermal cycling is caused by intermittently putting cadmium plates between the reactor and six of the experiments. These plates are moved by hydraulic cylinders.

Each fuel element is a 3/4-in.-OD, 0.020-in.-wall stainless steel tube that contains 12 UO_2 pellets 1/2 in. long by 0.705 in. OD. Each container is filled with helium at atmospheric pressure before it is sealed.

Measurement and Control. — The NaK is held at 300 psig with helium pressure. Two parallel helium pressure regulators and relief valves supply helium to the NaK annulus through double O-ring-sealed check valves. The 1/8-in.-OD tubes from the NaK annulus to the fission-gas traps pass by radiation detectors. The first pair of radiation detectors show whether fission products have leaked out of the pellet container and diffused through the tubes to the radiation detector. Helium is passed by the second pair of radiation detectors when gas is bled from one experiment at a time. Thus, the leaking experiment can be found.

Low NaK pressure causes an alarm. A lower pressure causes the reactor to set back. This protects the fuel element from possible rupture.

The fuel element wall temperature is assumed to be about the same as the NaK temperature. Thermocouples in the NaK annulus, held against the fuel element wall, measure temperature. The six thermocouples in each NaK annulus are 1/16-in.-OD, stainless-steel-sheathed Chromel-Alumel. After the grounded hot junction was made, the first 9 in. of the thermocouple was rolled to 0.045 in. because of limited space in the NaK annulus. All thermocouples were x-rayed and dye-penetrant checked. A flame was run along the sheath while the thermocouple was connected to a potentiometer. If the wires were shorted to each other, or to the sheath, the potentiometer would show this. The thermocouples passed through two bulkheads, one at the top of the NaK container, and one farther up the experiment tube. During fabrication, sheath failures occurred where the sheaths were brazed to the bulkheads. This was caused by the boron in the brazing material, which embrittled the stainless steel. The transition from sheath to thermocouple lead wire was made with special connectors which formed a hermetic seal.

Only two thermocouples did not read correctly when the experiments were initially operated. None have failed during 2 1/2 months of operation.

High temperature from either of two top thermocouples causes an alarm. A higher temperature causes the reactor to be set back. The top thermocouples are used because a NaK loss would first stop cooling at the top of the fuel element.

Mixtures of helium and nitrogen or argon can be put in the gas annulus in any proportions through two O-ring-sealed check valves. Both gas flows are measured with capillary flow elements and regulated with hand valves. The thermal conductivity of the mixture is measured. The approximate desired composition can then be put in each annulus that controls heat flow, one at a time. This composition is adjusted to give the proper fuel element temperature.

The control gas enters the annulus at the top on one side and leaves on the other side. Spiral strips about 0.008 in. thick wound around the fuel element were to guide this gas to the bottom of the capsule and back to the outlet. Gas leaked from inlet to outlet without traveling to the bottom of the capsule and back. The only way that the gas composition around the capsule could be changed was to cycle the pressure a number of

times. Any attempt to automatically control temperature by changing gas composition would require that the gas be put in one end of the capsule and taken out the other end, or that leaks between inlet and outlet be eliminated. The very long time lags in the system would make automatic control difficult unless gas flows are larger than now used. Fuel elements which run at 1600°F have a low-pressure alarm from the control gas pressure.

Low pressures in the cylinders that supply helium to the NaK annulus cause alarms. Any control instrument power failure causes an alarm.

INSTRUMENTS AND CONTROLS FOR THE MARITIME SHIP REACTOR PRESSURIZED WATER EXPERIMENT IN THE ORR

R. F. Hyland

Introduction

Proper fuel element performance at operating conditions is important to the Merchant Ship Reactor Program. Uranium dioxide fuel pellets in stainless steel capsules will be tested at the ORR in an experiment that will simulate NS "Savannah" operating conditions. The experiment will also be used for other development programs. Lattice positions A-1 and A-2 will be used. The average unperturbed flux is estimated to be 5×10^{13} thermal.

Description

The out-of-pile part of the experiment is designed to circulate 625°F water at 2250 psig. The first in-pile section has been designed for MSR operating conditions, which are 500°F and 1750 psig. A different section must be designed for higher pressures and temperatures.

Water will flow around two sets of fuel elements of six fuel pins each. One set will be irradiated. The other set is outside the reactor and will not be irradiated. Thus the effect of irradiation can be isolated.

The pumps, heat exchangers, and the like are in a cubicle which is in the basement of the ORR building. Wherever possible, type 347 stainless steel will be used in order to reduce corrosion and avoid the need for weld-joint heat treatment.

This test loop, the first pressurized water experiment to be put in the ORR, will consist of an in-pile test section, an out-of-pile test section, a water-cooled heat exchanger, Westinghouse type 150D canned-rotor pumps, pool water pumps, reactor water pumps, a surge tank and pressurizer, a water purification and makeup system, circulating water purification system, and a sampling system. The pressurizer and the main loop will be heated by contact-type electric resistance heaters. The in-pile section and the submerged piping are surrounded by a vacuum jacket, evacuated by a vacuum pump which operates continuously.

The in-pile section can be cooled by reactor cooling water if fuel pins are not to be irradiated, or if some part of the external apparatus needs repairs. To go from normal circulating-water cooling to reactor-water cooling, the reactor must be shut down and the loop cooled to ambient pressure and temperature. Manually operated valves are used for the changeover.

The heat exchanger and the circulating pumps are cooled with pool water from a pump, or its standby.

Measurement and Control

Pressure. — The experiment pressure is the vapor pressure of the water in the surge tank. This water is heated in four single-tube reboilers on the surge tank. Each tube is surrounded by a 6-kw resistance heater. Power for the heaters comes from continuously variable autotransformers which are pneumatically operated by the system pressure control. When the system pressure is too high an alarm sounds, and at a higher pressure the heaters are cut off. Low pressure must be prevented to keep the water in the in-pile section from boiling and possibly damaging the experiment. When the pressure drops, an alarm sounds and the loop heaters are cut off. If the pressure continues to drop, there is an alarm and cooling is increased. If the pressure drops further, the reactor is set back. In addition, argon from cylinders can be used to maintain loop pressure manually.

There are alarms caused by high in-pile tube differential pressure, high vacuum jacket pressure, low argon supply pressure, low instrument air pressure, high loop pressure, and failure of any rupture disk.

Disastrous overpressures in the loop, in the vacuum jacket, and in the surge tank are prevented by rupture disks and relief valves in series. These discharge to the flash condenser.

Circulating pump pressure is recorded. Pool water pump, reactor water pump, and makeup water pump pressures are indicated. Circulating pump differential pressure and out-of-pile section differential pressure are indicated.

Temperature. — A three-way valve mixes water that has been cooled in the heat exchanger with hot water from the in-pile tube. The valve is operated by a temperature control to give the proper pump inlet temperature. This method of control is used to avoid time lags in the control system.

Power to 60-kw heaters attached to the main loop piping is manually adjusted to put enough heat into the system to make up all heat losses, plus some heat to keep the temperature control valve in operation when there is no nuclear heat input. The heat exchanger has enough cooling capacity to remove all electric heat plus all nuclear heat. When there is nuclear heat input, the temperature control system dumps it into the heat exchanger along with any excess electric heat. Since the temperature control system has fast response, reactor startups and shutdowns should give no trouble.

The cooling control valve goes to maximum cooling when instrument air fails or when instrument power fails. Operating a panel switch will also cause maximum cooling.

High in-pile pressure-tube temperature first sounds an alarm. If the temperature continues to increase, the reactor is set back.

High in-pile section outlet-water temperature sounds an alarm and the loop heaters are cut off. If the temperature goes on up, cooling is in-

creased as much as possible and there is an alarm. Finally, the reactor is set back. This is to prevent boiling, which may damage the experiment.

High temperature of any heater section on the loop or on the pressurizer will sound an alarm and shut off the heaters while the temperature is high.

There are high-temperature alarms on the heat exchanger outlet pool water, the ion bed inlet, and the circulating pumps. High temperature of the operating circulating pump causes transfer to the first standby pump.

Flow. — The fuel elements and the in-pile tube must always be cooled while the reactor runs. The circulating water flow is measured by a venturi tube. Water is circulated by a canned-rotor pump with two standby pumps. Flow is regulated with a hand-operated valve.

If power fails, batteries and a motor generator can keep a circulating pump and a pool water pump operating for over 1/2 hr to remove afterheat.

A low loop water flow will cause an alarm. If flow decreases further, the first standby pump starts, an alarm is sounded, and after 1/2 sec the original pump stops. If after 2 sec the flow is still too low, the second standby pump starts, an alarm is sounded, the reactor scrams, and 1/2 sec later the first standby pump stops. At the same time, loop cooling is increased as much as possible, and the loop heaters are cut off.

When reactor cooling water is used to cool the in-pile section, the flow is measured with an orifice plate and a meter run. There are two reactor cooling water booster pumps, one a standby. If water flow gets low, an alarm sounds. If the flow decreases further, the reactor scrams, the standby pump starts, and after 1/2 sec the original pump stops.

Variable-area meters are used to measure flow of pool water through the heat exchanger and through all the circulating pump cooling coils. Any low flow sounds an alarm. Simultaneous low pool water flow through the cooling coils of any two circulating pumps will start the standby pool water pump, and 1/2 sec later the original pump stops. If, after 3 sec, flow is still too low, the reactor is set back, the loop heaters are cut off, and cooling is increased as much as possible.

Flow through the water purification system is measured by differential-pressure transmitters which have integral orifices.

Level. — Differential-pressure transmitters measure pressurizer surge tank level. The reference leg is external and cooled. The makeup pump adds water to the system to maintain the proper level. If the level gets below the top of the reboiler heaters, power to the heaters is cut off until the level rises, and an alarm is sounded. When the level is too high, the makeup pump circuit is broken, to prevent the manual addition of water, and an alarm sounds.

The flash condenser level is indicated only.

System Radioactivity. — The activity of the circulating water is recorded. Activity increases, such as that caused by a ruptured fuel element, will cause an alarm to be sounded. Alarms will also be sounded in the event of high activity in the purification system, the off-gas, the sampling station, the operating area, or the equipment room. A red light over the equipment room door is turned on by activity in that room.

Electrical. — Overload of the circulating water pump, the pool water pump, and the reactor water pump will cause an alarm and a transfer to a standby pump.

Failure of any control instrument power causes an alarm.

Battery room ventilation blower failure causes an alarm.

Electrical conductivities of the water entering and leaving the ion beds and of the demineralized water supply are recorded.

Engineering

All drawings have been made in accordance with ORNL standards.[1–3]

The instrument and control panel is shown in Fig. 66. The flow diagrams and sample copies of the control elementary diagrams and maintenance elementary diagrams are shown in Figs. 67–74.

---

[1]Instrumentation Flow Plan Symbols and Recommended Drawings, ORNL CF-57-2-1.

[2]Electrical and Electronic Drawing Standards Wiring and Device Coding, ORNL CF-58-12-141.

[3]ORNL Symbols List and Safety Procedures for Inpile Experiments in the LITR and the ORR, ORNL CF-57-12-58.

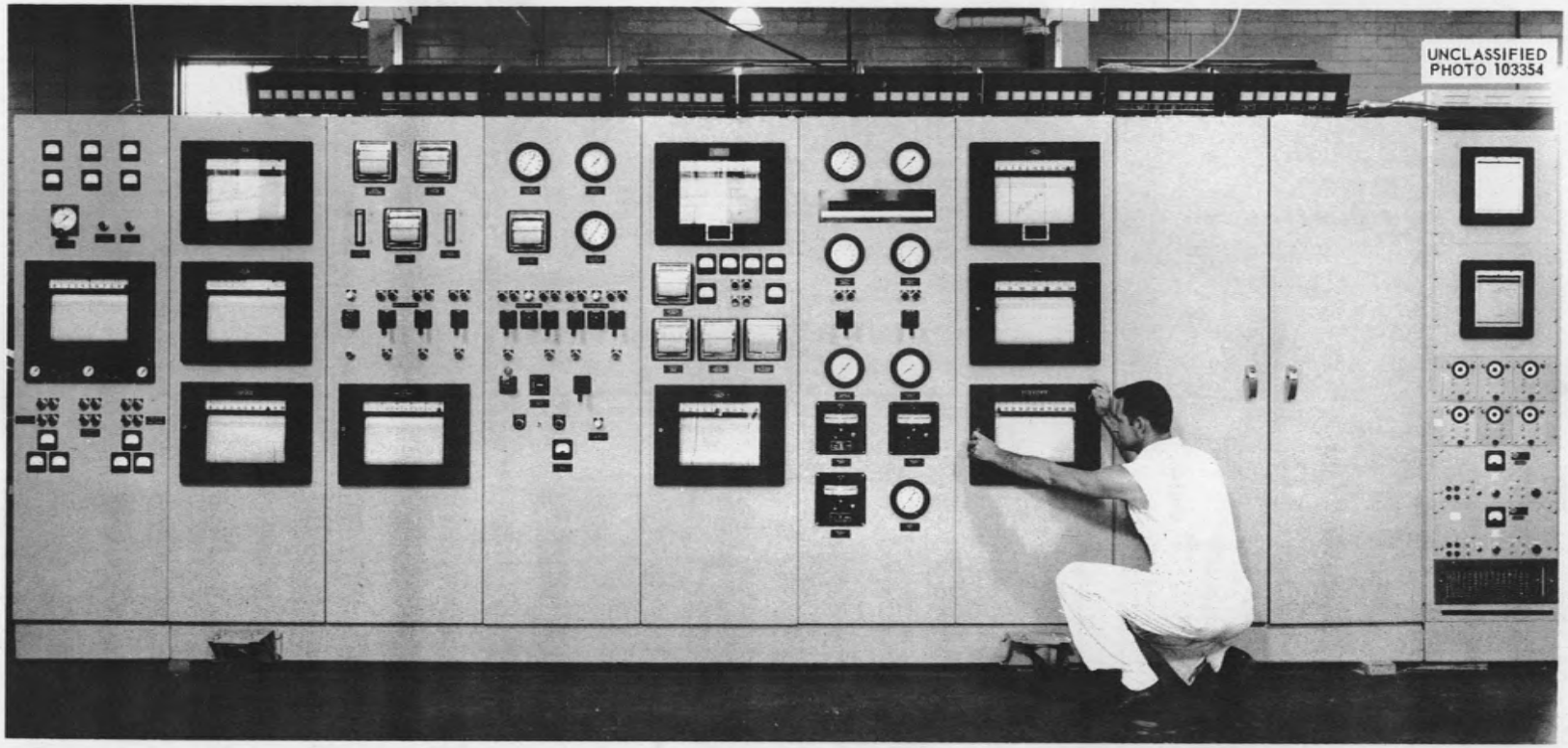

Fig. 66. Instrument and Control Panel for the Maritime Ship Reactor Pressurized Water Experiment in the ORR.

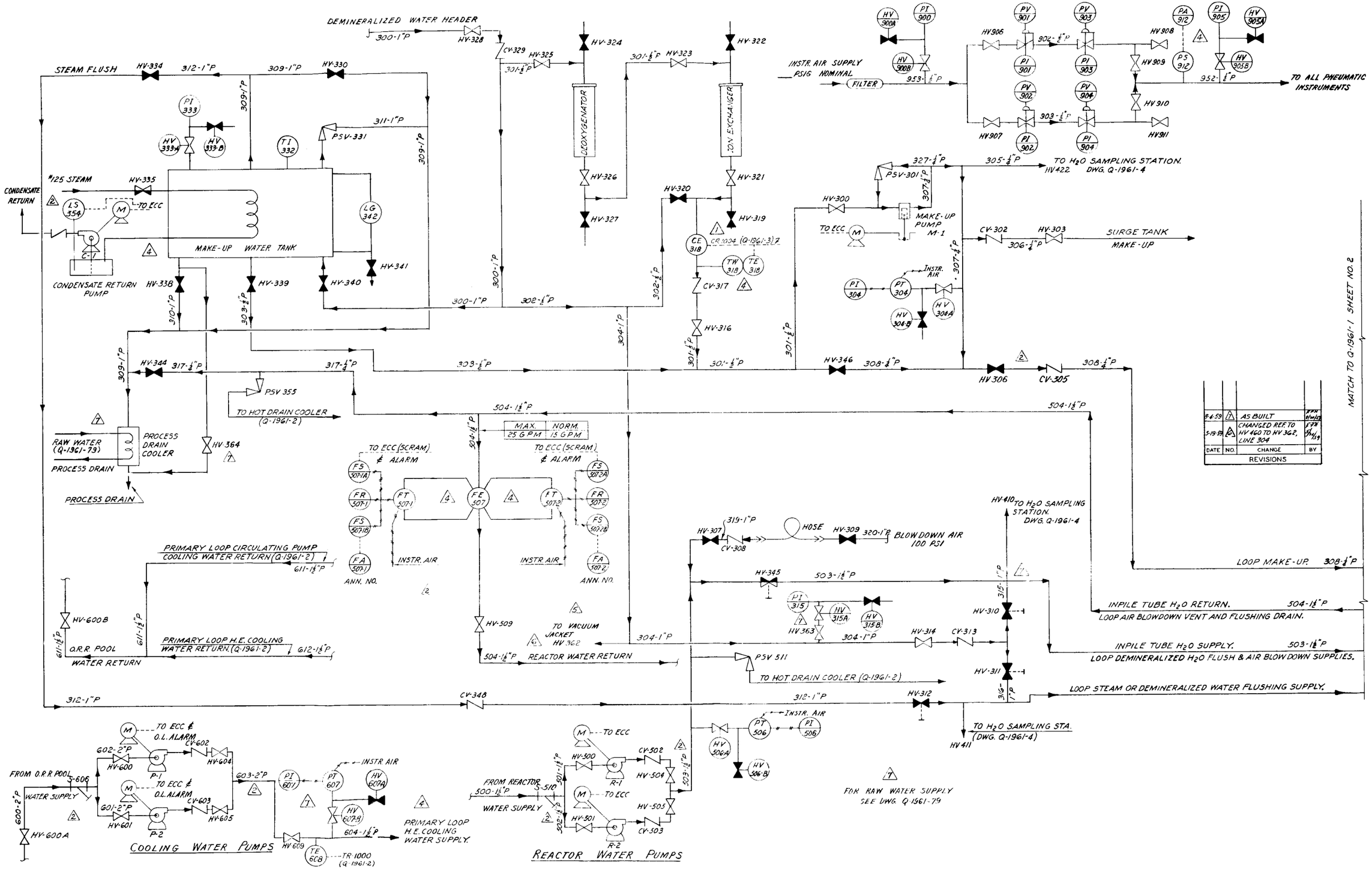

Fig. 67. MSR Pressurized Water In-Pile Loop: Instrument Flow Diagram for Auxiliary Systems.

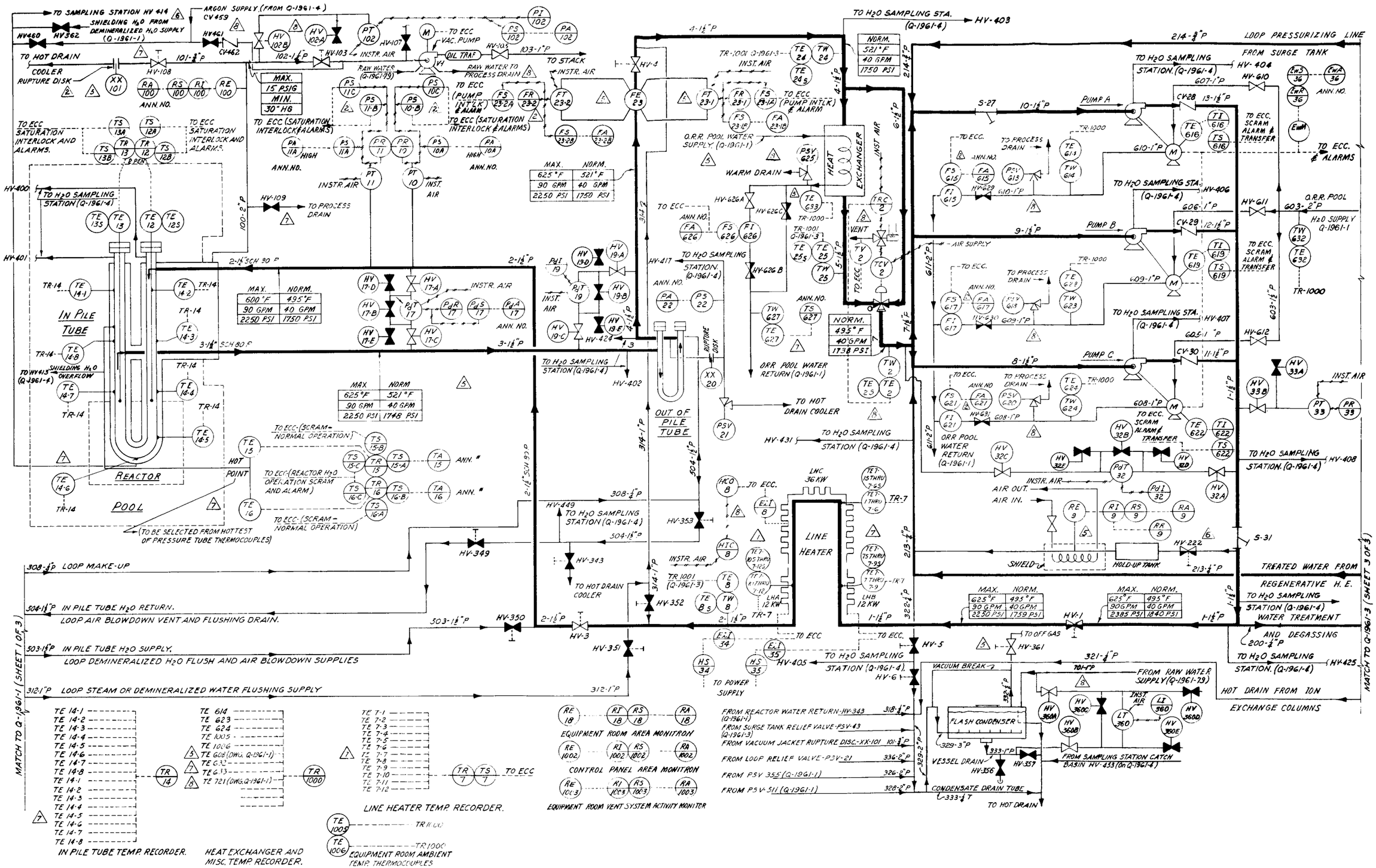

Fig. 68. MSR Pressurized Water In-Pile Loop: Instrument Flow Diagram for Primary Loop.

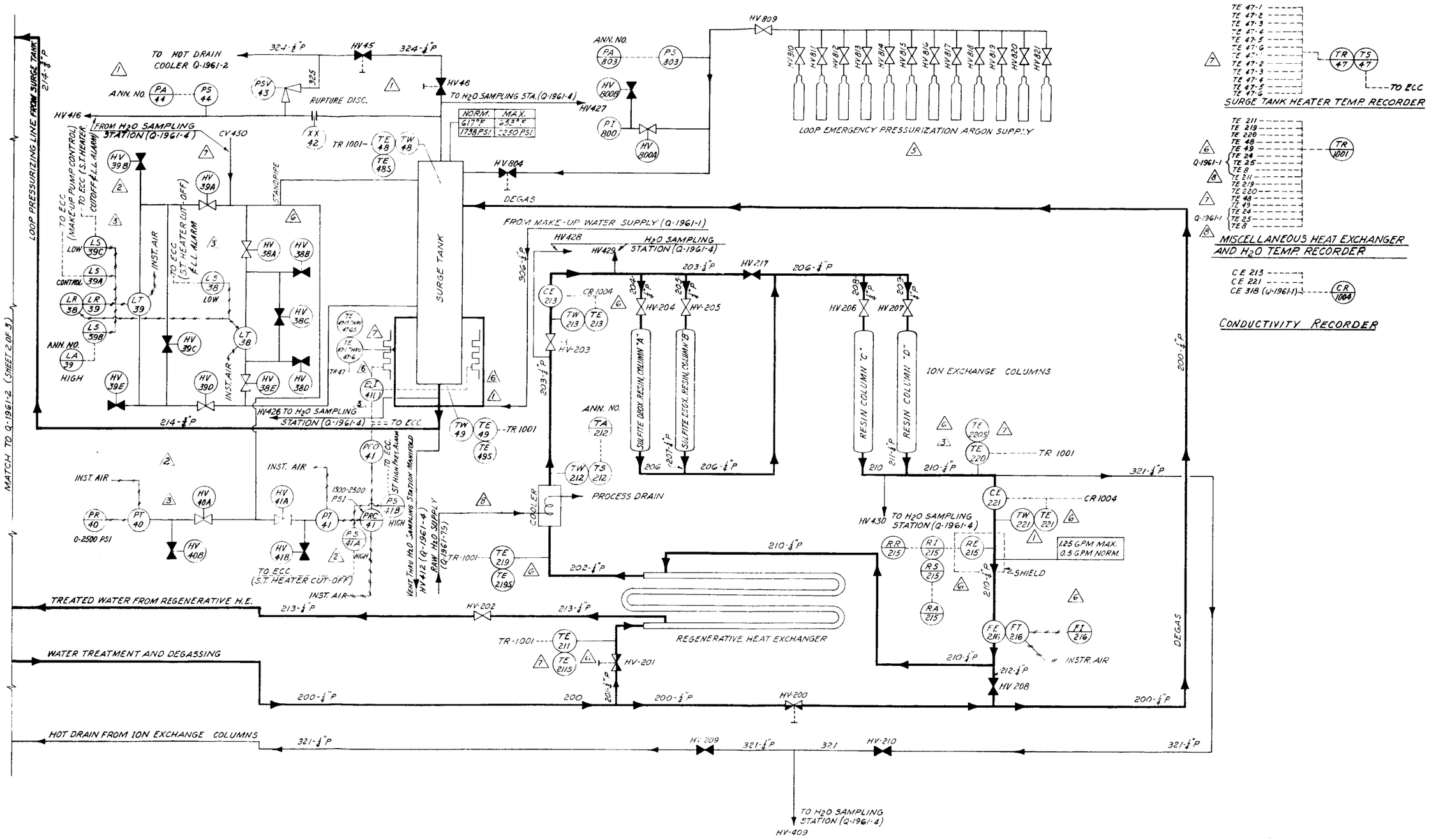

Fig. 69. MSR Pressurized Water In-Pile Loop: Instrument Flow Diagram for Pressurizer and Water Treatment Systems.

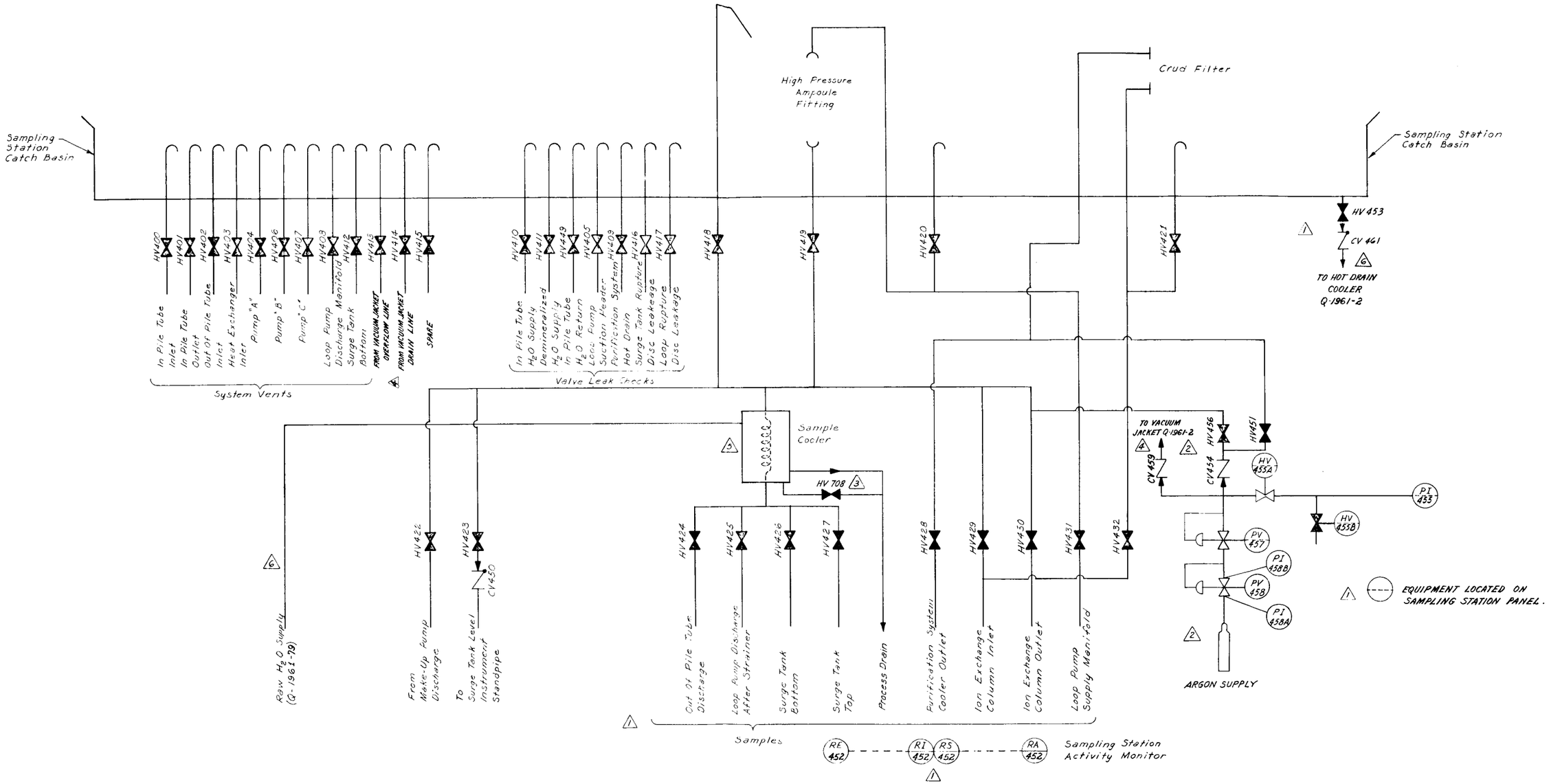

Fig. 70. MSR Pressurized Water In-Pile Loop: Instrument Flow Diagram for Water Sampling Station.

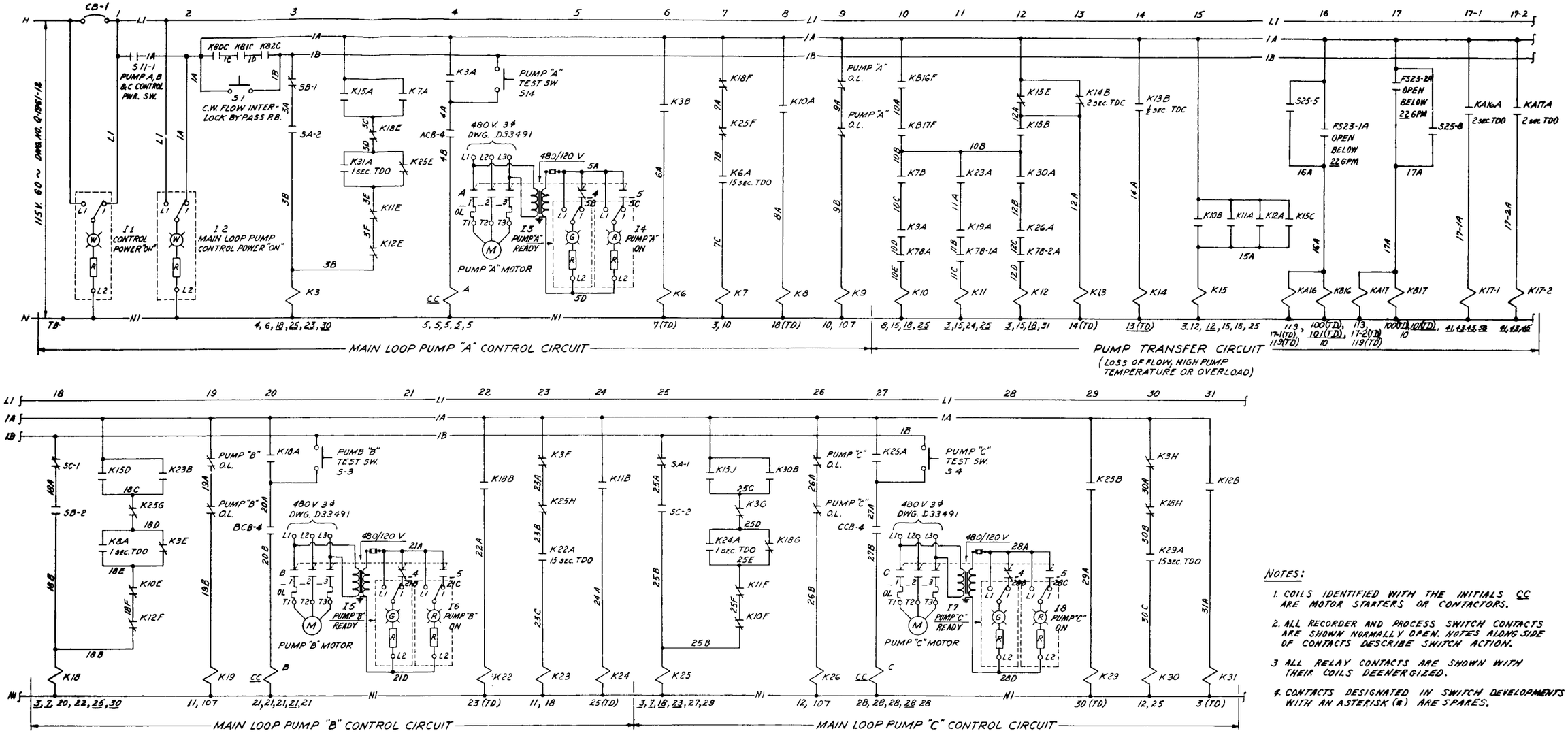

NOTES:

1. COILS IDENTIFIED WITH THE INITIALS CC ARE MOTOR STARTERS OR CONTACTORS.
2. ALL RECORDER AND PROCESS SWITCH CONTACTS ARE SHOWN NORMALLY OPEN. NOTES ALONG SIDE OF CONTACTS DESCRIBE SWITCH ACTION.
3. ALL RELAY CONTACTS ARE SHOWN WITH THEIR COILS DEENERGIZED.
4. CONTACTS DESIGNATED IN SWITCH DEVELOPMENTS WITH AN ASTERISK (*) ARE SPARES.

MAIN WATER PUMP CONTROL POWER
(MAINTAINED CONTACT)
SWITCH S11

CONTACTS HANDLE END	HANDLE POSITIONS (BACK VIEW)		
		ON	OFF
1 — 2	1	X	
	2	X *	

MAIN WATER PUMP "B"
(SPRING RETURN TO NORMAL)
SWITCH SB

CONTACTS HANDLE END	HANDLE POSITIONS (BACK VIEW)		
	START	NORMAL	START
1 — 2	1	X	
	2	X	X
3 — 4	3	X *	
	4	X *	X *

MAIN WATER PUMP "A"
(SPRING RETURN TO NORMAL)
SWITCH SA

CONTACTS HANDLE END	HANDLE POSITIONS (BACK VIEW)		
	START	NORMAL	START
1 — 2	1	X	
	2	X	X
3 — 4	3	X *	
	4	X *	X *

MAIN WATER PUMP "C"
(SPRING RETURN TO NORMAL)
SWITCH SC

CONTACTS HANDLE END	HANDLE POSITIONS (BACK VIEW)		
	START	NORMAL	START
1 — 2	1	X	
	2	X	X
3 — 4	3	X *	
	4	X *	X *

* SEE NOTE 4

REFERENCE DRAWINGS:

CONTROL ELEMENTARY DIAGRAMS.
Q-1961-6 SURGE TANK PRESSURE AND LOOP TEMPERATURE.
Q-1961-7 MISCELLANEOUS CIRCUITS.
Q-1961-8 REACTOR AND COOLING H_2O PUMPS.
Q-1961-9 SAFETY CIRCUITS.
Q-1961-10 ANNUNCIATORS - SHEET 1 OF 2.
Q-1961-11 ANNUNCIATORS - SHEET 2 OF 2.
Q-1961-12 115 V.A.C. POWER DISTRIBUTION.

Fig. 71. MSR Pressurized Water In-Pile Loop: Control Elementary Diagram for Primary Loop Pumps.

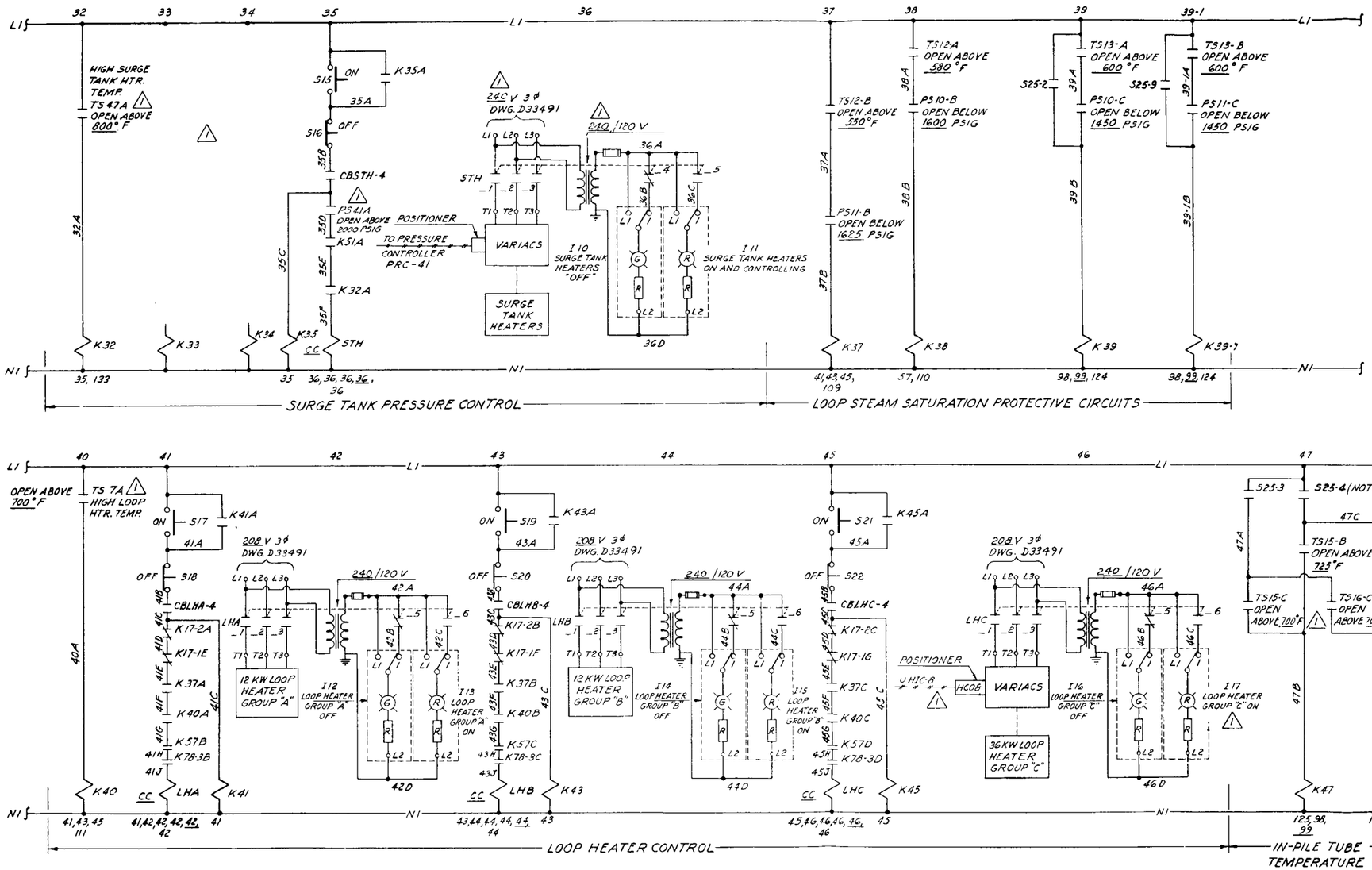

NOTES:

1. COILS IDENTIFIED WITH THE INITIALS CC ARE MOTOR STARTERS OR CONTACTORS.
2. ALL RECORDER AND PROCESS SWITCH CONTACTS ARE SHOWN NORMALLY OPEN. NOTES ALONG SIDE OF CONTACTS DESCRIBE SWITCH ACTION.
3. ALL RELAY CONTACTS ARE SHOWN WITH THEIR COILS DEENERGIZED.
4. SWITCH S25 DEVELOPMENT IS SHOWN ON DWG. Q-1961-9.

REFERENCE DRAWINGS:

CONTROL ELEMENTARY DIAGRAMS

Q-1961-5 PRIMARY LOOP PUMPS.
Q-1961-7 MISCELLANEOUS CIRCUITS.
Q-1961-8 REACTOR AND COOLING H_2O PUMPS.
Q-1961-9 SAFETY CIRCUITS.
Q-1961-10 ANNUNCIATORS - SHEET 1 OF 2.
Q-1961-11 ANNUNCIATORS - SHEET 2 OF 2.
Q-1961-12 115 V.A.C. POWER DISTRIBUTION.

Fig. 72. MSR Pressurized Water In-Pile Loop: Control Elementary Diagram for Surge Tank Pressure and Loop Temperature.

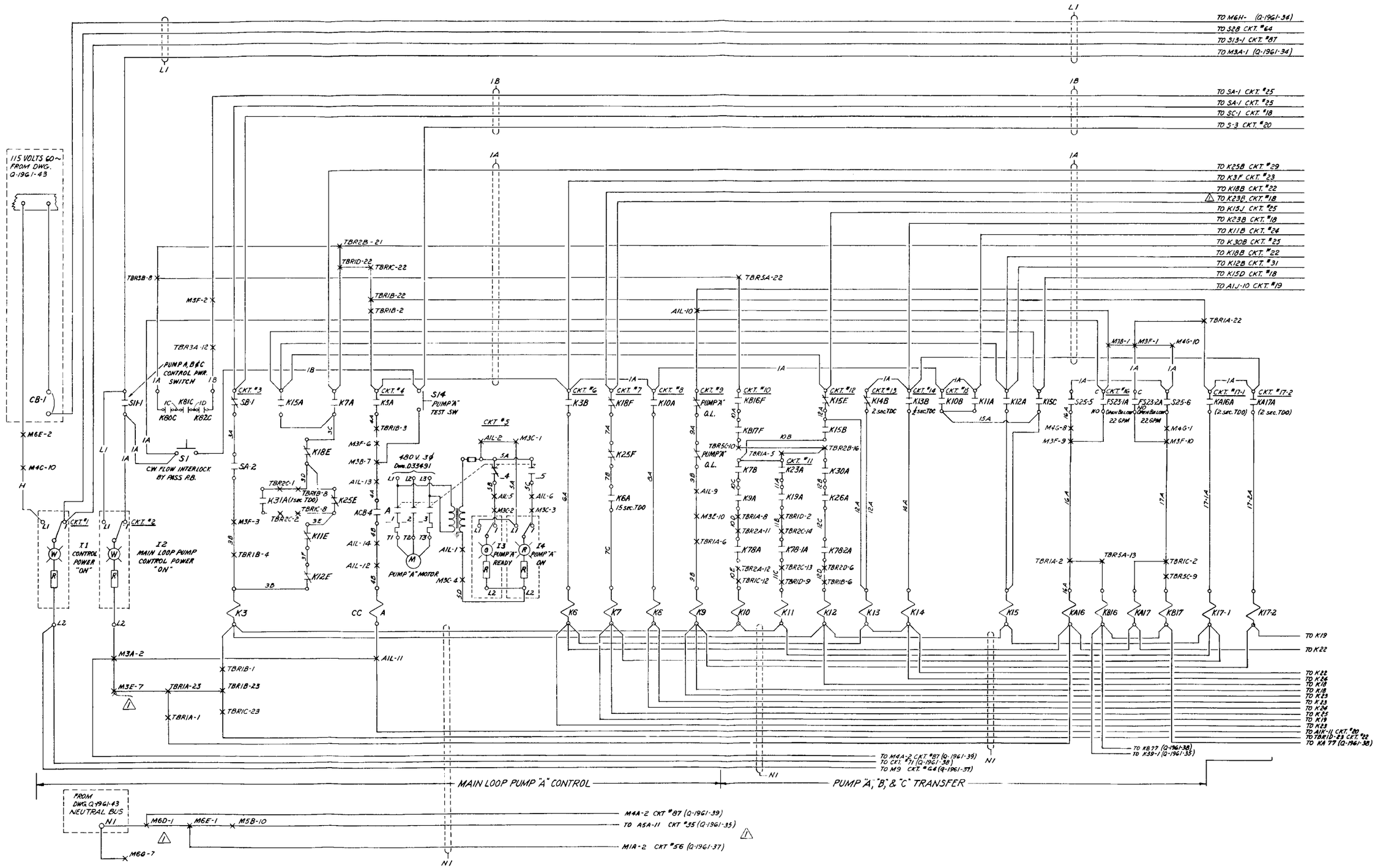

Fig. 73. MSR Pressurized Water In-Pile Loop: Maintenance Elementary Diagram for Main Loop Pump "A" and Pump Transfer.

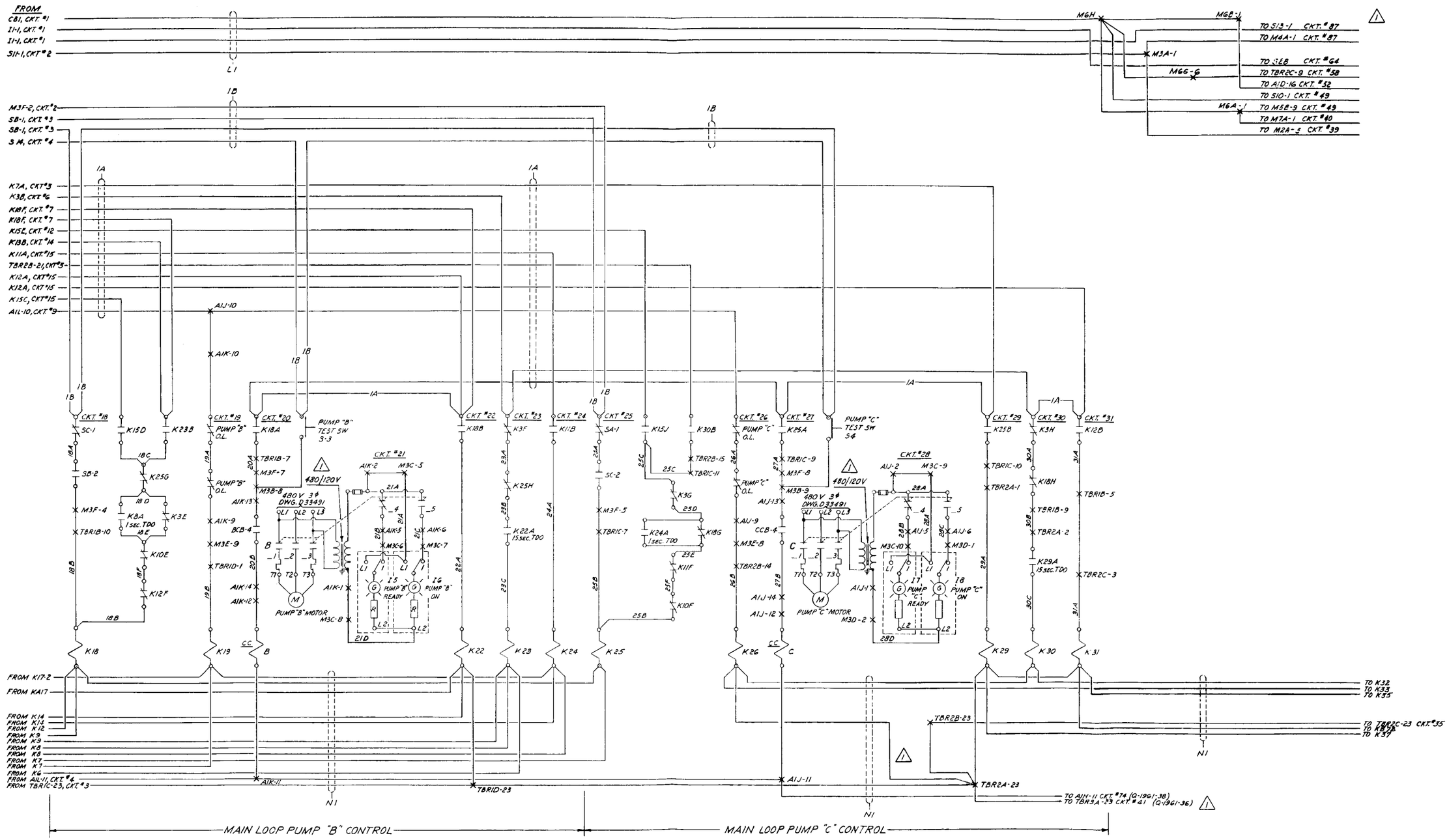

Fig. 74. MSR Pressurized Water In-Pile Loop: Maintenance Elementary Diagram for Main Loop Pumps "B" and "C."

TRANSIENT HEAT TRANSFER TEMPERATURE MEASUREMENTS

J. W. Krewson

Purpose

Turbulence in fully developed flow along a pipe wall that is transferring heat to a fluid will cause pipe-wall temperature fluctuations. To understand the phenomena, these temperature fluctuations must be measured.

Description

Water is passed through 8 ft of steam-jacketed 2-in. pipe. Water flow through the pipe and steam pressure in the jacket are changed to get different heat transfer rates. Wall temperature changes were plus or minus about 2°F.

Measurements

The turbulence frequency ranges from 0 to 20 kc. A gun-barrel thermocouple flush with the inside pipe wall measures the wall temperature. This thermocouple is one in which the junction is an electroplated film about 0.00005 in. thick deposited on an insulator. The time constant of the junction is less than 1 μsec. The thermocouple was Inconel to nickel, and its output was 15 to 30 μv.

A common-mode-rejection transistor amplifier operated by batteries was obtained from the Video Instruments Company (model No. 71). This amplifier rejected most of the common-mode pickup when it was balanced and when the rejection controls were adjusted for operating conditions at the time of use. This amplifier was connected to a high-speed Brush amplifier and recorder for use in the experiment.

Usable data on the magnitude and frequency of wall temperature changes were obtained when all leads were shielded as well as possible, when all a-c—operated amplifiers and recorders were kept several feet away from the Video amplifier, and when it was rotated to the position where pickup was smallest.

MOLTEN-SALT EXPERIMENTS IN THE MTR

G. H. Burger

Introduction

During the year two molten-salt in-pile test loops were operated in the MTR at Arco, Idaho, for the Molten-Salt Reactor Program. The purpose of the in-pile tests was to determine whether the molten salt and INOR-8 were compatible when irradiated. The molten salt consisted of uranium, beryllium, and lithium fluorides.

Description

A hydraulic-motor-driven pump circulated molten salt through 10 ft of 1/8-in. sched 40 INOR-8 pipe. Flow was from the pump to a 2 1/2-turn coil, through a cooler, and back to the pump. A surge tank absorbs volume changes. The coil of pipe was at the nose of the assembly and got the highest irradiation. Fission and other heat was removed by the air-cooled heat exchanger. Electric resistance heaters kept the salt molten when the loop was filled and before it was put into the beam hole. Operating conditions were: loop temperature, 1300°F; fission power, 7.5 kw; fission power density, 237 w/cc in the nose coil and 55.6 w/cc in total fuel; total heat, 2 kw; and salt flow, 1.3 gpm.

Measurement and Control

Temperature. — The pump-suction temperature control held the temperature constant by changing air flow through a cooler. The most serious condition that could develop was to have the salt freeze, which would stop flow and allow the nose coil temperature to rise 122°F/sec.

Low temperatures caused an alarm, followed by a reactor setback at a lower temperature. At the same time, air flow was cut off. High temperature caused an alarm, followed by a reactor scram at a higher temperature. If the pump suction was above 1200°F and at the same time the cooling air supply pressure was low, the reactor was set back and nitrogen from cylinders cooled the loop enough to remove afterheat. When the cold traps became warmer than -20°F an alarm sounded.

Flow. — Salt flow could not be measured, and so the hydraulic motor oil flow was measured to give an indication that the pump was operating. Low flow caused an alarm and then a junior scram, which is the release of shim safety rods No. 6 and 7. Pump speed was also an indication of salt flow. Below-normal speeds caused an alarm followed by a junior scram. The nose of the experiment was encased in a water jacket to absorb gamma heat. Below-normal flow to this jacket caused an alarm followed by a junior scram. Low nitrogen flow to the nose region caused an alarm, as well as low helium flows to the pump bearings and to the surge tank.

Pressure. – High nitrogen pressure in the nose of the experiment caused an alarm followed by a junior scram. This overpressure could be caused by a leak in the water jacket, or by a plugged vent line. Low instrument air pressure first alarmed and then caused a junior scram and closed the cooling air control valve. Low pressure in any of the nitrogen or helium supply systems caused an alarm.

Radiation. – High activity in the helium from the nose or high cooling air activity gave an alarm, followed by a scram. Activity in the area around the control panels, around the experiment cubicle, in the off-gas lines, and in the hydraulic oil, all caused alarms. A PCP chamber recorded reactor power, and when power dropped to 5 Mw, the rear electric heaters were turned on. At 2 Mw the front electric heaters came on.

HOMOGENEOUS REACTOR PROJECT INSTRUMENTATION AND CONTROLS

D. S. Toomb

S. J. Ball
E. H. Bell
A. M. Billings
J. R. Brown
D. G. Davis
G. W. Greene[1]
J. D. Grimes[1,2]
P. G. Herndon
R. L. Moore
J. L. Redford
J. A. Russell[1]
H. D. Wills

INSTRUMENT DEVELOPMENT

High-Temperature Radiation-Resistant Differential Transformer

A differential transformer for sensing the primary-element motions of sealed instruments and capable of operating for long periods at 300°C was developed.[3] There was no change in this transformer's characteristics when it was cycled from 25 to 350°C with a span setting of 0.025 in., and it shifted less than 2% in zero and span in a three-month test at 300°C. The transformer is wound with No. 24 AWG ceramic-insulated nickel-plated copper wire on an Inconel form. The wire was manufactured by the Secon Metals Corporation. The two secondary windings are wound on the Inconel form and are separated by a Lava spacer. The primary is wound over both secondaries, and the windings are impregnated with Allen PBX ceramic cement. The 1 1/8-in.-long movable transformer core is Armco iron.

The transformer has a sensitivity of 0.1 mv/v per 0.001 in. at 1000 cps when used with appropriate exciting and impedance-matching circuitry. Figure 75 illustrates the transformer, which is also sealed in an Inconel housing and has a 5/8-in.-dia bore for the instrument pressure housing extension. The lead wires are brought out through the housing in a 1/4-in.-OD tube.

The resistivity of the coil form was found to be a significant factor because the coil form acts as a shorted secondary turn on the transformer and causes a phase shift and reduction in amplitude of the output signal. For this reason materials of low resistivity and high temperature coefficient of resistivity, such as aluminum, were found not to be desirable. Inconel, which has a high resistivity and a very low coefficient of resistivity, now appears to be the best choice for a metal coil form material. Inconel is much better than the 300-series stainless steels in this respect since its temperature coefficient is about one-tenth that of stainless steel.

---

[1]Part time on project.

[2]On loan from TVA.

[3]R. L. Moore, "The Differential Transformer in High-Temperature Nuclear-Radiation Environments," ISA, Proceedings of the Second National Nuclear Instrumentation Symposium, Idaho Falls, June 1959.

Pressure Transmitter Evaluation

A Norwood Controls Division pressure transmitter was tested in conjunction with their magnetic amplifier and indicating receiver.[4] The transmitter, illustrated in Fig. 76, consists of a rotary differential transformer, a twisted Bourdon pressure tube, and a safety housing. The range of the transmitter tested was 0 to 2500 psi, and the Bourdon tube, safety housing, and pressure connection were fabricated from type 347 stainless steel. This transmitter has an exceptionally high test pressure rating of 5000 psi. An accuracy of ±1% of the range was noted in the ambient temperature range from 75 to 200°F. A block diagram of the complete measuring system is shown in Fig. 77.

Differential-Pressure Transmitter Evaluation

An electric-type differential-pressure transmitter with a 100-psi differential range and suitable for use at line pressures to 4000 psi was laboratory-tested and then installed in a process test loop. The transmitter, which is shown in Fig. 78, is available with ranges of 50 to 125 psi depending on the spring constant of the installed range bellows. The transmitter may be weld-sealed for use in radioactive fluid processes, and range bellows travel stops are provided to prevent permanent calibration shifts due to overranging. The movement of the ferrite core is sensed through a stainless steel shield and pressure housing by a center-tapped inductive coil. The inductive unbalance, which is proportional to differential pressure, is measured by conventional bridge-type instrumentation.

The tests indicated a maximum hysteresis error of 2% of range and freedom from temperature effects at 140°F. There was less than 1% zero shift due to pressure with 2000 psi applied simultaneously to the high and low sides. Overrange-induced shifts due to 2000 psi applied to the high side or 500 psi applied to the low side were correctable by applying a pressure higher than the rated range to the opposite side of the sensing bellows.

Sheathed Thermocouple Adapter

A special adapter was designed which allows greater flexibility in the application of the heated-thermocouple-probe liquid-level sensor described previously.[5] The adapter, which can also be used with sheathed thermocouples, is illustrated in Fig. 79. The adapter is designed around an Autoclave Engineers, Inc., high-pressure compression fitting and eliminates the difficult weld between the thin-walled probe sheath and the massive vessel wall found in the earlier design. The new design permits

---

[4]R. L. Moore and T. M. Cate, Performance Test of a Norwood Electrosyn Pressure Measuring System, ORNL CF-58-11-105 (Nov. 11, 1958).

[5]D. S. Toomb et al., Instrumentation and Controls Ann. Prog. Rep. July 1, 1958, ORNL-2647, p 95.

easy replacement of a failed unit and facilitates adjustment of the depth of insertion of the probe sensing tip. The stainless-steel-sheathed thermocouple is furnace-brazed to the stainless steel tubing adapter with General Electric Company brazing alloy GE-81 (66% Ni, 19% Cr, 10% Si, 4% Fe, 1% Mn).

Liquid-Level Alarm Transmitter

The measurement of liquid level in HRP high-pressure systems is necessary to indicate or control the vapor-liquid interface in process vessels. The liquid phase in such a system may be uranyl sulfate, thorium oxide slurry, or water.

The instruments now used for this application include differential-pressure and displacement-type transmitters, which have the disadvantages of lack of sensitivity and complexity, respectively.

A commercially available Copes-Vulcan boiler water-level alarm transmitter was tested to determine its suitability for these measurements.[6]

The instrument, illustrated in Fig. 80, develops a signal-producing motion from differential expansions caused by the difference in heat loss from the liquid and vapor sections of the measuring tubes. Since the parts of the sensing tubes which contain steam attain saturation temperature while the parts of the tubes which contain water operate at a lower temperature, a temperature gradient is established which produces sufficient motion when multiplied by a lever mechanism to operate alarm switches for high and low liquid-level conditions.

Performance tests on the test loop pressurizer shown in Fig. 81, which also illustrates the alarm transmitter, indicated that the steady-state temperature of the tubes containing steam was within 2°C of the saturation temperature at 1200 psi, while the tubes containing condensate operated at 65 to 95°C above the room ambient temperature of 25°C. The motion produced by the switch arms was approximately 0.050 in., and the time of response to a level change was between 1 and 2 min.

The instrument has the advantages for HRP applications of incorporating no thin-walled members and of being completely weld-sealed. It has the disadvantages of slow response, of being difficult to adjust remotely, and of being insensitive when the process vessel is at or near room temperature.

Capacitance-Type Liquid-Level Measuring System

A commercial capacitance-type liquid-level measuring system was also tested[7] to determine the suitability of this kind of instrument for HRP liquid-level applications.

---

[6]H. D. Wills, Performance Test of a Boiler Water-Level Alarm, ORNL CF-58-6-28 (June 10, 1958).

[7]J. L. Redford, Performance Test of "Jarco" Liquid-Level Indicating System, ORNL CF-58-5-91 (May 19, 1958).

The sensing element, illustrated in Fig. 82, consists of an electrode made of 3/8-in.-OD stainless steel rod covered with a 5/8-in.-OD Kel-F insulator and sealed in a 1-in. sched 80 stainless steel pipe by a nylon-Teflon compression seal. The entire assembly forms a coaxial condenser 21 in. long whose capacitance varies with the height of the liquid-level column in the annulus between the stainless steel pipe housing wall and the Kel-F electrode insulator.

The probe forms one leg of a capacitance bridge and is excited by a 30-kc oscillator. As the liquid level in the sensing element is changed, the capacitance bridge circuit is unbalanced; the resultant signal is amplified, rectified, and displayed on a microammeter.

The tests indicate that the measurement is nonlinear for the first 7 in. of the 21-in. range and that there is a 5% of full scale short-term hysteresis error due to water adhering to the electrodes and insulators. Increasing pressure caused a positive change in output at all levels and resulted in a 3 1/2% of full scale error at 2000 psi for a liquid level of 20% of full scale. This error increases with decreasing liquid level in the measuring element.

The instrument was also tested on a thorium oxide slurry with a composition of approximately 1000 g/liter. The result was a difference in output signal at full level of 3% from that obtained with water.

Evaluation of a Magnetic Amplifier Instrumentation System

A new Foxboro Company electric system for process instrumentation was tested in the laboratory and then installed as a pressure control loop in a high-pressure pump-test stand for investigation of long-term stability and reliability. The system is unique in that magnetic components and static rectifiers are used to amplify low-level signals and to derive the control functions. Previously available commercial equipment for general process instrumentation has been pneumatically powered or has utilized vacuum tubes which do not have the inherent reliability of electric solid state type component systems.

A block diagram of the pressure measuring and control system tested is shown in Fig. 83. The 0 to 2500 psi measured pressure is applied to a stainless steel helical sensing element which alters the position of a copper shorting ring, and thereby the flux linkage and output electric signal in a differentially connected electromechanical transducer, the Dynaformer. The low-level a-c output signal proportional to pressure is rectified and then amplified by a magnetic amplifier to provide a 10- to 50-ma d-c signal for the transmission line to the recorder or indicator, controller, and adjustable electric alarm-deriving chassis. An electric-to-air converter, to provide a pneumatic pressure signal for powering diaphragm control valves, is also available as part of the system. These components are pictured in Fig. 84.

The laboratory test of set-point stability, with the system connected as a closed loop, resulted in less than 1% change in control point when

the line voltage was varied from 105 to 125 v ac and no drift was observed during a period of two weeks of operation with constant line voltage.

Frequency response analysis of the controller indicated a characteristic curve flat to approximately 1 cps. It was also noted that the maximum reset time obtainable with the two-element flow controller was about 2 min per reset and the minimum proportional band setting was 50%. A general-purpose three-element controller has been designed by Foxboro and placed on order but is not yet available for testing. Figure 85 indicates how the magnetic amplifier components of the controller are arranged on a printed circuit wiring board. The controller assembly is connected to its housing by an easily removable plug-in connector.

Static-Component Power-Control System Evaluation

The presently used method of controlling the electric resistance elements used in HRP systems for supplying heat to the pressurizer vessels is a time-duration off-on mode. This control method functions by turning off and on the electric current to the heaters, the percentage on-time being varied in a fixed period. This system is inexpensive in the use of control equipment but suffers from the disadvantages of causing the temperature to cycle and of requiring that the relays and contactors be preventively maintained to ensure reliable operation. The temperature cycle is minimized by increasing the cycling rate of the control mode.

An alternate supply-voltage proportioning system utilizing static control components was investigated[8] to determine the control characteristic curves obtainable with available magnetic amplifiers and saturable reactors.

The test setup shown schematically in Fig. 86 consisted of a 0- to 10-ma current source, a magnetic amplifier connected as a self-saturating doubler with bridge rectifier output, and three saturable reactors. The reactors were connected with their inputs in parallel and their outputs Y-connected to a 30-kw resistive load. The load was conveniently supplied by connecting Calrod heating elements in parallel.

The over-all control-characteristic curve for the test system is shown in Fig. 87. The curve is nonlinear and neither zero nor full power output was obtained. However, the reliability to be gained from a system without moving parts and off-on contacts makes the scheme attractive for future applications.

---

[8]J. L. Redford, Static-Component Electric Power Control System Evaluation, ORNL CF-58-12-99 (Dec. 16, 1958).

Remote-Viewing Equipment

The miniature television camera designed for resistance to radiation, which was pictured in an earlier report,[9] was tested in a high gamma field. The only electronic components in the camera head are the Vidicon tube, the deflection coils, one ceramic capacitor, and a carbon resistor. The remaining electric components associated with the camera are in a preamplifier chassis which is connected to the camera by a 10-ft cable. By using this remote preamplifier most of the electric components can be kept out of the high radiation zone either by the use of intermediate shielding from strong sources or physical removal from weaker sources.

There was no observable initial effect on the camera operation when it was lowered into a 1.5×10^6-r/hr field. However, the picture then faded rapidly and after 20 min required maximum target voltage. After 1 hr of additional exposure in a reduced field of approximately 5×10^5 r/hr, the picture was not readable. After further exposure for a total dosage of 5×10^6 r, the camera head was removed and the camera lens was found to be practically opaque. After replacement of the lens, the camera operated satisfactorily with some loss of sensitivity, probably due to browning of the Vidicon tube face plate.

The test was performed in the canal of the ORNL Graphite Reactor using buckets of Co^{60} capsules as a source. As the source was under water, the camera was mounted in the test chamber shown in Fig. 88. An air purge for cooling was provided and the camera temperature was not allowed to exceed 110°F. A photographically reduced standard television test pattern was mounted at the bottom of the watertight chamber. Illumination was provided by two concentric rings of 12 General Electric No. 328 lamps. The intensity of illumination was of the order of 50 to 100 foot-candles. The glass in some of the lamps which were not energized darkened under irradiation. However, the heat generated by the illuminated lamps was sufficient to keep them clear.

The gamma dosage was monitored by cerium sulfate dosimeters.

A lens made from nonbrowning glass is now available from the Wollensak Optical Company and was ordered. The test will be repeated with this lens at a radiation level of about 10^5 r/hr.

Gamma Radiation Detector

A gamma-sensitive ionization chamber which utilizes alumina insulators to permit operation in high-temperature environments was acquired for evaluation.

The detector housing is weld-sealed, and a threaded cable-connector housing is provided so that the chamber may be operated while completely

---

[9]D. S. Toomb et al., Instrumentation and Controls Ann. Prog. Rep. July 1, 1958, ORNL-2647, p 114.

immersed by threading the detector onto a cable conduit. The chamber, which is illustrated in Fig. 89, is filled with nitrogen gas at 10 atm to increase sensitivity.

When the detector was temperature-cycled from ambient to 150°C, no appreciable change in output signal was observed. Although the manufacturer rated the detector for operation at temperatures to 400°C, the cable connectors now installed have Teflon insulators which would limit the maximum operating temperature to less than 200°C.

The detector should be useful as a radiation monitor in reactor steam-valve compartments and other locations where severe environmental conditions exist.

VALVE DEVELOPMENT

Stem Sealing Bellows

The longer flexible bellows assembly fabricated from grade Ti-55 titanium by the Fulton Sylphon Division on an ORNL contract passed the acceptance test. The 2 1/8-in.-long assemblies tested earlier[10] were not satisfactory. One of the 6 29/32-in.-long tandem bellows assemblies, which are made up from three 0.010-in. plies, was cycled 11,600 1/8-in. strokes in uranyl sulfate at 280°C and with a 2300-psi differential before failure occurred at the convolution indicated in Fig. 90. The bellows has an inside diameter of 13/16 in. and a spring rate of 300 lb/in.

Life testing of a larger bellows than those now used for control valve stem sealing in the HRT was begun, as a larger bellows may be required for future HRP systems. The bellows now being used in the HRT has an inside diameter of 0.875 in. The new bellows being tested is a seamless dual-stacked assembly with an inside diameter of 1 1/16 in. and constructed of three 0.0085-in. plies of type 347 stainless steel. In cycling the bellows 1/4 in. in uranyl sulfate at 1000 psi and 250°C, the first failed at 17,553 strokes and the second at 18,994. The larger bellows is Fulton Sylphon Division No. FS-001509-A01.

Slurry-Service Valve Trim

The Hammel-Dahl control valve[11] installed in the 30-gpm slurry loop was fitted with a Zircaloy-2 plug and seat after tungsten and chromium carbides proved unsatisfactory as trim materials. The valve has now operated satisfactorily for 2650 hr, including 125 hr in a 65% closed

---

[10] D. S. Toomb et al., Instrumentation and Controls Ann. Prog. Rep. July 1, 1958, ORNL-2647, p 105.

[11] D. S. Toomb et al., Instrumentation and Controls Ann. Prog. Rep. July 1, 1958, ORNL-2647, p 100.

position. During this time loop pressure and temperature were about 1650 psi and 275°C; slurry concentration has varied from 400 to 500 g of Th per kg of H_2O.

Another Hammel-Dahl valve installed in slurry loop 200B utilizing a long-radius pipe bend body design[12] and fitted with tungsten carbide trim was exposed to a 3-hr nitric acid loop rinse, during which the Colmonoy-faced stem was severely attacked. This stem was reinstalled in the loop and has performed satisfactorily for a total of 1600 hr to date, including 43 hr with 200 g of Th per kg of H_2O at 750 psi and 220°C during shakedown operation of the loop. Two sets of Zircaloy-2 replacement trim were fabricated for this valve, and it is hoped that a hardening procedure for this material can be developed to provide a more satisfactory slurry-service valve trim.

Valve Actuators

Life testing of the all-metal 40-in.^{2} effective-area control valve actuator described in an earlier report[13] was completed. Results obtained from the test stand illustrated in Fig. 91 were as follows:

Test No.	Failed Component	Stroke (in.)	Cycles to Failure
1	Stem sealing bellows	1	12,000
2	Stem sealing bellows	1	26,000
3	Stem sealing bellows	3/4	42,116
4	No failure	1	42,000
4	No failure	3/4	42,116

From the results obtained it is concluded that a longer stem sealing bellows is advisable for strokes exceeding 3/4 in. However, as the actuator was specified for 20,000 cycles at a 3/4-in. stroke, it is considered to be very satisfactory.

[12] Ibid., p 101.

[13] D. S. Toomb et al., Instrumentation and Controls Ann. Prog. Rep. July 1, 1958, ORNL-2647, p 108.

UNCLASSIFIED
PHOTO 33843

Fig. 75. High-Temperature Radiation-Resistant Differential Transformer.

UNCLASSIFIED
ORNL-LR-DWG 32332

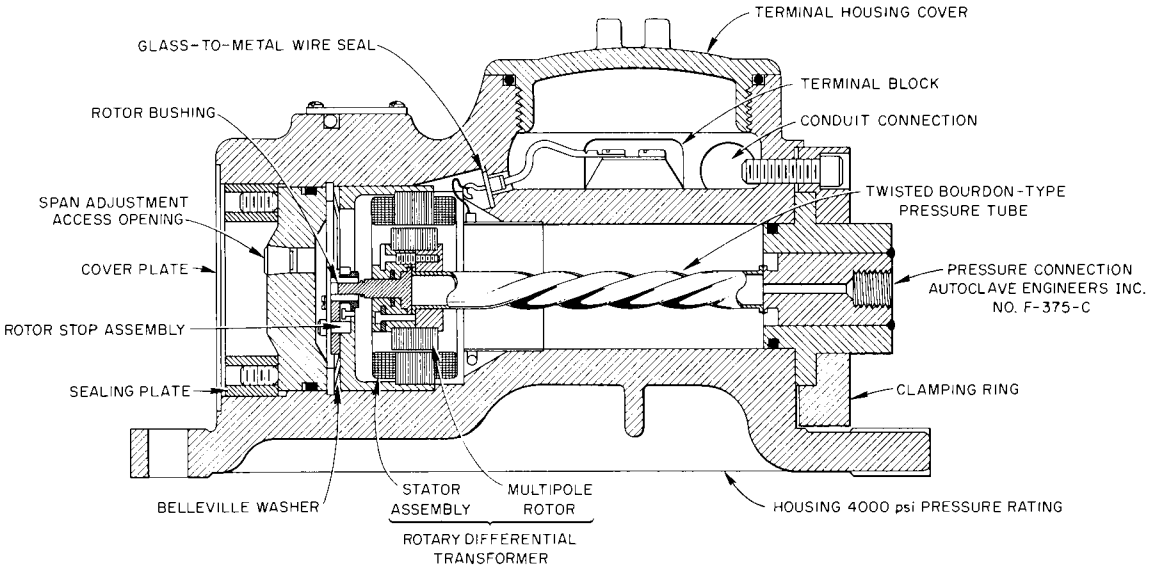

NOTES:
PROCESS CONTAINING PARTS—347 SS
RANGE—0-2500 psig
OUTPUT SIGNAL—0 TO 8.5 volts, 60 cps OPEN CIRCUIT
ERROR—±1%
TEST PRESSURE—5000 psig
PRESSURE RATING WITHOUT RUPTURE—12,500 psig
MAX.—ENVIRONMENTAL TEMP.-200°F
VENDOR—NORWOOD CONTROLS DIV.

Fig. 76. 0 to 2500 psi Pressure Transmitter.

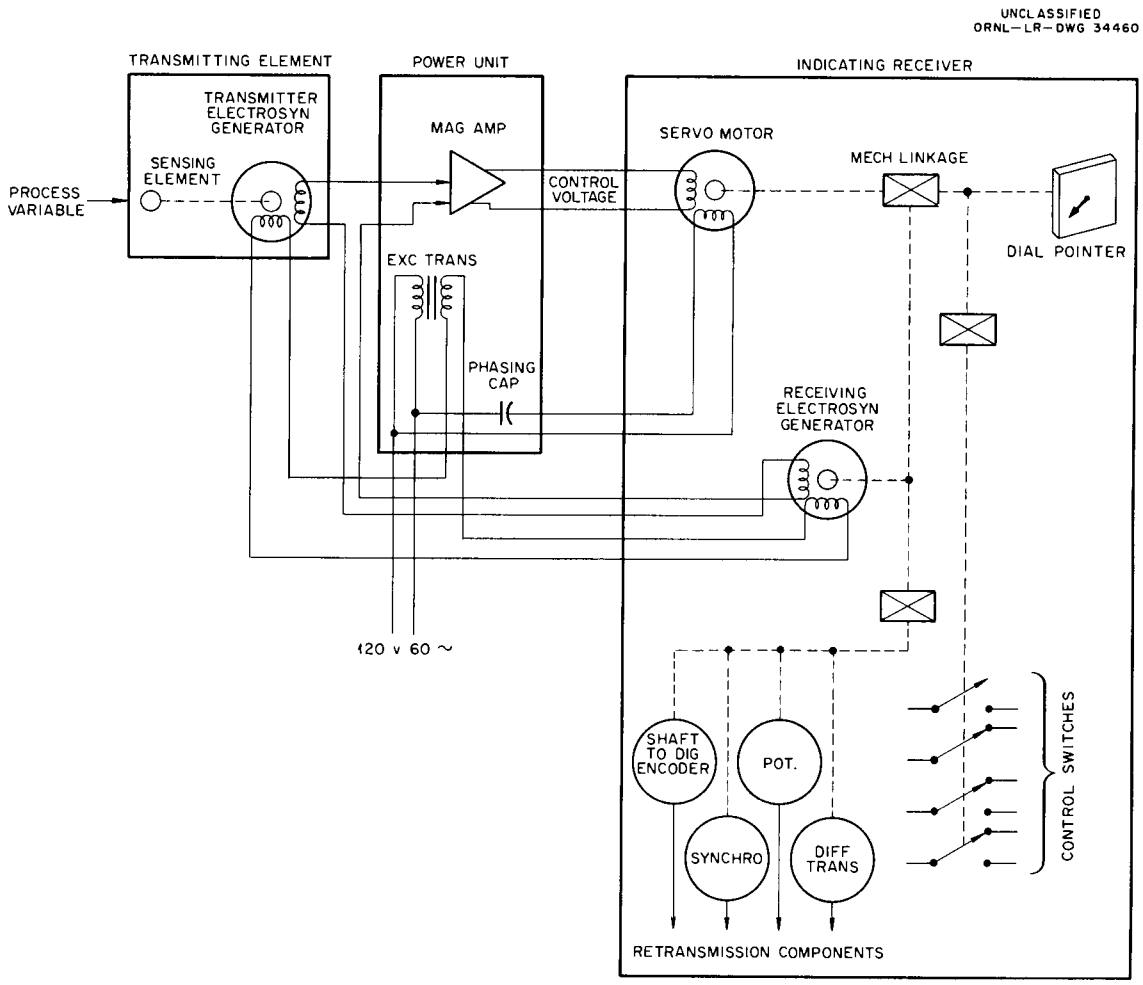

Fig. 77. Diagram of Norwood Controls Pressure Measuring System.

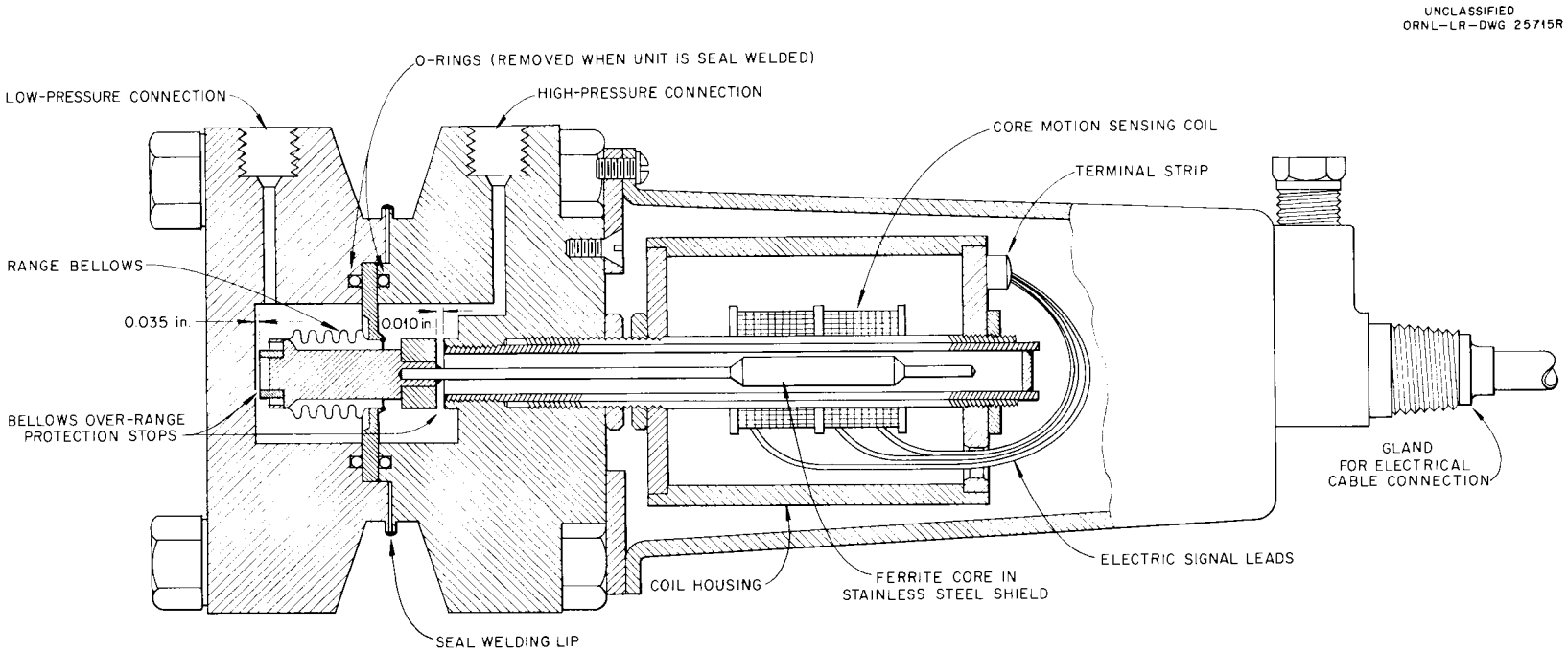

TYPE: INDUCTIVE BRIDGE FOR 1000 cps EXCITATION
RANGE: 0–50 psi TO 0–125 psi BY CHANGE OF RANGE BELLOWS
OVER-RANGE: HIGH SIDE–2000 psi, LOW SIDE–500 psi
ACCURACY: 3 %
BODY RATING: 4000 psi DESIGN, 6000 psi TEST
MATERIAL: 347 STAINLESS STEEL
VENDOR: THE FOXBORO CO.

Fig. 78. High-Range Differential-Pressure Transmitter.

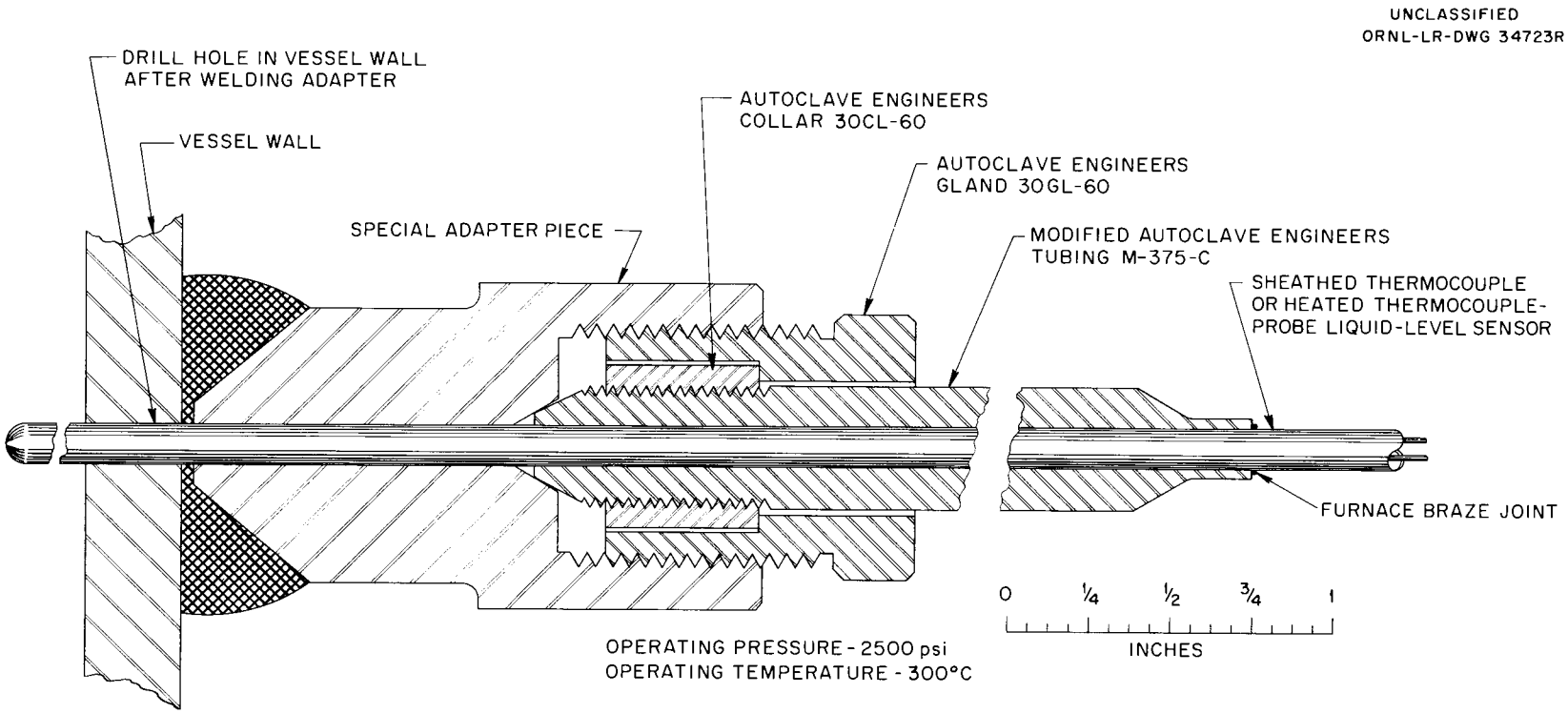

Fig. 79. Sheathed-Thermocouple Adapter.

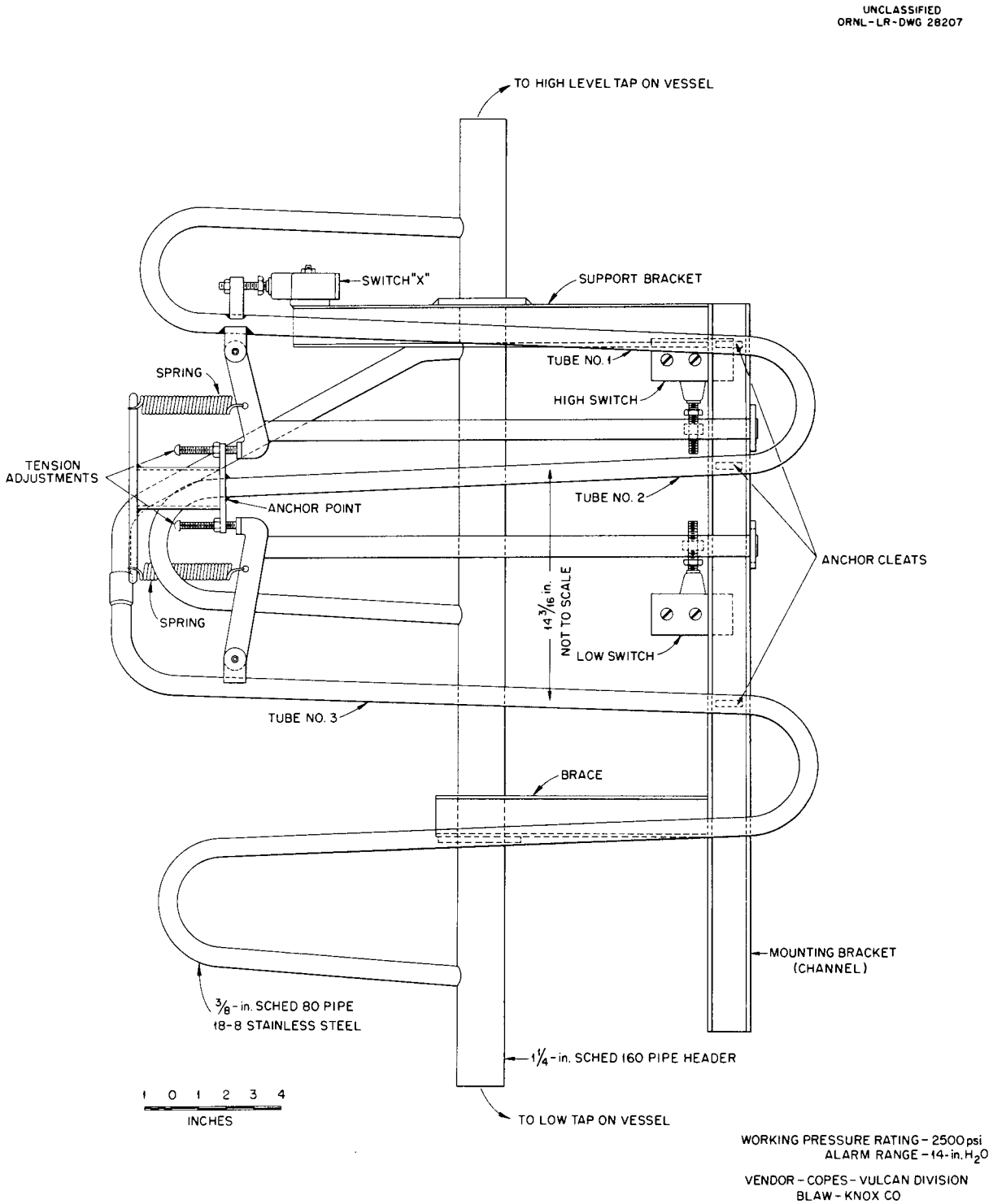

Fig. 80. High-Pressure Liquid-Level Alarm Transmitter.

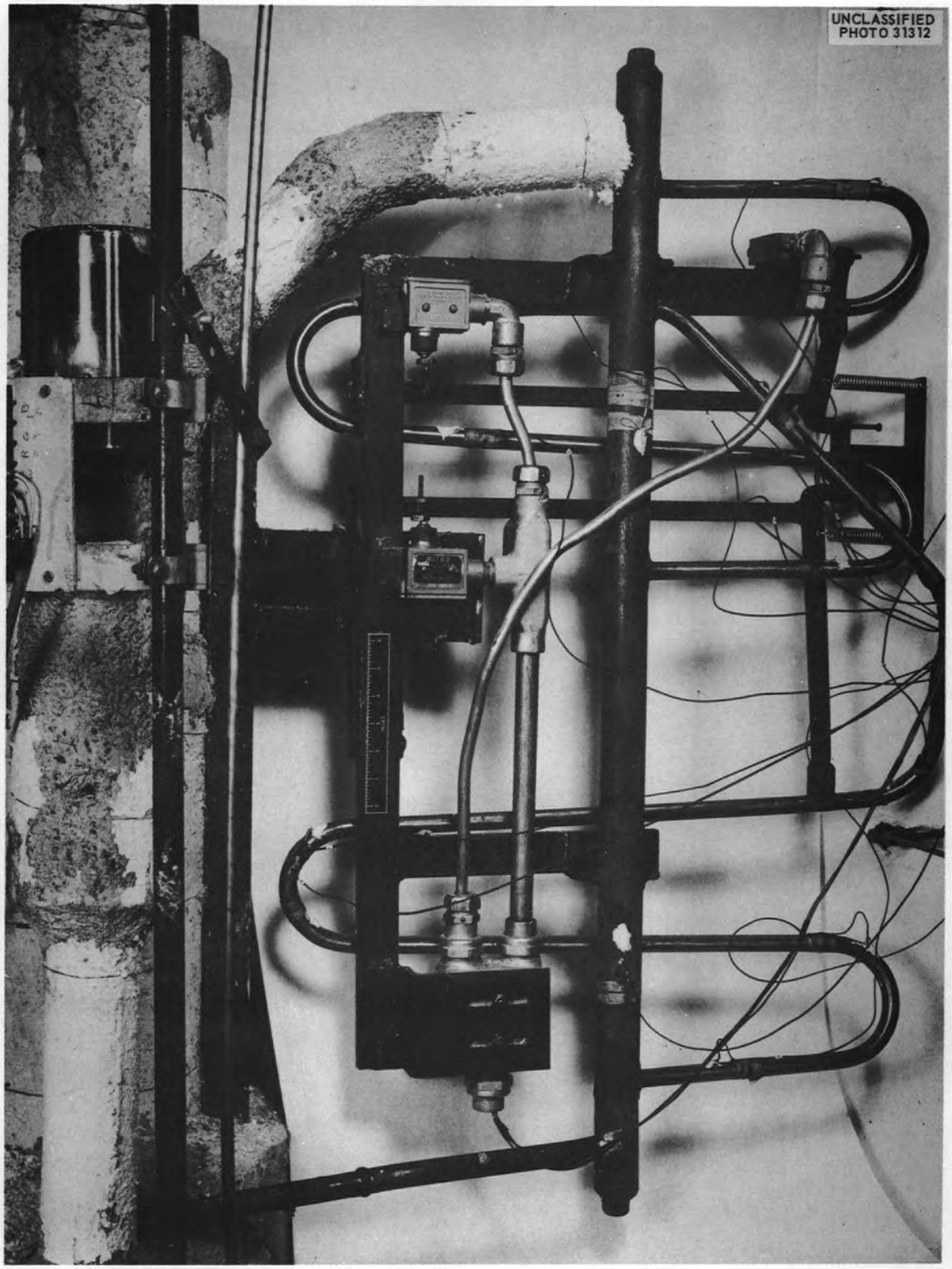

Fig. 81. High-Pressure Liquid-Level Alarm Transmitter Test Stand.

UNCLASSIFIED
ORNL-LR-DWG 30072R

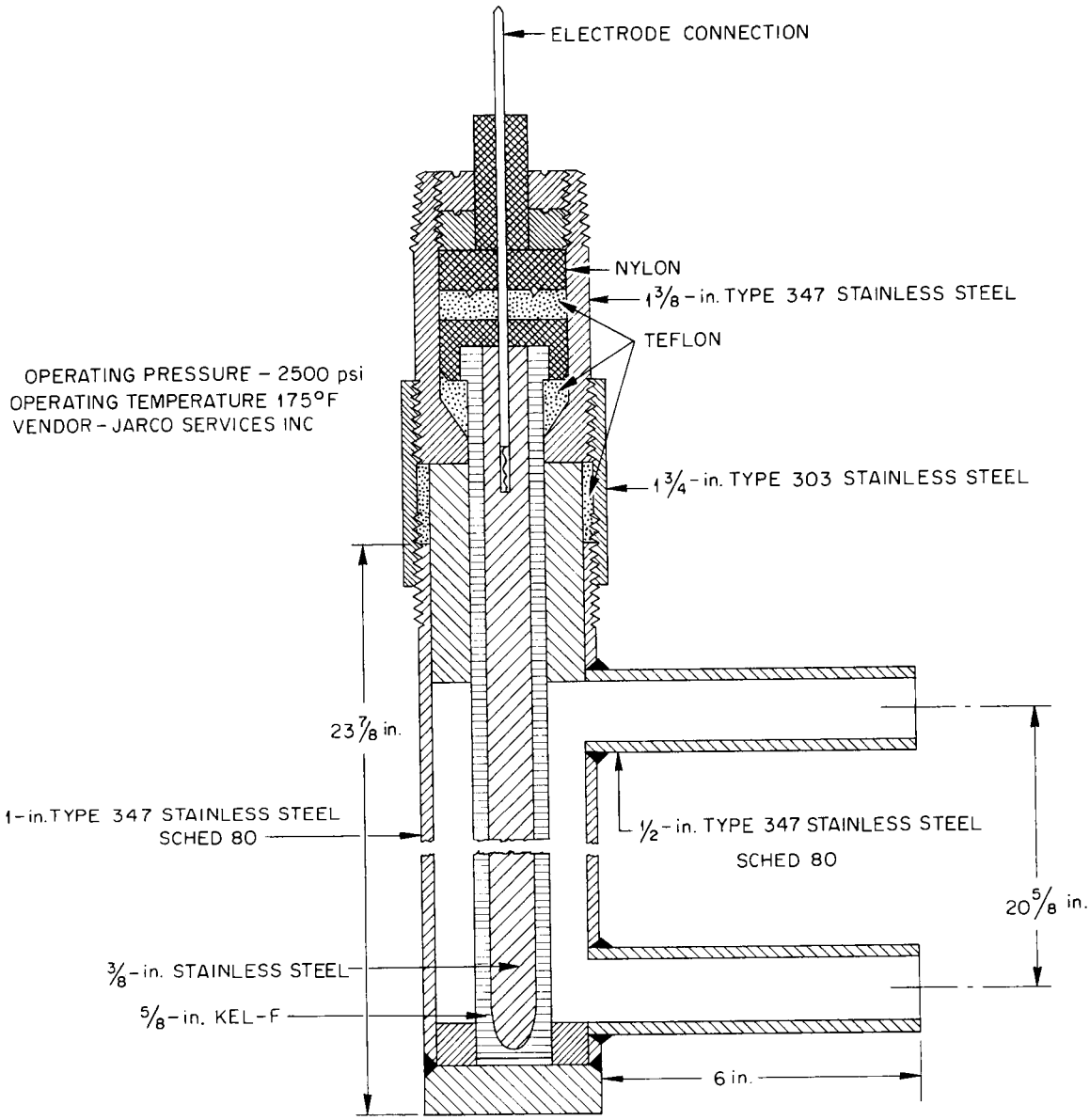

Fig. 82. Capacitance-Type Liquid-Level Sensing Element.

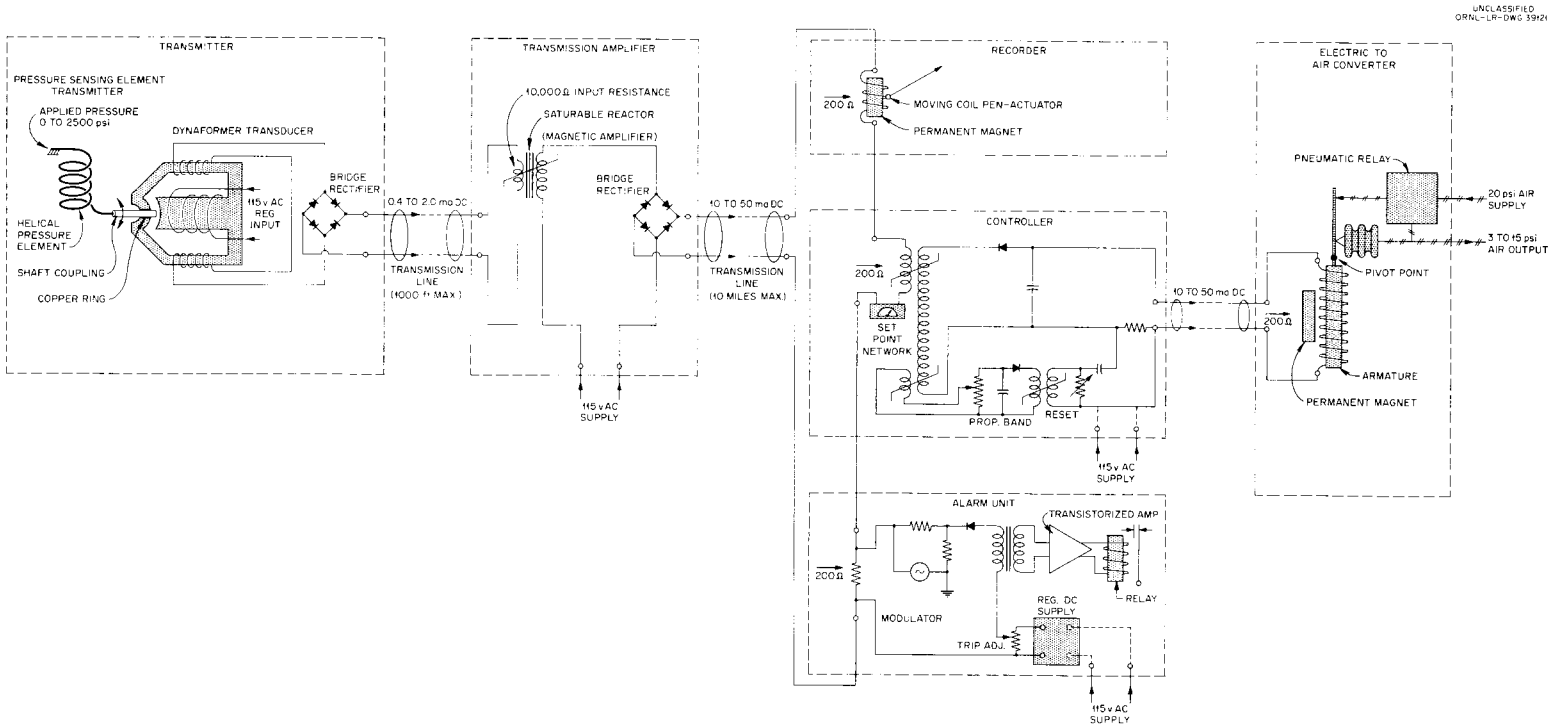

Fig. 83. Schematic Diagram of Pressure Recording-Controlling-Alarm System.

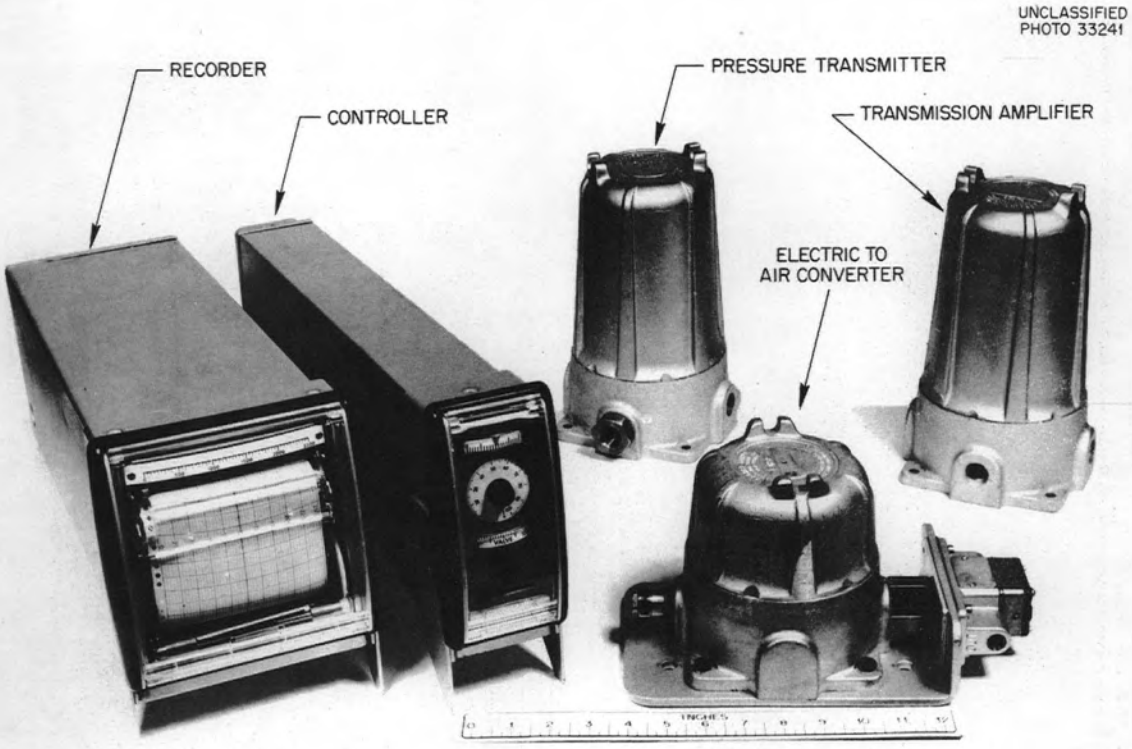

Fig. 84. Electronic Consotrol Instrumentation Components.

UNCLASSIFIED
PHOTO 33237

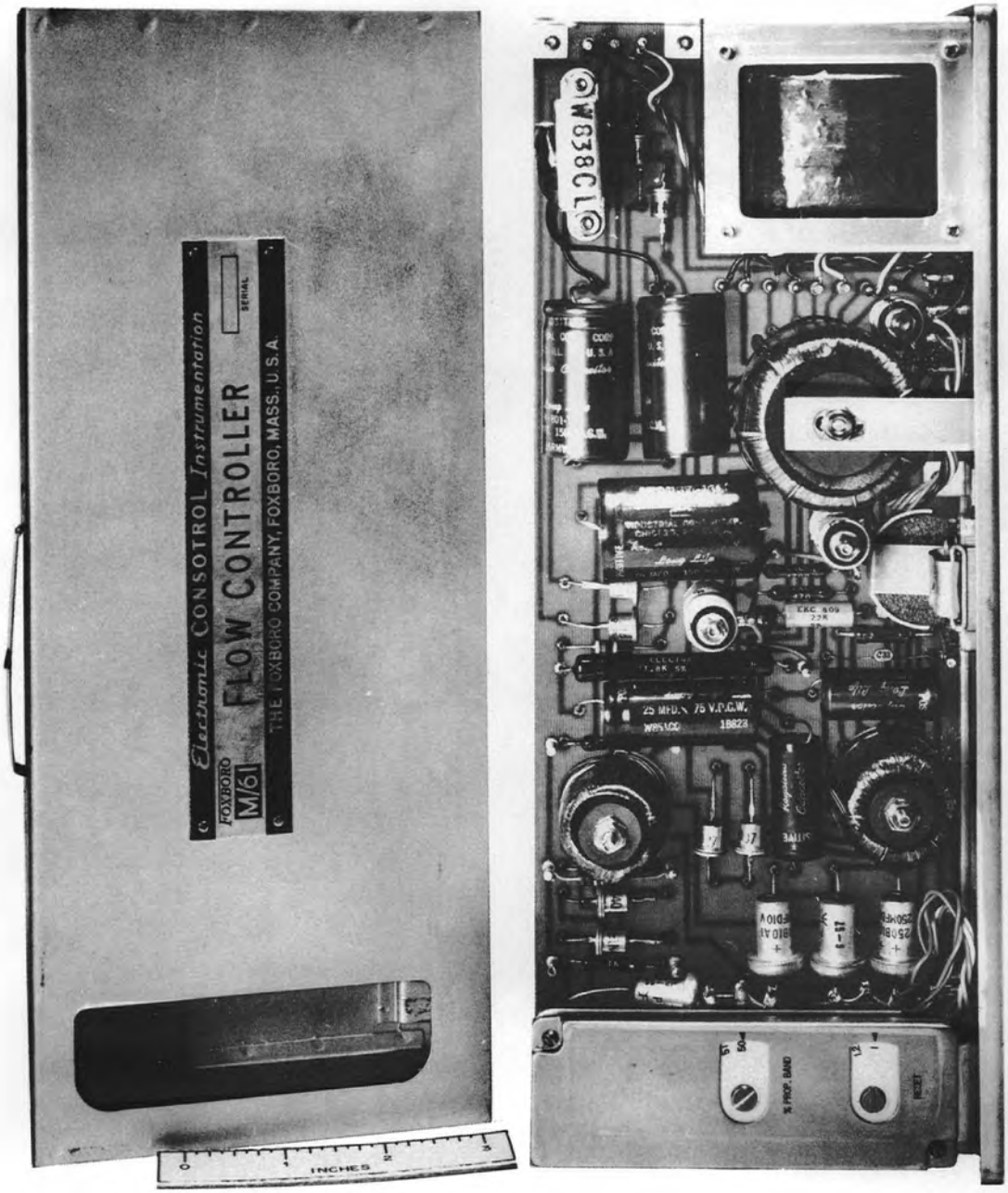

Fig. 85. Magnetic Amplifier Flow Controller.

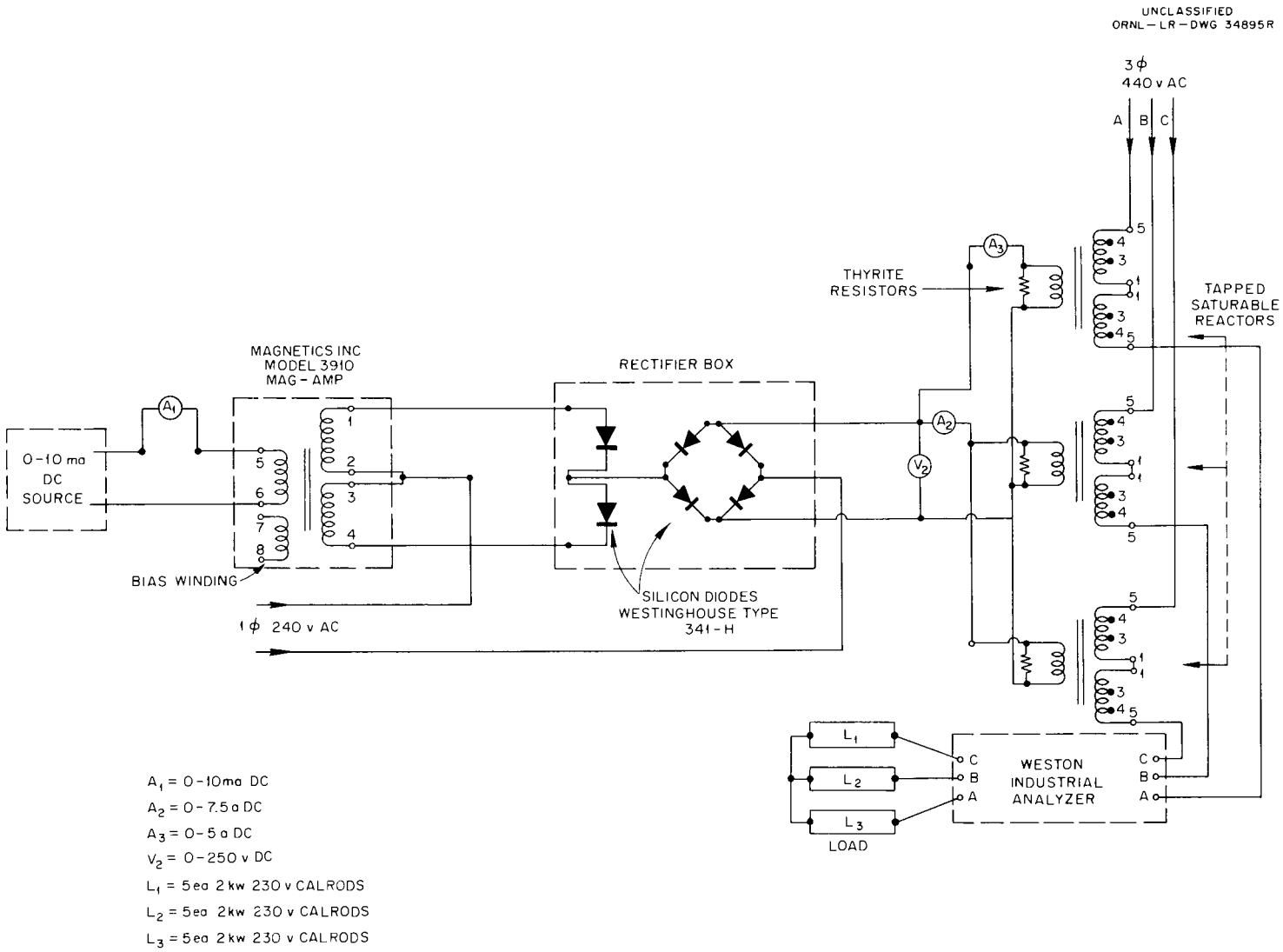

Fig. 86. Schematic Diagram of Static-Component Power-Control System Test.

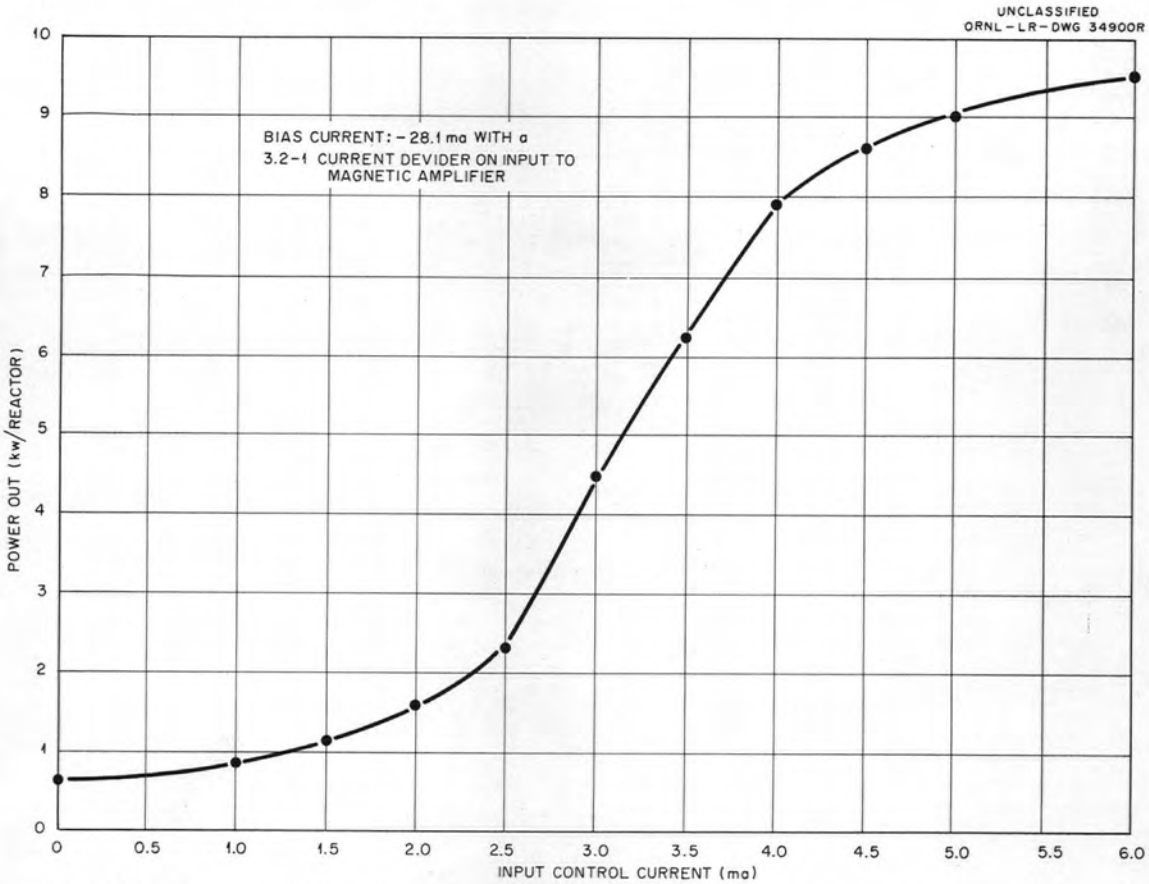

Fig. 87. Control Characteristic Curve of Static-Component Power-Control System Test.

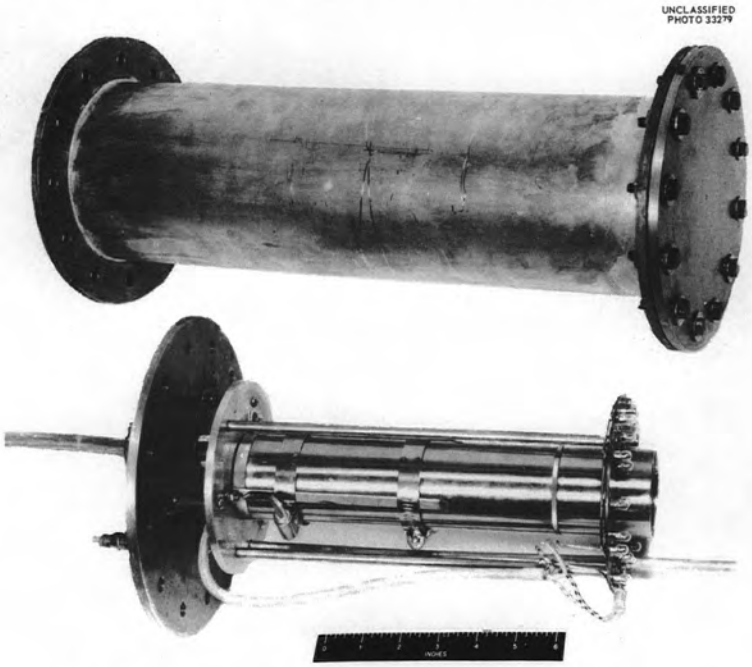

Fig. 88. Miniature TV Camera and Test Chamber.

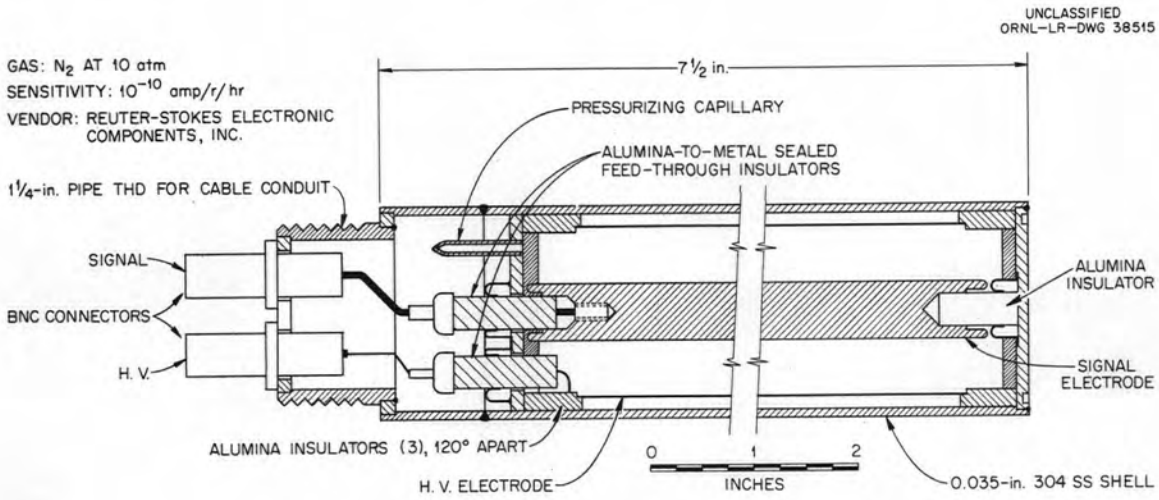

Fig. 89. High-Temperature Gamma Radiation Detector.

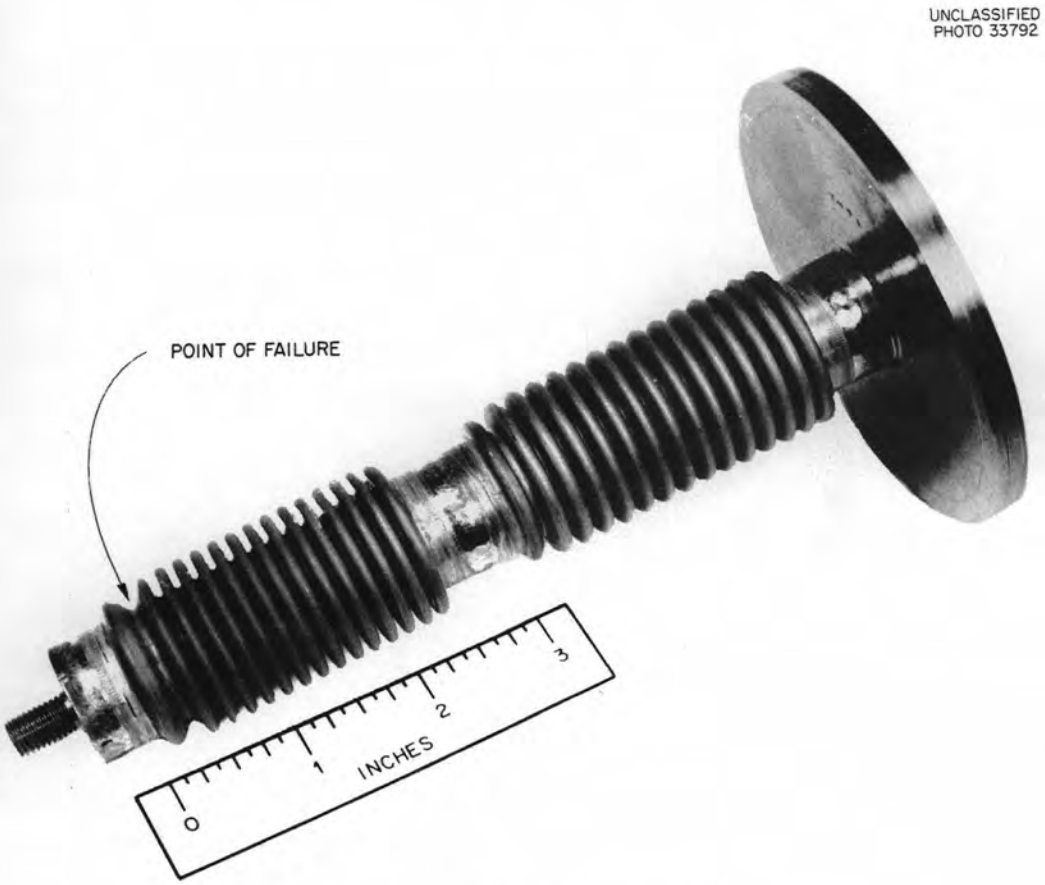

Fig. 90. Titanium Valve Stem Sealing Bellows.

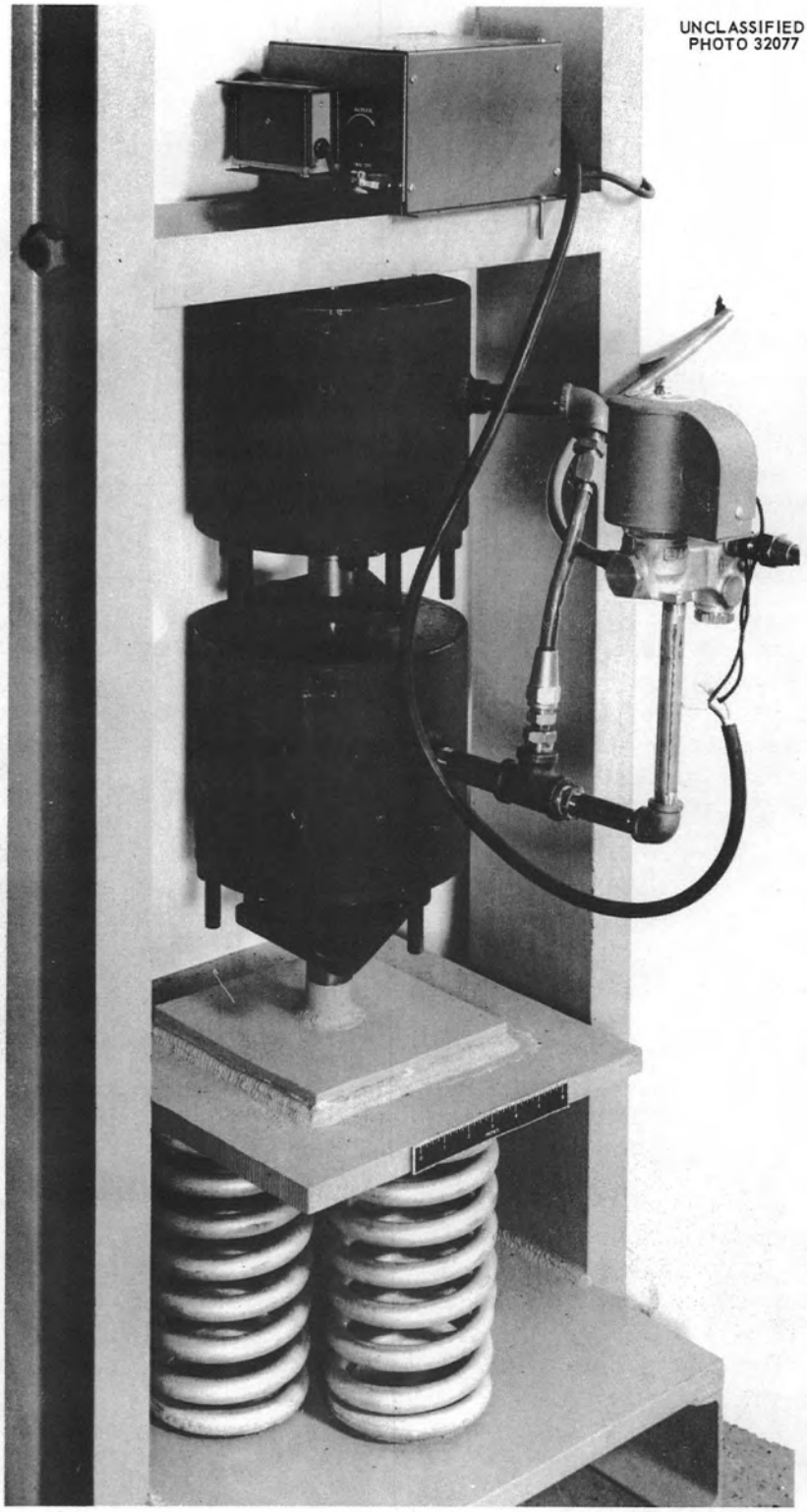

Fig. 91. Test Stand for Metal Bellows Valve Actuators.

PROBLEMS RELATING TO ORR OPERATION

S. J. Ditto, Jr. J. C. Gundlach

Two programs of general interest in the field of reactor control instrumentation are being carried out at the ORR.

The first involves the application of gamma-ray detectors in the level safety system. It has been observed that filling an experimental beam hole at the ORR with water may reduce the current in a nearby neutron-sensitive ionization chamber to as little as 20% of its reading when the beam hole is empty. Perturbations of more distant chambers are less, but since all neutron-sensing chambers are in the vicinity of the beam holes none is capable of indicating, unambiguously, the reactor level during changes in beam hole conditions. Since it is likely that experimenters will wish to drain and fill beam holes or beam hole liners periodically, and since it is possible that beam holes may be accidentally drained or filled during reactor operation, a study of the possible solution to the problem was begun.

Preliminary tests have shown that a gamma ionization chamber can be used to indicate neutron level with fair accuracy in the upper 1 1/2 decades of reactor operating power. Thus the gamma chambers can be used in this range to give a good indication of fission power. These chambers are relatively insensitive to beam hole changes in the ORR as compared with the neutron-sensitive chambers. However, it is found that loading changes and rod movements produce about the same perturbations of the outputs of the gamma chambers and the neutron chambers.

Four gamma chambers of an existing type[1] have been temporarily installed outside the reactor tank in a gamma flux of the order of 10^6 r/hr at 20-Mw reactor power, where they deliver approximately 10 μa. As a temporary measure, two of these chambers have been tied into the slow scram circuit through recorder switches. The ionization currents develop voltages across resistors to drive the 10-mv recorders directly. New gamma chambers are being designed to supplement neutron chambers in the permanent level safety system at the ORR.

The second program is concerned with the effects of deuterium photoneutrons on the log N information at the ORR during startup.

It has been generally accepted at ORNL that when the log N output level has increased above a certain point, the reliability of the log N channel has been established. On this basis, when "confidence" in the log N has been established certain operational procedures have been permitted through automatic permissive circuits. Recently, studies have been made to determine the validity of such a scheme. The results of preliminary experiments are enlightening.

---

[1]D. S. Toomb et al., HRP Quar. Prog. Rep. Jan. 31, 1957, ORNL-2272, pp 35, 36.

The neutron current in an ionization chamber separated from the reactor by water has two important components. One of these is due to neutrons from the vicinity of the core and the other is due to gamma-induced neutrons from the deuterium in the water. Previously the second component has been neglected on the assumption that it is so small that its effect is insignificant. Recent tests have indicated that the assumption is not correct under conditions prevailing at the ORR.

In a high-flux reactor, in order that the chamber and amplifier operate at their design neutron flux, the chamber must be farther from the core than in previous installations at the Laboratory. In this location the difference between neutron and gamma-ray attenuation in the water causes an increase in the ratio of photoneutrons to reactor-neutron flux at the chamber. For this reason it may be hazardous to rely on log N information alone during a reactor startup.

Plans are being formulated to further the investigation of the problem outlined and to correct any features of the system or its operation which need correction.

BULK SHIELDING REACTOR II–SPERT I TESTS

J. R. Tallackson R. T. Santoro

The principal effort in the safety program has been directed toward testing the BSR-II in the SPERT-I facility at the NRTS in Idaho. The design of the BSR-II has been thoroughly described.[1]

Tests at SPERT-I will be a joint effort by ORNL and Phillips Petroleum Company personnel. Test objectives are: (1) to meet the requirements[1] set forth by the Safeguards Committee, (2) to obtain transient and nuclear data (this reactor, because of its size and composition, will provide information in an area not covered by tests to date), and (3) to operationally test the performance of the ORNL safety system, which is widely employed in pool-type reactors throughout the world.

The test program will consist of a series of transients produced by both step and ramp insertions of excess reactivity. The usual nuclear and thermal data taken during SPERT-I tests will be taken. In addition, however, the performance of the safety system will be observed in detail. For example, it has been recognized that the log N amplifier, when operating at very low input currents and short periods, suffers a slight loss in amplitude response. Analog computer simulation and analysis have verified this situation. Measurements at SPERT-I will provide actual in-service operational data which describe log N performance as installed in the system. Other quantities of particular interest are period amplifier response and magnet release time as affected by transient water surges.

The analog computer will be used in an attempt to simulate the reactor transients prior to running the tests at SPERT-I.

Equipment built to conduct these experiments is simple. The control system contains only one channel of safety instruments instead of the usual three. All control is manual and contains a minimum of interlocks. Ramp inputs of reactivity will be accomplished by the simple expedient of shim rod withdrawal. A variable-frequency motor generator set will provide up to a 50% increase in rod velocity over that normally used in ORNL modular rod drives. Shim rod worth is estimated at approximately 3% per shim, and four shims are provided. Minimum periods so produced are expected to be in the 20-msec region.

Step insertions of reactivity will be provided by using a fifth spring-loaded modular rod drive with an inverted combination transient rod which contains fuel and boron with the boron section at the lower end. Total rod worth is of the order of 6%. The grid plate has been modified by the addition of rectangular slots to allow passage for the transient rod.

---

[1]J. G. Lewin and E. G. Silver, Safeguard Report for a Stainless Steel Research Reactor for the BSF (BSR-II), ORNL-2470 (July 1958).

SERVO FISSION CHAMBER

J. L. Anderson R. E. Wintenberg

The purpose of the servo fission chamber is to provide continuous indication of neutron flux and pile period of a reactor from source level to full power with a single detector (fission chamber). In a pool-type reactor this represents a range of about 10^{10}, or ten decades. The need for such a device can be illustrated by considering briefly the instruments presently used on pool reactors.

At source level the only instrument which is on scale is the log count rate meter, which is driven from a fission chamber and appropriate pulse amplifiers. The useful range of the log count rate meter is three or four decades, depending on source strength. The log N amplifier, which is supplied the signal from a compensated ion chamber, has a useful range of four to six decades, depending on reactor history and degree of compensation. The compensated ion chamber normally has a fixed position such that the log N will be on scale at full power. Thus, the four- to six-decade range of the log N is from the "top" downward, and the three- to four-decade range of the log count rate meter is from the bottom upward. Considering that the range of the reactor from source level to full power is ten decades, it is apparent that on good days the ranges of the two instruments will just meet with no overlap. On poor days there can be as much as three decades of "bare midriff," that is, reactor power range that cannot be instrumented without either repositioning chambers or providing an additional overlapping channel of information. This situation is illustrated in Fig. 92.

An additional channel is undesirable because of space limitations around the reactor. The usual startup procedure is to reposition the fission chamber when the upper counting limit of the log count rate meter is reached. Often this point is reached simultaneously with criticality. This is a particularly unhandy coincidence when automatic startup is employed. Both flux-level and period information are incapacitated while the chamber is in motion and for a period of time thereafter because of the long recovery time constant of the count rate meter.

The servo fission chamber positions the chamber slowly and continuously during flux-level changes so as to maintain a constant counting rate. A proportional servo controls the motion so that the counting instruments are never incapacitated due to overload. Flux level information is derived from chamber position and flux gradient in the shielding medium. Period information is derived from the rate of change of chamber position. Since flux-level and period information are obtained while the chamber is in motion, as well as while it is stationary, no blind spot, or "bare midriff," exists.

Since the system uses the existing reactor fission chamber, no additional space is required in the reactor. The additional electronics required is considerably less than would be needed for a second fission chamber channel.

Basic System

A block diagram of the system is shown in Fig. 93. It can be seen that the chamber, pulse amplifier, log count rate meter, and differentiator are connected in the usual fashion with the exception that the chamber and pulse amplifier also function as part of a servo loop. The output of the pulse amplifier drives a linear count rate meter. The output of the linear count rate meter feeds a summing junction, where it is compared with a reference. The difference signal from the junction drives a proportional servo which positions the fission chamber to maintain zero difference signal. In other words, the servo tries to maintain a constant counting rate by moving the chamber through the shielding medium. The reference is set to demand a relatively high counting rate (10^3–10^4 counts/sec) so that good counting statistics along with reasonably fast response times can be obtained. The linear count rate meter is used so that its time constant can be tailored for optimum response at the demand counting rate and so that better accuracy can be obtained. When the reactor is shut down (source level), the servo causes the chamber to move to a position of maximum sensitivity, where there are still not enough counts to satisfy the reference demand. At fluxes between source level and reference demand, the count rate indicated by the log count rate meter is a measure of the flux. As the reactor flux is increased from source level, the chamber remains fixed in the position of maximum sensitivity and the count rate rises until it reaches the reference demand. As the flux is increased further, the servo acts to maintain the counting rate constant at the reference demand level by moving the chamber. The output from the log count rate meter is now a constant and the chamber position is a measure of flux level. Since the neutron attenuation of the shielding medium (water) is nearly logarithmic, the chamber position is approximately proportional to the logarithm of neutron flux. The output of the log count rate meter and a signal proportional to chamber position are summed to produce a net signal which is proportional to the logarithm of the neutron flux from source level to the limit of chamber travel.

Since neutron attenuation in water is not exactly logarithmic, some corrections must be applied to the chamber position signal. Figure 94 shows the neutron attenuation in water vs distance from the reactor core as measured at the Bulk Shielding Facility. In close to the core is a region of irregularity which is to be avoided. By setting the fully inserted or maximum sensitivity position of the chamber slightly beyond this region, the irregularity is avoided without significant loss of sensitivity. Between 10 and 200 cm from the core the attenuation characteristic has uniform curvature. In this region the chamber position signal can easily be corrected to provide logarithmic output by means of a nonlinear potentiometer or similar device. Beyond 200 cm the rate of curvature changes to follow the gamma attenuation, since this far from the core the neutron population is primarily due to (γ,n) reactions in deuterium. However, this is academic because more than adequate range is available before this change in curvature is reached.

Performance

If the servo has insufficient speed to hold the counting rate constant for a particular rapid rate of rise, the output of the position potentiometer alone will not truly represent reactor neutron level. However, in such a case the deviation of the log count rate meter from demand level will be an exact measure of the amount by which the position potentiometer output is in error. Since the outputs of the log count rate meter and the position potentiometer are continuously summed, the errors are canceled and the output of the summer will be always a correct indication of the reactor flux. This situation has important bearing on the speed required of the servo. Without the summation the servo would have to be fast enough to follow the fastest rate of rise that is required to be indicated; for instance, a 3-sec period. The summing operation relaxes this requirement considerably. It is only necessary that the servo be fast enough to keep the log count rate meter within its operating range. Thus fast rates of rise which exceed the capability of the servo can be tolerated without error for short periods of time. In order to avoid an accumulated difference which would eventually drive the log count rate meter off scale, the servo must be as fast as the maximum sustained rate of rise encountered in normal operation of the reactor. Typical operating periods are 10 to 25 sec.

The transient response requirements are similarly lessened. It is advantageous to use the slowest permissible servo response so that the size of the drive motor and power amplifier can be proportionately reduced. A fast servo has some merit, in that it will tend to reduce the statistical variation of the counting rate information and present a smoother output, but this benefit is trivial.

The system was assembled using available instruments and operated in the Pool Critical Assembly. The purpose of the experiment was to determine optimum time constants, servo speed of response, and the neutron attenuation characteristics in typical chamber and drive locations. The equipment is shown in Fig. 95. The performance was entirely satisfactory, and another system is being constructed which will combine most of the instruments in a smaller package. This new system will be for extended use and evaluation in one of the pool reactors.

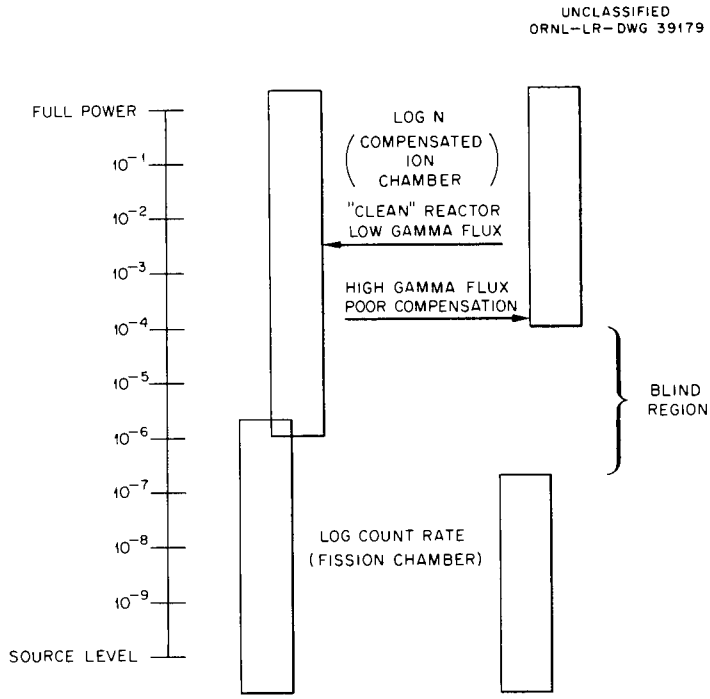

Fig. 92. Typical Instrument Ranges – Pool-Type Reactor.

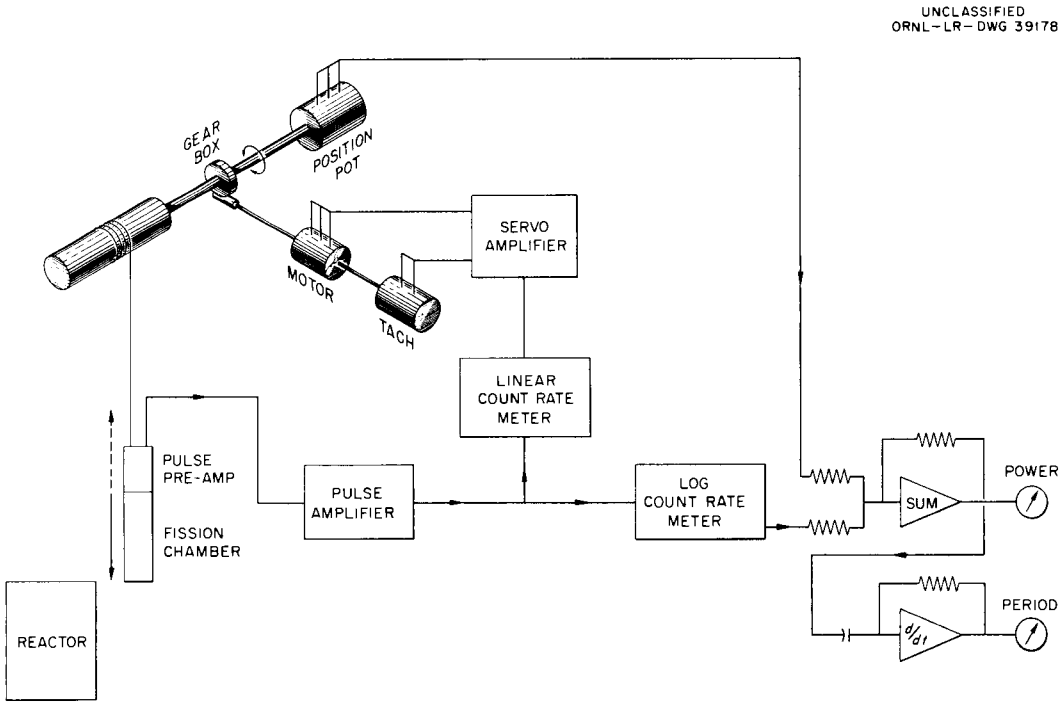

Fig. 93. Block Diagram of Servo Fission Chamber.

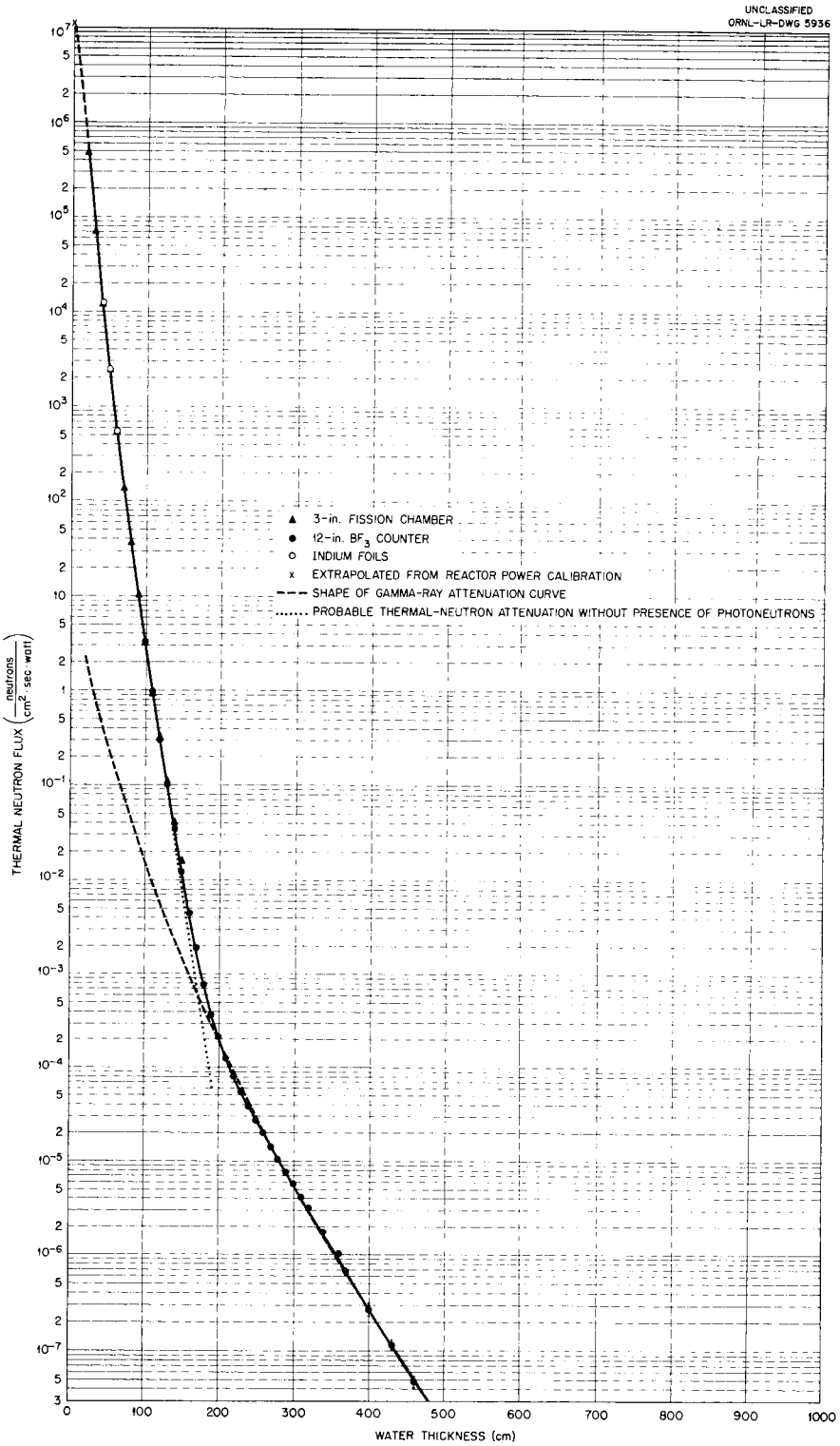

Fig. 94. Thermal-Neutron Flux as a Function of Distance from the Bulk Shielding Reactor.

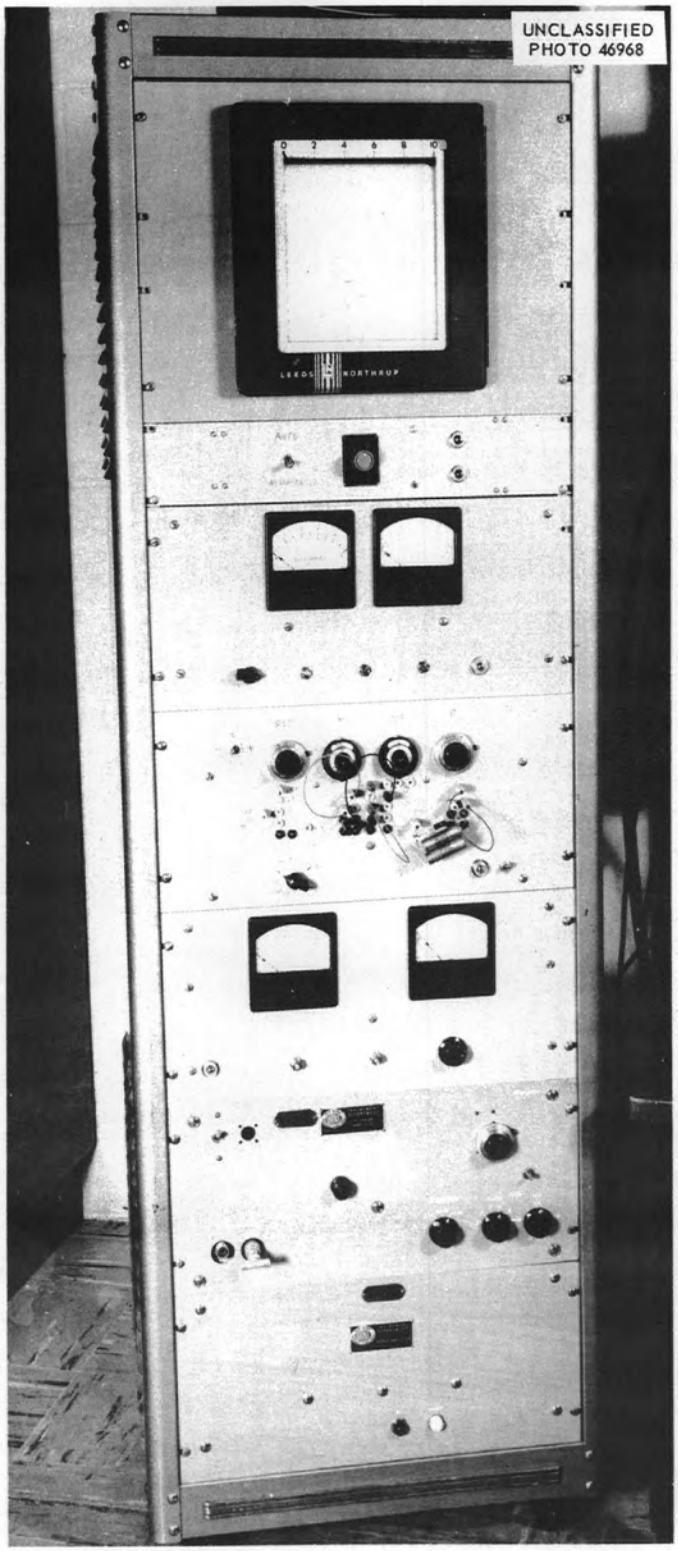

Fig. 95. Instrument Cabinet for Servo Fission Chamber.

ORNL-2787
Instruments
TID-4500 (15th ed.)

INTERNAL DISTRIBUTION

1. C. E. Center
2. Biology Library
3. Health Physics Library
4-6. Central Research Library
7. Reactor Experimental Engineering Library
8-128. Laboratory Records Department
129. Laboratory Records, ORNL R.C.
130. A. M. Weinberg
131. L. B. Emlet (K-25)
132. J. P. Murray (Y-12)
133. J. A. Swartout
134. E. H. Taylor
135. E. D. Shipley
136. C. S. Harrill
137. M. L. Nelson
138. W. H. Jordan
139. S. C. Lind
140. F. L. Culler
141. A. H. Snell
142. A. Hollaender
143. M. T. Kelley
144. K. Z. Morgan
145. T. A. Lincoln
146. A. S. Householder
147. C. E. Winters
148. H. E. Seagren
149. D. Phillips
150. C. J. Borkowski
151. P. R. Bell
152. J. L. Lovvorn
153. G. S. Hurst
154. R. S. Livingston
155. E. E. Fairstein
156. C. W. Sheppard
157. W. G. Stone
158. C. P. Keim
159. C. D. Susano
160. P. M. Reyling
161. G. C. Williams
162. M. J. Skinner
163. J. V. Francis
164. R. W. Johnson
165. D. J. Fisher
166. E. G. Struxness
167. J. R. McNally, Jr.
168. J. L. Gabbard
169. R. A. Charpie
170. T. V. Blosser
171. E. L. Olson
172. J. A. Auxier
173. R. K. Abele
174. J. R. Tallackson
175. H. E. Banta
176. E. W. Burdette
177. R. R. Dickison
178. C. A. Mossman
179. D. S. Toomb
180. R. G. Affel
181. H. J. Stripling
182. E. P. Epler
183. F. W. Manning
184. ORNL-Y-12 Technical Library, Document Reference Section

EXTERNAL DISTRIBUTION

185-186. Ohio State University (Professor of Naval Science)
187. R. Hofstadter, Stanford University
188. J. C. Nance, Consolidated-Vultee Aircraft Corporation
189. E. A. Rollor, ANP Project Office, Fort Worth
190. R. N. Keller, University of Colorado
191. Division of Research and Development, AEC, ORO
192. Office of Isotope Development, AEC, Washington (J. Hitch)
193-809. Given distribution as shown in TID-4500 (15th ed.) under Instruments category (100 copies, OTS)